KATHOLIEKE UNIVERSITEIT LEUVEN
FACULTEIT DER TOEGEPASTE WETENSCHAPPEN
DEPARTEMENT WERKTUIGKUNDE
AFDELING MECHANISCHE KONSTRUKTIE EN PRODUKTIE
Celestijnenlaan 300B — B-3001 Leuven (Heverlee), Belgium

PRODUCTION ORIENTED DESIGN OF FILAMENT WOUND COMPOSITES

Jury :
Voorzitter :
Prof. dr. ir. J. Berlamont,
vice-dekaan
Leden :
Prof. dr. h.c. ir. J. Peters
Prof. dr. ir. H. Van Brussel
Ing. P. Vanherck
Prof. dr. ir. G. De Roeck
Prof. dr. ir. I. Verpoest
Prof. dr. ir. W. De Wilde (VUB)

Proefschrift voorgedragen tot
het behalen van het doctoraat
in de toegepaste wetenschappen

door

ir. M. LOSSIE

UDC 621.763.001.13

April 1990

Graag zou ik een dankwoord willen richten tot iedereen die mij steun heeft verleend bij dit doktoraatswerk.

Ik dank Prof. J. Peters en Prof. H. Van Brussel die als promotor en co-promotor mijn onderzoek hebben begeleid.

In het bijzonder wens ik P. Vanherck te danken voor zijn dagelijkse motivatie en hulp. Pol, jouw onvoorwaardelijke paraatheid en interesse betekenden voor mij een onmisbare steun.

Ook dank ik mijn "komposiet"-kollega's J. Scholliers en D. Bastiaensen voor hun spontane en leerrijke samenwerking.

Mijn dank gaat verder uit naar alle medewerkers van Mechanika en van de K.U.L. - komposietgroep voor de aangename en sfeervolle uren.

Ook dank ik mijn ouders, schoonouders en familieleden voor hun steun en aanmoediging.

Tenslotte dank ik jou, Christophe, omdat je me bent blijven motiveren om dit doktoraat ook "thuis" nog verder af te werken.

Mieke Lossie
april 1990

Samenvatting

Produktie georiënteerd ontwerpen van gewikkelde vezelversterkte komposieten

Inleiding

In voorliggend werk wordt een ontwerpmethodologie voorgesteld voor gewikkelde, vezelversterkte kunststofkomponenten. Zij is bedoeld als leidraad voor de komposietontwerper, om uitgaande van een voorontwerp, via opeenvolgende stadia, een geschikt eindprodukt te ontwikkelen dat aan alle vooropgestelde eisen voldoet.

Het zwaartepunt bij deze ontwerpstrategie situeert zich rond het zoeken naar een optimaal kompromis tussen de bijna grenzeloze ontwerpmogelijkheden met vezelversterkte kunststoffen enerzijds, en de beperkingen opgelegd door het wikkelproces anderzijds; bij de opbouw van een komposietlaminaat kan men, door een zorgvuldig opeenstapelen van lagen met geschikte vezeloriëntatie, aan de meest uiteenlopende eisen van sterkte en stijfheid in verschillende richtingen beantwoorden. Deze vrijheid wordt echter in sterke mate beperkt wanneer beslist wordt de beoogde komponent geodetisch te gaan wikkelen. Bij geodetisch wikkelen ligt de weg die de vezel op de mal beschrijft immers volledig vast eens startpunt en starthoek gekozen zijn. Bijgevolg is de mogelijkheid om de vezels overal te richten overeenkomstig de gewenste sterkte en stijfheid dus eerder beperkt. Om desondanks toch zoveel mogelijk de intrinsieke komposietvoordelen te benutten, kan de komposietontwerper beroep doen op de voorgestelde ontwerpmethodologie.

De bestudeerde ontwerpproblematiek situeert zich in een ruimer kader van het komposietonderzoek aan de afdeling Mechanische Konstruktie en Produktie. Dit onderzoek spitst zich voornamelijk toe op het ontwerp en de produktie van gewikkelde komposietonderdelen voor de industrie. Hierbij werd gebruik gemaakt van twee wikkeleenheden; een numerisch gestuurde twee-assige wikkelmachine en een off-line programmeerbare wikkelrobot.

Door theoretische en praktische kennis in verband met het ontwerpen en berekenen van komposietstrukturen te kombineren met de praktische ervaring, opgedaan bij het wikkelen van diverse eenvoudige

komponenten op de NC-machine, kon voldoende inzicht worden opgebouwd om tot een geschikte ontwerpmethode te komen voor axisymmetrische komposieten. Later werd deze dan uitgebreid naar het wikkelen van niet-axisymmetrische komponenten.

Aangezien in dit doktoraatswerk *ontwerpen* en *wikkelen* centraal staan, ligt het dan ook voor de hand om het *ontwerp van gewikkelde komposieten* in te leiden met twee hoofdstukken die respektievelijk de problematiek rond het ontwerpen van komposieten in het algemeen en het wikkelen van komposieten als produktietechniek toelichten.

Hoofdstuk 1 : Ontwerp en analyse van komposietstrukturen

In vergelijking met klassieke, isotrope materialen bieden komposieten bijna onbegrensde ontwerpfaciliteiten; dit hebben zij te danken aan hun anisotroop karakter. Hierdoor kunnen immers sterkte en stijfheid zonder beperkingen worden gevarieerd en kunnen komposieten lokaal versterkt of juist soepeler gemaakt worden, om optimaal te beantwoorden aan de vooropgestelde strukturele eigenschappen. De interessante mechanische karakteristieken van vezelversterkte kunststoffen, en dit voor een slechts lage soortelijke massa, maakt hen bijzonder aantrekkelijk voor toepassingen waar het gewicht een kritische rol speelt. Dankzij hun uitmuntende korrosieweerstand zijn zij ook heel nuttig voor de chemische industrie. Verder bieden komposieten de mogelijkheid om ook grotere komponenten uit één stuk te vervaardigen en aldus het aantal onderdelen en verbindingen in komplexere konstrukties te reduceren.

Vezelversterkte kunststoffen worden meestal aangewend onder de vorm van platen of schalen, laminaten genoemd. Het zijn de vezels die, via hun richtingsafhankelijke sterkte en stijfheid, toelaten een laminaat *naar maat* te maken; immers, door een gelamineerde struktuur op te bouwen uit lagen met geschikte vezel/hars kombinatie, deze lagen goed te richten en in de juiste volgorde op elkaar te stapelen, kan een komponent worden verkregen die als het ware "*geknipt*" is voor de funktie die hij moet vervullen.

Ontwerpen houdt drie taken in : het kiezen van het materiaal, het definiëren van een geschikte konfiguratie en het vinden van een aangepast produktieproces. Deze benaderingswijze geldt zowel voor

konventionele materialen als voor komposieten. Komposieten vragen echter dat het materiaal samen met de struktuur mee wordt ontworpen. Bijgevolg vereisen zij, in tegenstelling tot metalen die volgens een lineair proces kunnen worden ontworpen, een meer geïntegreerde ontwerpprocedure, met meestal een iteratieve optimalisatie. Hiervoor beschikt de ontwerper over een aantal min of meer gesofistikeerde hulpmiddelen. Bij het voorontwerp volstaan gewoonlijk eenvoudige, analytische rekenmethodes zoals b.v. de *Netting Analyse* of de *Klassieke Laminaattheorie.* Naarmate het ontwerp echter verder evolueert en meer komplexe, gedetailleerde berekeningen nodig zijn, moet de ontwerper zich beroepen op numerieke rekentechnieken zoals de *eindige differentie-* en de *eindige elementen* methode.

De hoofdtaak van de ontwerper is een struktuur uit te denken en vorm te geven die aan een vooropgesteld geheel van funktionele eisen voldoet. Dikwijls worden deze ontwerpvereisten uitgedrukt in termen van stijfheid, sterkte of levensduur. Belangrijk hierbij is dat de ontwerper een *veilige* struktuur moet afleveren. Om zijn ontwerp te kunnen dimensioneren en te evalueren, moet hij beschikken over materiaalgegevens en notie hebben over de betrouwbaarheid waarmee deze gekend zijn. Om funktioneel te kunnen ontwerpen, moeten ook een aantal nevenaspekten van komposieten beschouwd worden, zoals b.v. anisotropieeffekten, die zich doen gelden onder de vorm van aanzienlijke interne spanningen bij temperatuursveranderingen of vochtabsorptie. Vocht en temperatuur kunnen het komposiet zelf ook aantasten. Vooral komposieten die aan cyclische temperatuurs- en vochtigheidskondities worden blootgesteld, lopen gevaar voor degradatie. Tot de funktionaliteit van een ontwerp draagt ook de kostprijs in sterke mate bij. Vaak ligt de zuivere kostprijs van een komposietstuk hoger dan die van een equivalente metalen komponent. Toch kunnen komposieten ekonomisch interessanter blijken omdat zij, door hun gewichtsbesparing, onrechtstreekse kosten zoals b.v. brandstofkosten kunnen reduceren. Verder zijn er ook een aantal fabrikageaspekten waaraan reeds bij het ontwerp aandacht moet besteed worden; bijzondere aandacht verdient de uitharding van de struktuur, die residuele spanningen en scheeftrekken kan veroorzaken. Een komposietkomponent moet ook veilig gehanteerd en vervoerd kunnen worden en meestal stemt de krachtwerking die daarbij optreedt niet overeen met de grootte en de richting van de ontwerpbelasting. Zwakke punten in een komposiet-

struktuur zijn heel dikwijls de verbindingen; deze verdienen dan ook extra aandacht in de ontwerpfase. Tenslotte zijn ook ontwerpaspekten met betrekking tot schade-tolerantie en onderhoud van belang. Kleine foutjes zoals luchtinsluitsels, delaminaties en scheurtjes kunnen immers reeds bij de fabrikage geïnduceerd worden maar ook tijdens het gebruik kan nog extra schade veroorzaakt worden door impakt van kiezelsteen of vallende voorwerpen. Reeds tijdens het ontwerp moet rekening gehouden worden met mogelijke kwaliteitskontroles en eventuele reparatietechnieken.

Naast al deze aspekten van komposietontwerp zijn er natuurlijk de hoofd-ontwerpkriteria, nl. de eisen waaraan het ontwerp ongetwijfeld wordt getoetst en moet voldoen. Deze kriteria kunnen allemaal vertaald worden naar de noodzaak het ontworpen stuk te beschermen tegen één of andere vorm van falen wanneer het wordt onderworpen aan de vooropgestelde krachtwerking. Deze ontwerpbelasting kan zowel mechanisch als thermisch zijn, zowel statisch als dynamisch. Het begrip *falen* kan ook op verschillende manieren worden geïnterpreteerd; zo kunnen de vervormingen de toelaatbare waarde overschrijden. Te grote spanningen kunnen tot overbelasting leiden en schade veroorzaken. Tijdsafhankelijke belastingen kunnen aanleiding geven tot een fatale dynamische respons met te grote verplaatsingen of te hoge spanningen. Vermoeiingsverschijnselen ten gevolge van een langdurige cyclische belasting kunnen een struktuur onherroepelijk beschadigen. Tenslotte kan ook knik een komponent onbruikbaar maken.

Om een statisch belaste struktuur op sterkte te kunnen berekenen en veilig te kunnen dimensioneren, moet de ontwerper de sterkte en stijfheid van zijn ontwerp kunnen voorspellen. Hierin zitten twee opeenvolgende stappen vervat: een analyse van spanningen en rekken, gevolgd door het nagaan van hun effekt op de stijfheid en de sterkte van de komponent. De eerste stap kan op verschillende niveau's worden uitgevoerd, met telkens een andere verfijningsgraad van de gebruikte rekenmodellen. Eens de spanningen en rekken berekend zijn, moet worden getracht de strukturele sterkte van de komponent te bepalen. Gezien de komplexiteit van schademechanismen in komposieten is dit geen eenvoudige taak; de sterkte van komposieten onder statische belasting wordt immers niet alleen beïnvloed door de initiatie van schade ter plaatse van scheurtjes, maar ook in sterke mate door het voortplanten, de groei en de akkumulatie van zulke mikroschade.

Momenteel wordt met heel wat inspanning gezocht naar modelleringswijzen die deze schadeakkumulatie inrekenen. In de praktijk stelt de doorsnee-ontwerper zich echter tevreden met sterktevoorspellingen op basis van een elastische spanningsanalyse, gevolgd door een elementair breukkriterium, zoals b.v. het *Tsai-Wu* kriterium.

Wanneer een struktuur wordt onderworpen aan een wisselende belasting, dan moet hij op vermoeiing worden berekend. Bij composieten gaat vermoeiing gepaard met schade die zich doorheen de ganse komponent voortplant, in tegenstelling tot het groeien van één enkele dominante scheur bij een stalen komponent. Zowel matrixscheurtjes, vezelbreuken, delaminaties als het loskomen van vezel en matrix zorgen ervoor dat met de tijd de sterkte en de stijfheid gaan afnemen. Bij vermoeiing staan twee punten centraal; het voorspellen van de nuttige levensduur van een komponent onder specifieke belastingskondities en het resulterende belastingsniveau waaraan een komponent nog veilig kan onderworpen worden, na een zekere levensduur. Om vermoeiing van composieten te behandelen wordt nog veelvuldig gebruik gemaakt van traditionele modellen voor metallieke materialen, zij het dan onder een lichtjes aangepaste vorm. Net zoals bij het voorspellen van statische sterkte wordt echter heel wat onderzoek verricht om de schadeakkumulatie ten gevolge van een cyclische belasting in de voorspellingsmodellen in te brengen.

Ook al kan de ontwerper een vrij behoorlijke schatting maken van de draagkracht van zijn ontwerp, toch moet hij afrekenen met een groot aantal vaagheden. Ten eerste kan er een aanzienlijke spreiding zitten op de materiaalgegevens die hij in zijn berekeningen heeft gehanteerd. Deze kunnen dan nog in sterke mate afwijken van de reële karakteristieken, zoals die in de werkelijke konstruktie voorkomen. Bovendien kunnen er onzekerheden optreden i.v.m. de aangrijpende belasting. Vooral de richting van de krachtwerking en de omgevingsvoorwaarden waarin deze op de struktuur inwerkt, spelen hierbij een belangrijke rol. Om zijn ontwerp veilig te stellen tegen al deze onzekerheden, moet de ontwerper een geschikte veiligheidsfaktor inrekenen. De literatuur biedt hierover weinig éénduidige richtlijnen. Gewoonlijk moet de ontwerper maar zelf uitmaken hoe gevoelig zijn ontwerp reageert en mag reageren op variaties in materiaaleigenschappen, hoe kritisch bepaalde schades zijn en in hoeverre de struktuur specifieke schadevormen moet kunnen doorstaan. Het gebrek aan uniformiteit in ontwerpregels blijkt

duidelijk uit een onderzoek, ingesteld door het *American Institute of Aeronautics and Astronautics* (Ref. [30]), betreffende breukkriteria en veiligheidsfaktoren bij het ontwerp van komposieten.

HOOFDSTUK 2 : WIKKELEN VAN VEZELVERSTERKTE KUNSTSTOF-KOMPONENTEN

Een veelvuldig toegepaste produktietechniek voor het vervaardigen van hoogwaardige komposietstrukturen is wikkelen. In het kort geschetst komt wikkelen neer op het onder gekontroleerde spanning aanbrengen van kontinue, met hars geïmpregneerde vezel op een meestal ronddraaiende mal, en dit volgens een op voorhand vastgelegd geometrisch patroon. Praktisch gezien houdt het komplete wikkelproces natuurlijk veel meer aspekten in.

Ten eerste moet een keuze gemaakt worden betreffende de te gebruiken vezels en harssoorten; waar vroeger hoofdzakelijk glasvezel werd aangewend, wordt nu ook veelvuldig gebruik gemaakt van aramide- en koolstofvezels. Bij de harsen kan men onderscheid maken tussen twee hoofdtypes : thermoharders zoals b.v. epoxyhars en thermoplasten, waarvan *peek* een typisch voorbeeld is. Thermoharders vormen bij het uitharden op verhoogde temperatuur drie-dimensionale bindingen, waardoor zij, eens definitief uitgehard, niet meer opnieuw gesmolten kunnen worden. Thermoplasten daarentegen kunnen telkens opnieuw door een gepaste temperatuursverhoging week worden gemaakt, zodat zij uitermate geschikt zijn voor vormgevingsprocessen in verschillende stappen en gemakkelijk hersteld kunnen worden bij eventuele schade.

Bij het wikkelen worden onvermijdelijk holtes en luchtinsluitsels gekreëerd, zowel tussen naburige vezels, daar waar vezels elkaar kruisen als tussen lagen met verschillende vezeloriëntatie. Om deze luchtbellen te verwijderen en een zo uniform mogelijke harsverdeling te verkrijgen, is een gepaste konsolidatie nodig. Het komposiet kan na het wikkelen gekonsolideerd worden, maar ook tijdens het wikkelen kan een geschikte spanning in de vezelbundels voor de nodige samendrukking zorgen. Door een nauwkeurige kontrole van de vezelspanning is het immers mogelijk een optimaal kompromis te sluiten tussen enerzijds, een voldoende vloeien van het hars waardoor de luchtbellen worden verwijderd, en anderzijds toch geen overdreven druk die al het hars uit het komposiet zou drukken.

Een belangrijke stap bij het wikkelproces is het impregneren van de vezel. Er zijn verschillende manieren om de vezels met hars te doordrengen. De meest voorkomende zijn *nat* wikkelen en *prepreg* wikkelen.

- Bij *natte* wikkelprocessen wordt het hars op de vezel aangebracht tijdens het wikkelen zelf, net voordat de vezel op de mal wordt gelegd. Hierbij wordt de vezel ofwel door een harsbadje getrokken, ofwel over een rol, die zelf deels in een harsbad rolt en een geschikte hoeveelheid hars via een harsfilm op de vezel overdraagt. Nat wikkelen is eenvoudig en goedkoop maar is moeilijk te kontroleren en levert dan ook geen hoogwaardige kwaliteit af. Het belangrijkste nadeel is echter dat nat wikkelen slechts weinig wrijving garandeert zodat een stabiel en slipvrij wikkelpatroon enkel door geodetisch wikkelen kan worden bereikt.

- Bij *prepreg* wikkelen worden de vezels met hars geïmpregneerd vóór het wikkelen en deels uitgehard. Prepregs zijn duurder maar geven kwalitatief betere resultaten. Vooral vanuit het gezichtspunt van de komposietontwerper zijn zij duidelijk interessanter aangezien zij toelaten om, zonder slipgevaar, af te wijken van geodeten, zodat de laminaatopbouw beter kan beantwoorden aan de vooropgestelde eisen van sterkte en stijfheid.

Na het wikkelen moet de komponent uitgehard worden tot een stevige struktuur die de gewenste draagkracht bezit. Dit vastwordingsproces begint op het ogenblik dat de verschillende harskomponenten met elkaar worden gemengd en verloopt in twee fasen; de eerste stap in de uithardingscyclus wordt *B-harden* genoemd. Hierbij bouwt het hars progressief hogere viskositeiten op tot het gelpunt bereikt wordt. Het hars is dan nog wel week en kleverig maar vloeit niet meer. Om tot het B-stadium uit te harden blijft de gewikkelde komponent meestal ronddraaien om het hars niet plaatselijk te laten afdruipen. De verdere uitharding van het komposiet (*C-harden*) tot de definitieve fysische eigenschappen zijn bereikt, gebeurt meestal bij verhoogde temperatuur in een oven of autoklaaf.

Bij het wikkelproces speelt de mal, het voorwerp waarrond de geïmpregneerde vezels worden gewikkeld, een belangrijke rol. Momenteel bestaat er een uigebreid gamma aan mogelijke malmaterialen en maltypes; zo zijn er eenvoudige metalen mallen uit één stuk, op-

klapbare of deelbare mallen en mallen die bestaan uit water-oplosbaar zand of uit oplosbare of smeltbare zouten. Ook laagsmeltende legeringen en oplosbare plaastersoorten worden gebruikt. Verder komen nog opblaasbare mallen voor. Voor hoogwaardige toepassingen worden voornamelijk *liners* aangewend; dit zijn dunne licht-metalen mallen die na het wikkelen deel blijven uitmaken van de struktuur en eventueel voor lucht- en waterdichtheid zorgen of mee belasting gaan opnemen.

Bij het wikkelen kunnen de vezels op diverse manieren op de mal worden aangebracht. De mogelijke vezeltrajekten kunnen op twee manieren worden opgesplitst :

- Wat wikkelstabiliteit betreft, kan men onderscheid maken tussen *geodetisch* en *niet-geodetisch* wikkelen.

  Geodeten zijn lijnen die twee punten op een oppervlak volgens de kortste afstand over dit oppervlak verbinden. Bijgevolg zal een vezel die volgens een geodeet gericht is geen neiging vertonen te gaan verschuiven en vergt geodetisch wikkelen dus geen wrijving om de vezels op hun plaats te houden.

  Men kan ook *semi-geodetisch* wikkelen, door lichtjes van de geodetische paden af te wijken. Hiertoe moet er wel voldoende wrijving voorhanden zijn, zoals b.v. bij prepregs, om te kunnen garanderen dat de vezels, eens geplaatst, hun positie ook blijven behouden.

- Een tweede klassifikatie is gebaseerd op de wijze waarop in-de-tijd-opeenvolgende wikkelingen ten opzichte van elkaar zijn gepositioneerd. Zo onderscheidt men drie types van wikkelpatronen : *polair-*, *helikoidaal-* en *omtrekswikkelen.*

  Polair wikkelen geeft aanleiding tot een gelaagde struktuur waarbij een volgende vezel net naast de vorige komt te liggen. *Helikoidale* wikkelprocessen leveren een eerder geweven struktuur met een voortdurend kruisen van de vezels. Naast polaire en helikoidale wikkelingen, die meestal de ganse struktuur overspannen, kan men ook nog *omtrekswikkelen*, waarbij naast elkaar gelegen wikkelingen worden aangebracht volgens de omtreksrichting van de mal.

Naast de verschillende stappen die samen deel uitmaken van het wikkelprocédé, zijn er nog een aantal technologische wikkelaspekten die bijzondere aandacht verdienen.

Zo zijn er de omgevingsomstandigheden van verhoogde temperatuur en vochtblootstelling tijdens de fabrikage, waaraan komposieten in het algemeen reeds gevoelig zijn en die nog eens extra gevaar betekenen voor gewikkelde stukken om wille van hun meestal laag harsgehalte.

Ook al laten komposieten toe het aantal elementen van een struktuur te reduceren, toch komen komposiet-metaal verbindingen nog zeer frekwent voor. Spijtig genoeg vormen deze verbindingen meestal de zwakste schakel in een struktuur en vereisen bovendien dure en tijdrovende machinale bewerkingen. Het wikkelproces biedt echter de mogelijkheid verbindingen direkt mee in de struktuur in te wikkelen en zo te integreren zonder bijkomende bewerkingsstappen.

Om volledig aan alle vooropgestelde eisen te kunnen voldoen, moeten gewikkelde komponenten meestal nog een aantal nabewerkingen ondergaan. Zo is er b.v. het buitenoppervlak dat zonder het gebruik van een vakuümzak of een buitenmal zeer ruw en oneffen is. Als de komponent deel moet uitmaken van een komplexere konstruktie, moeten vaak extra details, aansluitingsstukken en verbindingsmogelijkheden aangebracht worden. Hiertoe moeten meestal snij- of booroperaties worden uitgevoerd, die op hun beurt gespecialiseerde apparatuur en komposiet-aangepaste werktuigen vereisen.

Om een te wikkelen ontwerp te kunnen evalueren, heeft de komposietontwerper materiaalgegevens nodig die het gewikkelde karakter van het komposiet mee insluiten. Hiervoor staan hem een heel gamma testprocedures ter beschikking. De meest voorkomende testen worden uitgevoerd op gewikkelde buizen of ringen.

De technologie van het wikkelen heeft de laatste jaren een heuse evolutie ondergaan. Vroeger werd wikkelen eerder zelden toegepast; het wikkelproces was immers arbeidsintensief, vergde veel tijd en bleek enkel geschikt voor eenvoudige geometrieën. Het ontwerp moest zo worden opgevat dat de mal na het wikkelen en uitharden kon verwijderd worden. Deze mal was vaak komplex en duur. Verder was het wikkelen beperkt tot geodetische patronen en konden konkave vormen niet worden gewikkeld. Bovendien was de oppervlaktekwaliteit van de uitgeharde komponenten vaak slecht en bevatte het komposiet meestal vrij veel luchtinsluitsels.

Dankzij nieuwe technieken en materialen heeft het wikkelen deze zwakke punten echter weten te omzeilen. Momenteel is er een zeer

uitgebreid gamma aan malmaterialen op de markt beschikbaar, telkens beantwoordend aan weer andere vereisten. Uitwasbare en oplosbare malmaterialen hebben de vroegere problemen rond het verwijderen van de mal opgelost.

Nieuwe materiaalvormen, zoals het gebruik van prepregs en thermoplastische harssoorten, hebben aan het klassieke wikkelen heel wat flexibiliteit gegeven; er kan nu op stabiele wijze van de vroeger verplichte geodetische paden worden afgeweken, waardoor het mogelijk wordt de vezels beter te richten volgens de optredende krachtwerking. Bovendien kunnen nu ook konkave krommingen worden gewikkeld.

Ook de evolutie naar computergestuurde wikkelsystemen en wikkelrobots en vooral de integratie van CAD/CAM in het ontwerp en de produktie, hebben ertoe bijgedragen dat wikkelen is uitgegroeid tot een ekonomische fabrikagetechniek voor hoogwaardige komposietkomponenten, met een brede waaier van toepassingsmogelijkheden.

Ter illustratie van deze evolutie en tevens om dit wikkelhoofdstuk af te ronden, worden de twee wikkeleenheden besproken die gebruikt werden voor het wikkelonderzoek. Voor het wikkelen van eenvoudige, axisymmetrische komponenten werd een draaibank omgebouwd tot twee-assige, numerisch gestuurde wikkelmachine. Tevens werd een offline programmeerbare robot ingeschakeld, die meer komplexe, niet-axisymmetrische strukturen wikkelen kan.

De NC-machine, weergegeven in Fig. 0.1, heeft slechts twee vrijheidsgraden, de rotatie van de hoofdspil die de mal draagt en de rotatie van de wikkelarm die via het wikkeloog op zijn uiteinde de vezel aanvoert. Daarnaast is er de nodige apparatuur voorzien die zorgt voor het afwikkelen van de vezelbobijnen, de spanning in de vezels, de impregnatie van de vezels en het uitharden van de gewikkelde komponent. Om geodetisch te wikkelen, wordt de armbeweging gestuurd in funktie van de spil die aan vrij konstante snelheid ronddraait. Deze sturing gebeurt in twee stappen; eerst wordt een wikkeltabel aangemaakt, die de sturingsgegevens overeenkomstig de gewenste geodetische wikkelingen bevat, onder de vorm van spil- en bijhorende armposities. Tijdens het wikkelen zelf is de sturing gebaseerd op een *position feed-forward* principe, waarbij gebruik gemaakt wordt van de zonet vernoemde wikkeltabel. In vergelijking met de meeste kommerciële twee-assige wikkelmachines die met een zware langsslede zijn uitgerust, laat de lichte wikkelarm van de NC-machine veel hogere wikkelsnelheden

toe.

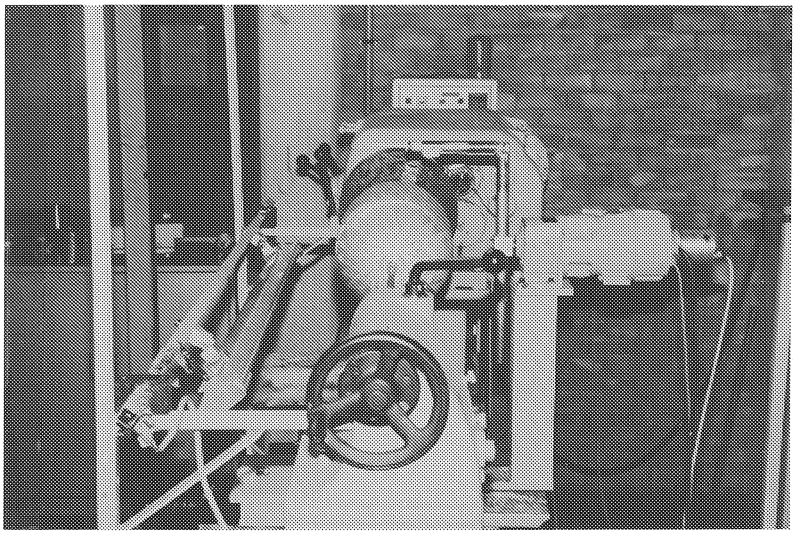

Figure 0.1: Numerisch gestuurde wikkelmachine.

Voor het wikkelen van niet-axisymmetrische komponenten volstaan twee-assige wikkelmachines niet meer. Hiervoor werd dan ook gebruik gemaakt van een *Puma* robot met zes vrijheidsgraden. Een externe as waarop de mal wordt aangebracht werd gesynchroniseerd met de robot en zorgt dus voor een bijkomende zevende vrijheidsgraad. Met een drie-dimensionaal CAD tekenprogramma wordt een tekening gemaakt van de te wikkelen geometrie. De bijhorende geometrische gegevens worden vertaald naar een leesbare vorm voor de geodeetprogrammatuur die werd ontwikkeld voor het berekenen van geodeten op komplexe oppervlakken. De berekende geodeten worden voortdurend op konkaviteit getest; immers, indien het vezelpad lokaal konkaaf wordt, zal de gewikkelde vezel nooit op zijn plaats blijven liggen maar een kortere weg door de lucht verkiezen. Daar torsie van de vezels bij bredere banden aanleiding kan geven tot plooien in het komposietoppervlak, wordt er ook een torsiekontrole uitgevoerd. Eens het geodetisch pad is berekend en goedgekeurd, kunnen de opeenvolgende posities van het voedingsoog, aangebracht op het uiteinde van de robotarm, en de daarbijhorende hoekposities van de externe as worden bepaald, die er samen voor zorgen dat de vezel op de juiste manier op

de mal wordt gelegd. Deze off-line sturingsgegevens kunnen dan naar de robot worden doorgestuurd en het wikkelen kan beginnen.

HOOFDSTUK 3 : ONTWERP VAN AXISYMMETRISCHE GEWIKKELDE KOMPOSIETEN

In het eerste hoofdstuk werd het ontwerp van komposieten in het algemeen besproken en werden de opeenvolgende stadia die de ontwerper moet doorlopen beschreven, alsook de hulpmiddelen waarover hij beschikt.
Hoofdstuk 2 werd volledig gewijd aan het wikkelproces als dusdanig en aan de technologische aspekten en beperkingen die onvermijdelijk met wikkelen samengaan.
Er werd reeds aangehaald dat komposietontwerp in belangrijke mate bemoeilijkt wordt door het feit dat konfiguratie, materiaal en produktiewijze simultaan gegenereerd worden en met elkaar interageren.
Vermits deze thesis zich heeft toegespitst op het ontwerp van gewikkelde komposieten, zal de ontwerpmethodologie die in dit derde hoofdstuk wordt voorgesteld moeten afrekenen met interakties en beperkingen, opgelegd door het wikkelproces.

Ten eerste zijn er de toleranties die rechtstreeks aan de wikkeltechnologie verbonden zijn. Bij wikkelen zijn er immers een groot aantal soms moeilijk te kontroleren parameters die de eigenschappen van de gewikkelde komponent gaan beïnvloeden. Zij moeten reeds van bij het ontwerp mee ingekalkuleerd worden om de ontwerper een idee te geven over de haalbare toleranties zodat hij geschikte veiligheidsfaktoren kan toepassen.

Zowel de harssamenstelling, zijn vermenging als zijn verdeling in het komposiet hebben een belangrijke weerslag op de uiteindelijke sterkte van het eindprodukt. Ook de dikwijls beperkte bruikbaarheidsduur van het nog niet uitgeharde hars moet reeds tijdens het ontwerp in acht worden genomen. Verder moet rekening gehouden worden met de haalbare en toegelaten variaties op de temperatuur en de snelheid van temperatuurswijzigingen tijdens het uitharden. Als het aanwenden van een vakuümtechniek wordt overwogen , moet dit reeds bij het ontwerp worden ingerekend. Ook de omgevingskondities waarbij de komponent wordt gefabriceerd moeten goed gekend zijn.

Naast parameters die betrekking hebben op het hars, is ook de

wikkelspanning in de vezels belangrijk aangezien ook zij in sterke mate de eigenschappen van het eindprodukt beïnvloedt. De ontwerper moet dus nagaan welke de spanningskontrolemogelijkheden zijn. Daarnaast moet hij ook bedenken dat scherpe kanten de vezels doen inscheuren en dat vlakke stukken voor een slechte konsolidatie zorgen.

Verder moet ook de nauwkeurigheid waarmee de vezels kunnen worden gelegd en gericht in acht genomen worden, omdat zij een idee geeft over de nauwkeurigheid waarmee een wikkelpatroon na een groot aantal cycli kan worden gesloten.

Tenslotte zijn er nog de vezelgeleidingsrolletjes en wikkeloogjes die niet alleen de vezels kunnen beschadigen of doen fibrileren maar ook in sterke mate de breedte van de vezelband op de mal beïnvloeden.

Naast voorgenoemde, met het wikkelproces geassocieerde punten, die allemaal gereflekteerd worden in het uiteindelijke gedrag van het komposiet, zijn er de ontwerpaspekten die verband houden met de mal. De mal en het komposiet blijven immers samen tot de laatste produktiestap en ondergaan dus beide de uithardingscyclus en daarbijhorend temperatuursverloop. Bijgevolg hangen de uiteindelijke afmetingen van de gewikkelde komponent en de toleranties op deze dimensies in sterke mate samen met het maltype en de thermische uitzettingskarakteristieken van het malmateriaal. Er moet ook opgelet worden voor thermische spanningen in de mal waardoor vormafwijkingen kunnen ontstaan. Verder is ook de kwaliteit van het buitenoppervlak van de komponent in ogenschouw te nemen. Is deze belangrijk, dan moet ofwel een vakuümzak, ofwel een buitenmal worden aangewend.

Ontwerp en produktie interageren met elkaar in die zin dat de haalbare komplexiteit van het ontwerp afhangt van de beschikbare wikkeltechnologie en wikkeluitrusting. Enerzijds is er de wikkelmachine zelf die de dimensies van de komponent beperkt en anderzijds speelt ook de gebruikte wikkeltechnologie een rol omdat zij de mogelijke wikkelpaden en laagopbouw bepaalt.

Het type van wikkelmachine, haar afmetingen en vrijheidsgraden, samen met haar kontrolekapaciteit, beperken de mogelijke geometrieën en haalbare dimensies. Hoe meer vrijheidsgraden een wikkeleenheid bezit, hoe komplexer de te wikkelen geometrie mag zijn, maar hoe ingewikkelder ook de sturing wordt.

Komposieten bieden de mogelijkheid maatwerk af te leveren door de vezels zodanig te gaan richten dat de resulterende sterkte en stijf-

heid perfekt beantwoorden aan de spanningstoestand die optreedt onder invloed van de uitwendige belasting. Bij het wikkelen kunnen echter, al naargelang de toegepaste wikkeltechniek, vrij strenge grenzen worden opgelegd aan de mogelijke vezelrichtingen. Wanneer b.v. geodetisch gewikkeld wordt, zoals ook het geval was in dit onderzoek, dan moet de wet van *Clairaut* in acht worden genomen. Deze wet drukt uit dat het verloop van geodetische paden volledig vastligt, eens het startpunt van de vezels en hun startrichting gekozen zijn.
Bijgevolg zijn de haalbare vezelrichtingen dus eerder beperkt en wordt het moeilijk optimaal aan de vooropgestelde eisen van sterkte en stijfheid in bepaalde richtingen te voldoen.

Om toch zoveel mogelijk van de komposietvoordelen gebruik te kunnen maken, ondanks deze beperkingen, werd een ontwerpmethodologie ontwikkeld die toelaat een voorontwerp in verschillende stappen verder uit te werken tot een eindprodukt dat aan alle eisen voldoet. Deze ontwerpmethodologie, geschematiseerd in Fig. 0.2, sluit in feite een kompromis tussen enerzijds, het optimale antwoord op de eisen van sterkte en stijfheid, en anderzijds, de beperkingen opgelegd door het wikkelproces.

Op basis van de eindproduktvereisten denkt de ontwerper een geschikte geometrie uit die vervolgens naar komposietmateriaal toe moet vertaald worden. Om een uitgangspunt te vinden voor de laminaatopbouw wordt op de vormgegeven komponent eerst een isotrope spanningsanalyse doorgevoerd. De hieruit volgende spanningstoestand kan dan, aan de hand van eenvoudige laminaatprogramma's, in diskrete delen van de komponent reeds een eerste indikatie van de nodige vezeloriëntaties geven. Meestal kunnen deze ideale vezelhoeken echter niet zonder meer gewikkeld worden. Bijgevolg moet er gezocht worden naar opeenvolgende wikkelstappen die samen zo goed mogelijk de ideale laagopbouw in de verschillende delen van de struktuur benaderen. Eens deze opeenvolgende wikkelfasen en overeenkomstige wikkelpatronen gevonden zijn, kan de daarbijhorende laagopbouw ingevoerd worden in een eindige elementen model voor een gedetailleerde kontroleberekening. Eventueel kunnen dan nog wat wijzigingen in de wikkelpatronen en dus in de laagopbouw aangebracht worden zodat uiteindelijk een komponent wordt verkregen die veilig zijn funktie kan vervullen.

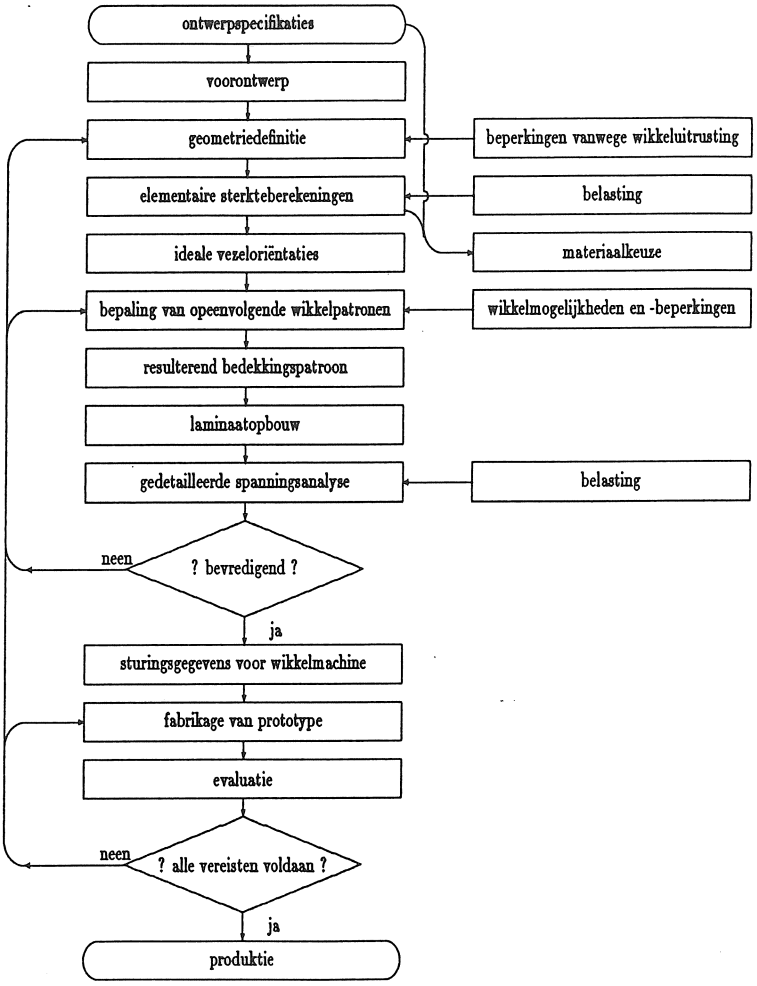

Figure 0.2: Ontwerpmethodologie voor gewikkelde komposietstrukturen.

Bij het wikkelen van axisymmetrische komponenten volstaan de data van één enkele geodetische lijn om een ganse wikkelstap te beschrijven; in geval van symmetrie kan immers een zelfde geodeet over de omtrek van de komponent herhaald worden tot het ganse oppervlak is bedekt. Deze geodetische data zijn eenvoudig te berekenen. De overeenkomstige laagopbouw varieert enkel met de lengtekoördinaat en kan meestal met de hand berekend worden. Bij niet-axisymmetrische stukken is echter een ganse set verschillende geodeten nodig om het op-

pervlak volledig te bedekken. Zoals in hoofdstuk 4 wordt beschreven, vraagt het berekenen hiervan heel wat meer rekenwerk en aangezien ook de laagopbouwdefinitie veel komplexer wordt, is het aangewezen de laagopbouwdata automatisch te laten genereren uitgaande van de beschrijving van het wikkelpatroon.

Ter illustratie van de voorgestelde ontwerpmethodologie werd zij toegepast op het ontwerp van spinpotten. Het betreft de substitutie van bestaande aluminium potten door een komposietversie met als hoofddoel een betere korrosieweerstand. Beide potten zij weergegeven in Fig. 0.3.

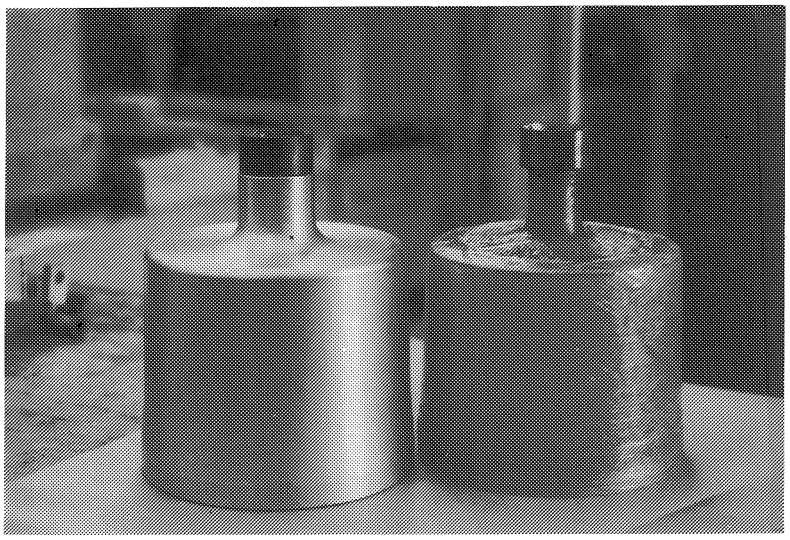

Figure 0.3: De originele aluminium spinpot en zijn korrosiebestendiger komposietequivalent.

Terwijl de potten aan hoog toerental ronddraaien in een zwavelzure atmosfeer, wordt een geleidelijk groeiende bobijn in de potten gesponnen. Om wille van aanwezige randapparatuur moest de vorm van de bestaande potten behouden blijven. Voorberekeningen op de isotrope potten hebben, samen met het onderzoek naar de mogelijke vezelhoeken, geleid tot een laagopbouw die vervolgens bijkomend werd gekontroleerd aan de hand van een eindige elementen analyse.

Om symmetrieredenen werd beslist twee potten samen te wikkelen en achteraf door te zagen. Ondanks het nadeel dat hiermee ook de

vezelversterking wordt doorgesneden, werd deze aanpak toch verkozen omdat de symmetrie hierdoor het wikkelproces sterk vereenvoudigde en toeliet te wikkelen op de NC-machine. Het vervaardigen van de potten was een proces in verschillende stappen. Om de sub-optimale laagopbouw die uit het ontwerp volgde te realiseren, werd het wikkelproces opgedeeld in drie stappen : globale wikkelingen, omtrekswikkelingen en daarop nog eens gordelwikkelingen. Na het uitharden en doorsnijden werden ringen op de potten gewikkeld die het deksel moesten dragen. Achteraf werd ook nog een valse bodem in de potten ingelamineerd. Tenslotte volgde nog een nabewerkingsproces om de potten van de vereiste buitenoppervlakkwaliteit te voorzien.

Een tweede ontwerpvoorbeeld betreft het vervaardigen van drukvaten voor de automobielindustrie. Hier was een werkelijk komposietontwerp mogelijk. De optimale eindkapvorm werd bepaald door gebruik te maken van de netting analyse en werd afgeleid door het numeriek oplossen van een tweede-orde differentiaalvergelijking. Deze optimale vorm biedt echter niet de mogelijkheid op optimale manier over te gaan in een cylinder. Bijgevolg moest het cylindrisch deel van het drukvat bijkomend door omtrekswikkelingen verstevigd worden, om over het ganse vat een zo uniform mogelijke barstdruk te realiseren.

Een belangrijke ontwerpparameter, bestudeerd in dit doktoraatswerk, is de *wikkelstrategie*, in feite een vrijheidsgraad die verband houdt met de verweving van de vezels. Met wikkelen kan men, al naargelang de toegepaste wikkeltechniek, een gelaagde struktuur verkrijgen, alsook een komposiet waarin de vezels in elkaar zijn verweven. De meeste wikkelexperten verkiezen een gelaagde wikkelwijze boven een verweven, vermits zij ervan uitgaan dat de vezelkruisingen bij het weefwikkelen aanleiding geven tot spanningskoncentraties. Nochtans hebben weefwikkelprocessen reeds interessante voordelen aan het licht gebracht; zij geven het wikkelproces veel meer flexibiliteit doordat zij geen bijzondere eisen stellen aan de geometrie. Om daarentegen een gelaagde struktuur te bekomen, moet de geometrie zodanig zijn dat na één cyclus, de volgende vezel net naast de vorige komt te liggen. Bovendien werd vastgesteld dat de verwevenheid van de vezels de sterkte van het komposiet in gunstige zin kon beïnvloeden. Om dit te bevestigen werd een onderzoek ingesteld naar de invloed van de wikkelstrategie, en dus de verweving, op het gedrag van gewikkelde buizen en drukvaten. Glasvezel/epoxy buizen werden gewikkeld met een wikkelhoek

van $\pm 25°$ volgens verschillende wikkelstrategieën. Na het wikkelen, uitharden en ontmallen, werden de buizen in individuele ringen gesneden. Deze ringen werden dan op sterkte en stijfheid getest via een twee-schijven testprocedure. Uit de testresultaten blijkt dat de wikkelstrategie slechts weinig invloed heeft op de stijfheid van de ringen. De sterkte van de verweven ringen daarentegen lag 30% hoger dan die van de gelaagde ringen.

De invloed van de wikkelstrategie werd ook nagegaan op drukvaten. Er werden zowel gelaagde als sterk verweven vaten gewikkeld. Beide bestonden uit een cylindrisch deel, afgesloten door twee optimaal gevormde eindkappen. Beide types werden onder druk gebracht met water en getest op lekken. Alvorens een statische barsttest uit te voeren werden de vaten eerst gedurende 33000 cycli vermoeid tussen 0.025 en 0.6 MPa aan een frekwentie van 1 Hz. Op de eindkappen gedroegen de verweven vaten zich het best, met een lekdruk van 1.8 MPa tegen 1.4 MPa voor de gelaagde vaten. Wat de cylinders betreft, konden de vaten met gelaagde laminaatopbouw veel hogere drukken weerstaan dan de verweven vaten. De verweven cylinders begonnen reeds te lekken bij 1.6 MPa terwijl de gelaagde cylinders met de beschikbare drukapparatuur niet tot lekken konden gebracht worden. Uit deze experimenten blijkt dat het ideale drukvat een eerder gematigde verwevingsgraad zou moeten hebben, zodat het lekken op de cylinder en op de eindkappen ongeveer bij een zelfde druk begint.

Hoofdstuk 4 : Ontwerp van niet-axisymmetrische gewikkelde komposieten

In hoofdstuk 3 is duidelijk gebleken dat bij het ontwerp van gewikkelde stukken, zelfs bij axisymmetrische komponenten, de beperkingen vanwege het wikkelproces dikwijls de ontwerpprocedure bemoeilijken. Wanneer men daarenboven ook niet-axisymmetrische vormen geodetisch wenst te wikkelen, ligt het voor de hand dat er nog bijkomende problemen zullen optreden, zowel op het niveau van het ontwerp als tijdens de kontrole.

Wat de ontwerpproblemen betreft, kan in eerste instantie gesteld worden dat het volledig bedekken van een niet-axisymmetrisch maloppervlak, moeilijkheden inhoudt die niet voorkomen wanneer de komponent een symmetrieas bezit. Initieel naast elkaar startende geodeten

kunnen immers vrij snel divergeren en zo op hun weg andere oppervlakken tegenkomen. Bijgevolg vragen niet-axisymmetrische oppervlakken een hele serie individuele wikkelpaden die samen het ganse maloppervlak bestrijken. Vermits al deze geodeten uniek zijn, bestaat een belangrijk onderdeel van het ontwerp hieruit, een geschikte selektie te maken van startposities en bijhorende geodetische paden, samen resulterend in een laminaatopbouw die aan de komposietstruktuur de gewenste sterkte en stijfheid kan garanderen.

Naast het zoeken naar geschikte geodeten is nu ook de berekening ervan veel komplexer. Deze kan onder meer gebeuren door het numeriek oplossen van de differentiaalvergelijkingen die het verloop van de geodeet beschrijven.

Naast een meer komplexe ontwerpprocedure komen er ook komplikaties voor op het niveau van de kontrole. Er zijn niet alleen veel meer data te verwerken om wille van het groot aantal verschillende geodeten maar meestal moeten ook meer vrijheidsgraden gestuurd worden. Verder kunnen er problemen optreden wanneer de mal lokale konkaviteiten vertoont, wat botsingsgevaar tussen de mal en het wikkeloog inhoudt en ook vezelbruggen, los van het maloppervlak, kan veroorzaken.

Vroeger werden niet-axisymmetrische komponenten meestal gewikkeld via een *leermode*. Hierbij werden de kontroledata experimenteel bepaald doordat de operator het wikkeloog *leerde* welke weg het moest beschrijven om de gewenste wikkelingen te realiseren. Deze methode was tijdrovend, niet erg produktief en leverde geen hoge nauwkeurigheid. Het is dan ook veel interessanter de sturingsgegevens op voorhand te berekenen en pas daarna door te sturen naar de wikkeleenheid. Dit *off-line* programmeren laat een hogere nauwkeurigheid toe en maakt ook een simulatie mogelijk om na te gaan of er geen botsingen zullen optreden.

Aangezien het ontwerp en het wikkelen van niet-axisymmetrische stukken vrij komplex blijken te zijn, werd besloten de ontwerpmethodologie voor axisymmetrische stukken uit te breiden tot ontwerp- en kontrolestrategieën voor niet-axisymmetrische gewikkelde stukken.

Van een serie mogelijke geodetische paden moet een geschikte selektie worden gemaakt. De oppervlaktebedekking die zij samen uitmaken stemt overeen met een welbepaalde laagopbouw die aan de hand van een struktuuranalyse moet geëvalueerd worden. Al naargelang de re-

sulterende spanningstoestand in de belaste struktuur, moeten extra geodeten of lagen voorzien worden om de zwakkere, overbelaste of onvoldoende bedekte zones bijkomend te versterken. Eens het resulterende komposiet kan beantwoorden aan de vooropgestelde sterkte- en stijfheidsvereisten, kunnen kontrolekommando's worden opgesteld om de vooropgestelde wikkelpatronen daadwerkelijk te gaan realiseren.

Een belangrijke stap in deze strategie is de overgang tussen een gegeven set wikkelpaden en de daarbijhorende laminaatopbouw. Gezien de komplexiteit en de grote hoeveelheid gegevens werd een programma ontwikkeld dat automatisch de laagopbouw genereert uitgaande van de beschrijving van het gewenste wikkelpatroon. Tot de belangrijkste invoerdata van dit programma behoren enerzijds, de punten die de ganse set geodeten beschrijven en anderzijds, gegevens betreffende de eindige elementen verdeling van de beoogde komponent. De resulterende laagopbouw is rechtstreeks gerefereerd naar het eindige elementen model en zijn individuele elementen en kan dus rechtstreeks voor de eindige elementen kontroleanalyse aangewend worden.

De voorgestelde strategie wordt integraal toegelicht aan de hand van een te wikkelen T-aansluitstuk. Fig. 0.4 geeft schematisch dit T-stuk weer, bedekt met enkele geodetisch gewikkelde vezelbanden.

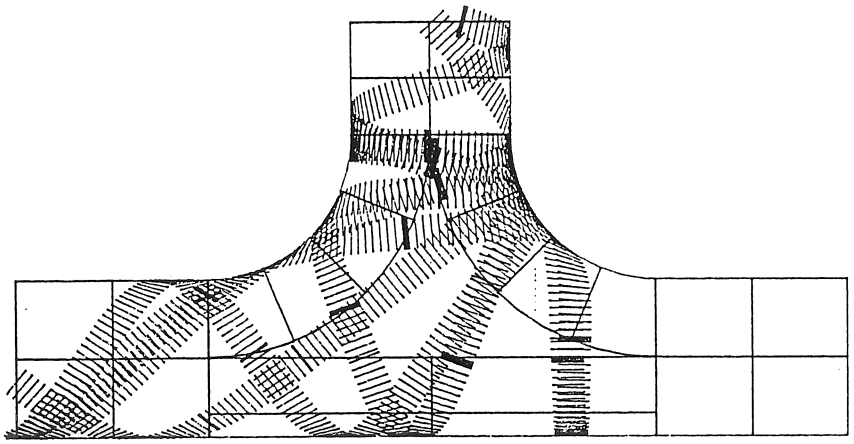

Figure 0.4: Het T-stuk met enkele geodetische wikkelingen.

Nadat de geometrie werd vastgelegd, werd een eindige elementen analyse uitgevoerd op een isotroop T-stuk. Het zou in pricipe mogelijk zijn de resulterende isotrope spanningstoestand te vertalen naar ideale vezelrichtingen over heel de struktuur. Maar, het vinden van een set geodeten die samen de mal volledig bedekken was op zich al een probleem, zodat het praktisch gezien onmogelijk was om overal rekening te gaan houden met de ideale vezelrichting. Daarom werd het ontwerpprobleem opgevat als een kontroleprobleem. Van een geschikte selektie van geodeten werd de equivalente laminaatopbouw berekend en ingevoerd in een eindige elementen kontroleanalyse. Lokaal overbelaste zones moesten dan versterkt worden door goed gerichte bijkomende vezels te voorzien. Want, de uiteindelijke set te wikkelen patronen moest het komposiet T-stuk de vereiste draagkracht geven.

BESLUIT

Komposietmaterialen bieden enorme ontwerpfaciliteiten. Het wikkelproces legt echter strenge beperkingen op aan deze ontwerpvrijheid. Om desondanks de intrinsieke voordelen van komposieten toch zo efficiënt mogelijk te benutten, werd een ontwerpmethodologie voorgesteld voor axisymmetrische gewikkelde komponenten. Na het toepassen op twee praktijksvoorbeelden werd deze methodologie uitgebreid naar ontwerp- en kontrolestrategieën voor niet-axisymmetrische stukken. Een onderzoek naar de invloed van de wikkelstrategie heeft belangrijke voordelen van de verweving van de vezels bij het wikkelen aan het licht gebracht.

List of symbols

On-axis, fibre direction related quantities

σ_x, σ_{ll} : longitudinal normal stress (in fibre direction) [MPa]
σ_y, σ_{tt} : transverse normal stress (perpendicular to fibre direction) [MPa]
σ_s, τ_{lt} : shear stress due to in-plane shear [MPa]
τ_{lz} : shear stress due to shear in a plane perpendicular to the composite element, but parallel to the fibre direction [MPa]
τ_{tz} : shear stress due to shear in a plane perpendicular to the composite element, and perpendicular to the fibre direction [MPa]

σ_f : fibre strand stress [MPa]

ϵ_x : longitudinal normal strain
ϵ_y : transverse normal strain
ϵ_s : in-plane shear strain

E_x, E_l : longitudinal stiffness modulus [MPa]
E_y, E_t : transverse stiffness modulus [MPa]
E_s, G_{lt}: in-plane shear modulus [MPa]
ν_x, ν_{lt} : longitudinal, in-plane Poisson ratio
ν_y, ν_{tl} : transverse, in-plane Poisson ratio

X_t : longitudinal tensile strength [MPa]
X_c : longitudinal compressive strength [MPa]
Y_t : transverse tensile strength [MPa]
Y_c : transverse compressive strength [MPa]
S : in-plane shear resistance [MPa]

Off-axis quantities

σ_1 : normal stress in the laminate's 1-direction [MPa]
σ_2 : normal stress in the laminate's 2-direction [MPa]
σ_6 : shear stress in the $1-2$ plane [MPa]

ϵ_1 : normal strain in the laminate's 1-direction
ϵ_2 : normal strain in the laminate's 2-direction
ϵ_6 : shear strain due to $1-2$ plane shear

N_1 : normal force pro unit length in the laminate's 1-direction [MN/m]
N_2 : normal force pro unit length in the laminate's 2-direction [MN/m]
N_6 : shear force pro unit length in the $1-2$ plane [MN/m]

M_1 : bending moment pro unit length in the laminate's 1-direction [MN]
M_2 : bending moment pro unit length in the laminate's 2-direction [MN]
M_6 : torsional moment pro unit length [MN]

E_{te} : tensile modulus of a particular laminate, in a particular direction [MPa], [GPa]
σ_{te} : tensile strength of a particular laminate, in a particular direction [MPa]
σ_c : compressive strength of a particular laminate, in a particular direction [MPa]
G : shear modulus of a particular laminate [GPa]
τ : shear strength of a particular laminate [MPa]
V_f : fibre volume fraction [%]

Filament winding related quantities

Component related symbols

t : filament wound component thickness
t_1 : longitudinal layer thickness
t_2 : hoop layer thickness
N : number of windings along the component's circumference
A : cross-section of the impregnated fibre strand

List of symbols

α : fibre angle with respect to the meridian curve of an axisymmetric component
R, Y : mandrel radius at a particular cross-section of an axisymmetric component
Y_0 : radius at the nozzle of an axisymmetric component

Numerical control related symbols

R_a : winding arm radius
Z_a : distance between the winding eye's plane of movement and the spindle
Y_a : vertical distance between the winding eye's position at a particular moment and the spindle
(X_i, R_i) : coordinates describing the mandrel's geometry :
X_i : length coordinate, parallel to the axis of rotation
R_i : radius at a particular cross-section
ψ_i : sector described by the geodesic path between the starting point and point i
γ_i : additional angle over which the spindle must be turned to make the tangent to the geodesic line in point i intersect the circular path of the winding eye
θ_i : angular arm position, corresponding to the winding of point i
is_spindle : measured spindle position
is_arm : measured arm position
will_spindle : predicted next spindle position
will_arm : desired next arm position
ref_spindle : reference spindle position, for which corresponding arm positions are tabulated in the WINDING TABLE

Contents

Introduction

Fibre composites represent a class of new materials providing high strength and stiffness together with low weight and excellent chemical resistance. Consequently, they are nowadays preferred as construction materials in many areas of the aerospace, automotive, machine tooling and chemical industries.

Thanks to their anisotropic character, fibre reinforced plastics have opened up new dimensions of design freedom, that have never been available with isotropic materials; by judiciously building up a composite laminate out of plies with properly selected fibre/resin combinations, appropriately oriented and stacked according to a proper sequence, composite components can be tailored as to optimally answer the performance requirements. This tailoring potential is obviously accompanied by a more complex design process and requires adequate, composite-specific analysis and design tools.

Due to the highly directional nature of continuous fibre reinforcement, a major concern in composite design and manufacturing is to precisely place the fibres along carefully chosen directions, to align them with the orientations of the applied loads.

In filament winding, continuous fibre, impregnated with resin, is applied under controlled tension to a usually rotating mandrel, along a predescribed geometrical pattern. Hence, filament winding is a production method allowing to fabricate composites with well-aligned fibres.

Filament winding once used to be a stand-alone process that was labour-intensive, time-consuming and only capable of producing simple geometries. However, the integration of CAD/CAM and numerically controlled and robotic systems, together with the adaptation to handle new fibres and resin materials, have made filament winding evolve towards an economical and advanced composite fabrication technique with versatile application facilities.

It is obvious that the allowed complexity and realizability of a design depend upon the available manufacturing equipment; there is the winding machine itself, limiting the dimensions of the component, but there is also the applied winding technology, which determines the feasible winding patterns and laminate lay-up.

The type of winding unit used, its size and degrees of freedom,

together with its control capacities, restrict the attainable geometries and the dimensions that can be wound. For example, two-axis winding machines are confined to simple axisymmetric structures, whereas robotic winding cells with up to seven degrees of freedom can handle more complex non-axisymmetric shapes. Along with symmetry aspects, also concavity must be considered. In fact, concave parts have been unwindable for a long time. However, thanks to new technologies, as e.g. the use of thermoplastic prepregs, winding concave shapes has become possible.

Composites offer the great potential of being tailored to perfectly suit their application, as they allow the fibres to be aligned with the principal load directions. In filament winding however, the freedom of choosing the fibre angles can be quite restrictive, depending on the applied winding technique. When for example geodesic winding is performed, the law of *Clairaut* must be regarded, which, for a surface of revolution, can be expressed as :

$$r \cdot \sin \alpha = constant$$

indicating that the product of the radius r, at a specific point on the mandrel, and the corresponding fibre angle α, with respect to the meridian curve through that point, equals a constant value. This means that once a starting position and starting angle of the fibre path have been chosen, the whole trajectory is uniquely defined and only depends on the mandrel's geometry. This restricted freedom in fibre orientations and laminate lay-up clearly indicates that, when performing geodesic winding, the scope for obtaining a winding pattern, which is optimal with respect to the applied mechanical loads, is rather limited. On the contrary, semi-geodesic winding, in which friction effects are used to deviate from the geodesic lines, allows much more flexibility, thereby enabling a better alignment of the reinforcement with the principal load directions. In the course of this thesis however, only wet filament winding is performed, in which the fibre is impregnated with resin just before being wound onto the mandrel. Since wet winding does not provide much friction, the fibre paths are to be limited to geodesic patterns.

In order to take optimal benefit of the great potential offered by fibre reinforcement anyhow, in spite of the only limited fibre orientation possibilities, a design methodology will be presented for geodesically wound composites. The main concern of this design strategy is

finding an optimal compromise between, on the one hand, the almost unlimited tailoring facilities of composites, and, on the other hand, the restrictions imposed by the winding process. The design finally leads to a semi-optimal geometry and winding pattern.

In illustration, the proposed design methodology will be discussed in detail, by referring to some practical axisymmetric applications. A first example regards composite spinning pots, which "unfortunately" are just a substitution of their aluminum equivalents. The second example concerns pressure vessel design, allowing an optimal definition of the dome shape. Both components are wound on a numerically controlled winding machine, using a combination of an epoxy matrix, reinforced by E-glass fibres.

But even if the design of a filament wound component has evolved in so far that the laminate lay-up has been defined, there remains a final degree of freedom, being the winding strategy. Winding strategy refers to the time sequence of the fibre lay-down and is related to the interweaving of the fibres. With filament winding, depending on the winding strategy, layered structures as well as components with interwoven fibres can be obtained. Most filament winding experts prefer a layered way of winding. However, an investigation of the influence of the winding strategy, including the interweaving of the fibres, on the performance of filament wound tubes and pressure vessels will show that interweaving winding methods can have positive influences on the composite's performance.

It has already been mentioned that in filament winding design, even in case of only axisymmetric components, the restrictions imposed by the winding process very much complicate the design procedure. If, moreover, non-axisymmetrical shapes are concerned, which have to be wound geodesically, the design's complexity will be even more pronounced. Furthermore, also the control of the winding process will include more difficulties. Therefore, as an extension of the axisymmetric design methodology, design and control strategies will be presented for non-axisymmetric filament wound composites. From a series of feasible geodesic patterns, a proper selection has to be made. Their coverage will correspond to a specific laminate lay-up which must be checked through analyzing the structure and if necessary, some additional patterns or layers must be provided to strengthen the overloaded or undercovered areas. Once the resulting composite can answer to the

strength and stiffness requirements, control commands can be set up to materialize the proposed winding patterns.

An important step in this strategy is the transition between a given set of winding paths and the corresponding laminate lay-up, required to be introduced in the finite element model. To realize this link, software is developed to automatically generate the lay-up data out of the winding pattern description.

In illustration, the proposed design method will be applied to a filament wound T-connection. After the geometry is defined, a finite element analysis is performed on an isotropic T-part. Theoretically, it would be possible to translate the resulting isotropic stress state into ideal fibre orientations all over the structure. However, finding a set of geodesic paths, which together completely cover the mandrel, is already such a problem, that in practice it is impossible to take into account the ideal fibre direction everywhere on the T-part. Therefore, the design is conceived as a problem of verification. From a proper selection of geodesic patterns, the equivalent laminate lay-up is computed, which is then used as input to a finite element control analysis. Locally overloaded areas are then to be reinforced by supplying additional, well-oriented fibres. For, the final set of patterns to be wound must provide the composite T-part with the required load-bearing capacities.

Chapter 1

Composite design and analysis

1.1 Introduction

This chapter will treat the design of composites in general, but will concentrate on fibre reinforced composites in particular.

Thanks to their anisotropy, composite structures have opened up new dimensions of design freedom, that have never been available with isotropic materials; since stiffness and strength can be varied freely within one single component, composites can be locally softened or strengthened as to optimally answer to the performance requirements. The fact that composites show interesting mechanical properties, combined with only small densities, makes them particularly attractive for low-weight applications. Thanks to their outstanding corrosion resistance potential, composites can also be of great value to chemical industries. Further, they allow for large one-piece structures to be designed and manufactured, with a reduced number of fasteners and parts.

Fibre reinforced materials are mostly used as plates or shells, called laminates. They owe their tailoring potential to the highly directional nature of their fibre reinforcement. By judiciously building up the composite laminate out of plies with properly selected fibre/resin combinations, appropriately oriented and stacked according to a proper sequence, composite components can be tailored to optimally suit their application.

Consequently, composites allow for the material to be designed along with the structure. This potential of designing the material as well as the structure, of course offers the designer more flexibility, but it obviously also complicates the design process.

Successively, attention will be given to functional design requirements, often expressed in terms of stiffness, strength or lifetime, and to the the problem of safety factors to be applied in the design process. Further, manufacturing and maintenance related design aspects will be considered. And finally, a composite design cycle will be discussed, together with the tools at the designer's disposal.

1.2 Composite notions

1.2.1 Composites in general

The term "*composites*" refers to a material, made by dispersing particles of one or more materials in another material, which forms a substantially continuous network around them. Their basic purpose is to combine interesting properties of different individual materials into one single composite material (additive effect), which will thereby present surprising new characteristics (synergetic effect).

Composites stand for a whole range of products, consequently they can be classed in several ways :

- A classification can be based on the form of the structural constituents, distinguishing between e.g. fibre composites or flake or particulate composites.
- The components can be randomly arranged or organized in some sort of pattern. Their distribution can be continuous or discontinuous, e.g. continuous fibre reinforcement or chopped fibres, embedded in a resin matrix. Generally, the arrangement will have a large effect on the properties.
- Several basic material combinations are possible :
  e.g. metal/organic, metal/ceramic, etc ....

1.2.2 Fibre-matrix composites

Of all composite materials, the fibre type has evoked the most interest among engineers concerned with structural applications.

Fibre reinforced materials can look back upon a whole history, as they have been used by men for a very long time.

The first fibre composites to be used were naturally occurring composites, such as wood. But long ago, men also found out that there were advantages to be gained from using artificial mixtures with a fibrous component, such as straw in clay for bricks or horse hair in plaster for ceilings.

Nowadays, a whole series of matrix and fibre reinforcement types has become available. Beside glass, carbon and aramid fibres, also boron, silicon carbide or aluminum oxide, as well as nylon or polyester are made use of. Their cross-section can vary from solid and circular to hollow and even non-circular. The matrices can be metals, ceramics or polymers. The widely used thermosets are currently facing the competition of their thermoplastic rivals.

1.2.3 Role of fibre and matrix

In a continuous fibre reinforced composite, the fibres provide virtually all of the load carrying capacity. Their orientation, length, shape and composition to a large extent contribute to the composite's engineering performance.

The matrix is the weak link in the composite, yet, it nevertheless provides essential functions. The matrix must bundle the fibres together and keep them in the proper position and orientation. The matrix must also distribute the loads to and between the fibres. Moreover, the matrix serves as to protect the fibres from their environment and from handling effects. It also supplies the composite with resistance to crack propagation and damage and provides all of the interlaminar shear strength. Furthermore, the matrix generally determines the overall service temperature of the composite and usually controls its environmental resistance.

Fibre composites are able to withstand higher stresses than either of their individual constituents, thanks to the fibres and the matrix interacting and redistributing the stresses. Their capability of exchanging stresses critically depends on the effectiveness of the coupling or bonding between them. The fibre-matrix bond is often in a state of shear when the composite is loaded. When this bond is broken, the fibre separates from the matrix and leaves discontinuities that may cause failure. Coupling agents and special types of fibre finishes can

be used to strengthen these bonds against shear forces.

1.3 Fibre composite design potential

In most practical composite structures, the fibre reinforced material is usually applied as thin plates or shells, called laminates. For, the superior composite properties permit the use of thin-walled structures. Laminates are obtained by stacking various thin layers or laminae on top of each other. Each lamina consists of long, parallel fibres, embedded in a resin matrix and oriented at a particular angle. Over and above the excellent strength and stiffness properties that composites possess, the ability to stack the laminae one on the other, in a varied but unique fashion, allows for an optimal design with respect to a given structural size and set of loads. The parameters at the designer's disposal are, the selection of the fibre/matrix combination, which can be different for the different plies (hybrids), the orientation of the laminae, their stacking sequence, and the number of plies in each direction. To make a justified choice, the designer must have at his disposal adequate methods to determine the stiffness and strength properties of the laminate, and further, of the entire structure. The designer also needs information about the evolution of these properties with time, which is the problem of durability. Although composites allow for the amount of joints to be reduced, joints remain quite important in composite design and manufacture and therefore call for the designer's attention.

1.4 Design cycle

Approaching any structural design problem implies three tasks : select a material, define an appropriate configuration and find a process to manufacture. This approach is essentially the same for all materials, conventionals as well as composites. However, unlike e.g. metals, which can be designed according to a linear process, composites need a more integrated design procedure as they require the material to be designed along with the structure.

In many structural designs, either stress level or deformation is the material-limiting factor. With conventional materials, a material is chosen, the modulus is set, and deformations and stress levels are con-

trolled by cross-sectional design. For composites however, the scenario is usually one of iterative optimization; changing the angles of certain layers implies changes in structural stiffness which in turn affect the load pattern, requiring again a change in fibre orientation ...

The ability of composites to design the material as well as the structure obviously complicates the design process, but at the same time, offers the designer a great design freedom.

For composites, an integrated design method usually consists of following steps :

- In a first phase, a set of functionality requirements, such as cost, size, weight and performance must be specified. By performance can be understood mechanical, electrical, as well as thermal or chemical behaviour, each of which being related to the loading and environmental conditions.

- In a next step, a preliminary design is developed; the material is chosen, a rudimental lay-up is defined, a configuration is selected and a process for manufacturing is chosen. All of these design elements must be individually evaluated and their compatibility must be verified. For they can very much interfere with one another : for example, with filament winding, not every fibre/resin combination can be applied and feasible fibre orientations can be significantly limited. Eventually, if necessary, a compromise must be considered.

  Thanks to their highly directional nature, fibre composites offer the possibility to tailor the design and provide stiffness and strength in the direction and at the place where they are needed. Hence, the lay-up definition is one of the major design aspects. The designer has to assemble basic unidirectional plies into a global, multidirectional lay-up, enabling the structure to suit the application. However, there exist no closed governing equations to derive the overall optimal laminate lay-up. Moreover, as already mentioned, feasible angles can be quite restricted. Hence, the ply assembly and lay-up generation will have to be incorporated in an iterative design process. The tools the designer disposes of for this iterative design cycle will be discussed in the last section of this chapter. The further the design is developed, the more sophisticated these tools will be. In the preliminary

design phase however, usually simple laminate programs are applied.

- At an intermediate design stage, more sophisticated analysis of competing design concepts must be performed. If required, simple models of critical components can be fabricated and tested.

- In a further step, the selected design concept is verified as a last check by more detailed finite element analysis, paying special attention to critical areas as e.g. discontinuities, holes, joints and stiffeners.

- And finally, a full-scale prototype is fabricated and evaluated for cost, performance capabilities and effects from environmental factors. If all specifications are satisfied, production can start.

In the past (and even today), direct substitution by composites rather than new part design has usually been the design engineer's approach, his major concern being to lower the weight and the cost of existing components. Consequently, the composite was forced to be compatible with the existing neighbouring hardware. These too many constraints often kept favouring metals as no optimal advantage could be taken from the composite's higher specific strength and stiffness. However, there exists a great potential for original design in composites, when directing the constraints towards the inherent composite nature. But an original composite design must start at a preliminary design stage, before metal's thinking fixes the configuration. Yet, before leaving classical design approaches and turning over to original composite design, composites will still have first to further prove themselves.

1.5 Design for functionality

The task of a designer is to tailor a composite part as to optimally answer to a specified set of functional requirements.

Functionality is a measure of performance capabilities versus e.g. cost, weight, size, time .... A composite design should not only be evaluated, based on stiffness and strength. Obviously also cost aspects should be regarded, since the price for which a specified performance can be obtained is an important design parameter. Furthermore, also

manufacturing and maintenance related aspects should be considered in the design stage.

In this section, first the principal design criteria will be reviewed, being the criteria against which the design is undoubtedly checked. All these criteria can be translated into the need to protect the part from some sort of failure, when subjected to the loads it has to be designed for. These can vary from mechanical loads, including static, cyclic or impact loads, to thermal and other environmental loads. Failure can be interpreted in various ways; a stiffness-critical structure is said to fail in case of excessive deflection or deformation. A component which is strength-critical, tends to fail from the moment the occurring stress state becomes too severe, leading to overloading and ensuing damage. Further, a structure can become damaged through a dynamic response to time dependent loads, again resulting in too large deflections or too high stresses. Dynamic loading can vary from a reoccurring cyclic loading of the same repeated magnitude, to a short time, intense and non-reoccurring load, termed shock or impact. Between these two extremes of harmonic oscillation and impact, there exists a continuous infinity of dynamic loads. Finally, a structure can fail or become useless through the occurrence of an elastic instability, termed buckling. Design considerations with respect to these different failure alternatives will be discussed in the following paragraphs.

1.5.1 Design for static strength

When subjected to a sufficiently large static loading combination, structural components run the risk of failing. A part can fail to maintain a desired stiffness, or it can fail to support the loads it was designed for.

To obtain an appropriate, failure-safe composite design, the designer must be able to predict the strength and stiffness (and their loss) of his designed component. There are two successive steps in this prediction : the analysis of stresses and strains, followed by determining their effect on the component's stiffness and strength.

1.5.1.1 Stress analysis

The first step, being an analysis of stresses and strains in the loaded structure, is fairly straightforward, at least in the linear range of struc-

tural behaviour. There exist several basic models to analyze simple structures as plates, shells or beams etc .... For more complicated components, finite element codes enable stress analyses to be performed.

Stress analyses can be conducted on three levels :

- on *microscale*, where fibres and matrix are treated as separate elastic phases.
- on *miniscale*, considering each individual lamina as a separate, homogeneous, orthotropic elastic body.
- on *macroscale*, where the entire composite laminate is manipulated as a homogeneous, anisotropic elastic body.

Only the two latter scales apply to design purposes. On both levels, there exist models for determining the equivalent homogeneous elastic properties (Ref. [78]); more or less sophisticated mixture rules for predicting laminae characteristics out of individual properties of fibre and matrix, and e.g, *classical laminate plate theory*, to combine the properties of the individual laminae into laminate characteristics. The resulting elastic properties can be used as input to the analytical or numerical stress analysis models. These permit to determine the stresses in the composite structure, due to the design load or combination of loading conditions. These same models can be reversed, thereby enabling the stresses in the individual fibres or matrix (microscale), or in the individual laminae (miniscale) to be obtained from the macro stress analysis.

1.5.1.2 Strength prediction

The second step, once stresses and strains have been computed, is to determine their effect on the component's stiffness or strength. Predicting the structural strength of a composite component is rather difficult for two major reasons :

- Unlike stiffness, which depends on "averaged" properties, the *initiation* of failure is highly affected by flaws, randomly and impredictably distributed throughout the structure. These flaws are too numerous to be readily characterized or modelled, yet are responsible for the onset of failure.

- The strength of composite structures is not only affected by the initiation of failure at flaws, but to a large extent by the *progression*, *growth* and *accumulation* of such microfailures (Ref. [69]). These microfailures result in stiffness changes and stress redistributions that ultimately lead to the inability of the structure to carry on its design load.

Due to the inhomogeneous nature, inherent in composites, the progressive growth of microfailures can proceed along an enormous number of different paths, both within and between the individual laminae. Consequently, this progressive failure process is very difficult to model. So, on a practical level, the designer has to content himself with a strength prediction, based on linear elastic stress analysis, combined with a rudimental failure criterion.

Rudimental strength prediction, based on elastic analysis

Strengths can be considered on different levels; *lamina* strength e.g. obviously depends on how the lamina is loaded. When loaded in its fibre direction, a lamina is very strong because the failure mode involves fibre breakage or buckling. However, when loaded normal to the fibre direction or in shear, a different failure mode, typically only involving matrix failure, occurs and the strength is more than an order of magnitude lower. When considering *laminate strengths*, it must be noticed that structural laminates are mostly multidirectionally reinforced, being built out of a number of laminae, stacked together, whith their fibres oriented in a number of different directions. When predicting strength, based on stress analysis, the first step is to resolve the structural stresses into the stresses in each lamina, using e.g. simple laminate plate theory. With the stresses in each lamina known, strength prediction can be performed according to several more or less sophisticated principles.

The simplest one is called *first ply failure* (Ref. [78]). Stresses in each ply are combined according to a rudimental failure criterion. If the substitution of the stresses, acting on one of the plies, into the particular failure criterion results in a value exceeding 1, the considered ply is said to fail. Further in this thesis, composite structural strength will be predicted using the *Tsai-Wu* criterion :

$$\frac{\sigma_x^2}{X_t X_c} + \frac{\sigma_y^2}{Y_t Y_c} + (\frac{1}{X_t} - \frac{1}{X_c})\sigma_x + (\frac{1}{Y_t} - \frac{1}{Y_c})\sigma_y + 2F_{xy}\sigma_x\sigma_y + \frac{\sigma_s^2}{S^2} \quad (1.1)$$

where : σ_x : longitudinal normal stress (in fibre direction)
σ_y : transverse normal stress (perpendicular to the fibres)
σ_s : shear stress due to in-plane shear

and

X_t : longitudinal tensile strength (in fibre direction)
X_c : longitudinal compressive strength
Y_t : transverse tensile strength (perpendicular to the fibres)
Y_c : transverse compressive strength
S : in-plane shear resistance

The value F_{xy} from the coupling term between the longitudinal and transverse normal stresses is defined as :

$$F_{xy} = F^*_{xy}\sqrt{\frac{1}{X_t X_c Y_t Y_c}}$$

where $-1 < F^*_{xy} < 1$.

Usually F^*_{xy} is taken to be -0.5, so the criterion links on to the *Von Mises* criterion for isotropic materials.

The strength of the structure is now taken to be the lowest load level at which any of the laminae satisfies the selected failure criterion. The problem with this prediction method is that the predicted failure is almost always a matrix failure in only one of the laminae. This implies that though some matrix damage will occur in that particular ply, the laminate or the entire structure is nowhere near ultimate failure or does not yet show any significant stiffness reduction. Thus, for most design purposes, the *first ply failure* is far too conservative for practical use.

Ultimate fibre failure is a second simple method to predict laminate strength. In this approach, the longitudinal stresses or strains in the fibres of each ply are determined from the stress analysis and compared to the ultimate allowables. Strength is predicted to be the load at which the fibre stresses in any lamina first equal the allowable value. The major difficulty here is that this criterion can be too optimistic in its prediction, overpredicting strength by a considerable margin, due

to the progressive nature of composite failure, which is not taken into account.

This progressive microdamage growth leads to redistributions in lamina load shearing and results in stress concentrations, that are not incorporated in the typical stress analysis, conducted to predict structural strength. Hence, predictions based on elastic analysis must be handled with care.

Progressive failure models

To allow for composite structural strength to be properly predicted, microdamage growth and accumulation should be taken into account. At the present, such progressive failure models are at the laboratory stage, rather than being in general use. Current finite element codes do not exhibit progressive failure capabilities. For, progressive failure in composites, although fairly well understood qualitatively, has not yet been quantitatively modelled. However, there exist quantitative models of microdamage modes but they typically concern only one particular type of damage, such as fibre failure, matrix cracking or delamination growth. A not yet established, but very important step is to model the interaction between these individual modes.

Although progressive failure models are still being developed, certain rudimental concepts of progressive failure are used to predict composite strength.

First, there is the idea of reducing the laminae stiffnesses in the stress analysis, to account for matrix failure. This reduction can be performed radically, by setting the stiffness of a failured lamina to zero after first ply matrix failure has been predicted. More recently, elastic models have been developed, which give the effective lamina stiffness of a matrix cracked lamina, as a function of the crack spacing (Ref. [54]). This method allows for the stiffness of damaged plies to be appropriately lowered as the structural load increases, resulting in more load to be carried by other, not-yet damaged plies. Consequently, this approach provides more realistic strength predictions than the rudimental *first ply failure* based prediction methods.

A more sophisticated approach is to include the effect of delamination on composite failure. Modelling delamination growth can be accomplished, using the principles of fracture mechanics (Ref. [65]). It allows for the effects of delamination on stress distribution to be

determined and strength to be properly estimated. The problem encountered is however that the analysis is mostly three-dimensional and hence very complex.

1.5.2 Design for fatigue

Material damage or local failure can accumulate in time under sustained loading. This can happen under creep conditions in which the load magnitude is held constant, or under fatigue conditions, in which a cyclic loading, with magnitude varying in time, is applied.

Due to their anisotropy, composite materials exhibit very complex failure mechanisms under fatigue loading conditions (Ref. [32] and Ref. [70]). Fatigue failure is usually accompanied by extensive damage, multiplying throughout the composite component, unlike the localized formation of a single, predominant crack, as is common in isotropic, brittle materials. The four basic failure mechanisms in composites are : matrix cracking, delamination, fibre breakage and fibre-matrix interfacial debonding. Any combination of these can cause fatigue damage, resulting in reduced strength and stiffness. Both, the type and intensity of the damage vary widely, depending on fibre and resin characteristics, laminate stacking sequence and type of fatigue loading. It has been observed (Ref. [32]) that in general, damage development under fatigue loading is similar to that under static loading, except that fatigue at a specified stress level causes additional damage as fatigue cycles increase.

The two major design concerns in fatigue are, first, to predict the useful lifetime of the component in specified loading conditions, and, second, to predict the safe load limit that can be applied to the component, after a certain lifetime. The latter issue concerns residual strength. Unlike for metals, using crack length, residual strength is chosen to describe the severity of the damage, because composite failure is characterized by a multitude of matrix cracks and fibre breaks, rather than a single dominant crack growth (Ref. [6]).

1.5.2.1 Traditional fatigue failure approaches

To treat fatigue failure in composites, general approaches, traditionally applied to metals, have been adopted. These approaches follow essentially the same failure concepts as in case of static failure.

According to the *point stress failure* approach (Ref. [84]), failure can be described by the stress state at one particular point, without regarding the actual failure modes. Let $\sigma_i (i = 1, \ldots 6)$ be the stress state at the considered point, with the stresses σ_i oscillating between σ_{imax} and σ_{imin}. As already mentioned above, the problem of fatigue failure can be approached from two different views, fatigue life and residual strength.

- *fatigue life :* this approach concerns failure at a particular point or in one individual ply, where the fluctuating stress state, determined e.g. using laminate plate theory, satisfies a certain mathematical criterion. Such a criterion can be expressed as :

$$F(\sigma_{imax}, R, N) = 1 \tag{1.2}$$

  where R is the stress amplitude ratio and N is the number of cycles, required to cause failure. This equation is usually determined empirically, by fitting a large series of experimental data. A fatigue failure model based on (Eq. 1.2) can be used to predict the fatigue life N, given the dynamic loading condition of the structure. However, in practice this model does only apply to fatigue involving uniform, uniaxial stress states. For, in case of multidirectional loading or stress conditions, involving sharp gradients as e.g. at stress concentrations, the application and evaluation of (Eq. 1.2) become quite cumbersome and impractical.

- *residual strength :* the alternative view is to consider the strength of the composite component, after it has been subjected to a prescribed number of fatigue cycles. In this context, the material is presumed to be damaged, but has not yet totally failed. Hence, the remaining material strength is enough to resist the applied load. In this case, the residual strength can be empirically expressed as :

$$\sigma_{k,r} = f_k(\sigma_{imax}, R, n) \; ; \; n < N \tag{1.3}$$

  where n is the number of sustained cycles, N the lifetime when maintaining σ_{imax} and R, and the subscript k refers to the various strength components of the material. The empirical procedure to obtain enough data for determining (Eq. 1.3), however,

is again primarily suited for simple loading cases, involving only uniform stress states.

The *point stress failure* approach, neither the fatigue life, neither the residual strength view, take into consideration any of the possible failure modes. Neither do they include any of the possible interfacial stress redistribution mechanisms, which can occur between the different plies.

The *crack propagation* approach (Ref. [84]) is concerned with the prediction of the slow growth of a dominant crack in the material, due to cyclic loading. Since this method incorporates the concepts of failure mechanics, it can follow the actual mode of failure. Crack propagation investigations are carried out on laminates with a known dominant through-thickness crack or a man-made through-thickness notch. Usually, the laminate itself is treated as a homogeneous plate, with a severe stress concentration modelled near the tip of the crack. It is assumed that cyclic stressing will, like in metals, cause a stable crack growth from the crack tip. If this were real, a crack growth rate rule, analogous to the *Paris formula* for metals, could be applied to predict composite crack growth behaviour :

$$\frac{da}{dn} = \alpha(\triangle K)^{\beta} \tag{1.4}$$

where : a : crack size
K : stress intensity at crack tip
$\triangle K$: $K_{max} - K_{min}$
α, β : material related constants

All these methods have an only limited application potential, due to their empirical nature and because failure in composites is actually a with time evolving process, with many local failures occurring and interacting. Rather than the growth of one single dominant crack in fatigued metals, fatigue of composites often appears to result in the formation and distribution of sublaminate cracks, to a large extent depending on local reinforcement constraints.

1.5.2.2 Fatigue failure approaches including the damage accumulation, proper to composites

Recently, researchers have tried to relate the sublaminate matrix crack accumulation to the fatigue load history and to bring this relation into their fatigue models. There are two ways to introduce damage accumulation into a predictive fatigue model.

The first is to identify the actual damage modes (Ref. [87]) and to follow their growth or progression in space and time, thus requiring a complete description of the various damage mechanisms at the sublaminate level. This obviously turns out to be an almost endless work, at least in case of complex failure modes.

A second approach is to indirectly represent the damage accumulation by some global, measurable quantity. This requires the quantity to be uniquely related to the damage development process. Fatigue experiments on composites have shown that the development of sublaminate damages can be associated with a measurable decrease of stiffness. Consequently, an empirical model, describing the laminate stiffness loss in terms of the applied fatigue loading, can be established from a set of test data, without prior analysis of the failure or damage mechanisms themselves. However, the extent of damage must be evaluated from the amount of stiffness loss, which can be difficult in case of complex failure modes.

1.5.3 Instability considerations

The structural forms in which composite materials are most generally employed are thin-walled bodies. If thin plates or shell panels are subjected to in-plane compression or shear loads, they can fail through buckling, which is an instability problem. At these critical loads, usually far below the material's ultimate or yield stresses, a severe decrease of the element's transverse stiffness may arise, resulting in large lateral deflections which can be disastrous. Specifically, if a very small static loading is applied perpendicular to the plate or shell surface, when the component is at or near one of its critical limits, a large transverse displacement will occur, referred to as *buckling*. In a dynamic situation, as the in-plane loading approaches a critical limit, all of the component's natural frequencies are reduced and one of them falls to zero. Consequently, if the element is then subjected to a transverse

vibrating excitation, while it is in or near its critical loading state, its vibratory response amplitude would probably become unexpectedly large (Ref. [41]).

Instability phenomena can be considered on different levels, on a structural scale or on a lamina scale. For, compressive loads can render an entire structural component instable, but also individual fibres can, on their own or together, buckle when being compressed.

If no matrix would be present, the fibres would immediately buckle when under compression. In a composite however, the matrix acts as lateral support, resulting in an enhanced compression resistance. Yet, under compression load, fibre buckling can still occur. Three modes of fibre buckling can be distinguished :

- *tension buckling :* fibres are buckled in opposition, the matrix being subjected to alternating tension/compression (Fig. 1.1 (a)). This mode only occurs in case of a very flexible matrix and a low fibre volume.

- *buckling in shear :* appears as an in-phase buckling, in which the matrix is subjected to a shear stress state (Fig. 1.1 (b)). This type of buckling requires a flexible matrix together with a higher fibre volume fraction.

- *localized shear :* (Fig. 1.1 (c)) initiates in matrix-rich zones, at voids or in areas where the fibres are not oriented parallel to the compression load. The difference in Poisson ratio between matrix and fibres causes debonding at the interfaces. Further, this failure propagates in a 45° plane with respect to the compressive force, causing a double rupture of the fibres in bending. This mode occurs in case of rigid matrices which are multidirectionally reinforced.

When considering structural instability, one should realize that buckling analysis for composite plates and shells is far more complicated than it is for isotropic, homogeneous materials. Moreover, in case the plies are not symmetrically stacked, coupling will exist between bending and mid-plane stretching as transverse deflection takes place, which further complicates the problem. Reliable experimental results are also more difficult to obtain, particularly because of increased difficulty in simulating desired edge constraints.

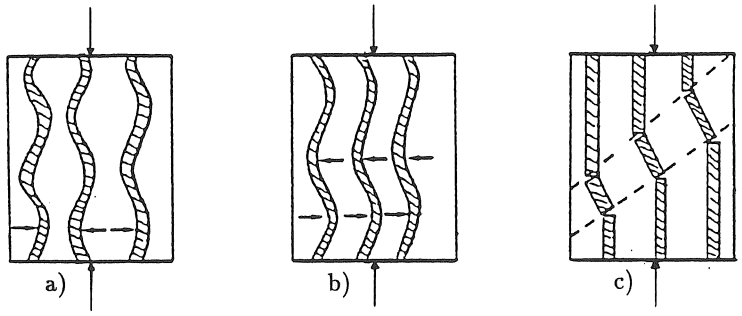

Figure 1.1: Fibre buckling modes : (a) tension buckling, (b) buckling in shear, and (c) localized shear buckling.

There exist several less or more sophisticated analysis methods to determine the critical buckling loads of rectangular composite plates (Ref. [41]). For the simple case of unidirectional plates, with the fibres oriented parallel to a set of plate edges, orthotropic plate theory can be applied for buckling analysis. For symmetric cross-plies, where the fibres are not parallel to the plate edges but skewed, general anisotropic plate theory will permit the critical buckling loads of the rectangular plates to be determined, corresponding to particular support conditions. In case of unsymmetrically laminated plates, an additional problem arises in that coupling between bending and midplane stretching will occur in the buckled mode shape. Several closed-form exact solutions have however been derived for particular cases of well-defined stacking sequence, loading condition and edge support.

A very frequently used application of composite shells showing tendency to buckle, are filament wound vessels subjected to hydrostatic external pressure. In (Ref. [55]) several procedures are discussed which predict the corresponding buckling pressure.

When applying *classical laminate plate theory* for buckling analysis, one should realize that this simple theory is based on the *Kirchhoff* hypothesis : normals to the midplane remain straight and normal to the midplane during deformation. This assumption ignores the transverse shear deformation. Considering shear deformation however results in added flexibility, which becomes significant as the plate's thickness increases relative to its length and width. This non accounted for flexibility can be considerably more important for laminates than for

isotropic plates.

As for isotropic materials, buckling of composite plates and shells does not always have to include immediate failure; although the critical buckling load, where instability is found to occur, has been reached, a plate can, depending on the support conditions, be able to carry considerable additional load before collapsing. Ultimate failure will only occur when excessive stress levels, causing severe damage, are reached within the material. Consequently, a structure which has not failed through buckling, can still dispose of some post-buckling load-carrying capacity.

1.5.4 Safety factors

A structural component is always designed with respect to a specific set of loading conditions. For preliminary sizing and further verification whether a designed component can meet the loading requirements, the designer must dispose of appropriate material characteristics. Both data types, loads and material properties, must be assessed and on both, a significant, unknown scatter can be present. Consequently, in order to design a safe component, relevant safety factors must be incorporated within the design process.

A variation among material properties occurs on two levels. First there are the basic material data, e.g. unidirectional stiffness and strength, which are used for computational purposes to predict structural behaviour. To establish these design allowables, a statistical study must be conducted, which can be very laborious. The results of extensive testing provide A-basis, B-basis, S-basis and typical-basis design allowables. An A-basis allowable is the value that 99% of the population of values should exceed, with 95% confidence. A B-basis corresponds to a 90% exceeding, the S-basis is the minimum expected value, while the typical-basis is the average value expected. Far more unknown and therefore more critical are the property reducing factors, included in real world manufacture and service : stress concentrations, insufficient fibre wet-out, fibre undulation, improper fibre alignment, resin-rich areas, voids, etc .... Although the laboratory values give preliminary design directions, a substantial reduction in mechanical properties can be expected, depending on part complexity and manufacture conditions. The designer must also consider to what degree the properties of the laminate will change throughout its life time. For,

environmental effects including heat, cold, moisture, ultraviolet light and acids can, over time, degrade the mechanical properties. Analyzing their influence can be very costly and time-consuming because not all accelerated test procedures provide consistently accurate predictions of final properties.

Often, the exact loads the designed structure will be subjected to are not known in detail. For composites, it are particularly the direction of the loads together with the environmental condition in which they act onto the component, that are critical, more than the scatter on the load's magnitude, which is easier to incorporate within the design.

In literature, very few data or directives are provided concerning safety factors. Usually the designer himself has to decide how sensitive the design reacts and is allowed to react to variations among material properties, how critical certain failures are and how tolerant the material must be against specific damages.

Recently, the *American Institute of Aeronautics and Astronautics* (AIAA) has conducted an inquiry on composite failure criteria and applied safety factors. This survey shows that among composite designers, no uniformity in design rules has yet been established, each designer observing his own design philosophy. Following data result from the AIAA inquiry (Ref. [30]) :

- 55% of composite designers use either the *maximum strain* or *maximum stress* failure criterion, which are known to give only poor results for composites. The much more suited *Tsai-Hill* or *Tsai-Wu* criteria account for only 30%.
- The applied safety factors are primarily situated between 1 and 1.5 with a 55% maximum at 1.5. Also 2 and 2.5 are frequently used.
- On the question whether matrix cracking was allowed below ultimate load, 65% of the designers answered "yes". Among these "yes" responses, 40% allowed matrix cracking at the limit load, 20% only above the limit load and 10% even beneath the limit load. According to Jones (Ref. [30]), the 35% designers allowing no matrix cracking below ultimate load are "wish full thinkers".
- 55% designers use unidirectional and 30% cross-ply laminate tests to determine matrix failure. 7.5% refer to tests on pure

matrix material, although this behaves otherwise than in situ, when combined with fibres.

- Another question concerned fibre failure below ultimate load. More than 80% answered "no". From the "yes"answerers, 40% only allowed fibre failure starting at a load, varying between 1.1 and 1.5 times the limit load.
- 65% designers defined fibre failure from unidirectional laminate tests, 25% from cross-plies and only a few percentages from fibre tows.
- 60% of the designers considered fibre failure much more important than matrix failure.
- For 20%, failure stresses and strains are based on cross-ply laminate tests. 35% use unidirectional tests, combined with laminate theory and again 35% rely on a combination of both previous ones.
- About allowing buckling below ultimate load, the meanings were equally distributed, but there was no agreement on at what times the limit level the line has to be drawn.

A major conclusion from this inquiry obviously is a regrettable shortage of uniformity and standardization among composite design rules, which certainly does not simplify the designer's assignment.

1.5.5 Anisotropy effects

The anisotropic properties, inherent in composites, are the key to developing highly efficient structures, as stiffness and strength can be engineered to meet specific needs. However, differences in e.g. coefficients of thermal and moisture expansion can also become a concern, due to the large stresses that might result from temperature and moisture variations. Symmetry is often an important requirement; for, in order to avoid coupling between bending, torsion and stretching, or to reduce residual stresses, the plies of a laminate must be stacked symmetrically and an overall balance must be maintained. And even altough laminate lay-ups can be designed as to optimally answer the stiffness and strength requirements, their practical realization is often limited by manufacturing imposed restrictions.

1.5.6 Environmental effects

Moisture and temperature are two key environmental concerns in designing composite structures (Ref. [77]). Moisture can attack composites by migrating along fibre-resin boundaries and destroying the adhesive interface but can attack the fibres as well. The result is a gradual softening of the structure. High temperatures also soften and weaken a composite structure. The worst case is a hot/wet combined condition, especially when varying in time. Since hot/wet cycling mostly affects the matrix, it is a concern when matrix performance is important. Therefore, testing under the expected environmental conditions is required.

An important benefit of composites for industrial applications is their corrosion resistance. However, relevant testing is required to determine the effects of long time exposure to chemicals and corrosive environments on the composite properties.

1.5.7 Cost aspects

Reducing costs is one of the major concerns of today's designers (Ref. [53]). Composite designs are often compared for cost to equivalent metal concepts. However, to give a fair comparison, the total system cost must be considered.

In case of a metal by composite replacement, the composite is almost certain to be the more expensive alternative. First, the composite's raw material cost is higher and second, the composite manufacture can be quite labour-intensive. However, composites offer the possibility to significantly reduce their total system cost. With composites e.g. the number of joining steps can be lowered, which reduces the requirements for manufacturing, assembly, inventory, inspection and machining. Fewer joints can also improve dimensional control and provide better tolerances, thereby reducing rejection and rework rates for the overall structure. Further, composites show important saving potential by reducing either total structural weight or the inertia of rotating and translating parts, thereby making machinery more fuel-efficient. Decreased weight can also result in improved performance, such as increased range, speed or payload.

To incorporate these advantages, the total cost should be considered, when comparing composites against metals.

1.6 Design for manufacturing

Production processes often restrict the attainable designs, since they can only deliver a limited range of configurations and details. Furthermore, final composite properties can be very much affected by the way the component has been manufactured. Therefore, following aspects, co-contributing to the design's functionality, deserve some special attention.

1.6.1 Curing and residual stresses

When selecting materials, one must consider the availability of the specific equipment required for curing. For, cure cycle requirements vary significantly from one material to another. Moreover, the cure cycle must also be fast enough to suit the desired production needs.

Residual stresses must also be considered in designing composite parts. When metal components are heated or cooled down in an unconstrained state, dimensions will change but internal stresses will not necessarily result. Composites on the other hand, can be designed to be dimensionally stable, with a low coefficient of thermal expansion, and yet being subjected to significant internal stresses. These residual stresses are superimposed on the external loads which are acting on the composite component during handling and operation.

During cure, part warpage can occur. Usually this is caused by poor mould design or an inappropriate cure cycle. Part warpage can however also be due to an asymmetric stacking of the laminate. Using symmetric and balanced laminates will balance out residual curing stresses.

1.6.2 Joints

Joints are used to transfer a load from one part to another. As the full stiffness and strength characteristics of the laminate usually can not be transferred through the joint without significant penalties, joints and other fastening devices are critical to the successful use of composite materials.

Joints are usually accompanied by high loads and stress concentrations (Ref. [14]). Due to their often brittle nature, composites are very sensitive to these stress concentrations. For, most thermoset ma-

trix laminates have only a very limited yielding capacity. When the stresses exceed the allowable limit, the laminate develops microcracks or can fail catastrophically, unlike most metals which can yield and thereby redistribute the stresses.

Moreover, most types of joints, whether they are adhesively bonded or mechanically fastened, involve some cutting or machining of the strength providing fibres.

Thus, there is an especially high concern for joint configurations to be carefully planned, designed and manufactured (Ref. [60], Ref. [81] and Ref. [28]).

1.6.3 Handling

Handling composite structures includes moving and storing. Unlike isotropic materials, anisotropic composites are primarily designed to meet specific stiffness and strength requirements in specific directions and at specific locations. Therefore, imposing loads somewhere on the composite structure, in an unexpected direction or magnitude, should be avoided. Hence, composite parts require being handled and moved with care, to preclude premature failure before they are even in service.

1.7 Design for maintenance

1.7.1 Damage tolerance

Damage tolerance is a measure of the ability of a structure to tolerate a reasonable level of damage, defects or flaws, that might be encountered during manufacture or while in service.

Flaws include scratches, dents, holes, voids, delaminations and cracks. Furthermore, holes for fasteners or step changes in laminate lay-up, although planned, also cause stress concentrations and act as flaws. Flaws can result from improper manufacturing or handling techniques, but can also be introduced during service, by impact due to kicked-up stones or dropped tools.

Safety is a primary goal of damage tolerance. The designer should ensure, through analysis and testing (Ref. [40]), the existence of alternative load paths, enabling the composite structure to keep functioning adequately, even with flaws. In this respect, damage tolerance

is closely related to the material's ductility. The greater the ductility of the material, the greater its damage tolerance and resistance to impact. Thermosets e.g. lack ductility whereas toughened matrix materials, such as thermoplastics, show high impact damage resistance.

Other important considerations are however, that damage tolerance must be achieved with maximum structural efficiency (minimum weight) and with minimum manufacturing, maintenance and supportability costs.

From economical point of view it is very important to make composites very damage tolerant. For they have a definite advantage over metals in that they can significantly better resist corrosion and fatigue. This lower cost maintenance advantage can however get lost due to too expensive repairs that are often required if the material is not reasonably tolerant to damage caused by foreign objects.

1.7.2 Inspection and repair

Not all damaged areas are visible. Furthermore, those that are visible can not be quantified by visual techniques. It is essential to locate and ascertain the extent of damage to determine whether repair can and should be attempted. Nondestructive evaluation techniques can, although expensive and time-consuming, be used to inspect composite components (Ref. [15]). These usually transmit nondestructive electrical, ultrasonic or X-ray signals through the material. Automatic scanning equipment maps the area in question and identifies cracks, voids, debonding or delamination. The inspection schedule and nondestructive testing, required to recertify the parts, must be specified within the design process.

Repair techniques have been developed for various types of damages encountered in service. Recommended techniques can vary, depending on the location where the repair must be carried out, and should be considered in advance during the design.

1.8 Design / analysis tools

There are several elements of analysis present in design, each corresponding to a specific failure mode that must be avoided. These elements include :

- stiffness analysis
- buckling and post-buckling analysis
- vibration and dynamic response analysis
- prediction of static and fatigue strength
- analysis of joints

Although analysis is incorporated in design, design represents more than just the inverse of analysis. For, analyzing means determining the load which a specific configuration can take. So, analysis is a deterministic process, evaluating the response of a specific structure to a specific loading. Designing on the contrary, means finding a nonunique structure which satisfies specified requirements of strength, stiffness, weight, cost etc. ..., which is a nondeterministic process.

Analysis can appear at different stages of design, in preliminary design, at an intermediate design level or in the final, detailed design stage. The emphasis of the designer's and analyst's task however is not uniformly distributed within the design process. Designers are generally involved heaviest in early design / analysis stages, for they have to think of and create a functional, but not yet existing, structure. Unlike the designer, the analyst must analyze a specific structure to various levels of sophistication. He is usually involved heaviest in late design / analysis stages, to analyze refined structure models, including all configuration details.

The type and degree of sophistication of the analysis obviously depend on the level that the design phase has reached.

In preliminary design stages, usually most structural parts are considered individually and simplified, allowing elementary ANALYTICAL methods to be used. For a fast, rudimental dimensioning, *Netting theory* (appendix B) can be applied, in which only the fibres are supposed taking up the loads, the matrix not being considered. Generally applied is however *Classical laminate plate theory* (appendix A), offering the possibility of stiffness and strength prediction and allowing to assess structural response of simple, laminated plates or shells.

Classical laminate plate theory can yet become too rudimental for more advanced analysis, as it neglects through the thickness effects. Therefore, in recent analytical studies, considerable attention is being

paid to the development of appropriate shell theories that can accurately simulate the effects of shear deformations and transverse normal strains in laminated shells (Ref. [31] and Ref. [82]).

But, as the design further evolves and more detailed computations must be performed on more complex configurations, the designer / analyst often finds that closed form analysis methods are somewhat limited in defining the state of stress or strain. Analytical difficulties may arise in areas where geometric discontinuities and stress concentrations exist because of joints, cutouts, edge effects, complex support conditions, etc. ...In addition, through the thickness stress gradients, multiple materials and hydrothermal effects may be difficult to characterize, using closed form techniques. Moreover, large structures usually have a number of interrelated structural elements, precluding hand analysis methods to be used. To adress local stress phenomena as well as large assembly problems, NUMERICAL analyses can be applied.

The primary tools used today for numerical analysis of composite structures are the *finite difference* method (Ref. [17]) and in particular the *finite element* method (Ref. [17], Ref. [29] and Ref. [80]).

The approach in the *finite difference* method is to approximate the differentials in the governing differential equations of a structure by means of finite differences. This results in a system of linear equations which must be fulfilled in a grid of discrete points, distributed over the structure. The drawback of closed-form elasticity analysis is that only the simpler boundary conditions can be easily accomodated. Finite difference approaches however, allow for more complex boundary conditions to be analyzed.

The *finite element* method models a structure by subdividing it into "small" but discrete elements that are connected together at the corner nodes. Once conveniently subdivided, the individual element stiffness matrices are summed together to form the global structural matrix, which is used to determine the total structural response to external loads. Early finite element codes were based on the *classical laminate plate theory*; shear effects were neglected and the so-called *A-B-D* matrix (appendix A) was used to represent the structural behaviour. Recently, sophisticated finite element programs have been developed, capable of modelling shear deformable shells, material nonlinearities, geometrical (large deformation) nonlinearities, structural instability and fracture mechanics (Ref. [7]).

However, one should realize that these numerical tools, although very powerful for analysis purposes, usually have no incorporated design facilities. On a lower level, there exist several basic laminate ranking programs for lay-up optimization. Frequently used laminate sizing tools are *Lamrank* (Ref. [78]), *Class* (Ref. [46]) and *Decomps* (Ref. [44]). When however more detailed analytical or numerical computations are required, an eventual optimization will have to result from an iterative, adaptive process.

1.9 Conclusion

Before introducing the reader into filament winding design, it has been considered relevant to devote a first chapter to the issue of composite design in general.

Thanks to their anisotropic nature, composite materials provide the designer with a powerful tool to tailor light-weight and corrosion resistant structural components, which optimally answer a specific set of needs.

This tailoring potential is obviously accompanied by a more complex design process and requires adequate, composite-specific analysis and design tools.

A key problem in composite design is strength prediction. For, failure mechanisms in composites are usually very complicated and hence difficult to model. Moreover, obtaining relevant material data, applicable to "real" laminates, is not self-evident.

To take maximum benefit of composite advantages, an original composite minded design should be performed. Unfortunately, conservatism together with imposed boundary conditions, often restrict composite design to substitutions for metals.

Chapter 2

Filament winding of composites

2.1 Introduction

In this chapter, filament winding, being a widely applied manufacturing alternative for advanced composite components, will be treated.

The highly directional nature of continuous fibre reinforcement requires that the fibres are precisely placed along carefully chosen directions, to align them with the orientations of the applied loads. In filament winding, continuous fibre, impregnated with resin, is applied under controlled tension to a usually rotating mandrel, along a predetermined geometrical pattern (Fig. 2.1(Ref. [73])). Hence, filament winding allows producing composites with well-aligned fibres.

Filament winding once used to be a stand-alone process that was labour-intensive, time-consuming and only capable of producing simple geometries. However, the integration of CAD/CAM and numerically controlled and robotic systems, together with the adaptation to handle new fibres and resin materials, have made filament winding evolve towards an economical, advanced composite fabrication technique with versatile application facilities.

After an introduction into filament winding applications, the successive processing steps which together constitute the winding process are discussed thoroughly. Further, attention will also be paid to several technological aspects, which are directly or indirectly related to filament winding and hence will reflect in the following chapters.

Finally, the winding equipment, used to produce the design examples, treated in chapters 3 and 4, will be described in detail.

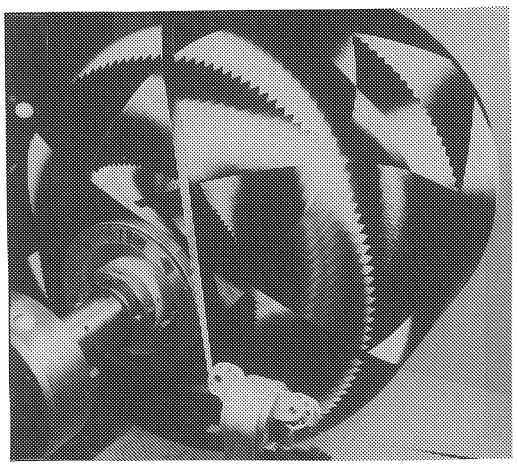

Figure 2.1: Fibre placement in filament winding.

2.2 Filament winding applications

Filament wound composites appear in many industrial areas, covering simple geometries as well as products with considerable complexity. Winding applications range from small diameter water pipes to large diameter sewage pipes and from grain storage tanks to rocket motor cases. Beside pipes, vessels and tanks, also springs, drive shafts, helicopter and wind turbine blades are being filament wound.

Recent filament winding developments can be found in power transmission, including pump and compressor couplings and cooling tower shafts (Ref. [74]). The automotive industry has started winding steering wheel armatures and even entire car frames (Ref. [92]). Finally, filament winding is also applied to manufacture recreational products such as oar shafts and blades, ski poles and softball bats (Ref. [57]).

2.3 Winding process

2.3.1 Material processing

2.3.1.1 Material choice

Fibres

As for other composite applications, the reinforcement used for filament winding purposes has evolved from glass fibres, over aramid fibres, towards carbon fibres.

At first and even today, the most widely used fibre in filament winding is glass fibre. Types of useful glass fibres for filament wound structures are shown in Table 2.1. The low cost of the E-glass fibre, its dimensional stability, moderate strength and modulus, together with its ease of handling, make E-glass suitable for components for which stiffness and weight are not critical.

Type	Tensile modulus [Gpa]	Tensile strength [Mpa]	Maximum number of filaments / strand	Fibre density $[g/cm^3]$
E	72.4	3447	4000	2.60
R	86.2	2068	60	2.49
S	86.9	4585	...	2.55

Table 2.1: Glass fibres for filament winding, normalized to 100% fibre volume.

Aramid fibres (Table 2.2) show higher strength- and modulus-to-weight ratios and are therefore capable of answering more critical application requirements. When compared to glass and carbon, aramid fibres are surprisingly damage tolerant. Unfortunately they show a tendency to absorb water. Furthermore, aramid fibres have only low compressive strength and poor adhesion to matrices. Consequently, aramid components have relatively poor compression and shear properties.

Type	Tensile modulus [Gpa]	Tensile strength [Mpa]	Maximum number of filaments/strand	Fibre density $[g/cm^3]$
Aramid(medium modulus)	62	2758	1000	1.44
Oriented polyethylene(a)	117	2585	118	0.97
Aramid(a)	121	4067	...	1.44
Aramid	124	3792	5000	1.44
Oriented polyethylene(b)	170	3274	...	0.97

Table 2.2: Organic fibres for filament winding, normalized to 100% fibre volume. (a) Development status, (b) research and development status.

Carbon fibres (Table 2.3) provide the largest variety of strengths and stiffnesses, but they are more costly. Problems arise in delivering the fibres from the tension system to the mandrel; high-modulus fibres have a tendency to break and roll back on the delivery system, so special attention must be given to the carbon fibre handling.

Class of fibre	Tensile modulus [Mpa]	Tensile strength [Mpa]	Maximum number of filaments/strand	Fibre density $[g/cm^3]$
High tensile strength	227	3102	12000	1.75
High strain	234	4100	6000	1.79
Intermediate modulus	275	4295	12000	1.74
High modulus	358	2482	3000	1.81
High modulus pitch	379	2068	4000	2.0
Ultra-high modulus	517	1816	384	1.96

Table 2.3: Carbon and graphite fibres, normalized to 100% fibre volume.

Resins

Resin chemistry

Two main types of resins can be distinguished : thermosets and thermoplastics. Both are chemically reactive compounds which solidify into load-bearing materials.

In case of thermosets, the chemical reaction builds up a three-dimensional bonding. Because of this three-dimensional structure, the

cured material never melts or flows, but will soften a little as temperature is increased, and will even ignite or burn at sufficiently high temperatures. Examples of usual thermosets are epoxies, polyesters and polyimides.

Thermoplastic resins however, are materials which are already fully polymerized in a linear fashion. Their high performance properties are achieved through backbone stiffness, whereas thermosets achieve their properties through their high degree of cross-linking. Unlike thermosets, thermoplastic polymers soften and flow at elevated temperatures. Subjecting them for a brief time to temperatures above the melting point, together with the application of pressure, is sufficient to melt or fuse them. Polyether etherketone (peek), polysulphone and nylon are some typical thermoplastic resins.

Filament winding resins

Among current filament winding resins both thermosets and thermoplastics are present (Ref. [47]).

Thermosets have been commonly used for filament winding purposes. They have low viscosities, impregnate tows easily and can be wet wound. Thanks to their ease of use, long history, familiarity and low material cost, they will probably maintain their leading position among the filament winding resins. Weak points are however, their long cure times and the quite limited freedom in winding pattern selection.

In an attempt to meet these thermoset drawbacks, thermoplastic prepregs have recently joined the filament winding materials family (Ref. [18] and Ref. [73]). Once made, it suffices to briefly heat and compress the prepreg during the winding operation. No further heating is needed to cure the composite, as in the case of thermoset resins. From winding pattern point of view, the major benefit of thermoplastics is that they permit non-geodesic winding. In fact, winding a thermoplastic prepreg tape can be considered as a non-stop welding process in which pressure is applied to the pre-heated fibre, at the moment the fibre makes contact with the mandrel. This provides a high friction coefficient and allows a wide freedom in choosing the fibre paths. Even concave parts can be wound. And as thermoplastics allow reshaping after manufacture by winding, the filament winding technique has opened its doors for new applications.

However, filament winding thermoplastics has also to deal with some problem areas. A first difficulty appears when impregnating thermoplastics, since these show very high viscosities at their flow temperatures. Consequently, special heating and impregnating equipment is required to ensure full fibre wet-out and impregnation at the high temperature needed to melt the thermoplastic. The second difficulty concerns the winding itself. Special attention must be given to select a proper heat source and an appropriate pressure system. As the latter has to be continuously in contact with the mandrel and instantaneously follow the fibre on its winding pattern, it is obvious that additional control facilities are required.

2.3.1.2 Fibre tension

Necessity of fibre tension

The filament winding process generates many possible void sites between fibres, at roving cross-overs and between layers with different fibre orientations. Voids can be removed by an appropriate compaction of the layers during the winding or curing operations. However, subsequent debulking processes can be avoided by performing a close control of the fibre tension, which acts to consolidate the part during winding.

When filament winding, the compaction pressure is determined by the tension in the fibre, the curvature of the mandrel surface and the fibre band width, according to following equation (Ref. [22]) :

$$P = \frac{T \cdot \chi}{W} \tag{2.1}$$

where : P : compaction pressure in N/m^2
T : fibre tension in N
χ : mandrel curvature in $1/m$
W: fibre band width in m

It is obvious that for a geometry with varying diameter, the fibre tension must be altered if uniform compaction is mandatory. So, a close control of fibre tension during the winding process is required to ensure a high-quality end product with uniform properties. Composite properties are very much influenced by resin content and distribution.

And resin content, especially in wet winding, is closely related to the winding tension. A certain amount of flow is beneficial in removing trapped air or volatiles but excessive tension does squeeze the underlying layers and produces marked differences in the amount of resin in the inner and outer layers. In case of insufficient tension however, there is no squeeze at all, resulting in fibre looseness and high external dimensions.

In Ref. [10] a model is presented which can be used to determine appropriate values of the process variables for filament winding of cylinders. Beside temperature, viscosity and degree of cure, fibre position and tension are computed as a function of position and time during filament winding and subsequent cure.

Tensioning systems

Most filament winding reinforcements are provided on externally unwinding bobbins, enabling tension to be introduced at the roll.

Automatic unwinders comprise several independent axes, each carrying an externally unwinding fibre package. Usually, adaptations are available for centre-pull packages. The spindle driving and braking are managed by more or less sophisticated devices, in order to ensure constant regulation of the pull on each fibre.

Most commercially available unwinding systems control the fibre tension just by means of weights, thereby introducing significant forces of inertia.

The more advanced tensioning systems are servo-controlled and have the capability to rewind, thereby enabling excess threads, for example created by overtravel at the domes, to be taken up. Servo-controlled tensioners, as presented in Fig. 2.2 (Ref. [4]), operate in the following way : the spool axis is driven by a DC servo motor with a reduction gear. The motor is controlled by a transistorized amplifier such that the pivot bracket, which is activated by a smoothly operating pneumatic cylinder, is held in the horizontal neutral position. The pivot bracket is provided with a position transducer. As soon as the pivot is pulled down out of the neutral position (increase of fibre tension), the braking torque of the motor is reduced until the neutral position is achieved again. When the pivot bracket swings upwards (reduction of fibre tension), the braking torque is increased until the neutral position is again attained. The required fibre pull-off force is

set by the pressure at the pneumatic cylinder of the pivot bracket. This pressure can be either controlled by a manually adjustable precision pressure regulator, either by a motorized regulator with a feed-back potentiometer. In this last case, the fibre pull-off force can be continuously controlled.

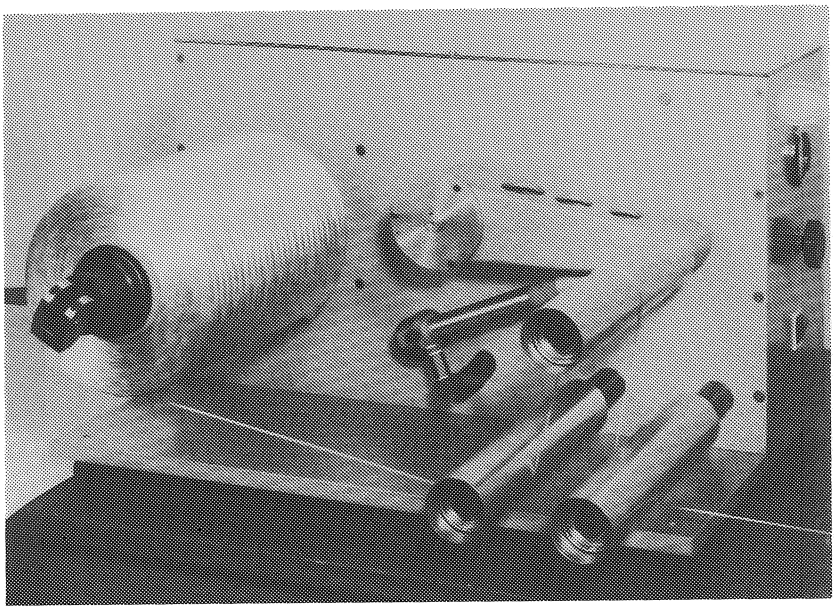

Figure 2.2: Servo-controlled tensioning device.

A weak point of the tensioning system, shown in Fig. 2.2, is the fact that it only provides a small fibre buffer. Filament winding processes however require a fast reaction onto sudden variations in fibre feed and velocity. Due to the inertia of heavy fibre bobbins, these can not be sufficiently fast accelerated or decelerated. Therefore a larger fibre buffer is needed, as for example the buffer of the fibre tensioning system used in the course of this research (Fig. 2.13).

2.3.1.3 Fibre impregnation

During the impregnation process, resin and reinforcement are joined together. Following types of impregnation methods, preceding the winding act, are commonly used : wet winding, pre-impregnated rovings (prepregs) and wet rerolled winding. Sometimes dry winding with

post-impregnation is performed, in which the fibre is only impregnated after the winding is completed.

In a wet winding process, the resin is applied to the fibre at the time of winding, just before the fibre is laid onto the mandrel. Wet fibre impregnation can be accomplished by pulling the reinforcement either through a resin bath or directly over a roller, which contains a metered volume of resin, controlled by a scraper blade. Wet winding offers several economical and practical advantages (Ref. [37]). Thanks to using neat resin and fibres, wet winding can benefit from a substantial material cost reduction over methods using prepreg materials. The resin can be stored at room temperature, unlike prepregs which require a freezer. Further, wet winding offers a good fibre wet-out and consolidation of the resin-wet fibre bundles. Moreover, the amount of resin can be varied as required.

However, due to the type of impregnation, wet winding is limited to low viscosity materials such as polyesters and most epoxies. In order for the resin to flow easily into the fibre bundles, it is possible to heat the resin mixture to reduce the viscosity, although this usually shortens the working life of the resin.

With wet winding, reproducibility in resin content and uniformity in fibre band width are difficult to obtain and to control. This is due to several parameters such as resin viscosity, interface pressure at mandrel surface, winding tension, number of layers pro unit length and mandrel diameter, which all affect the resin distribution.

Wet winding's major penalty is its rather small friction coefficient, which causes geodesic winding to be recommended in order to ensure a stable, non-slipping winding process.

In prepreg winding, the resin is impregnated into the fibres prior to the winding process, using hot-melt or solvent dip processes, and gelled to a partly cured level, called B-stage, as prepreg. Prepreg winding is often used in case the resin is a rigid amine, polyimide or high viscosity epoxy. Prepregged components are more expensive but show several advantages. They can be used at higher temperatures, provide better quality with lower resin content and less variation among their properties. Quality control is easier and can be performed away from the winding operation. The major benefit of prepregs, with respect to the design point of view, is that fibre movement is much easier to prevent, implying that winding can take place along non-stable paths

without slipping.

However, prepreg winding has also to deal with some practical difficulties. To extend their storage life, often solvents or preservatives are added to the resin formulation. But these can affect the tack of the roving, making it difficult to remove the roving from the spool during winding. These same solvents can also become trapped during B-staging and curing. Trapped volatiles can promote void incubation, which decreases the mechanical strength of the final composite. Particularly shear and compression strength are affected. Therefore often intermediate compaction and heating operations are required to remove the solvents and to reduce voids and delaminations between the wound layers.

In case of wet rerolled winding, rovings are impregnated and respooled without B-staging and either being used promptly or refrigerated. This combining method is very cost-effective for obtaining pre-impregnated rovings and eliminating the penalties of both wet and prepreg winding; unlike in wet winding, the quality control can now be uncoupled from the winding process and the prepreg problems with solvents or preservatives are withdrawn as these are not required anymore because the roving is either used immediately or stored in a freezer for future use.

The least-used technique is called dry winding, where the dry fibres are wound onto the mandrel, which is then enclosed in a mould. The mould is evacuated and liquid resin is injected. The advantage of this method is that the composite can afterwards be cured in the mould, yielding very smooth inner and outer surfaces, which conform to the tolerances, designed into the mould. Resins used for this technique must however have very low viscosities in order to fully penetrate the fibre form, without leaving dry areas.

2.3.1.4 Winding of the fibre

During the winding operation, continuous filaments, drawn from the storage spools and carrying with them the desired amount of resin, are applied under controlled tension onto a rotating male mandrel, along pre-described patterns.

The fibre path is determined by controlling the position and direction of the fibre as it is guided onto the mandrel surface. The last guidance of the fibre occurs in the fibre pay-out system or feed-eye.

So, consequently, it is the feed-eye motion with respect to the mandrel spindle revolution which has to be controlled in order to obtain the desired fibre lay-down. The type of control and its complexity of course depend on the winding machine used. This can vary from a simple mechanically controlled machine to a numerically controlled multi-axis winding unit and even a winding robot. The more sophisticated the winding equipment is, the more degrees of freedom there are to be controlled to realize the wished for winding pattern and the lower the winding speed usually will be.

In order to produce a high quality composite component, the fibres must be laid down very accurately, to ensure total and uniform coverage and prevent structural faults as overlaps or gaps. In case of band winding, uniformity in fibre band width is an important issue. Band geometry is partly determined by handling, tensioning and impregnating procedures, but also strongly depends on pay-out eye shape and orientation. Often improved band control can be obtained if the pay-out eye rotation is used as additional machine axis, permitting the fibre bands to be properly positioned and oriented as they are wound onto the mandrel.

2.3.1.5 Curing

B- and C-staging

In order to yield a load-bearing structure, the liquid resin must chemically react or cure into a strong solid. This is achieved by cross-linking, thereby creating a three-dimensional structure. This solidification process begins at the moment the resin components are mixed and can be subdivided in two steps.

The first step in the cure cycle is called B-staging. The mixture progressively builds up higher viscosities until the gel point is reached. At that moment, the resin is still soft and sticky but does not flow anymore. B-staging components are often rotated until gelation is achieved. Otherwise the resin will tend to flow to the lowest point, resulting in a non-uniform resin distribution. If necessary, excess resin can be removed before proceeding with the curing process.

During further cure, called C-staging, exposure to higher temperatures or additional time is required to develop the composite's full physical properties. As a general rule, the temperature of cure is somewhat below the maximum temperature capability of the com-

posite. Thus, room temperature cured resins will only perform at or slightly above room temperature.

Since being appropriately cured is a major requirement for high end product quality, many researchers have been concentrating on simulating cure cycles (Ref. [75]). Hence, models have been developed, which provide optimum cure cycles, including cure temperature and cure pressure as a function of time (Ref. [76]).

Curing equipment

Commonly used curing equipments are infra-red lamps, electric or gas-fired ovens, autoclaves, induction and microwave ovens. Controlled cure cycles are required to ensure sufficient (but not excessive) resin flow and to minimize fibre movement. In critical applications, vacuum bag and autoclave techniques provide a control of resin flow and fibre movement as well as a reduction of void content. Microwave cure significantly reduces energy costs and cure times but requires special heating supplements.

Thermosets and thermoplastics

In case of thermosets, the curing operation is a time-consuming production step; a long period is needed for the molecules to react and to achieve the fully cured state. To assure high quality, epoxy systems require vacuum degassing, heating under vacuum and at high temperatures for a period exceeding six hours.

On the contrary, thermoplastic resins are already fully reacted. They only require heat and pressure for a short time at their softening or melting point, followed by pressure cooling below their melting point, in order to solidify and to obtain their desired load-bearing capacities (Ref. [23] and Ref. [18]).

2.3.2 Tooling

The tool around which the impregnated fibres are wrapped is the mandrel. Mandrels are very critical in that poor mandrel design can result in damage of fibres, deviations in dimensions and excessive residual stresses. Three factors determine the choice of tooling : part geometry, tolerance requirements and life cycle costs.

Following types of mandrels are frequently used in the filament winding industry :
one-piece metal mandrels, collapsible or segmented mandrels, water-soluble sand mandrels, soluble or meltable salts, low melting alloys, soluble plasters, inflatable mandrels, expandable mandrels and unremovable liners.

For small parts with simple, open-ended geometric shapes, a one-piece metal mandrel can be used.

Larger or closed shape components require a collapsible or segmented tool, so the component can be removed. Collapsible or segmented mandrels are specialized and expensive, but since they are reusable, their cost can be justified for large lot sizes. However, care must be taken when only small polar openings are present, since these may complicate segment removal.

Water-soluble sand mandrels provide a low-cost solution for small-to-medium-sized parts with good repeatability, but their use is limited for larger parts because of the weight and deflections encountered. Also fibre tension has to remain low due to insufficient compression strength.

Soluble or meltable salts offer high temperature resistance and good repeatability, so they can be used for large series of relative small components. However, the need for an external mould makes removable salts very costly, particularly the melting salts, since these require an additional melting installation.

Low-melting alloys are very hard and can be reused but they are expensive and heavy, so they have to be made very thin and can only be applied for small structures. Furthermore, they have the undesirable tendency to creep, even under moderate loads.

Plaster is hard and form consistent. It is cheap and can be finished afterwards so that high tolerances can be achieved. Unfortunatelly it is very heavy. However, for development projects and short production runs, often a plaster shell over a metal structure is used, offering flexibility for planned configuration changes. Plaster mandrels can be either removed by shaking, eventually combined with applying pressurized air (e.g. Cara PNF 102 R) or by washing out (e.g. Kerr DMM) (Ref. [63]).

Foams (e.g. polystyrene (Ref. [63])) show poor mechanical properties, especially at high temperatures. They are not reusable but

give a good and cheap solution in case only small series have to be wound, using room temperature curing resins and requiring no special dimensional tolerances.

Inflatable rubber mandrels are a low cost choice for programs which do not require high tolerance control. If no supporting structure is present, these mandrels are impractical. However, past problems of torque transmission and dimensional control have been overcome with improved designs, which make this technique currently attractive.

Expandable mandrels can be very effective for winding cylindrical shells; a controlled expansion of the mandrel parts applies pressure to the inner surface while the shell is being formed, thus increasing the density and the mechanical strength of the formed shell. Various concepts of expandable mandrel designs are available; rubber or plastic bags, filled with liquid or gas, as well as movable pushers and wedges (Ref. [50]).

Unremovable liners are used e.g. for metal-lined pressure vessels, combining the high strength-to-density advantage of composites with a thin, impermeable metal liner. The liner prevents leakage, provides a boss for the valve, serves as mandrel and carries a small part of the pressure load during service. Liners used are low-strength ductile metals such as aluminum, stainless steel, nickel and titanium (Ref. [51]).

2.3.3 Winding equipment

In this paragraph, the evolution and automation of filament winding equipment are discussed.

Early filament winding machines had only two degrees of freedom. They were controlled by mechanical means such as gears or chains. Nowadays, they still continue to be popular and are entirely adequate for simple, repetitive geometries.

However, the demands imposed by more complex product geometries, together with the advent of microprocessor control, have led to the development of more flexible, multi-axis machines. Currently used are winding machines with five or six axes of motion : spindle rotation, carriage axis, cross-feed, and two or three delivery axes. Their motory functions are driven by a computerized numerical control. Furthermore, also auxiliary operations such as fibre tensioning and heat application can be controlled.

Recently, robots have joined the today's winding equipment. Their

six axes of motion, combined with the rotation of the spindle, being a seventh degree of freedom, allow filament winding of complicated, three-dimensional components.

Not only the winding equipment but also its programming and control have evolved. Numerically controlled machines and winding robots were originally programmed *on-line*, by the time-consuming and not very accurate *teach-in* method. Last years, most filament winders have been concentrating on developing direct machine input programs which take machine and winding constraints into account and produce precise fibre paths (Ref. [85]). Recently this *off-line* programming is being integrated within the introduction of CAD/CAM in filament winding design and manufacturing (Ref. [73]). Nowadays winding machines are being interfaced with computers, capable of surface modelling, fibre path generation, finite element analysis and optimization of winding parameters.

Thanks to the integration of CAD/CAM and the application of NC and robotic systems, filament winding has evolved towards an economical, advanced composite fabrication technique, with reduced labour-intensive part design, development and manufacturing costs (Ref. [88] and Ref. [64]).

2.3.4 Winding patterns

2.3.4.1 Classification

With filament winding, fibres can be applied onto the mandrel along several trajectories. However, there are two main ways to classify possible winding patterns.

geodesic / non-geodesic

From geometrical stability point of view, winding patterns can be classed under either geodesic, either non-geodesic families.

Geodesic lines are lines for which the second order derivative is perpendicular to the surface. Mathematically this can be expressed by a system of two second order differential equations (Ref. [9]). Starting position and orientation of the geodesic trajectory constitute the initial conditions for solving this system.

In case of surfaces of revolution, geodesic paths can be easily computed using the law of *Clairaut* (Ref. [66]),

$$r \times \sin\alpha = constant \tag{2.2}$$

relating the fibre angle α with respect to the meridian curve in a particular point, to the radius r in that point.

Geodesic lines connect two successive points along the shortest distance over the surface. Consequently, if a fibre is laid down onto the mandrel in a geodesic way, it will not move when being pulled along its axis. With geodesic winding, no friction force is required to keep the fibre from slipping, as it follows a self-stable trajectory. So, if there is no significant friction to rely on, as in case of wet winding where the friction coefficient is rather small, geodesic winding is recommended in order to guarantee a stable and accurate fibre placement.

However, when winding with prepregs, which stick and provide more friction, these friction forces can be counted on to prevent the fibre from slipping across the mandrel's surface. Consequently, with prepreg winding, also semi-geodesic or non-geodesic winding can be performed. By slightly deviating from the geodesic lines, e.g. along paths of equal slip safety (Ref. [86] and Ref. [94]), it is possible to obtain stable winding patterns which can closer approximate the optimal lay-up.

The freedom of choosing appropriate fibre trajectories is even more pronounced when winding with thermoplastic resins. As the thermoplastic prepreg is immediately welded onto the prior windings, fibre paths can be freely chosen to meet the loaded stress state.

polar / helical / hoop

A second classification is based on how successive windings are positioned with respect to the preceding ones. Three types of winding patterns can be distinguished : polar or planar winding, helical, and hoop winding.

Polar or planar winding (Fig. 2.3(Ref. [72])) provides a layered laminate lay-up with a minimum of voids and cross-overs. A next fibre is immediately adjacent to the previous one and there is almost no interweaving of the fibres. With polar winding, the mandrel can be stationary while the delivery system revolves around it. Or both delivery system and mandrel may be fixed while the machine, supporting

the mandrel, revolves. After each rotation, the mandrel advances over one band width. Polar winding is widely used for spherical and other bottle-like shapes, rather than for open-end structures.

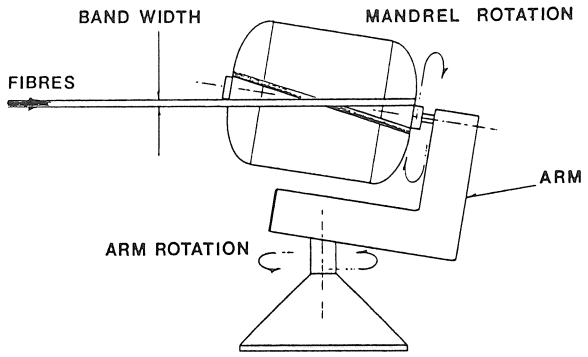

Figure 2.3: Polar or planar winding.

Helical winding (Fig. 2.4) is usually performed on machines with translating feed carriage. With helical winding, a woven structure is created in which both voids and cross-overs do occur. Here, the composite is built up by a more random fibre lay-down and fibres will only be adjacent after a given number of cycles.

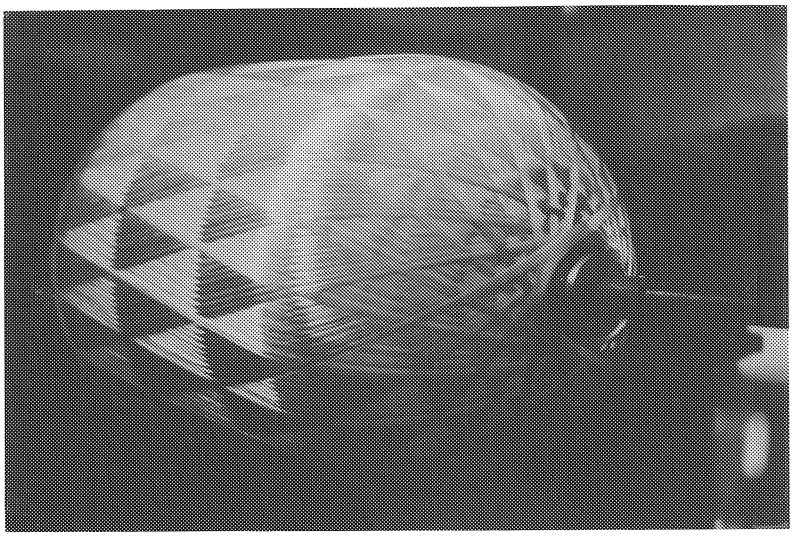

Figure 2.4: Helical winding.

The third type of patterns is called hoop windings (Fig. 2.5). In fact, these are extreme helical windings, almost circumferentially placed, with an angle close to 90°.

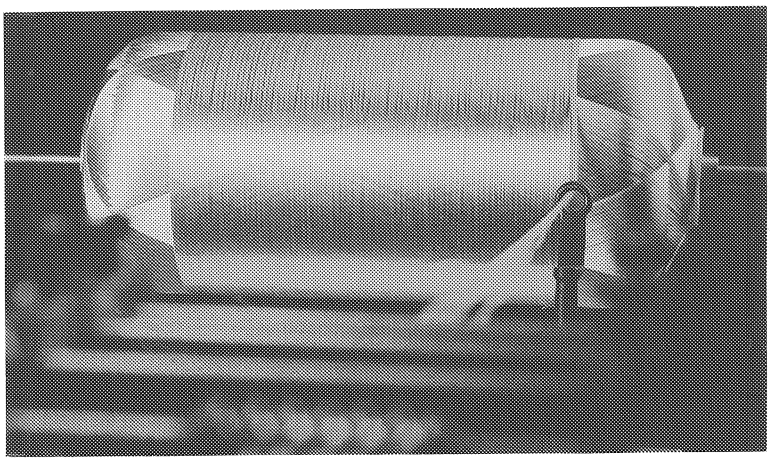

Figure 2.5: Hoop winding.

In order to generate a particular winding pattern, the fibre has to be returned after each winding cycle. This reversal can be accomplished either by winding over a dome, by winding around pins or by deviating from the geodesic lines and returning the fibre, counting on friction.

2.3.4.2 Winding strategy

By winding strategy is understood the time sequence of the fibre laydown of one single layer in a particular cross-section of the wound structure. The winding strategy is closely related to the winding pattern and together they determine the interweaving of the fibres. The influence of the winding strategy on the performance of a filament wound structure will be discussed in 3.4.

2.3.4.3 Winding sequence

In order to provide the filament wound component with an as uniform as possible safety factor with respect to the loading conditions, the

winding process often has to be subdivided into successive steps. Each step corresponds to a specific layer of windings, which all together closely reach the optimal overall lay-up. Continuity between successive patterns can cause difficulties in fixing the fibre to the prior windings at the new starting location, somewhere on the mandrel.

2.3.5 Filament winding evolution

In earlier days, filament winding applications were limited by several drawbacks. A mandrel was required which could be complex and expensive. The shape of the component had to be such that the mandrel could be removed. Winding was restricted to geodesic patterns and reverse curvatures were impossible to wind. Furthermore, the cured structure had a poor external surface and often showed a lot of voids.

However, thanks to new technologies and new materials, filament winding has become a versatile production method, able to circumvent the original disadvantages.

Nowadays, many types of mandrel materials are available to suit individual applications. Mandrel removal difficulties have been solved thanks to the advent of soluble or washable mandrel materials (2.3.2).

New material forms, the use of prepregs and thermoplastic matrices, have rendered the winding process more flexible in that deviating from geodesic paths is now possible, allowing the fibre orientations and laminate lay-up to closely meet the loading conditions. Reverse curvatures can now be wound, also thanks to reshaping possibilities after winding.

New technologies and equipment, together with computer control, have made a closer control of winding parameters, fibre tension, fibre placement, resin distribution, curing and compaction cycles possible, resulting in a higher quality product. Integrated CAD/CAM has reduced design problems and cost and has led to the automation of filament winding design, development and manufacturing. Filament winding products now show high mechanical properties, excellent reproducibility and are ready to be manufactured on industrial scale.

Concerning the future, Wilson (Ref. [89]) claims that the growth in filament wound products and in the equipment to produce them will continue. Moreover, filament winding will maintain its leadership among the manufacturing processes of the ever increasing number of composite products.

2.4 Technological aspects related to filament winding

2.4.1 Environmental effects

The properties of filament wound composites are affected by temperature, weathering, aging and other environmental conditions. In general, the response to these factors is similar to that of other reinforced plastics. One complication is that the usually lower resin content of filament wound composites might render them more susceptible to moisture penetration and damage by exposure to high relative humidity.

Water is a pervasive substance which is present during the manufacture and service life of any composite. Moisture can be a problem in manufacturing operations, because it affects fibre and resin systems to various degrees. Moisture can attack a cross-linking component during cure. But even if adequately cured, the structure remains permeable to water throughout its life cycle. Moisture can be even more a problem when the composite is in field service and exposed to temperature and humidity, especially when combined and driven by cyclic changes in environmental conditions. Investigation of moisture and humidity exposures has indicated that filament wound composites, immersed in water, only lose a little of their strength in case they are unloaded or only loaded statically. If however, they are subjected to cyclic temperature and humidity exposure, an appreciable loss of strength, sometimes up to 30 %, can occur (Ref. [71]). It are mainly the matrix sensitive mechanical properties which significantly degrade, particularly at higher temperatures. On the contrary, fibre-controlled composite properties are relatively unaffected.

The degree of moisture sensitivity depends on the type of matrix used. Resin systems with low cross-linking density and low heat-distorsion temperature have very little resistance to severe environmental conditions; many epoxies, e.g., become flexibilized through absorption of moisture. Conversely, the same epoxy laminate becomes increasingly brittle as this moisture is removed from the composite. Other resins, formulated for high-temperature service, offer better moisture resistance.

The deleterious effect of temperature-humidity cycling can be minimized by using superior finishes, less moisture-sensitive resins and

improved cure conditions.

2.4.2 Joints

Filament winding offers the possibility to wind continuous fibre over an entire component, thereby allowing the overall number of parts and joints to be reduced.

However, composite-metal joints are still being used in many application areas. The reason is that until now, composite design has only evolved in so far that nowadays, many individual metal components have been replaced by composites. But it has not yet come to a completely composite minded design. So, the individual composite parts are still to be integrated within the global structure. Hence, joining techniques remain quite important, even indispensable. Yet, as composite stiffness and strength are quite different from those of ordinary materials to which they are fastened, the full characteristics of the laminate cannot be transferred through the joint without a significant weight penalty. Consequently, joints are critical to the successful use of composite materials.
Beside planned joints at predetermined locations in the structure, also unplanned repairs can be needed anywhere in the component.

The requirements for a filament wound composite joint are the same as for any other; the joint should be light-weight and non-corrosive and should not act as stress concentrator. Joints can vary from adhesively bonded joints to mechanically fastened joints, using bolts or rivets.

In a filament wound structure, two major types of composite-metal joints are frequently used.

In case of an in-situ joint (Fig. 2.6(Ref. [8])), the composite is wound while being joined to a shear ply or immediately to the metal surface. This joint type is often used in rocket motors. The in-situ joint takes advantage of the filament winding process and eliminates complex machining. However, it has also to deal with some geometrical restrictions. First, the joint must be quite smooth and should not have any abrupt discontinuity in contour. If there are changes in elevation present, they must be made at a small angle to the mandrel centre-line, in order to avoid fibre slipping and bridging.

Second, there may not be any protrusions above the composite surface, since these could interfere with the fibre path near the joint.

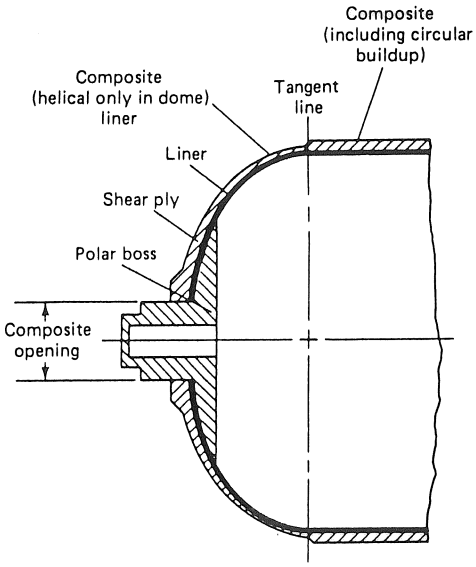

Figure 2.6: In-situ joint in a pressure vessel.

A second type of joint is machined or changed in some way after curing the composite. Commonly used are single lap (Fig. 2.7) or double lap (Fig. 2.8) joints (Ref. [56]). Usually, these joints require drilling and/or machining of both the composite and the metal, which can be time-consuming and expensive and which can damage the wound component.

Obviously, it would be beneficial to make a transition to the metal part without a joint, a contradiction in terms. However, this is not inconceivable, as it appears from pressure vessel technology, where load-shearing metal liners are combined with a filament wound coverage for high pressure applications.

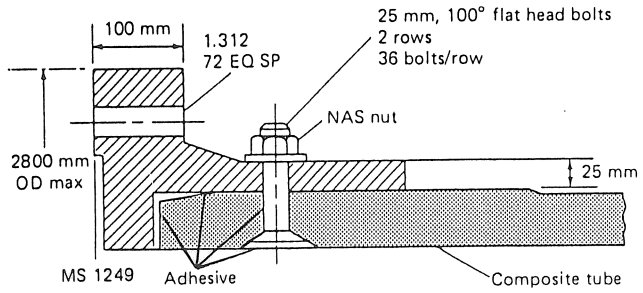

Figure 2.7: Single lap metal-to-composite joint.

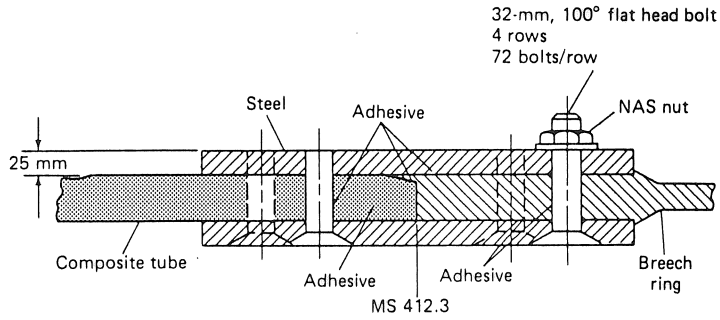

Figure 2.8: Double lap metal-to-composite joint.

2.4.3 Finishing

Filament wound components often require an additional finishing step as a final manufacturing phase, in order to satisfy all end product specifications. The composite usually has to be trimmed to the finally wished for size, shape and surface condition and, if necessary, details must be introduced to allow for joints and attachments to the final assembly.

If a filament wound component is cured under pressure to an external mould, the outer surface quality is usually irreproachable. Also vacuum bag curing and applying special surface tapes or cloths yield

good surface conditions. If however, during cure, no attention is given to the outer surface and the end product's outer surface requirements are critical, additional surface machining will be necessary.

In order to finally shape the composite and provide attachment facilities, often turning, cutting, milling and drilling operations must be performed. These finishing processes can be accomplished using either traditional solid-tool methods, or newer machining technologies. In each case, special considerations must be made with respect to the application on composite materials.

Due to their generally abrasive nature, solid-tool cutting and drilling of composites require appropriate tooling (Ref. [34]). Tool materials, cutter shapes, feeds and speeds will vary, depending on the type of composite. During machining operations, precautions must be taken to avoid damage of the workpiece, as e.g. delaminations, fibre fraying and drill break-through, and premature dulling of the tool.

The newer machining methods, such as water-jet, abrasive water-jet, laser or ultrasonic cutting, fortunately meet some of these problem areas (Ref. [35]). Yet, they introduce their own complications in terms of equipment size, high noise levels and other inherent restrictions when used on composites.

2.4.4 Testing

Testing and evaluating composites and their basic raw materials account for a major phase of composite and hence of filament winding technology. Tests are performed to determine resin and reinforcement properties, to supply design allowables and to provide quality control. Furthermore, testing also allows for proof and burst strength evaluations.

The majority of standard test specifications for composites, however, only apply to flat laminate properties. But, the mechanical behaviour of filament wound structures is typically different from flat laminate behaviour. Differences result from the type of cure, resin void content, microcracking and free edge construction. Still, filament wound structures require the same mechanical property data for design and analysis as general laminated structures. Consequently, industry-wide standards for material characterization of filament wound components is indispensable.

In industry, a whole series of test methods, standardized as well as

non-standardized, are used to support filament winding. Almost all of them are performed on wound tubes or rings. Test specimens and corresponding methods are shown in Fig. 2.9(Ref. [56]).

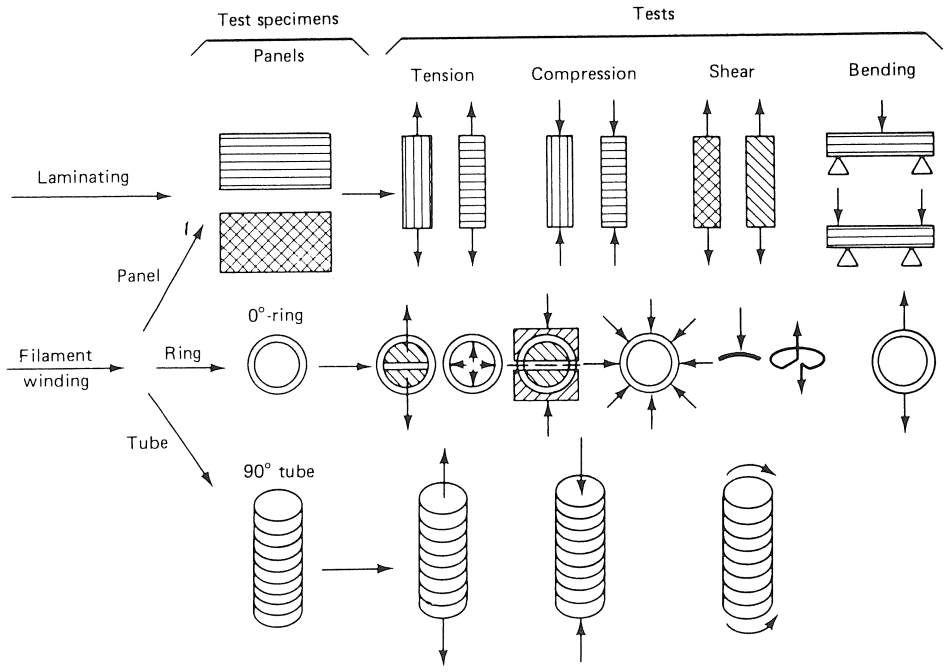

Figure 2.9: Filament winding test specimens and methods.

Yet, filament winding permits any classical test procedure to be carried out. Flat unidirectional tensile test specimens, for example, can be built by winding unidirectional, impregnated fibres circumferentially around a large mandrel, cutting and removing them from the mandrel, followed by plying and then consolidating and curing. However, since in filament winding additional consolidation is usually neglected, these specimens do not reflect the properties, obtained by ordinary filament winding and may even be more costly and time-consuming to fabricate. Flat specimens might also be produced by winding over a flat-sided drum. However, this results in less than optimum characteristics, because of the lack of compaction across the flat area, which leads to an excessive void or resin content unless other compaction methods are applied.

Fabrication and testing of a filament wound ring, using split disks or hydraulic pressure, is simpler than testing parallel straight-sided specimens; in the N.O.L. rings (*ASTM D2290*) the fibre orientation is easier to control. The ring, cured without requiring compaction aid such as a vacuum bag or an autoclave, needs no other processing. On the contrary, a flat-sided tensile specimen requires machining and adhesively bonded end tabs. The N.O.L. ring (Fig. 2.10) is reasonably self-aligning, unlike the flat-sided specimen, which must be carefully aligned in the test machine. However, the flat-sided specimen has the advantage of an easier strain gage attachment.

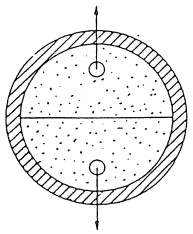

Figure 2.10: N.O.L. ring tensile test.

The N.O.L. ring specimen can be fabricated as an individual ring or by machining rings off a cylinder. Obviously, the individual rings are preferred since they do not imply fibre cutting.

Beside the N.O.L. tensile test, the N.O.L. ring short-beam shear test is also frequenly performed (*ASTM D2344*). Further, all kinds of tests are carried out to supply data concerning tensile and compression strength and stiffness, both in the radial or longitudinal direction, shear stiffness and strength, etc .... Beside test methods to control the properties of finished components, there obviously also exist lower level test procedures to characterize the raw filament winding material.

Both, standardized as well as non-standardized ring test methods however, all supply test data that can only be used for comparative purposes. They are not designed to give basic engineering data, but are intended to reveal differences in fabrication or materials such as resin type, fibre type and sizing; or processing variables such as fibre tension, resin viscosity or resin content and cure cycle. Ring test data appear to be not immediately suitable for design purposes. Consequently, material properties, needed to be introduced in the design, must be obtained by a roundabout way (3.4.5.1).

In order to provide realistic data which closely correspond to in-use loading conditions, filament wound composites have also to be tested for their biaxial strain performance. Of all composite specimens, pressure vessels best serve this purpose. Since pressure vessels account for a great percentage of all filament winding applications, it is obvious that in literature, much attention is given to pressure vessel design and test methods. Beside the *ASTM standards* (Ref. [3]), also the *ASME Boiler and Pressure Vessel Code* (Ref. [1]) prescribes detailed vessel test procedures.

2.5 Winding units at the K.U.Leuven

At the Production Engineering Division, two winding units have been set up : a numerically controlled machine for geodesic winding of axisymmetric components and a winding robot to handle more complex, non-axisymmetric shapes.

Up to now, only wet winding has been experienced, which does not provide much friction as compared to prepreg winding. Therefore fibre patterns have been limited to geodesic paths. Hence, the control of both NC machine and robot is based on geodesic principles.

2.5.1 Numerically controlled winding machine

To avoid the slowness of most commercially available machines, which are limited in speed due to their heavy carriages, a winding unit with a light-weight winding arm has been built. Through an adequate numerical control, this machine allows for a high-speed winding of axisymmetric geometries. Originally this NC machine was planned to wind fibre reinforcements for the tire industry. Thanks to its interesting control capacities, the NC winding unit has also been very useful within the course of this composite research.

2.5.1.1 Equipment description

The numerically controlled winding unit consists of following components :

- a rebuilt lathe
- a winding arm

- an impregnation element
- a tension controller and unwinding unit
- an heating system for curing

The impregnated fibre is applied onto a mandrel which is mounted on the spindle of the lathe (Fig. 2.11). This main axis rotates at a constant velocity, which can be manually adjusted by a frequency regulator, controlling the speed of the asynchronous driving motor.

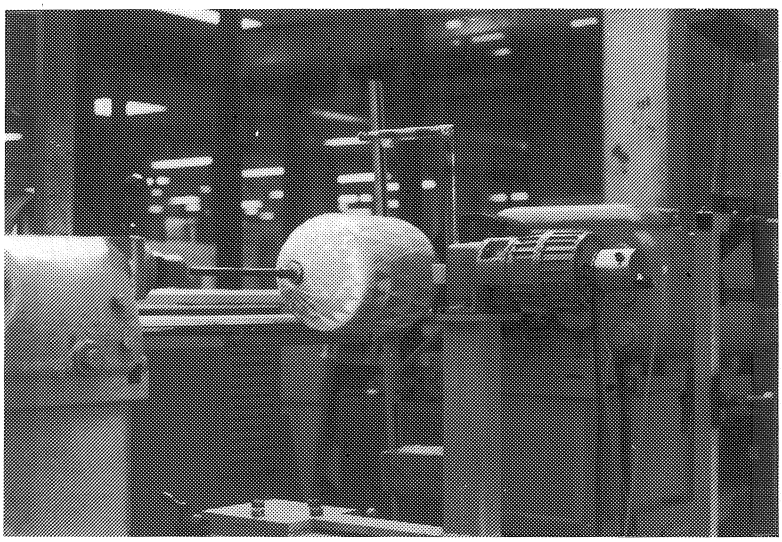

Figure 2.11: Numerically controlled winding unit.

The fibre is guided through the pay-out eye at the end of the winding arm (Fig. 2.11). This winding arm is controlled by a DC servo motor with a 100 Hz bandwidth, which is mounted on the cross-carriage of the lathe. The numerical control of the arm motion is discussed in detail in the next paragraph. The winding feed-eye describes a circular pattern in a vertical plane, parallel to the spindle, and thus has only one degree of freedom. However, the arm length can be varied between 0 and 500 mm and also the distance between the arm motion plane and the spindle, as well as the vertical position of the arm axis, can be adjusted to suit the mandrel's geometry. Thanks to this flexibility,

collisions between arm and mandrel can be avoided and arm velocities and accelerations can be reduced.

The fibres are impregnated while being pulled over a roller which is mounted in a resin bath (Fig. 2.12). The fibre makes the roller rotate due to friction and so, the resin film, carried by the roller surface, is transferred to the fibre. The thickness of the resin film can be manually controlled by means of a scraper. In order to obtain the desired resin viscosity, the resin is heated in a water bath.

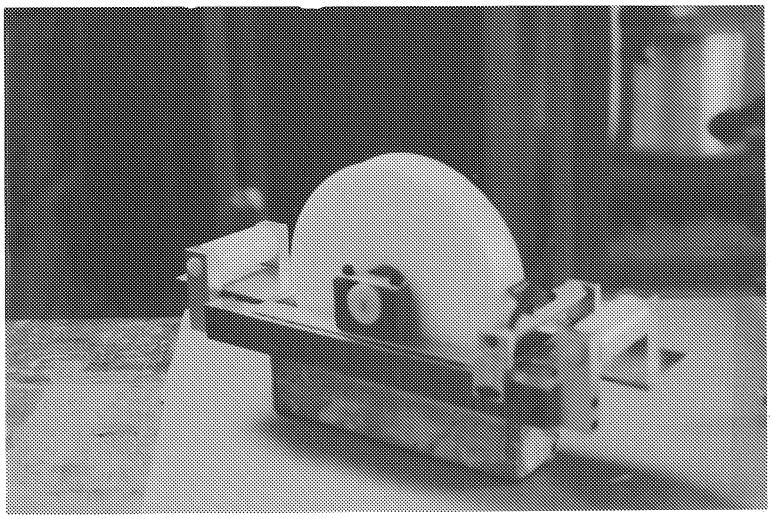

Figure 2.12: Fibre impregnation system.

The unwinding system (Fig. 2.13) is constructed as to meet the fibre need at every moment. The dry fibre is stored on a bobbin which is externally unwound by an asynchronous motor. The control mechanism functions as follows : in principle, the feeding motor of the bobbin is in rest when the lever remains in its reference position. But, if more fibre is required at the feed-eye, the lever goes up as the bobbin does not move. When however the lever is pulled upwards by the fibre need and gets out of its reference, a potentiometer, connected to the lever axis, returns a certain voltage. This signal regulates, by means of a PD control, the frequency-controlled unwinding motor. The higher the voltage is, the faster the motor will rotate. So, an equilibrium

between the fibre need and the fibre supply can be obtained. The lever will almost always retain the same position. It can, however, also serve as fibre buffer, if suddenly, a high portion of fibre is needed, but afterwards, the lever will again return to its equilibrium position.

The fibre can be tensioned by pulling on the lever with a specific force, applied to the lever by means of a pneumatic cylinder with adjustable pressure.

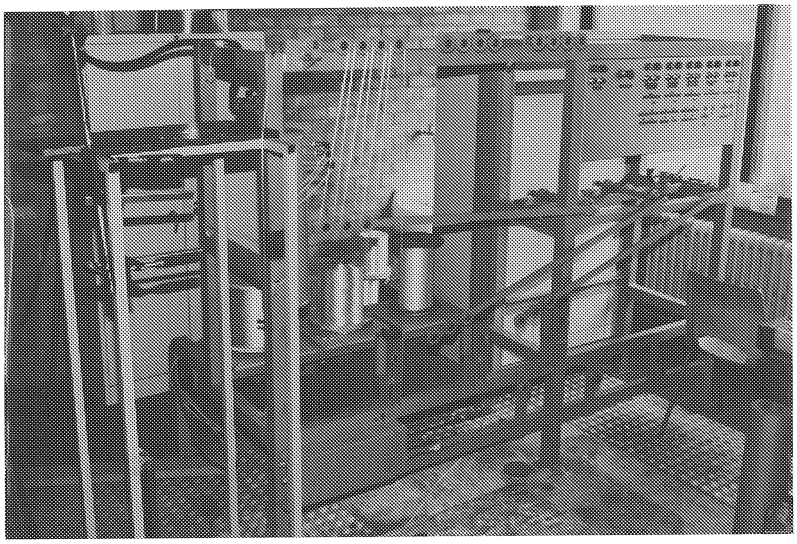

Figure 2.13: Fibre tensioning system.

B-staging is usually performed on the winding machine itself, using an heating lamp, which also serves for pre-heating the mandrel. To prevent resin flow, the structure is kept rotating. For further cure, an oven is used, in which a more uniform temperature distribution can be obtained.

2.5.1.2 Numerical control for geodesic winding of axisymmetric composites

Control principles

When performing geodesic winding, the fibres are forced to follow pre-described geodesic paths on the mandrel's surface. These patterns

are fixed, once a starting point and starting angle have been chosen and only depend on the geometry of the mandrel. In order to wind the fibre along the desired geodesic trajectory, the arm motion must be adequately controlled.

The enclosed rules to be observed require that at every moment the tangent to the geodesic line, -in the point on the mandrel that is wound at that particular moment-, passes through the winding eye. This requirement can be translated into a relation between the described sector of mandrel or spindle rotation and the angular position of the winding arm. Based on this relation, the arm can be controlled as a function of the spindle position.

In case of axisymmetric structures, the winding process has a repetitive character; the mandrel can be completely covered by a series of geodesic lines which are identical, except for being shifted over a certain sector of mandrel and spindle rotation. Since the associated fibre windings can be obtained by the same arm-spindle relation, one single geodesic line, corresponding to one arm cycle, forward and backward, provides enough data to control the whole winding process.

When however, beside axisymmetry, the part to be wound also shows an additional symmetry around a vertical cross-plane, the back motion of the arm can be described by the same function as the coming motion, but with reversed sign. Consequently, it is sufficient to only set up a arm-spindle relation for one single forward motion, called one half winding cycle, and corresponding to a geodesic line which crosses the mandrel's surface from one end to the other.

To compute and tabulate the arm-spindle relation into the ARM-SPINDLE table, the *geo-computing* program has been developed. A *postprocessing* module transfers this table into a directly usable form for the *controlling* program, referred to as WINDING table. Also a STARTING table is created, containing the exact spindle positions where a new winding cycle with reversed motion must be started. The *controlling* program is based on a POSITION FEED-FORWARD principle, using both WINDING and STARTING tables.

Beside the *geo-computing*, *postprocessing* and *controlling* routines, a *strategy* program has been developed, computing feasible winding strategies. In the next sections, these four routines will be successively discussed.

Strategy program

By winding strategy is understood the time sequence of the fibre lay-down in a particular cross-section of the mandrel. A detailed description of winding strategy and its influence on the composite's performance is given in (3.4). This section however will concentrate on the realization and practical implications of a specific winding strategy.

To close a winding circuit, it should be taken care of that the circumference is completely covered at the moment the prescribed number of windings is reached. In a particular cross-section, perpendicular to the axis of rotational symmetry, this wished-for number N is determined by the required (from strength analysis) thickness t of the composite layer, the radius r of the structure in the considered section, the wet fibre cross-section A and the fibre angle α :

$$N = \frac{t \cdot \cos\alpha \cdot 2\pi r}{A} \tag{2.3}$$

Obviously also the shape or width/height ratio of the fibre band's cross-section must be considered. In case a thin layer must be wound using thick fibre strands, N windings will not suffice and additional windings will be required to cover all empty spaces. Once N is known for the highest loaded section, an appropriate strategy, corresponding to these N windings, can be looked for.

A strategy is characterized by the angular shift between two successive (whole) winding cycles. If the circumference is subdivided into a number of segments, equal to the total number of windings, this shift can be expressed by the ratio of the number of positions, shifted at the beginning of a new cycle, and the total number of considered positions or windings along the circumference. For the case presented in Fig. 2.14, the strategy is referred to as *5/8*, indicating that at every new cycle, the mandrel has turned over a fraction *5/8* of one complete revolution.

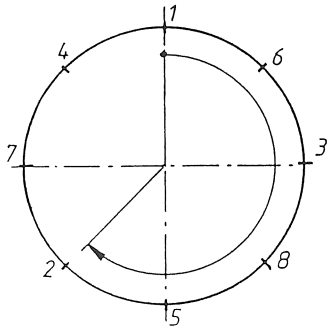

Figure 2.14: A winding strategy called *5/8*.

In order to avoid overlapping fibres, the number of shifted positions and the total number should have no common divisor. For, only after winding all cycles, the fibre may overlap already covered positions. In case of a common divisor, however, the fibre already returns to the starting point before all empty spaces have been filled up. As the pattern keeps repeating itself, these will never be capped. Consequently, for a specific number of windings along the circumference, only those strategies are valid with the shifted positions and total number having no common divisor. These appropriate strategies, computed in the *strategy* program, allow for the fibres to be distributed as uniformly as possible over the mandrel's surface.

To obtain a prescribed strategy, it must be taken care of that at the end of each complete arm cycle, -coming and back motion-, the spindle has turned over a number of rotations from which the resulting sector corresponds to the prescribed fraction.

Realizing a prescribed fraction usually requires one or more mandrel dimensions or the starting location to be varied, since a geodesic line is completely determined by the starting conditions and the geometry. In case of e.g. a pressure vessel, consisting of a cylinder, closed by two end caps, the winding strategy can be varied by slightly changing the length of the cylinder. Small changes in nozzle or cylinder radius also enable other strategies to be achieved, but they also affect the winding angles.

Varying the dimensions and thereby imposing a specific strategy is performed in the *geo-computing* program. Usually, the winding strategy choice is not very critical. In that case, one computes the fraction

corresponding to the designed geometry and chooses from all possible strategies the one that suits best this fraction. This way significant changes in geometry can be avoided and the computed stresses and strains, closely associated with the geometry-determined fibre angles, remain relevant.

Geo-computing program

This program computes geodesic lines on specified axisymmetric surfaces with cross-plane symmetry and for specific starting conditions. In addition, an ARM-SPINDLE table is set up which represents the relation between arm and spindle positions, corresponding to the winding of the computed geodesic pattern. Thanks to cross-plane symmetry, it suffices to compute only the geodesic line corresponding to one half winding cycle. With each point describing the geodesic pattern corresponding spindle and arm positions can be associated. To compute the geodesic data and set up the ARM-SPINDLE table, a stepped, iterative procedure is performed as shown in Fig. 2.15.

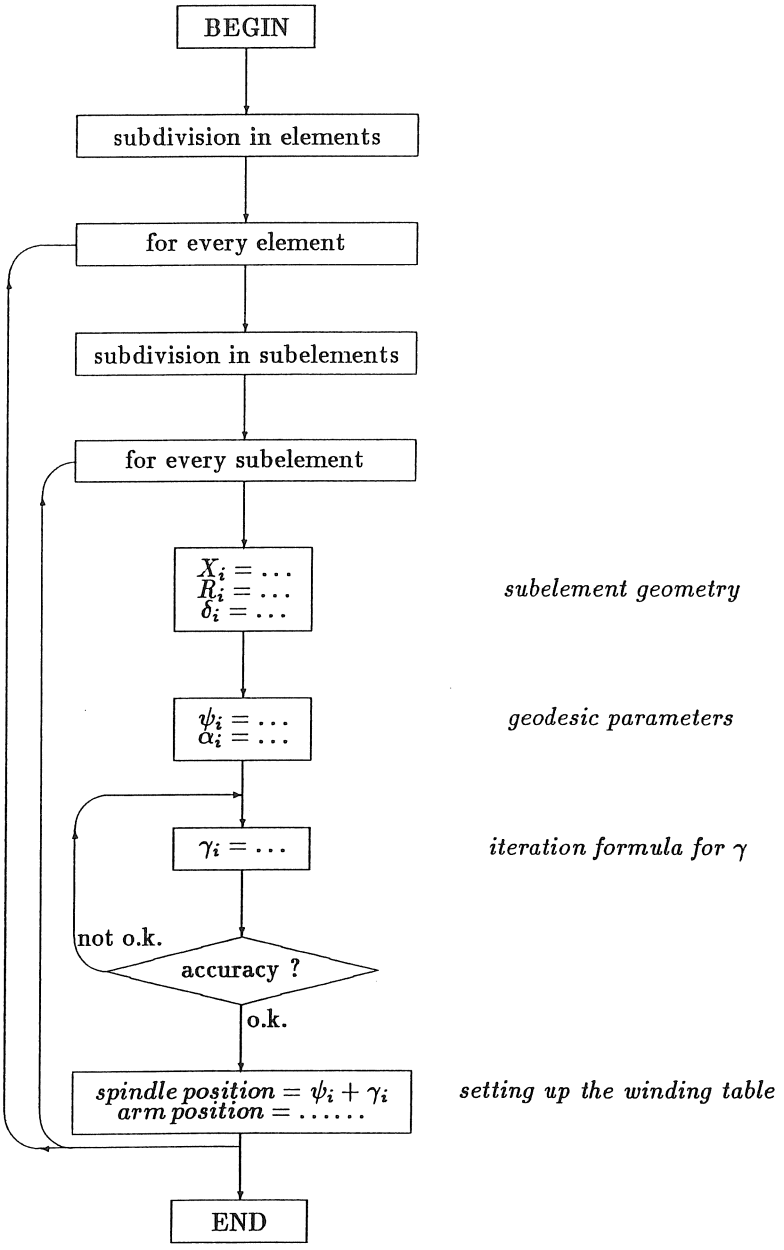

Figure 2.15: Scheme followed to compute the geodesic data and set up the corresponding ARM-SPINDLE table.

The geometry is divided up into several elements, such as cylinders, spherical, conical or torus segments. Further, each element is cut by a number of cross-planes, perpendicular to the axis of rotation, with their mutual distances chosen as to stabilize the subsequent iteration procedure (Fig. 2.16). The resulting sub-elements are approximated by conical segments.

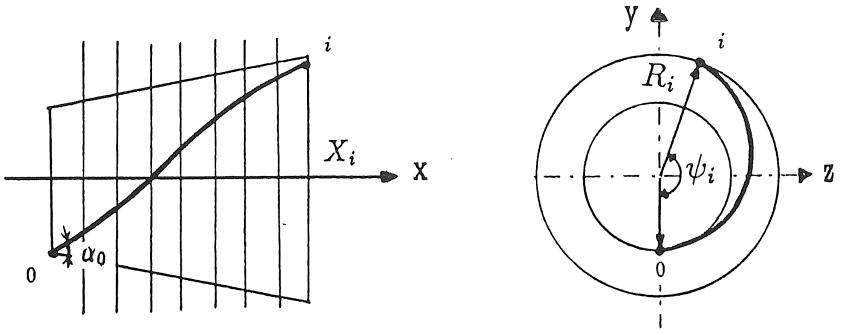

Figure 2.16: Computing geodesic lines on axisymmetric structures.

The computations start in the starting point, which is assumed to be situated at the top of the start cross-section . The starting point is usually chosen at the extremity of the mandrel. To allow for the fibre's returning in that end section, the starting angle α_0 with respect to the meridian curve must be 90°, perpendicular to the axis of rotation.

Successively, at every computation step a next point of the geodesic line is determined in the right-side plane of the next considered sub-element. Each new point is characterized by its coordinates (X_i,R_i) and by the span ψ_i with respect to the starting point and corresponding to the angle over which the spindle must turn to bring the considered point at the top of the cross-section.

Then, for every geodesic point, the angle γ_i is computed, over which the spindle must rotate in addition to make the tangent to the geodesic line cross the path of the winding eye (Fig. 2.17). This intersection determines as well the associated arm position, which is characterized by the angle θ_i between the vertical y-axis and the arm. Finally, the values to be tabulated are the spindle position ($\psi_i + \gamma_i$) and the arm angle θ_i.

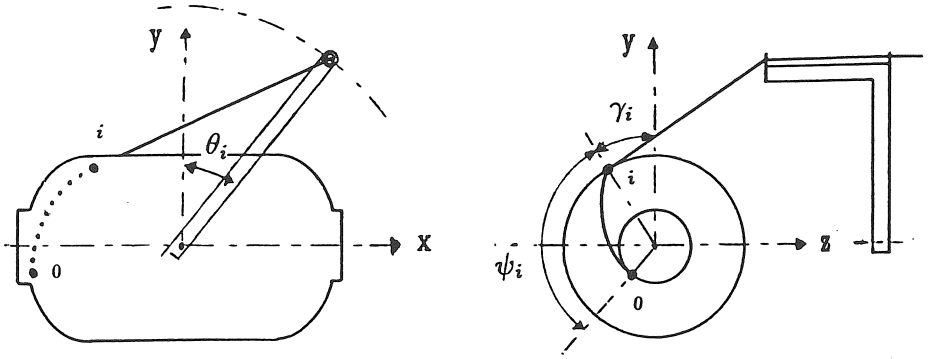

Figure 2.17: Additional spindle rotation γ_i, making the tangent to the geodesic line intersect with the winding eye path.

STARTING POINT

For the first point, the spindle rotation and corresponding arm position can be computed exactly, since the fibre angle α_0 is known to be 90°. The tangent to the geodesic line is then tangent to the starting cross-sectional circle of the mandrel. The spindle position is the angle γ_0 over which the mandrel must be turned to make the tangent intersect the circular path of the winding eye.

From Fig. 2.18 one can derive that :

$$\sin\gamma_0 = \frac{-R_0 \cdot Z_a + \sqrt{R_0^2 \cdot Z_a^2 - (Z_a^2 + Y_a^2) \cdot (R_0^2 - Y_a^2)}}{Z_a^2 + Y_a^2} \qquad (2.4)$$

In this equation it is assumed that the spindle and the axis of arm rotation are situated at the same height. Only simple adaptations are required for extension to non-equal height levels. Since the fibre is leaving perpendicular to the spindle, the arm angle θ_0 equals arcsin $\frac{X_0}{R_a}$. With $Y_a = R_a \cdot \cos\theta_0$, γ_0 can be computed. Both γ_0 and θ_0 constitute the initial conditions to be tabulated.

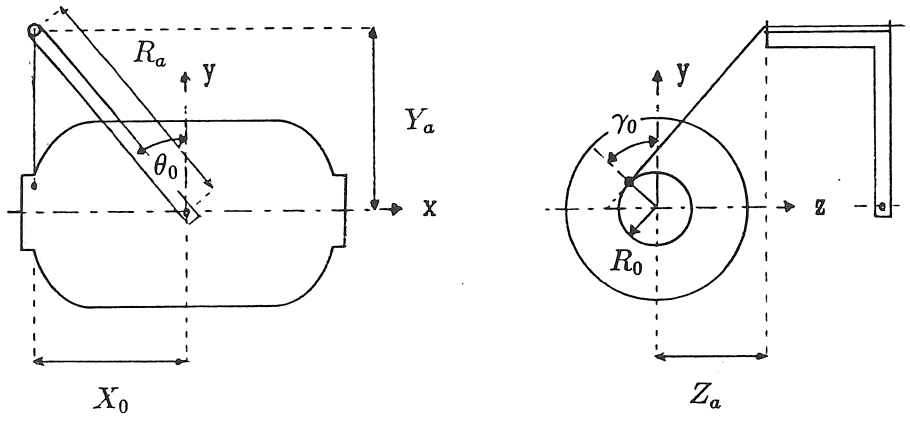

Figure 2.18: Starting conditions.

GEODESIC LINE COMPUTATION

The successive points representing the geodesic pattern are computed at the right side of each sub-element. The sub-elements are assumed to be conical, since this simplifies the geodesic calculations and does not significantly detract from the computation's accuracy. The coordinates X_i, R_i and ψ_i from the geodesic line at the right side of the sub-element are derived from the ones at the left side, which in their turn are end point coordinates from the previous sub-element.

Applying the law of *Clairaut* (Eq. 2.2) yields :

$$\sin\alpha_i = \sin\alpha_{i-1} \cdot \frac{R_{i-1}}{R_i} \tag{2.5}$$

The spanned sector ψ_i can be written as :

$$\psi_i = \psi_{i-1} + \triangle\psi \tag{2.6}$$

with

$$\triangle\psi = \frac{\alpha_{i-1} - \alpha_i}{\cos\delta_i} \tag{2.7}$$

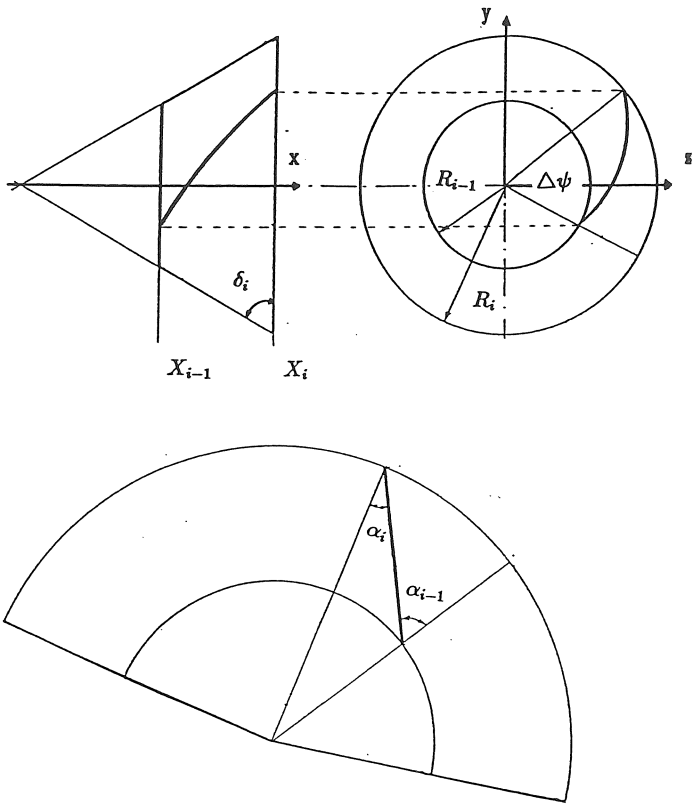

Figure 2.19: Stepped geodesic line computation on a conical surface.

DETERMINING THE TANGENT TO THE GEODESIC LINE

The equation of the tangent can be derived in two steps :

- First, the tangent to the geodesic line is computed, assuming that the considered point is situated at the top of the cross-section, in the vertical $x' - y'$ plane through the axis of rotation. The equation of the tangent in case the considered point, together with the spindle and mandrel, have turned over an angle γ_i, can then be obtained by an axis transformation, corresponding to a rotation γ_i around the x-axis.

The tangent to the geodesic line is defined as the intersection of two planes : (Fig. 2.20)

- (a) the tangent plane to the surface in the considered point
- (b) the plane through the considered point, making an angle α_i with the $x' - y'$ plane.

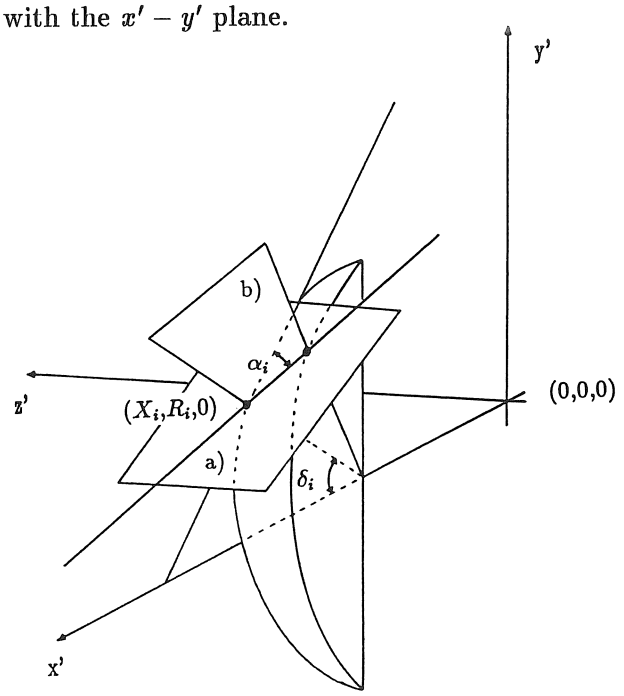

Figure 2.20: Tangent to the geodesic line, being the intersection of planes (a) en (b).

The tangent plane (a) can be described by :

$$\cos\delta_i \cdot (x' - X_i) + \sin\delta_i \cdot (y' - R_i) = 0 \qquad (2.8)$$

The equation of plane (b) can be expressed as :

$$x' - \frac{y'}{\tan\delta_i} + \frac{\cot\alpha_i}{\sin\delta_i} \cdot z' - X_i + \frac{R_i}{\tan\delta_i} = 0 \qquad (2.9)$$

- During winding, the instantaneously wound point is usually not situated at the top of the cross-section, but has already turned beyond that top. The angle γ_i, corresponding to this additional

rotation, can be computed by executing a transformation from the (x', y', z') coordinate system to the (x, y, z) system of coordinates : (Fig. 2.21)

$$\begin{aligned} x' &= x \\ y' &= y \cdot \cos\gamma_i + z \cdot \sin\gamma_i \\ z' &= y \cdot \sin\gamma_i - z \cdot \cos\gamma_i \end{aligned} \tag{2.10}$$

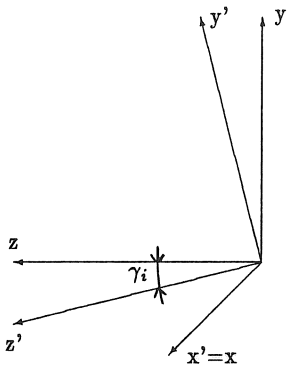

Figure 2.21: Axis transformation, corresponding to a rotation over an angle γ_i around the $x = x'$-axis.

The tangent equations then become :

$$\begin{aligned} \cos\delta_i \cdot (x - X_i) + \sin\delta_i \cdot (y\cos\gamma_i - z\sin\gamma_i - R_i) &= 0 \\ x - \frac{y\cos\gamma_i - z\sin\gamma_i}{\tan\delta_i} + \frac{\cot\alpha_i}{\sin\delta_i} \cdot (y\sin\gamma_i + z\cos\gamma_i) + \frac{R_i}{\tan\delta_i} - X_i &= 0 \end{aligned} \tag{2.11}$$

DETERMINING THE INTERSECTION AND THE ANGLE γ

The tangent must intersect the circular path of the winding eye, which has following equation :

$$\begin{aligned} x^2 + y^2 + (z - Z_a)^2 &= R_a^2 \\ z &= Z_a \end{aligned} \tag{2.12}$$

Together, (Eq. 2.11) and (Eq. 2.12) represent a 4×4 system in the unknowns x, y, z and γ_i. Since this system can not be solved analytically, following iterative procedure is applied :

First, a 3×3 system is solved, from which the coordinates of the intersection (X_h, Y_h, Z_h) can be expressed as a function of the unknown angle γ_i :

$$\begin{aligned} X_h &= f_1(\gamma_i) \\ Y_h &= f_2(\gamma_i) \\ Z_h &= Z_a \end{aligned} \tag{2.13}$$

Further, the angle γ_i must be searched, for which (X_h, Y_h) lies on a circle with radius $R = R_a$:

$$X_h^2 + Y_h^2 = R_a^2 \tag{2.14}$$

Since this equation in the unknown γ_i is not analytically solvable, γ_i will be determined by iteration, until the difference between the computed radius and the arm radius becomes smaller than a specified accuracy.

SETTING UP THE ARM-SPINDLE TABLE

From (X_h, Y_h) and γ_i, the spindle and arm positions, associated with the considered geodesic point, can be determined :

$$spindle\,position_i = \psi_i + \gamma_i \tag{2.15}$$

$$arm\,position_i = \arctan \frac{X_h}{Y_h} \tag{2.16}$$

After writing both values to the ARM-AXIS table, the process can continue with the next geodesic point, at the right side of the next sub-element. To allow for an element substitution by means of cones without affecting too much the accuracy, and in order for the iteration procedure to converge fast enough, a sufficient number of sub-elements must be defined.

Postprocessing routine

The postprocessor serves as interface between the *geo-computing* and the *controlling* program, and performs following tasks :

- Translating the tabulated spindle and arm positions into bits and setting up the WINDING table for a constant spindle step.

- Eventually smoothing sudden jumps in the continuity of the WINDING table profile. Although computed correctly, these jumps should be avoided, since they imply unwanted high arm accelerations.
- Setting up the STARTING table, which contains the spindle positions at every new half winding cycle.

In the following paragraphs, these tasks will be individually discussed.

SETTING UP THE WINDING TABLE

Translating angular positions into bits

During the winding process, the spindle and arm positions are measured by encoders. The spindle encoder returns two series of 1024 pulses pro revolution, with a 90° shift. Hence, the total number of pulses pro spindle encoder revolution is 4096. Analogous for the arm encoder, 4000 pulses pro encoder revolution are obtained. Further, the transmission ratio between the encoder axis and the axis to be measured must be taken into account. This ratio is 10 for the spindle and 15.17 for the arm axis. Consequently, every revolution is subdivided into :

- $10 \times 4096 = 40960$ bits for the spindle, and
- $15.17 \times 4000 = 60680$ bits for the arm axis.

To transform the computed arm and spindle positions from *radians* into *bits*, these must be multiplied by respectively a factor $\frac{60680}{2\pi}$ and $\frac{40960}{2\pi}$.

Computing the arm positions for a constant step of spindle rotation

In the *geo-computing* module, the computational step for the spindle or mandrel rotation was not taken constant; the tabulated values corresponded to geodesic points at the right side of each sub-element and the division in sub-elements was optimized as to guarantee a fast iteration convergence. However, to control the arm motion as a function of the spindle position, a constant spindle step is recommended.

This step can be chosen by the user. If too high, the WINDING table is "oversmoothed", thereby decreasing the winding's accuracy. A step which is too small on the contrary provides better accuracy but causes long computer runs. Once the spindle step has been defined, the arm positions to be tabulated can be determined by linear interpolation between the previously tabulated values.

SMOOTHING PROCEDURE

In order to smooth out eventual abrupt variations in angular velocity, a quadratic smoothing operation is carried out, with the number of incorporated adjacent points adjustable between 2 and 14.

SETTING UP THE STARTING TABLE

Usually, when transforming the ARM-SPINDLE table into a table with constant spindle step, the last tabulated point will not correspond to a multiple of the spindle step. Consequently, the end of the WINDING table will not coincide with the exact spindle position, where a next half winding cycle or reverse motion should be started. However, since the winding process consists of a long series of half winding cycles, which all use the same WINDING table, small errors are very easily accumulated. To avoid this error accumulation, each new half cycle must be started at the correct position. Therefore, the spindle positions at each new start are determined exactly and stored in the STARTING table.

Controlling program

CONTROL PROCEDURE FOR GEODESIC WINDING

During the winding process, the *controlling* program must take care that, by a proper arm control, the fibres are laid down onto the mandrel along the desired geodesic pattern. For this control purpose, the program uses the WINDING and STARTING tables, resulting from the *geo-computing* and *postprocessing* programs. These tables contain data concerning the motion which the arm must describe in function of the mandrel rotation for one half winding cycle, and the exact successive spindle positions where new half cycles should start.

The control is based on a POSITION FEED-FORWARD principle; the basic idea is to force the arm to move to a position, corresponding (according to the table) to the position the spindle will have reached at the next control step. To perform this control, the actual spindle position and speed, together with the actual arm position must be known. Since the spindle velocity remains quite stable, the spindle position at the next control step, at the next interrupt, can be quite well predicted (*will_spindle*). To this *will_spindle*, an associated *will_arm* can be computed, by interpolating between the known arm positions from the WINDING table, corresponding to the spindle positions just before and beyond the predicted *will_spindle*.

At every interrupt, e.g. 5 ms, the actual spindle and arm positions are measured (*is_spindle*, *is_arm*). It must be noticed that, due to a 16 bit representation of integers, these can only vary between - 32768 and 32767. The *is_spindle*, which should continuously increase, must be situated within this interval. When exceeding 32767, the counter will continue by overflow from - 32768.

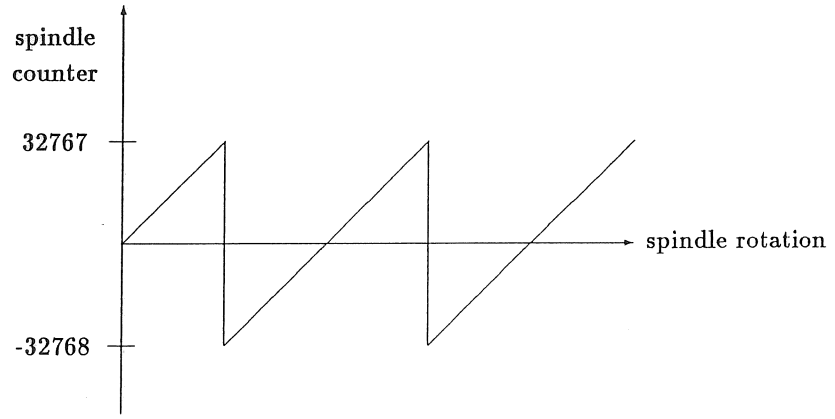

Figure 2.22: Spindle counter.

By a simple binary manipulation, putting the most significant bit, -the parity bit-, to zero, it is taken care of that only the 15 least significant bits of the *is_spindle* value are considered. Consequently, the *is_spindle* value is always positive and varying between 0 and 32767, which simplifies the computations.

Following steps are executed :

Determining the position error

First the measured arm position (*is_arm*) is compared to the predicted value from the previous step, which is the previous *will_arm*. Their difference represents the arm position error, in case the actual spindle position corresponds to the predicted one, (the old *will_spindle*).

$$error = (is\_arm) - (will\_arm) \tag{2.17}$$

Since the spindle position can be quite well predicted, - the spindle velocity being more or less stable -, this computed position error provides a good approximation of the real error. Only at the start and at the end of the winding process, the spindle will respectively accelerate and slow down.

Determining the next spindle position

The next spindle position is determined, assuming a constant speed. The difference between the actual and the previous spindle position will probably also be the step between the actual and the expected position in the next control step. In the computation of the future position, again an eventual integer overflow must be considered, so a *will_spindle* will be obtained between 0 and 32767.

Determining the reference spindle position

The next step looks for a further spindle position (*ref_spindle*), for which there has been computed a tabulated arm position. In the WINDING table, the reference spindle positions have constant mutual distances. For every new cycle, the new reference positions can be computed by adding the start position of that particular cycle to the tabulated reference positions. These references are manipulated as to only vary between 0 and 32767.

For control purposes it is always the reference spindle position beyond the computed *will_spindle* that must be determined. Since the measured spindle position describes a sawtooth, four different cases can occur when searching the proper reference :

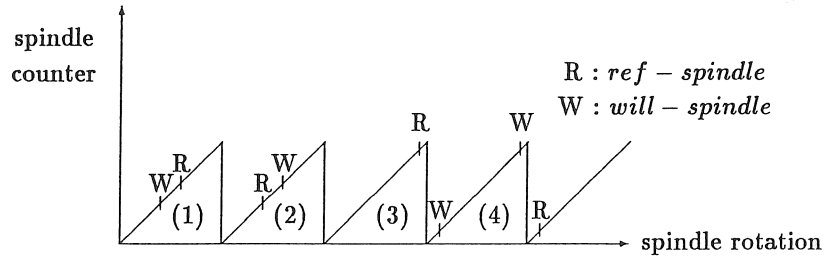

Figure 2.23: Determining the reference spindle position.

In the cases 1 and 4, the *ref_spindle* lies at the right side of the *will_spindle*, and the desired result is obtained. In the situations 2 and 3, a further *ref_spindle* must be looked for, beyond the *will_spindle*. In case the actual half winding cycle is not yet finished, a next candidate-reference position can be found by adding the table step to the previous reference. However, in case the previous reference spindle position corresponded to the last point in the WINDING table, one should continue with the first reference point of the next cycle, which can be found in the STARTING table.

Determining the next arm position

To determine the *will_arm* position, corresponding to the *will_spindle* position, a linear interpolation is carried out between the tabulated reference positions.

P-I - control of the output voltage to the arm motor

With the desired *will_arm* position, the value of the output voltage to the DC arm motor must be determined. This voltage corresponds to a certain speed which is given to the arm axis.

In case only a proportional action is accounted for, the output voltage becomes :

$$U_{out} = K' \times ((will\_arm) - (is\_arm)) \tag{2.18}$$

The D/A convertor has been adjusted as to make 2048 bits correspond to an output voltage of 10 V. 10 V input makes the motor rotate at

3000 rpm. With in addition a transmission ratio of the gear casing equal to 25.4, the proportional constant K' has been found to be $\frac{11}{I}$, I being the interrupt time. However, when only incorporating a proportional action, small residual errors occur, which detract from the winding's accuracy. To remove these errors, an integrated action is included in the output voltage determination. Each time, the position errors are summed and a term, proportional to this sum, is added to U_{out}, yielding :

$$U_{out} = K \times ((will\_arm) - (is\_arm)) + L \times \sum(position\ errors) \qquad (2.19)$$

Experimentally, following control constants have been obtained :

- L (integration constant) : $\frac{0.4}{I}$
- K (proportional constant) : $\frac{10.5}{I}$

For stability reasons, adding an integrating action must be compensated by a slight decrease of the proportional action. In case the influence of the summed position errors becomes too high, the integration is set to zero.

HOOP WINDINGS

In the controlling program also the facility is provided to directly control the arm as a function of the spindle rotation, to apply hoop windings on a cylindrical surface. The arm is controlled as to lay down the fibres adjacent to each other in the circumferential direction and over a certain length, eventually in several layers.

ZERO AND START ARM POSITION

Before the winding process can start, the arm must be calibrated to know its zero reference position. This zero reference corresponds to the vertical arm position with the winding eye above, and must be manually installed. From here, the arm can be moved to the position from which the winding process is to start. In case of geodesic winding, this point corresponds to the first arm position in the WINDING table. In case of hoop winding, the start arm angle is determined within the control program from the cylinder and arm length.

ACCURACY OF POSITION FEED-FORWARD

For applications where no abrupt changes in arm speed occur, as e.g. for winding tubes, position feed-forward control provides high accuracies, with arm encoder errors being smaller than 1 bit. In case of the spinning pots however, described in 3.3.3.1, the arm had to move quite discontinuously and errors of 20 to 30 bits did occur. In this context it would be interesting to also control the spindle, since this would allow for sudden winding speed variations to be met, without affecting the winding's accuracy.

FURTHER FACILITIES

- The user can choose the start side of the mandrel, depending on where the fibre can most easily be fixed.
- The axis can be given an initial speed before starting the winding process.
- During winding, positions and position errors are stored, which can be checked and graphically presented afterwards. From the successive positions, also arm speeds and accelerations can be computed. This error control can be useful to experimentally determine the P-I - constants.

2.5.2 Winding robot

2.5.2.1 Equipment description

For winding non-axisymmetrical components, a winding robot has been used.

The robotic filament winding cell (Fig. 2.24) consists of a fibre feeding unit, which takes care of fibre tension and impregnation, a robot to which the fibre pay-out eye is fixed, and a mandrel support on which the motor for the mandrel rotation is mounted.

The robot is an articulated PUMA-762 with six degrees of freedom. The axis carrying the mandrel is through a specially developed hardware board linked with the robot and thereby provides a seventh degree of freedom. The robot is off-line programmable in the VAL-II language of Unimation. A software routine takes care of the synchronization between the robot and the external axis.

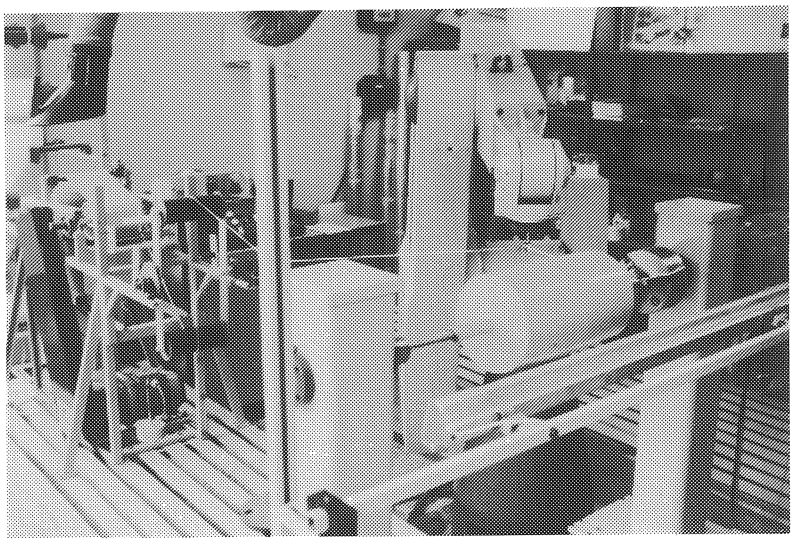

Figure 2.24: Robotic filament winding cell.

2.5.2.2 Robot control for geodesic winding of non-axisymmetric components

Controlled filament winding of non-axisymmetric structures is far more complicated than in case the component has an axis of symmetry (4.2); since the winding process does not show a repetitive character anymore, a whole series of geodesic lines are required for a complete mandrel coverage. Further, generating these geodesic data is also more complex because the simple law of *Clairaut* (Eq. 2.2) does only apply to surfaces of revolution.

In order to control the robot as to move along trajectories which result into the wished-for fibre placement, following steps are taken; first, the mandrel geometry is drawn within the ANVIL-5000 CAD system, which is a three-dimensional CAD surface modeller. The corresponding geometrical data are made accessible for an external program by creating an IGES file. IGES (*Initial Graphics Exchange Specification*) stands for an international standardized format for interchanging data between CAD systems. Thanks to the IGES format, the mathematical parameters which describe the mandrel's geometry can be extracted

and used in subsequent calculations.

Once the geometry has been defined, the computation of winding paths can start. A computer code *CAWAR* (*Computer Aided filament Winding of Asymmetrical shapes using Robots*)(Ref. [68]) has been developed to compute geodesic paths on components which are composed of several individual surfaces of revolution. The calculations are based on solving the differential equation for a geodesic line (Ref. [9]), the parameters of the differential equation being determined by the geometry of the surface, stored in the IGES file.

Beside computing geodesic lines, *CAWAR* continuously checks their curvatures, to assure that no local concavities do occur. For, in case the geodesic line is locally concave, the fibre will be released from the mandrel's surface and follow a shorter path through the air.

Twisting of the fibre is also checked. When tapes are used, large twists can lead to wrinkles in the surface. Fibre twisting however depends on the support conditions and the robot strategy. Therefore, a model of the robot is incorporated within the geodesic winding software.

Once the successive geodesic fibre paths have been determined and linked together, the corresponding pay-out eye positions and according angular positions of the mandrel axis can be calculated. These off-line winding data can then be down-loaded to the robot controller and winding can start.

A more detailed description of the robotic control is given in chapter 4, in the light of geodesic winding a T-connection.

2.6 Conclusion

As an introduction to the whole issue of filament winding design, a detailed discussion on winding processes and attending aspects has been considered to be relevant. Consequently, chapter 2 has treated the successive processing steps involved in filament winding. Beside common winding processes, equipments and their evolution, also the winding units available at the Department of Mechanical Engineering have been described.

Chapter 3

Design of axisymmetric filament wound composites

3.1 Introduction

The first chapter has discussed composite design in general, the successive steps the designer has to go through and the tools he disposes of. It has been emphasized that an important complication in composite design is the fact that configuration, material and means of manufacture are generated simultaneously and interact with one another. Hence, a more integrated design method must be followed, taking into account all occurring interplays.

Since this thesis treats the design of filament wound composites, it is obvious that the design methodology that will be presented deals with filament winding interactions and limitations. First, the filament winding related design considerations, including the tolerances joining the manufacturing process, design aspects related to the tooling and restrictions imposed by the applied winding technique, will be discussed. Afterwards, a design methodology, in which these additional winding related aspects are integrated, is described and applied to two practical examples.

A not yet fully investigated design parameter in filament winding is the winding strategy, in fact a degree of freedom, determining the interweaving of the fibres. Therefore, an investigation of the influence

of winding strategy on the composite's performance has been carried out, which will be summarized in the fourth section.

To conclude, some reflections will be made concerning the application of detailed stress analysis in filament winding design.

3.2 Additional design considerations, related to filament winding

3.2.1 Tolerances related to the manufacturing process

3.2.1.1 Resin handling

In the filament winding process, there exists a variety of manufacturing factors which affect the structural properties of the filament wound component. In view of a realistic quality insurance, all these factors should be considered during the design stage, in order to give the designer a notion about the feasible tolerances so that he can apply appropriate safety factors.

Resin handling during fabrication is a first important factor in that it strongly influences the final matrix composition. The possibility of errors in the resin formulation and the lack of uniformity in the mixing process should be evaluated during the design stage for their effect on the ultimate strength of the product.

Further, resin content and distribution are of importance for the weight and thickness control. From a strength point of view, excessive variation results in uneven stress distributions and areas where failures can be initiated. When compared to wet winding, prepreg tapes allow for the resin content to be easier controlled.

Also important are the time aspects involved in materials handling. Resins in both mixed state and prepregged materials have very precise specifications for the period of time they can be stored at room temperature; exposure to room temperature conditions results for either of these forms in some degree of resin advancement. This limited pot-life should be taken into account in the design process.

A further consideration for resin systems is the allowable tolerance band on temperature during a cure cycle. Both rate of temperature increase and level of cure temperature should be regarded. A ramp-up that is too fast will cause a surface skin curing and may ultimately inhibit resin flow through the composite structure during cure. Con-

versely, a slow ramp-up will result in a viscosity reduction before cross-linking of the resin system begins to take place. This could imply the resin draining from the part as it becomes too fluid. If the actual cure temperature sustained for a resin system is either too high or too low, it will also affect the final part properties; if too high, it may cause the resin to embrittle, which could result in discoloration and charring of the product. Too low cure temperatures could cause inadequate curing, which possibly only occurs internally in the structure and therefore might be undetectable for non-destructive inspection methods.

An additional consideration is the care with which autoclave parts are bagged for vacuum conditioning and pressure application. Both designers and manufacturers should take care that bagging can take place without any wrinkling of the bag during vacuum application, because this would cause a crease in the final part, acting as stress riser and resulting in premature failure. Also the application of the bleeder cloth must be considered. Applying too much bleeder and a too open cloth might cause resin deficiency in critical areas, resulting in a high void content, strength degradation and unacceptable surface condition.

Last but important factor to be mentioned is the moisture environment during manufacture. Nowadays, many manufacturing buildings are being converted to a controlled moisture condition. However, if the manufacturing environment does contain moisture, safety factors must be incorporated in the design to allow for the degradation effects.

3.2.1.2 Fibre handling

Prior to their application, the fibres must be stored at appropriate environmental conditions in order to maintain their full physical properties.

Also during manufacture, a poor fibre guidance, over pulleys and through pay-out systems, can affect the fibre quality and should therefore be reviewed during the design. For example, common carbon fibres require a specific minimum pulley diameter (75 to 100 mm) to minimize breakage of the high-modulus filaments. Aramid fibres impose special demands to the pulley's or roller's surface quality; they require a 1.5 to 1.75 μm satin finish in order to minimize the wear on the pulley from the fibre and ultimately the abrasion of the fibre by the worn pulley.

Fibre pay-out systems also have an effect on the variation in band width, the amount of gapping, the fibre band density and uniformity. Variations in band width result in resin-rich areas between fibre strands, thereby causing structural weak points.

3.2.1.3 Winding tension

Winding tension strongly influences the final properties of a filament wound component (2.3.1.2) and should therefore also be incorporated in the design process. In addition to the influence of winding tension on the resin content and distribution, also its effects on fibre prestress and mandrel deflection must be considered. The "optimum" winding tension differs from manufacturer to manufacturer, the limits generally varying between 1.1 and 4.5 N pro fibre strand (Ref. [71]).

Concerning winding tension, first a problem of limited control can be mentioned. Although there exist advanced tension control systems, many industrial winding units primitively control the fibre tension by means of weights. Hence, the resulting tolerances on the delivered strength of the composite structure must be translated into appropriate safety factors.

Second, the designer has to deal with some practical problems, automatically involved when winding certain shapes. Sharp edges, for example, will cause the tensioned fibre to cut in at the edges. On the contrary, laying fibres across a wide flat surface will result in very low tension conditions. So, it is important for the designer to evaluate these aspects prior to his design.

3.2.1.4 Winding angle

A last but important consideration is the effect of winding angle tolerance and pattern-closing errors on the strength and stiffness properties, designed into the composite. Each winding machine is limited in the accuracy with which winding angles can be realized. Depending on the number of winding circuits, needed to close a winding pattern, the slightest deviation in winding angle, e.g. only of the order of minutes of arc, can result in significant closing errors of a dozen of millimeters.

3.2.2 Design aspects related to tooling

3.2.2.1 Dimensional tolerances

The final dimensions of a filament wound component and their tolerances very much depend upon the type of mandrel used and the thermal expansion characteristics of the mandrel material (Ref. [90]). As the mandrel is associated with the composite through its final phase of manufacturing, it is subjected to the same temperature history of the cure cycle as the composite component itself. Hence, the designer must consider the dimensions of the mandrel at the specific temperature of cure.
Temperature effects can be useful to simplify mandrel removal. In case of pure cylindrical tubes, for example, mandrels can be used with higher expansion coefficients than the composite. Curing of the wound part around the expanded mandrel dimensions helps to reduce the size of voids and to densify the composite. When cooling down, the mandrel contracts more than the composite, thereby allowing an easy mandrel removal by pushing off or through.

Another tooling consideration is the residual stress state which could be built up in the mandrel during fabrication and which could result in some changes in mandrel shape upon heat-up during cure of the composite.

A third important aspect is the surface condition required on the final composite part. The internal surface is always smooth because it conforms to the mandrel. The external surface however will always be rough, unless the component is cured under pressure to an external shell. Applying vacuum techniques also improves the surface quality but often a finishing step is required. After winding, composites are frequently ground to their final dimensions, sometimes using an external sacrificial glass fibre wrap.

3.2.2.2 Cost aspects

Nowadays, designers dispose of a whole series of mandrel types and mandrel materials (2.3.2), from which they have to make an appropriate choice to suit the application. In this choice, not only technological requirements but also cost is an important factor. Mandrel cost is partly determined by the mandrel material but also by its complexity. Here the designer has to deal with a trade-off between the simplicity

of mandrel design, accompanied by low mandrel cost, and the ability of composites to reduce the number of required parts, which yields a lower assembly cost. Hence, a compromise will have to be considered, resulting in a reduction of the total cost of the final structure.

3.2.3 Restrictions imposed by the winding technique

It is obvious that the allowed complexity and realizability of the design depend upon the available manufacturing equipment. There is the winding machine itself, limiting the dimensions of the component and there is the applied winding technology, determining the feasible winding patterns and laminate lay-up.

The type of winding unit used, its size and degrees of freedom, together with its control capacities, restrict the attainable geometries and the dimensions that can be wound. For example, two-axis winding machines are confined to simple axisymmetric structures, whereas robotic winding cells with up to seven degrees of freedom can handle more complex non-axisymmetric shapes. Along with symmetry aspects, also concavity must be considered. In fact, concave parts have been unwindable for a long time. However, thanks to new technologies, as e.g. the use of thermoplastic prepregs, winding concave shapes has become possible.

Composites offer the great potential to tailor the design to optimally suit the application, as they allow the fibres to be aligned with the principal load directions. In filament winding however, the freedom of choosing the fibre angles can be quite restrictive, depending on the applied winding technique.

When performing geodesic winding (2.3.4.1), the law of *Clairaut* must be regarded, which, for a surface of revolution, can be expressed as : (Ref. [66])

$$r \cdot \sin\alpha = constant \tag{3.1}$$

indicating that the product of the radius r at a specific point on the mandrel and the corresponding fibre angle α, -with respect to the meridian curve through that point-, equals a constant value. This means that once a starting position and starting angle of the fibre path have been chosen, the whole trajectory is uniquely defined and only depends on the mandrel's geometry.

For the simple case of a pressure vessel, where the fibre is returned

at the nozzle, α being 90° there, the constant value is equal to the outer nozzle radius R_0 (Fig. 3.1).

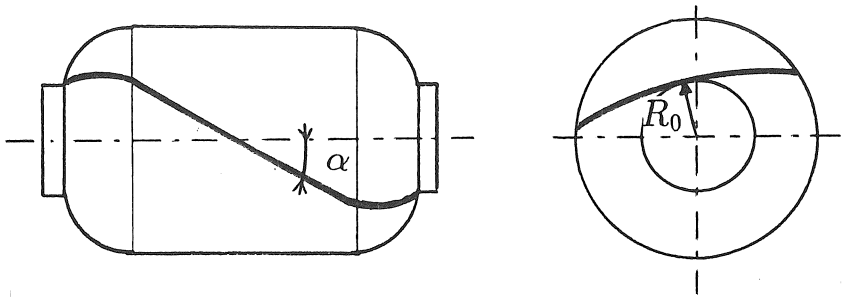

Figure 3.1: Geodesic line on a pressure vessel.

As the geodesic path, the laminate thickness in every point is also related to geometry. Suppose the pressure vessel is covered by $N/2$ half windings in the $+\alpha$ direction and $N/2$ half, returning windings in the $-\alpha$ direction. Assume the fibre strand which is wrapped around the vessel's mandrel has a wet (fibre + resin) cross-section A. The thickness t of the corresponding laminated shell at a section with radius r can then be expressed by following equation :

$$t = \frac{N \cdot A}{\cos\alpha \cdot 2\pi r} \tag{3.2}$$

where : t : composite thickness
N: number of windings along the circumference
A: wet fibre cross-section
α: fibre angle with respect to the meridian curve
r : radius

The restricted freedom in fibre orientations and laminate lay-up clearly indicates that, when performing geodesic winding, the scope for obtaining a winding pattern which is optimal with respect to the applied mechanical loads is rather limited.

On the contrary, semi-geodesic winding, in which friction effects are used to deviate from the geodesic lines, allows much more flexibility, thereby enabling a better alignment of the reinforcement with the principal load directions.

Hence, from the design point of view, it is recommended to use e.g. prepregs or thermoplastics, which do not require restrictive geodesic winding and consequently provide more optimization potential.

Not only geodesic paths but also winding strategy, standing for the time sequence of the fibre lay-down, is determined by geometry (3.4). Once the geometry is defined, also the winding strategy is completely fixed. However, small changes in geometry or dimensions can result in significant variations in winding strategy. For a fixed geometry, winding strategy can yet be varied by deviating from geodesic lines or by indexing. In case of indexing, the mandrel axis is additionally turned over a certain angle at the end of each winding cycle, to make the fibre restart and continue its pattern at the desired location.

As with geodesic winding the fibre angle and ply thickness definitely vary across the filament wound component, it would be a coincidence that one single winding pattern could meet the required laminate thickness all over the structure. Consequently, the design will have to be translated into several successive manufacturing steps, each of them corresponding to a specific layer of windings, which together enable the structure to resist the applied loads.

3.3 Design methodology

3.3.1 Design idea

A composite designer has to be composite minded and should tailor his design as to make optimal use of the great potential offered by fibre reinforcement. Unfortunately, designing composites is often just a substitution of metals in previously designed metal components. To avoid this substitution, a composite philosophy should be applied from a preliminary design stage on, before metal's thinking fixes the configuration.

The design is a compromise between, on the one hand, what is optimal according to stiffness and strength and, on the other hand, the restrictions imposed by the winding process. Additionally, the result must meet all the requirements of the customer. The design then finally leads to a semi-optimal geometry and winding pattern.

Further on, a design methodology for filament winding will be discussed, by referring to some practical design applications. A first example regards composite spinning pots, which "unfortunately" are just

a substitution of their aluminum equivalents. The second example concerns pressure vessel design, allowing an optimal definition of the dome shape. In both cases, a combination of an epoxy matrix, reinforced by E-glass fibres has been used. The corresponding strength- and stiffness computations have been performed with Scotchply data (Table 3.8), as these closely conform to the filament wound properties (3.4.5.1).

But before going into details about these examples, first the applied design methodology, presented in Fig. 3.2 will be explained.

3.3.2 Design steps

Starting from the specifications of the end product, the designer tries to materialize his design into a well-defined geometry, which afterwards has to be "compositized".

In order to provide a starting-point for building up the laminate, a simulation of the loaded geometry with an isotropic material is performed. The resulting stresses are then transferred to the composite structure which can be subdivided into parts of simple geometry. To define optimal fibre angles and ply sequences in these subdivisions, the transferred stresses can be used as input for *netting analysis* (appendix B) or *classical laminate theory* calculations (appendix A).

Unfortunately, due to the restrictions imposed by the winding process, the ideal fibre angles and ply thicknesses can not always be achieved. Consequently, successive winding steps must be investigated to meet as good as possible the optimal laminate lay-up in the different subdivisions of the structure.

Once the successive winding steps, resulting in a global coverage pattern and a sub-optimal ply stacking, have been defined, the laminate lay-up in every point can be determined. This lay-up can then be used as input to some more detailed finite element analysis. The lay-up is then adapted until enough strength and stiffness are achieved to permit the structure to operate safely.

In case of axisymmetric structures, a winding step can be defined using the data of one single geodesic circuit, which is repeated until the whole surface is covered. These geodesic data are very easy to calculate when using *Clairaut's* law (Eq. 3.1). The corresponding lay-up only varies with the length coordinate and can be introduced manually into the finite element code.

For non-axisymmetric structures however, a whole set of different

geodesic lines are needed to totally cover the surface. Computing geodesic lines now requires solving differential equations (Ref. [9]). As the lay-up definition is much more complicated, it is interesting to automatically generate the lay-up data for the finite element analysis out of the winding patterns (4.4).

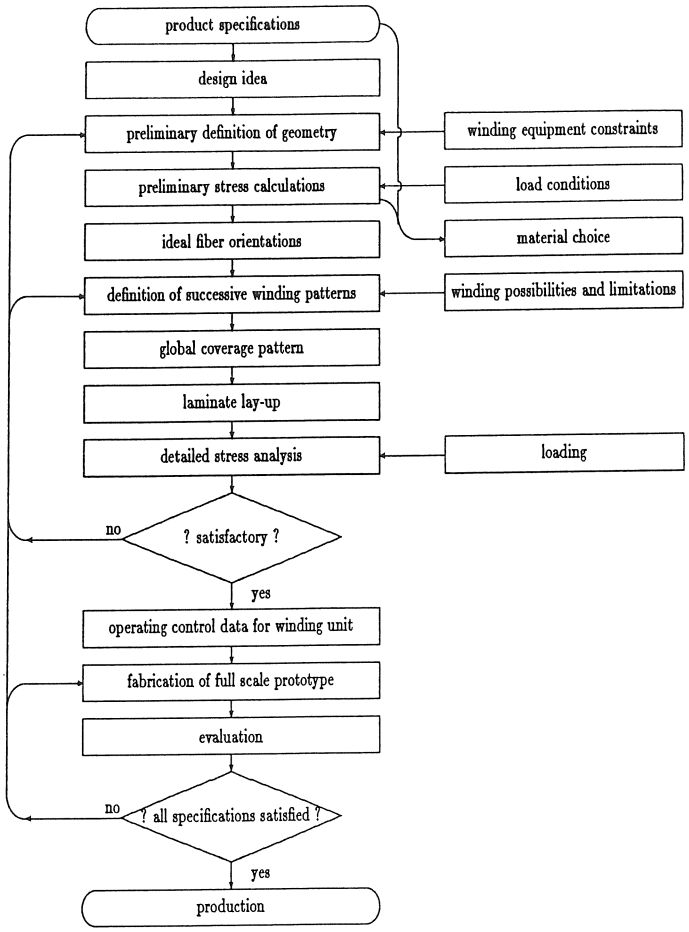

Figure 3.2: Design methodology for filament winding.

3.3.3 Design examples

3.3.3.1 Spinning pots

To illustrate the above mentioned design strategy, a practical example of filament wound pots for spinning textile thread bobbins will be presented. This project concerns a substitution of existing aluminum spinning pots by a fibre reinforced composite copy to provide better corrosion resistance and to allow for more thread production pro spinning unit, thanks to a smaller wall thickness.

The thread spinning process

A classical aluminum spinning unit consists of following parts :

- A centrifugal spinning box, made of an Al Mg Si alloy and shown in cross-section in Fig. 3.3. The pots are made by shell moulding, followed by a turning operation and thereby showing only poor corrosion resistance.
- The box is closed by a 400 g bakelite cover and sealed, when rotating, by a self-tightening, glass fibre reinforced polypropylene spring. The aluminum pot, with cover and spring, is shown in Fig. 3.4.
- The spinning boxes are driven by non-standardized 300 to 400 W motors, by means of bronze coupling parts, shown in Fig. 3.5. The motors have a lifetime of 2 to 3 years. To obtain an efficient spinning operation, the boxes must rotate at 7000 rotations pro minute. The acceleration from 0 to 7000 rpm takes 30 to 40 seconds. The motor slows down in 80 to 100 seconds.

While the pots are rotating, a glass tube translates 30 times pro minute up- and downwards through a hole in the cover. This tube continuously delivers the thread to be spun. The thread reacts in contact with the sulphuric acid atmosphere in the pot, while being slung against the inner wall of the pot, and generates there an internally wound thread bobbin.

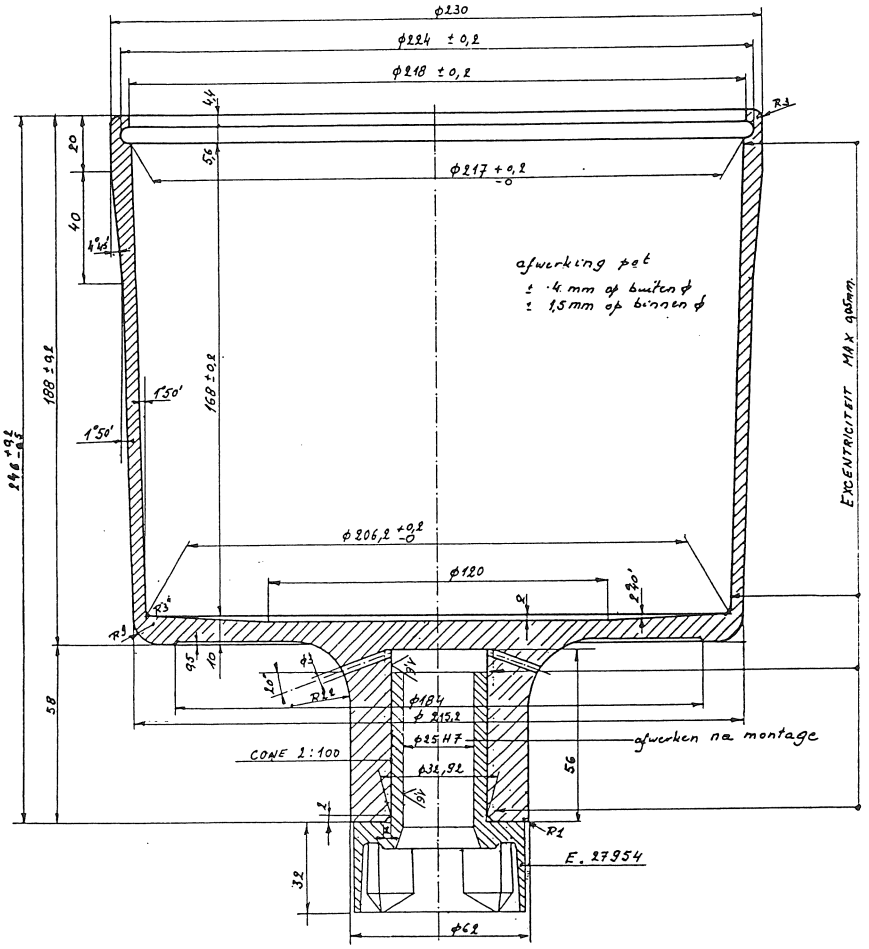

Figure 3.3: Cross-section of the aluminum spinning pot with bronze coupling part to the driving motor.

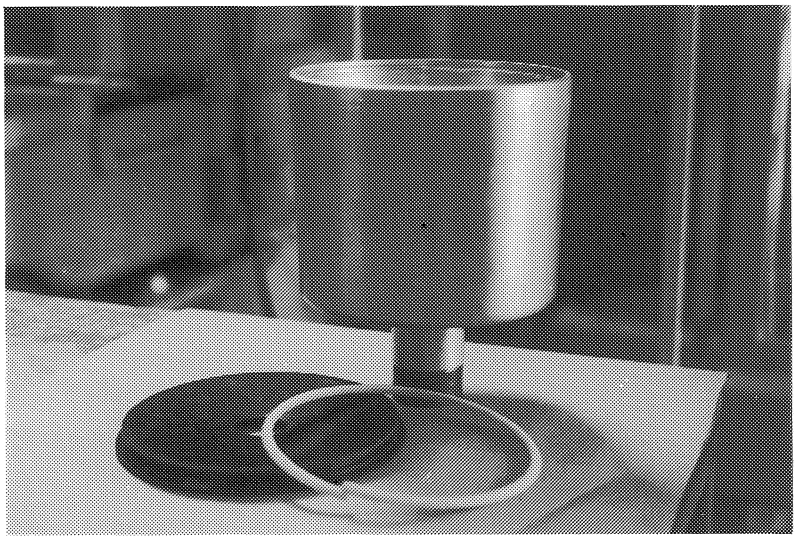

Figure 3.4: The aluminum spinning box with bakelite cover and polypropylene sealing spring.

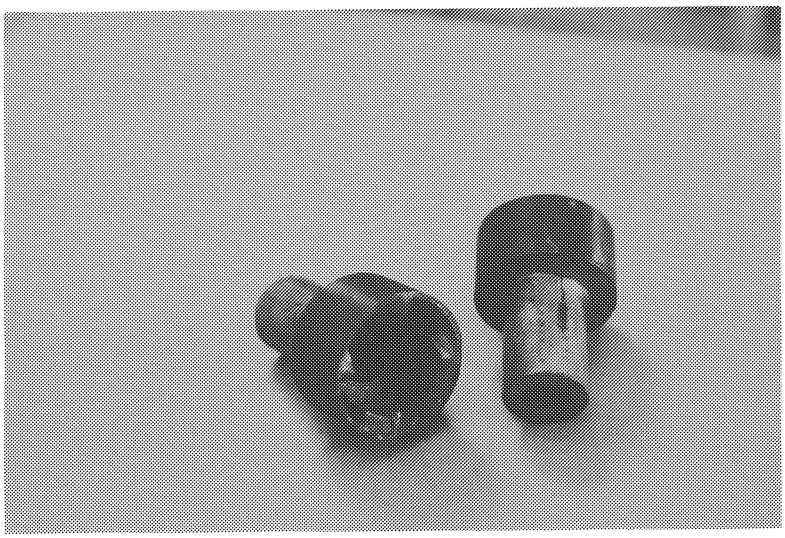

Figure 3.5: Bronze coupling parts to the driving motor.

Motives for substitution by composites

During spinning, 1 liter acid drops move upwards inside the pot, causing a severe corrosion of the aluminum at the upper edge, on the spot of the groove which is supporting the cover (Fig. 3.6).

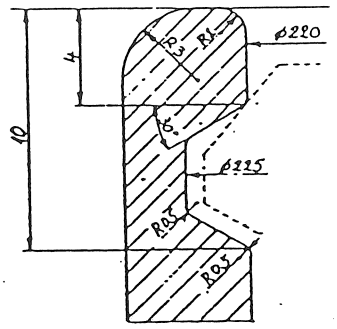

Figure 3.6: Cover support groove, location of corrosion.

To protect the aluminum, the cylinder surface is covered by a phenol paint. However, at the ring groove, this coating is difficult to be applied and hence, the paint can not provide sufficient protection. Furthermore, at the outside of the pot, the acid drips downwards and cristallizes. The resulting salt also contributes to significant corrosion. Replacing the aluminum by a corrosion resistant composite could solve the corrosion problem, thereby increasing the boxes' life time and reducing the maintenance costs.

Beside an improved corrosion resistance, there is a second composite asset, enabling larger bobbins to be produced within one pot. For, the distance between adjacent spinning units is 260 mm and since the boxes have a 240 mm diameter, a closer positioning is impossible. Consequently, exploiting the wall thickness, thereby increasing the internal diameter for constant external dimensions, would provide important economical advantages in that it would allow the end products to become larger; hence, with the same number of spinning positions, more thread length could be produced. With this object in view, composite spinning boxes surely are attractive, since they would show reduced centrifugal stresses thanks to their lower density. Furthermore, by appropriately orienting the reinforcement, the intrinsic strength of the fibre reinforced composite could result in a smaller wall thickness.

Composite spinning pot concept

Because of the boundary conditions imposed by the environment, the shape of the aluminum pots had to be copied. As no geometry optimization was allowed, the design was constrained to the material choice and the investigation of successive winding patterns, resulting in a satisfying pot with the desired performance.

The selection of matrix and fibres has been largely determined by the experience at K.U.Leuven and by the cost and delivery terms of these materials. Consequently, a decision was made in favour of an acid resistant epoxy, reinforced by cheap E-glass fibres.

To be able to design glass/epoxy composite versions of the existing aluminum pots, these were first thoroughly examined. A finite element model has been set up, from which the mesh is shown in Fig. 3.7.

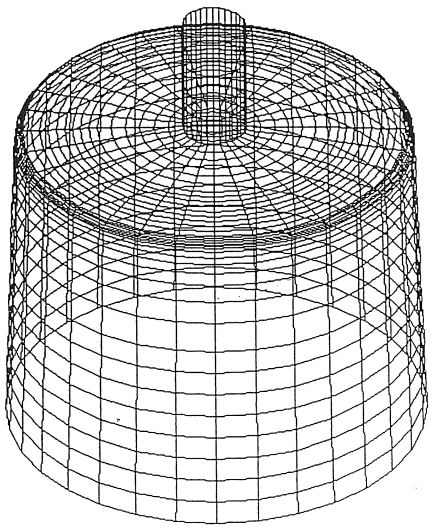

Figure 3.7: Finite element mesh of the centrifugal spinning box.

Later on, the same mesh has been used to analyze the composite spinning box. In the finite element computations, the in-service load has been divided into two sub-loads; on the one hand, the centrifugal forces resulting from the high speed rotation of the pot, and, on the other hand, the internal pressure onto the cylinder wall, caused by the rotation of the produced thread bobbin. For safety reasons, the bobbin was assumed to exhibit no strength at all and therefore was considered as a fluid. Taking into account the bobbin's density and dimensions, one could compute that, at a speed of 7000 rpm, the bobbin would press against the cylinder's internal surface with a 2 Mpa pressure. In a next step, the stresses corresponding to the aluminum pot analysis were transferred to the composite pots. Based on these stresses, a possible laminate lay-up was developed, taking into account the feasible fibre angles and ply thicknesses. This lay-up was then used as input to the finite element program and adapted until enough strength was achieved to permit the pots to operate safely.

On the cylinder, the final laminate has a 3.2 mm thickness and consists of 1 mm of $\pm$ 13° layers with respect to the axial direction, 1.5 mm of circumferential windings at 90° and 0.7 mm of $\pm$ 65° layers.

Definition of fabrication steps

To realize the final laminate lay-up, following steps have been proposed :

- winding of the pot : global, circumferential and belt windings
- winding of the ring to create the groove for the spring, which closes the cover during operation
- laminating the false bottom

For symmetry reasons, it was decided to wind two pots together, which had to be cut after the winding process. Although this solution implies fibre cutting, which is against the composite philosophy, it was preferred because it strongly simplified the winding process. Moreover, the ring groove for the spring had to be wound in a seperate step, which could take care of the cut surface. The mandrel used for winding the pots is shown in Fig. 3.8 and Fig. 3.9.

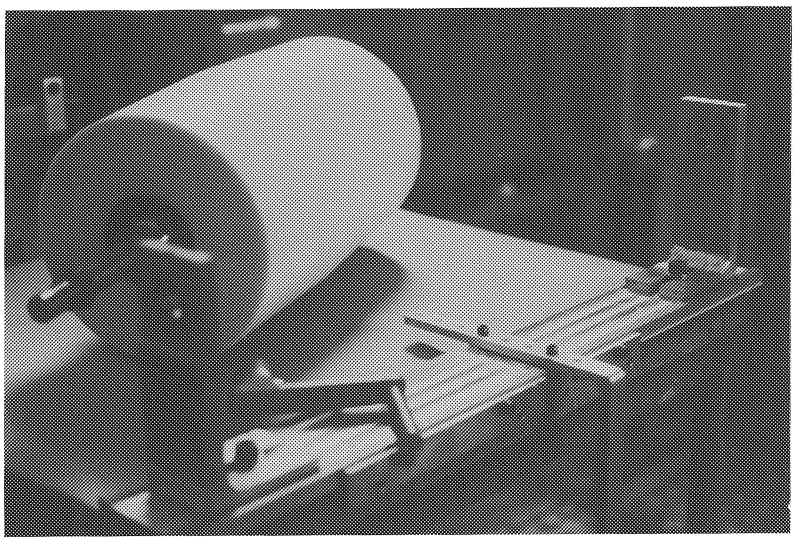

Figure 3.8: Mandrel for two spinning pots.

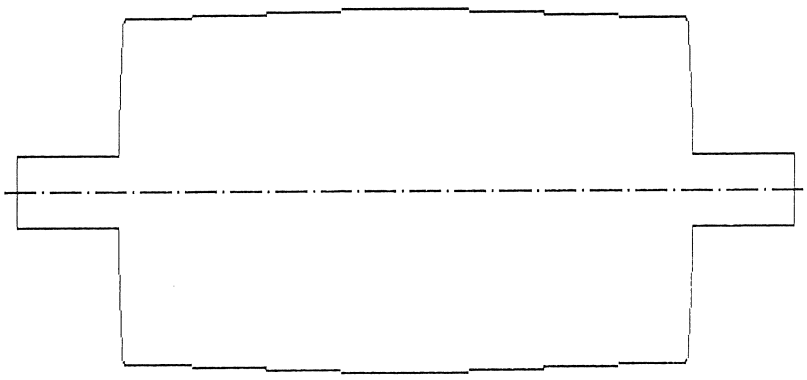

Figure 3.9: Scheme of the spinning pots' mandrel.

At both sides, a bronze coupling part to the driving motor was pressed against the ertalon mandrel, thereby allowing them to be automatically integrated within the filament wound structure.

After the cutting operation with a diamond saw, the rings were wound. Because of the groove, the ring mandrel had to be dismountable, so it was assembled out of several segments (Fig. 3.10).

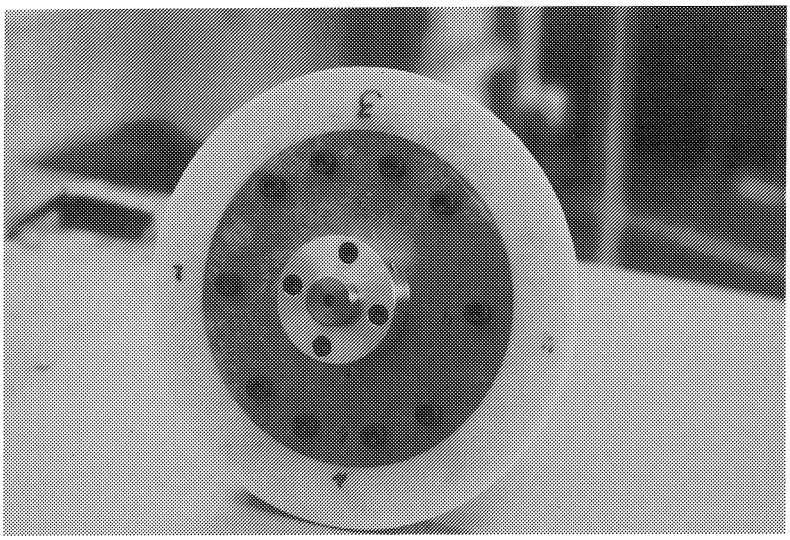

Figure 3.10: Ring mandrel.

Winding of the pot

Global windings

To assure continuity between the bronze coupling parts and the cylinder, it was necessary to provide windings starting on the bronze parts and continuing over the bottom and the cylinder towards the other side. These windings produce fibre angles of about 13° on the cylinder surface (Fig. 3.11).

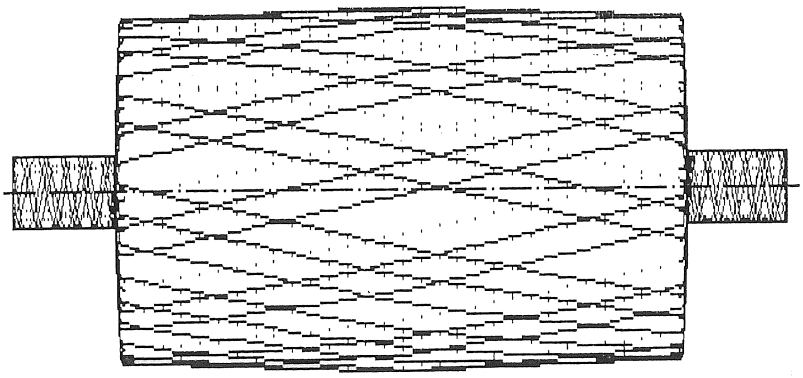

Figure 3.11: Global windings.

But, the internal pressure on the cylinder wall, together with the centrifugal forces, cause high circumferential stresses in the cylinder, loading the global windings almost transversally to their fibre direction. Although the global windings cannot contribute very much in taking up this load, they guarantee the continuity between the different parts. So, on the one hand, their thickness should be as low as possible, but on the other hand, they must give enough stiffness and strength to the bottom to assure that the pots can be handled safely without damage during the cutting and ring-winding operations.

Hoop windings

To assure that the cylinder can resist the high circumferential stresses, some hoop layers have been wound (Fig. 3.12). Now the cylinder satisfied the design requirements but the connection between the cylinder and the bottom remained rather weak.

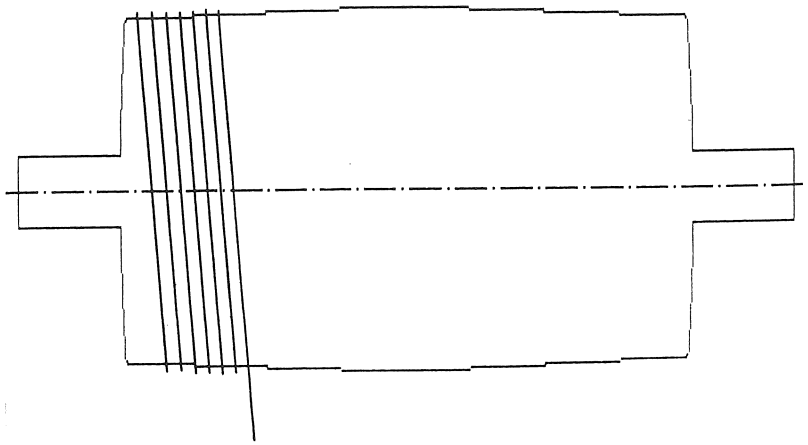

Figure 3.12: Hoop windings.

Belt windings

To strengthen this cylinder-bottom transition, an additional layer of belt windings was wound around a fictive hole with a slightly smaller diameter than the cylinder diameter, giving rise to a fibre angle of 65° on the cylinder (Fig. 3.13, Fig. 3.15).

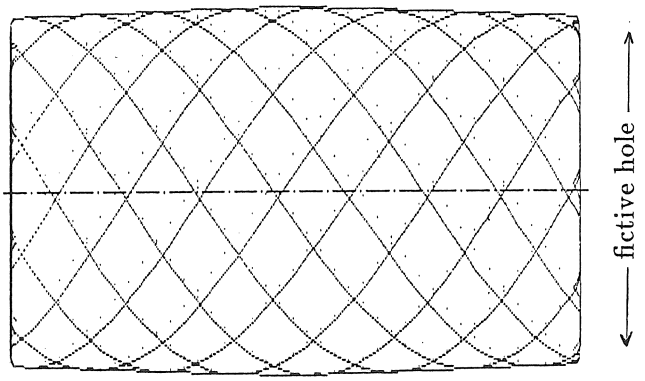

Figure 3.13: Belt windings.

Winding of the ring

Following on the winding process, the structure was kept rotating under an infra-red lamp in order to "B-stage". After further cure in an oven at 75°C and cutting the filament wound structure into two separate boxes, the winding of the rings could be started with. The ring mandrel (Fig. 3.14) was fixed into the pot and hoop windings were wound in the negative form of the groove and also over a small part of the cylinder, to guarantee continuity between the ring and the pot. To strengthen the ring in the axial direction, some woven glass strips were also applied in between the hoop windings.

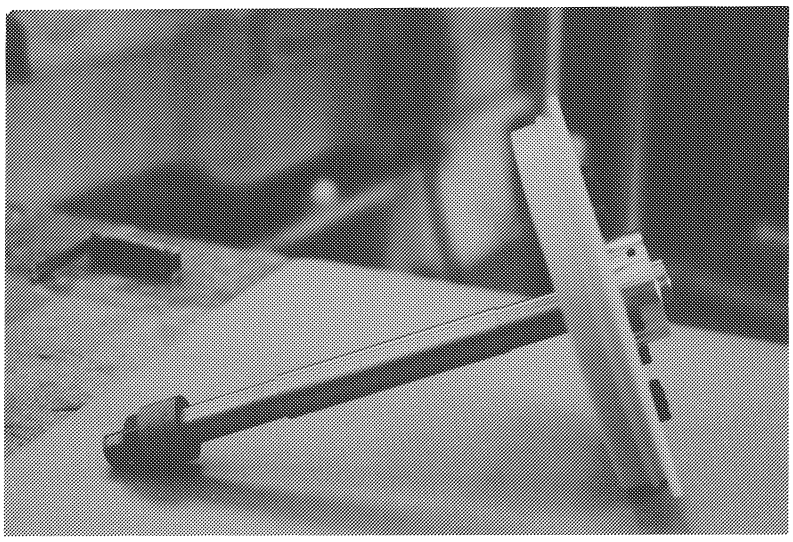

Figure 3.14: Mandrel used for winding the ring.

Bottom laminating

After curing of the ring and dismounting of the segmented mandrel, the pots received their false bottom. This time-consuming production step, which was made by hand lay-up, can be justified as follows; the layer of global windings on its own does not give enough thickness to the bottom. And increasing the amount of global windings produces too much superfluous thickness on the cylinder wall. Furthermore, the inside of the bottom must fulfill very accurate requirements. But, the fibres on the bottom are twisted when coming from the bronze part and continuing over the cylinder (Fig.3.15). Because of their twist and interweaving, they do not form a flat internal nor external surface. Instead, they give rise to a three-dimensional, open structure. Therefore, some woven fabrics have been laminated into the pot, creating a false bottom, which was shaped definitively by using a stamp while being cured.

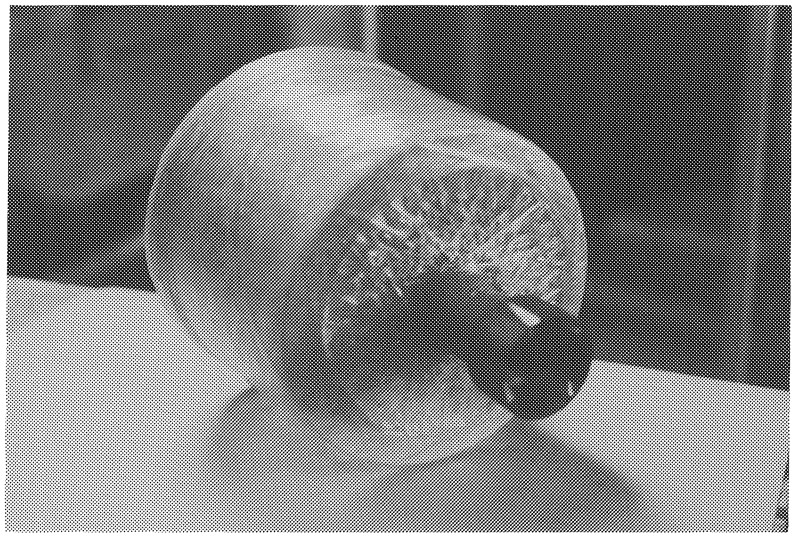

Figure 3.15: View on the spinning pot's bottom, showing the fictive hole of the belt windings and the fibre interweaving of the global windings.

Preprocessing

After the whole production process was planned, programming could start. The headlines of the winding program can be summarized as follows : the geometry of the mandrel must be introduced as input to the program. For this geometry, the geodesic path is calculated, starting from a specific point, with a specific radius and starting angle (see 2.5.1.2). For this geodesic winding the corresponding arm and spindle positions are computed by means of iteration. The results of these preprocessing calculations are gathered in a table, containing the arm positions as a function of the corresponding spindle positions. Fig. 3.16 shows a graphical representation of this table for the case of the global windings. Because of the high diameter ratio of the cylinder to the bronze coupling part, the laminate thickness at the bronze part would have become too thick before all global windings would have been applied. Therefore it was programmed, when starting on one bronze part, to perform five cylinder windings, before continuing on the other bronze part.

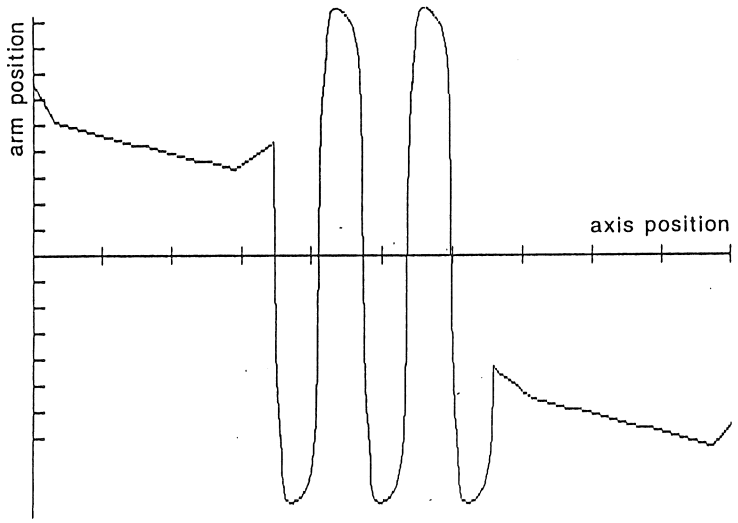

Figure 3.16: Graphical representation of the preprocessing results for the global windings, showing the winding arm motion as a function of the spindle rotation.

Filament winding

During the winding process, the on-line control of the arm motion guarantees that the fibres are wound onto the mandrel along the desired geodesic paths. This on-line control is based on a position feed-forward principle, using the data from the preprocessing step.

As the winding process was divided into different steps, starting a new step required fixing the fibres to the prior windings. For the hoop windings, this fixing operation caused no problems as the fibre could be clamped by the following windings. But in case of the belt, the fibre had to be sewed into the bottom layers, at the correct radius.

Finishing

Because of the high speed rotation of the pots in close fitting compartments, a high quality outer surface was required to avoid noise nuisance. In order to assure a smooth surface, perfectly fitting peel-ply and bleeder-breather coats have been sewed and used while applying a vacuum technique. But as this did not yet answer the smoothness expectations, especially at the bottom, an additional finishing step was inevitable; the cylinder's outer surface has been ground, a special surface cloth has been applied and the bottom has been filled up.

Concluding remarks

The design and manufacturing of filament wound spinning pots to replace existing aluminum boxes has been described in detail. The thereby pursued object has for the greater part been attained. The composite spinning pots show excellent corrosion resistance and thanks to their smaller wall thickness, larger thread bobbins can be produced within one single spinning unit. However, two aspects need some further investigation; a first issue to be improved is the cylinder's outer surface, which was too rough and thereby caused too much resistance. Secondly, more attention should be given to aligning the spinning pot's axis with the axes of the bronze coupling parts, since the slightest unbalance can, with time, damage the driving motor.

3.3.3.2 Pressure vessels

Introduction

A second example regards the design and manufacturing of composite pressure vessels for the automotive industry (Ref. [63]). Unlike in the previous spinning pot case, here a real composite design was possible. This design has been carried out in successive steps; *netting analysis* (appendix B) has been applied to obtain the optimal dome shape. This shape is defined by a second order differential equation, which can be solved using a numerical integration technique. Appropriate thicknesses of both longitudinal and hoop windings have been determined to resist the required internal pressure. Further, the optimal shape and lay-up, at least according to netting theory, have been checked by means of finite element analysis. And finally, the designed vessels have been filament wound and tested for their burst pressure, in order to provide a feed-back to the design's safety factor.

In this paragraph, several mathematical formulae will be referred to. Their derivations are described in detail in appendix B.

Design requirements

The vessels are meant to operate as water or oil reservoirs in a room temperature environment at a work pressure of 0.4 MPa. According to the *ASME Boiler and Pressure Vessel Code* (Ref. [1]), the vessels should be designed for at least five times their work pressure. Boundary conditions require that the vessels consist of a cylindrical part, closed by two domes and resulting in a 20 liter content. The cylinder and nozzle radius are respectively 125 and 20 mm.

Material choice

To avoid unnecessary mandrel costs, polystyrene foam mandrels have been used, which could be washed out with acetone after curing. The mandrels were turned to their final dimensions, the domes being shaped on a lathe with a special cutting tool, made by sparkerosion. Two aluminum fittings have been glued onto the foam mandrel. As the vessels were only designed for low pressure applications, a gelcoat liner would satisfy to prevent leakage. For the composite, a glass fibre reinforced epoxy has been chosen. Due to the foam mandrel, the resin had to be room temperature curing. Data concerning the applied materials are presented in Table 3.1.

fibre	E-glass Cosmostrand 859
resin	epoxy Ciba Geigy LW 561
liner	gelcoat Ciba Geigy SW 404
mandrel	polystyrene faom BASF Styrodur 3000S

Table 3.1: Material choice for the pressure vessel manufacturing.

Optimal dome shape

The principal design idea is trying to take up the load with a minimum amount of material. Hence, the composite must be loaded in its strongest direction, being the fibre direction. However, when using geodesic fibre paths, aligning the fibres with the principal load directions is not always possible. Therefore, the geometric form will be defined as to nevertheless take maximum benefit of the inherent fibre strength.

To define the optimal dome shape, *netting analysis* (appendix B) has been applied. According to *netting theory*, the fibres are the only load carriers, the matrix not being taken into account. Consequently, the fibres must be equally stressed all over the structure. *Netting analysis* is conservative but permits a fast dimensioning.

To obtain the optimal shape, equilibrium equations of a stressed membrane under internal pressure are combined with equations describing its curvatures. When in addition the uniform stress state in the fibres and the geodesic patterns of the fibres are taken into account, following differential equation defining the optimal end contour is obtained :

$$\frac{-y \cdot y''}{1 + y'^2} = \frac{2y^2 - 3Y_0^2}{y^2 - Y_0^2} \tag{3.3}$$

where : y : radius at a particular x-coordinate
Y_0 : radius at the nozzle

To solve this non-linear differential equation, a numerical method is recommended. Hence, a computer code has been written, using a *Runge-Kutta* method of the fourth order to solve a system of two first order differential equations (Ref. [58]). Therefore, equation 3.3 has to be rewritten as :

$$y_1' = f_1(x, y_1, y_2) \tag{3.4}$$

and

$$y_2' = f_2(x, y_1, y_2) \tag{3.5}$$

where : $y_1 = y'$
$y_2 = y$

resulting in :

$$y_1' = -\frac{2y_2^2 - 3Y_0^2}{y_2^2 - Y_0^2} \cdot \frac{1 + y_1^2}{y_2} \tag{3.6}$$

and

$$y_2' = y_1 \tag{3.7}$$

When numerically solving this system of differential equations, starting from the appropriate boundary conditions on the cylinder ($y_1 = 0$ and $y_2 = \textit{cylinder radius}$), an optimal dome shape is obtained, as presented in Fig. 3.17.

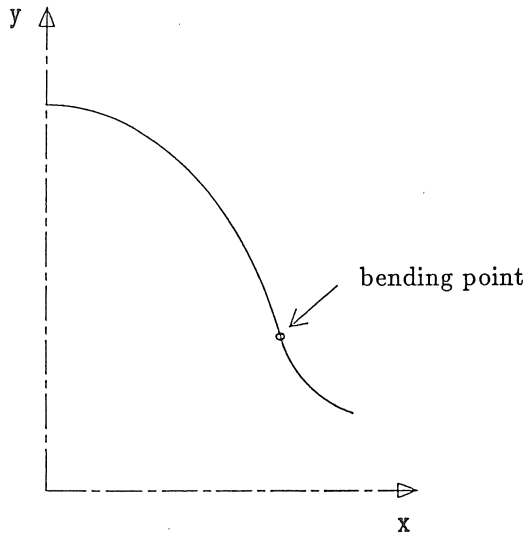

Figure 3.17: Optimal dome shape according to netting analysis.

However, when solving equation (3.3), problems arise as soon as the right side of the equation becomes zero or negative, this is for values

$y \leq \sqrt{\frac{3}{2}} \cdot Y_0$. In this case, the sign of the curvature changes and a bending point occurs. As such a profile is difficult to wind, it has been decided to replace the concave part by a convex, spherical surface. In fact, this can be easily justified because the bending point generally lies close to the nozzle. Moreover, the real shape is of no importance, because in practice the internal part of the nozzle is dimensioned as to just reach that bending point.

Cylinder - dome transition

To optimally proceed on a cylindrical surface, the same differential equation (3.3) should also be valid on the cylinder. Hence, there must exist a point on the netting profile, where y' and y'' both equal zero at the same time. Such a point could then belong to the cylinder. $y'' = 0$ translates into :

$$2y^2 - 3Y_0^2 = 0 \tag{3.8}$$

or

$$Y_{cyl} = \sqrt{\frac{3}{2}} \cdot Y_0 \tag{3.9}$$

With this equation, the radius of the cylindrical part is immediately fixed, the radius being not much greater than the nozzle radius. Besides, curvature changes its sign for points with $y < Y_{cyl}$. Consequently, an ideal netting dome profile can not optimally proceed onto a cylinder and vice versa. Therefore, the cylindrical part will have to be additionally reinforced.

Determination of the composite's thickness

Thickness variation over the end contour

Let N be the number of fibres along the circumference of any cross-section of the structure and A the cross-sectional area of the wet fibre. The composite's thickness t in a particular point can then be expressed as a function of the radius y and the fibre angle α with respect to the meridian curve :

$$t = \frac{N \cdot A}{\cos\alpha \cdot 2\pi y} \tag{3.10}$$

Required thickness

The wall thickness of the pressure vessel must fulfil two requirements; first, there must be enough fibres along the circumference to ensure a uniform surface coverage. Second, the stress and strain allowables may not be exceeded.

When using *netting analysis*, a simple equation can be derived, expressing the fibre tension as a function of the composite thickness. Consequently, the vessel thickness can be defined just by requiring the fibre tension not to exceed the maximum fibre strength. In fact, this dimensioning facility is only relevant in case metal liners are applied, as these allow the fibres to become very much stressed without danger for leaking (Ref. [21]). Nevertheless, because of safety reasons, metal-lined vessels are designed as to first start leaking before bursting (Ref. [52] and Ref. [38]). In case of vessels with a gelcoat liner, however, the direct *netting analysis* dimensioning is not at all significant because leakage will occur as soon as liner and matrix cracks appear. And this will happen long before the tensile resistance of the fibres is reached. Therefore, the dimensioning will be performed in two steps, a proposal followed by a check and, if necessary, an iterative optimization.

Based on the experience with previous vessel design and basic hand computations, it has been proposed to supply 460 fibres along the circumference, that is 230 in both the $+\alpha$ and $-\alpha$ direction. This amount of fibre strands should sufficiently cover the domes.

According to *Clairaut's* law (Eq. 3.1), the winding angle on the cylinder is :

$$\alpha = \arcsin \frac{20}{125} = 9°12'25'' \tag{3.11}$$

with 20 mm being the nozzle radius and 125 mm the radius of the cylinder. Knowing that the impregnated fibre has a 1.57 mm^2 cross-section, the corresponding laminate thickness on the cylinder can be computed according to equation 3.10 :

$$T_{cyl} = \frac{460 \cdot 1.57}{\cos 9°12' \cdot 2\pi 125} = 0.93mm \tag{3.12}$$

However, as the cylindrical part is not an optimal elongation of the ideal end cap shape, it will have to be additionally reinforced. *Netting analysis* can be applied to determine the required number of hoop windings to strengthen the cylinder. Expressing that both longitudinal and hoop windings have to be stressed to the same value yields

following relation between the longitudinal layer thickness t_{1-cyl} and the hoop layer thickness t_{2-cyl} :

$$\frac{t_{2-cyl}}{t_{1-cyl}} = 3\cos^2\alpha_{1-cyl} - 1 \tag{3.13}$$

Using the appropriate numerical data, the required thickness of the circumferential layer becomes :

$$T_{2-cyl} = (3\cos^2 9°12' - 1) \times 0.93 = 1.78mm \tag{3.14}$$

The corresponding number of hoop windings of course depends on the cylinder length L. As the ideally shaped domes have a content of 2.711 liter, a total 20 liter pressure vessel content requires a cylinder length :

$$L = \frac{(20 - 2 \cdot 2.711) \cdot 10^6}{\pi 125^2} = 297mm \tag{3.15}$$

However, for winding strategy reasons, it has been decided to elongate the cylinder up to 326 mm; with this length, a winding strategy 19/230 could be obtained, corresponding to a quite interwoven laminate lay-up (3.4.4) as it is only the 109th fibre that becomes adjacent to the first one.

With a cylinder length of 326 mm, a 1.78 mm circumferential layer thickness requires :

$$\frac{1.78 \cdot 326}{1.57} = 372\ windings \tag{3.16}$$

Consequently, the cylindrical part of the vessel has been reinforced by winding 372 hoop windings, distributed over the cylinder length, around its circumference.

Evaluation by means of finite element analysis

The finite element analysis is performed using a model with *shell* elements. Because of symmetry, only one half of the structure has to be modelled. A *sector generator* allows to only introduce one fourth of a longitudinal cross-section of the vessel whereas the computations are nevertheless three-dimensional. The finite element mesh is presented in Fig. 3.18.

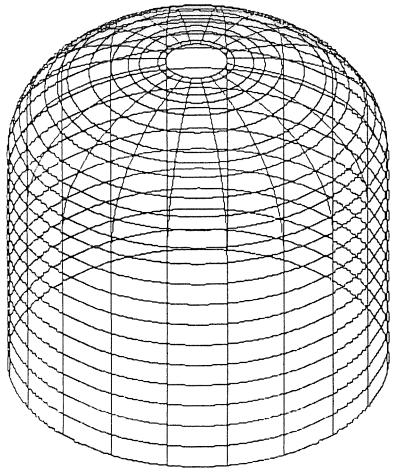

Figure 3.18: Finite element mesh of the pressure vessel.

The dome is modelled by means of 14 conical rings. The cylinder length is subdivided into 10 rings. All rings are circumferentially subdivided into 20 elements. The elements of the longitudinal cross-section are numbered from 1 to 441 with a step of 20, beginning with 1 on the cylinder and ending by 441 at the nozzle (Fig. 3.19).

The upper ring at the nozzle is supposed not to show any deformation, due to the aluminum nozzle to which the composite is fixed. The varying layer thicknesses and fibre angles are shown in Table 3.2. The layer thicknesses are calculated using equation 3.10. The fibre angles are referred to the circumferential direction and have been computed according to *Clairaut's* law (Eq. 3.1). Elements 1 to 200 have an additional hoop layer of 1.78 mm.

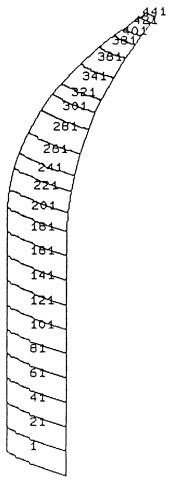

Figure 3.19: Finite element mesh numbering.

element	ψ	thickness [mm]
1 to 181	$\pm 80.79°$	0.465
201	$\pm 80.71°$	0.467
221	$\pm 80.43°$	0.48
241	$\pm 80.11°$	0.50
261	$\pm 79.48°$	0.53
281	$\pm 78.41°$	0.59
301	$\pm 77.35°$	0.64
321	$\pm 76.29°$	0.70
341	$\pm 73.50°$	0.85
361	$\pm 69.08°$	1.10
381	$\pm 63.51°$	1.43
401	$\pm 57.66°$	1.82
421	$\pm 36.77°$	3.84
441	$\pm 17.75°$	8.96

Table 3.2: Variation of layer thickness and fibre angle over the pressure vessel.

The vessel is subjected to an internal pressure of 1 MPa. The deformed mesh is shown in Fig. 3.20.

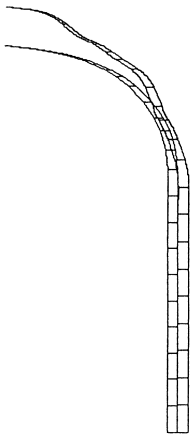

Figure 3.20: Deformed pressure vessel due to an internal pressure loading.

The safety factors, based on Scotchply data (Table 3.8) are given in Table 3.3.

These results show that the vessel can resist a pressure of 2.2 MPa on the cylinder. Failure is predicted to occur in the elements 161 to 180, close to the cylinder-dome transition, at a 2.2 MPa pressure. Consequently, taking into account that the design burst pressure should be five times the work pressure, the vessels can safely operate at a work pressure of 0.4 MPa.

It must be considered that this finite element analysis has been carried out assuming a layered laminate lay-up, whereas in the real filament wound vessel the fibres are interwoven. Within the available finite element code, the interweaving effect of the fibres can not be modelled. Layered computations will however prove to be satisfactory.

From Table 3.3 one can also conclude that the local effects at the dome-cylinder transition do not propagate very far. Therefore it was decided to wind analogous vessels with shorter length, in order to investigate the influence of winding strategy on the vessel's fatigue performance (3.4.5.2). For, the analysis results have shown the validity of a fatigue performance comparison of shorter and longer vessels. These vessels are shown in Fig. 3.21.

element	layer 1	layer 2	layer 3
1	2.26	2.27	3.04
21	2.26	2.27	3.04
41	2.26	2.27	3.04
61	2.26	2.27	3.04
81	2.26	2.27	3.04
101	2.27	2.27	3.04
121	2.27	2.27	3.05
141	2.24	2.25	3.08
161	2.21	2.20	2.88
181	2.54	2.47	2.25
201	3.79	3.95	
221	7.88	7.24	
241	8.46	8.00	
261	8.05	7.54	
281	5.73	4.59	
301	5.25	6.75	
321	4.10	5.44	
341	3.79	3.00	
361	3.37	2.90	
381	3.47	3.44	
401	3.23	4.07	
421	2.90	3.93	
441	3.96	5.36	

Table 3.3: Safety factors in the different layers of the pressure vessel.

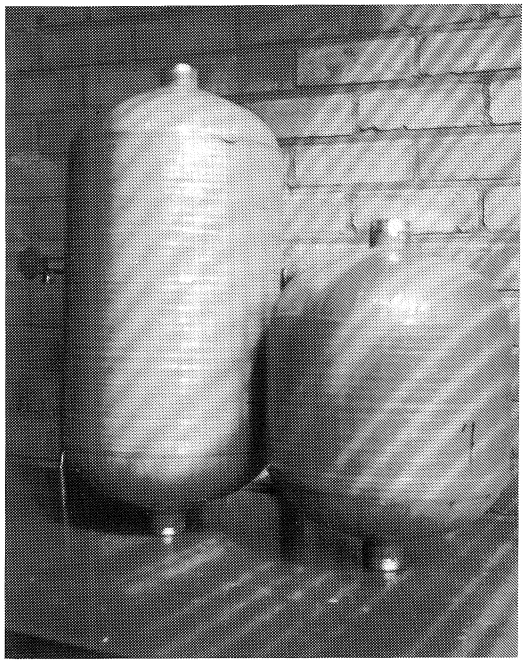

Figure 3.21: Filament wound vessels with optimal dome shape.

Concluding evaluation by means of burst tests

The designed vessels have been filament wound and tested by pumping them up with water very slowly, using a hand pump. The pressure at which the first structural leak occured is considered as the failure load. By *structural leak* is understood a clear leak or a series of small holes in a particular direction, unlike a local leak, which results from a local error, created during the manufacturing process. All vessels showed structural leakage on the cylinder surface between 1.5 and 2.0 MPa, with an average of 1.8 MPa. The visual leaks in the outer hoop layers were all oriented in the circumferential direction. Finite element analysis predicted first failure on the cylinder surface at 2.2 MPa. According to this analysis, the hoop and longitudinal cylinder layers would approximately fail at the same pressure, which was also pursued when determining the optimal hoop layer thickness.

Taking into account the sensitivity of leakage to the application and curing of the gelcoat, it can be stated that predicted and measured failure loads correspond quite well.

3.4 Winding strategy and its influence on the composite's performance

3.4.1 Terms of reference

Even when the design of a filament wound component has evolved in so far that the laminate lay-up has been defined, there remains a final degree of freedom, being the winding strategy. In this paragraph, the influence of the winding strategy on the performance of a filament wound component will be discussed.

In fact, there are two ways to wind a composite structure (2.3.4.1); on the one hand, the polar or planar winding, in which each layer of fibres is wound with a minimum of voids and cross-overs. In this case, a next fibre is immediately adjacent to the previous one and there is almost no interweaving. On the other hand, with helical winding, a woven structure is generated, containing both voids and cross-overs. Here, the composite is built up by a more disorderly fibre lay-down and fibres will only be placed nearby each other after a given number of cycles. So, with filament winding, either a woven or a layered composition can be obtained.

Most filament winders disapprove of the interweaving way of winding because they assume that the cross-over points act as stress raisers and therefore should result in lower strength properties.

According to literature however, woven fabrics show several advantages, which could also be expected in case of interweaving filament winding.

Therefore, research has been performed in the course of this doctoral thesis to prove that interweaving winding patterns can be quite beneficial for the composite's performance. In the argumentation, following subjects will be treated : first a literature review on winding method comments will be given, followed by a comparative survey on woven fabric and cross-ply characteristics. Afterwards, a definition of winding strategy will be enunciated, which is an important winding parameter indicating the degree of interweaving. Further, some test procedures will be described, carried out to investigate the influence of the weaving effect on the performance of filament wound tubes. Also an investigation on pressure vessels, wound to different degrees of interweaving, will be summarized. And to conclude, the measured test results will be discussed and compared with literature.

The issue of this research finds expression in that allowing interweaving filament winding has considerable implications on winding flexibility. For, the complete geodesic path on a specific geometry is fixed once a certain starting point and starting angle have been chosen. It would be very coincidential that this path corresponds to a layered winding path. Small changes in geometry could influence the winding strategy, but normally, indexing or deviating from geodesic lines would be necessary to ensure that a next fibre is lying just adjacent to the previous one. However, all this extra programming becomes redundant as it will be shown that interweaving helical winding, which does not require special geometrical demands, results in a product of the same quality.

3.4.2 Literature review on winding method comments

Most filament winders consider polar winding as the most suitable technique. To confirm their conviction, some author statements will be cited.

In a United States patent (1977), Dritt (Ref. [16]) claims :
"It has been found that a helical pattern of filaments results in multiple cross-overs of filament wound material...further, the presence of the filamentary cross-overs results in a considerable volume of voids or interstices between contiguous filaments so as to considerably detract from the strength of the winding for a given thickness." The same remarks were given for completely random winding patterns.

At the university of Nottingham, Middleton, Young, Ellimar and Owen give the following comments : (Ref. [49])
"There are two extreme types of structures which can be produced :

- *a layered structure with few fibre cross-over points, and*
- *a basket weave structure with many cross-over points.*

For most filament winding applications a layered structure is required. This gives fewer voids, fewer crimps in the fibres and higher fibre volume fractions. In order to produce such a laminate, each fibre must be laid immediately adjacent to the previous one. Most geodesic patterns do not do this but there are two methods by which this condition can be forced :

- *indexing, where a small arc of hoop winding is added onto the end of each pattern to alter the position of start of the next pattern.*
- *progression, where all mandrel rotation in the pattern is scaled by a factor close to 1.0. This alters the position of the start of the next pattern, in effect by twisting each pattern slightly."*

Hull, Spencer and Legg (Ref. [26]) were also convinced that cross-over points had to be avoided. They performed ...
"mandrel indexing to ensure that each roving slightly overlaps the previous one to produce a uniform lay-up of fibres."

Schwartz (Ref. [71]) on the other hand is more cautious when he claims :
"The filament cross-over effect is the most important factor in comparing helical and polar winding patterns. It has been assumed that the cross-over points act as stress raisers and should result in lower burst pressures. Three conclusions can be drawn :

- *while differences may exist because of filament cross-over, their exact interpretation depends on a detailed analysis of the local stress condition.*
- *deviation of fibre paths from theoretical positions may be more decisive than filament cross-over.*
- *for practical purposes, there is no significant difference between polar and helical patterns in ultimate burst strength."*

3.4.3 Comparative literature survey on woven fabric and layered cross-ply characteristics

3.4.3.1 Fabric definitions

All woven fabrics consist of two sets of interlaced threads, known as the *warp* and the *fill* threads. Different types of fabrics can be identified by the repetitive pattern of the interlaced regions as shown in Fig. 3.22 (Ref. [27]).

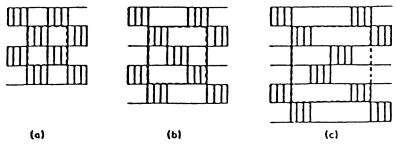

a) plain weave
b) twill weave
c) 4-harness satin weave
d) 8-harness satin weave

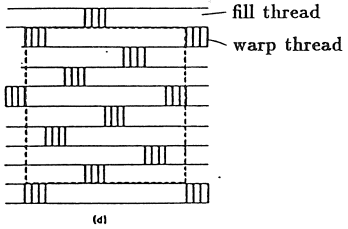

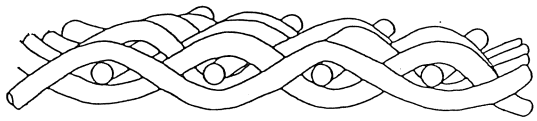

plain weave

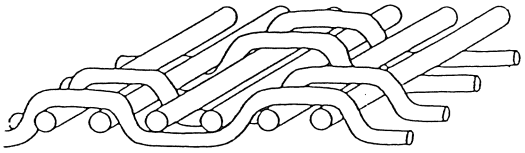

twill weave

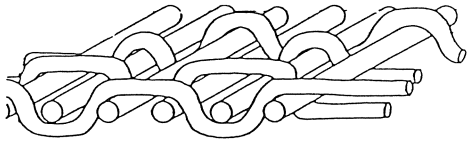

basket weave

five-harness satin weave

Figure 3.22: Examples of woven fabric patterns.

Two geometrical parameters can be defined to characterize a fabric; n_{fg} denotes that a warp thread is interlaced with every n_{fg}-th fill thread and n_{wg} indicates that a fill thread is interlaced with every n_{wg}-th warp thread. Fabrics with $n_{fg} = n_{wg} = n_g > 4$ and where the interlaced regions are not connected are called *satin weaves.*
As defined by their n_g-values, the fabrics in Fig. 3.22 are called *plain weave* ($n_g = 2$), *twill weave* ($n_g = 3$), *4-harness satin* ($n_g = 4$) and *8-harness satin* ($n_g = 8$). The *plain weave* is the simplest fabric form, with one warp yarn running over and under one fill yarn. The *plain weave* is also the most stable; it maintains its shape and prevents the threads from slipping. *Satin weaves* are more complex and flexible than the *plain weaves.* In a *5-harness satin weave*, one warp yarn runs over four and under one fill yarn. The *satin weave* is quite pliable, thereby allowing to conform to complex shapes.

3.4.3.2 Mechanical properties

[0,90] laminates

Stiffness modulus

In fabrics made by conventional weaving processes, the fibres are considerably curved. Consequently, some fibre aligning can occur when the fabric is stretched, which results in a relatively low-modulus composite.

Tensile strength

Because the fibres are necessarily kinked, it is obvious that the product can not be expected to yield its full strength potential. Cross-over points are assumed to act as strength reducers by causing stress concentrations.

Curtis and Bishop (Ref. [11]) report two series of tests on carbon/epoxy [0,90] cross-plies and 5-harness satin fabrics. The tensile strengths were significantly lower in the woven case, e.g. 25 % and 15 %. In the second test, the *Young* modulus for the woven material was 20 % lower (Table 3.4). The lower fibre volume fraction of the woven material was expected to give values of strength and *Young* modulus approximately 10 % lower. Undulations caused by weaving the load bearing 0° fibres accounted for further reductions in strength and stiffness.

The more the fibre interweaving is pronounced, the more significant the expected reduction of strength and stiffness is. This corresponds to Hanaqud's conclusions concerning glass fibre reinforced plastics (Ref. [24]). His research showed that weaves with less distortion of the fibre tows, such as *satin weaves*, result in a smaller reduction of mechanical properties as compared to *plain weave* fabrics.

Compression strength

When considering the compression strength of a fabric, one could again anticipate that the kinks, inevitably present in a woven fabric, would initiate premature failure. However, unlike these expectations, fibre kinking in the weave does not induce weakness. For, in a woven structure, impregnated with a tough matrix, any local instability due to fibre kinking can be stabilized by a counter direction buckling in an adjacent layer. This self-stabilizing mode may be further strengthened by the relatively short distances, determined by the weave cross-overs.

Support for this theory is given by compression test results by Measuria and Cogswell (Ref. [48]) on carbon/peek [0,90] cross-plies and 5-harness satin weaves (Table 3.4).

Shear strength

With woven fabrics, an enhanced product toughness with respect to delamination processes can be expected. The kinking of the fibres tends to deflect interlaminar cracking, resulting in a higher fracture toughness. In a woven product, any tendency to split is suppressed because there is no weak transverse direction. The absence of this weak transverse direction may reduce crack initiation or rapidly stop such cracks at the next fibre cross-over.

Winkel and Adams (Ref [91]) compared E-glass/epoxy [0,90] cross-plies and plain weave fabrics. They found a higher shear strength (124 MPa) for the fabric as compared to the cross-ply (108 MPa), in spite of the lower fibre volume fraction of the fabric (Table 3.4).

[± 45] laminates

The strength and stiffness behaviour of fabrics very much depends on the load direction with respect to the fibre orientations.

Curtis and Bishop (Ref. [11]) have done comparative tests on [± 45] carbon/epoxy cross-plies and 5-harness satin weaves. They conclude that : *"Woven material, oriented at ±45°, offers some improvement in mechanical properties compared to non-woven material and should be seriously considered for structural applications."*
Similar values of tensile strength and elastic properties were obtained for woven and non-woven material, despite of the lower volume fraction of the fibres in the woven material (Table 3.4). These results correspond to computed plots (Ref. [59]) of stiffness and strength in woven fabrics and cross-plies, at different load directions with respect to the fibre orientations. In these plots (Fig. 3.23) the fibres are assumed to lie along the 0° and 90° directions, while the tensile load orientation can vary between 0° and 90°. These plots reveal that, in case of intermediate loading directions, woven fabrics show even higher values of stiffness and strength than their cross-plied equivalents. The increased load-carrying capacity of the fibres in the woven fabric, when loaded along a direction in between the fibre orientations, is probably due to the inhibition of in-plane shear deformation and delamination, thanks to the woven and undulating nature of the fabric.

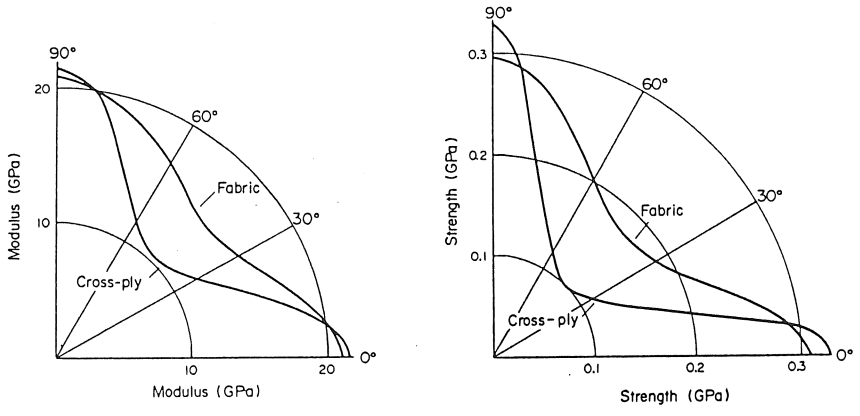

Figure 3.23: Stiffness and strength plots for wovens and cross-plies.

	E_{te} [GPa]	σ_{te} [MPa]	σ_c [MPa]	G [GPa]	τ [MPa]	Vf [%]
Graphite/epoxy						
cross-ply [0, 90]	52.6	535		3.31	157	42.8
plain weave fabric	65.2	697		3.86	150	49.7
(Ref. [91])						
Carbon/epoxy						
cross-ply [0, 90]		757				
	60.1	644	430			
5-harness satin		584				
	50.2	545	400			
(Ref. [11])						
Carbon/epoxy						
cross-ply [±45°]	17.1	190	216			
5-harness satin	16.3	216	21			
(Ref. [11])						
Kevlar/epoxy						
cross-ply [0, 90]	26.1	470		1.79	95	42.9
plain weave	29.5	437		1.59	99	46.2
(Ref. [91])						
E-glass/epoxy						
cross-ply [0, 90]	22.2	340		4.41	108	45
plain weave	20.8	157		4.28	124	36.6
(Ref. [91])						
Carbon/peek						
cross-ply [0, 90]	67	1065	717 warp			60
			637 weft			
5-harness satin	73 warp	779 warp	720 warp			60
	67 weft	759 weft	669 weft			
(Ref. [48])						

Table 3.4: Mechanical characteristics of cross-plied and woven laminates (literature survey).

3.4.3.3 Impact resistance

[0,90] laminates

Measuria and Cogswell (Ref. [48]) have done comparative falling weight impact tests on carbon fibre reinforced peek [0,90] cross-plies and 5-harness satin weaves. They have observed an encouraging improvement in impact performance for woven fabrics compared to cross-plied laminates. The woven fabric showed less tendency to delaminate than did the cross-ply.

Winkel and Adams (Ref. [91]) also reported smaller impact damage areas for AS4 graphite/epoxy and E-glass/epoxy plain weave fabrics, compared to corresponding [0,90] cross-plies.

Curtis and Bishop (Ref. [11]) also claimed that the impact damage was more contained in the laminates made of woven fabrics. They stated :

"The use of woven material restricted the extent of delamination and particularly the splitting along the fibre direction in the back surface layers."

After impact, further investigations were performed on the damaged material. Curtis and Bishop found that the impact damage significantly reduced the residual tensile strength of both woven and non-woven carbon/epoxy [0,90] laminates. The reduction was more pronounced in the woven case, with only 29 % of the original tensile strength remaining, compared to 53 % for the cross-ply material. Thus, the stress concentration effect of the impact damage must have been more significant in the woven material than in the non-woven laminates. In compression, the non-woven [0,90] was slightly stronger (430 MPa) than the woven material (400 MPa), but this was probably due to lower fibre volume fraction of the woven laminate. Large reductions appeared in the residual compressive strength of the [0,90] laminates after impact, although the woven material faired slightly better than the non-woven. The lower residual compressive strength for the non-woven material (only 45 % left against 59 % for the woven case) was probably due to the more extensive delaminations since these would lead to increased buckling instability.

[± 45] laminates

Curtis and Bishop (Ref. [11]) also performed impact tests on [±45] laminates. The residual strengths of these materials were consider-

ably less sensitive to impact damage than in case of [0,90] laminates. The non-wovens showed more damage than the wovens and a small reduction in both tensile and compressive strength was observed after impact. The effect of impact on the woven material was neglectable.

3.4.3.4 Fatigue resistance

To investigate the influence of interweaving, Curtis and Moore (Ref. [12]) have performed fatigue tests on carbon fibre reinforced plastics. According to their results (Fig. 3.24), [0,90] non-wovens, dynamically loaded along the 0° direction, show better fatigue performance as compared to the woven fabrics. The fabrics suffer more from stiffness and strength reduction, due to the cross-over points which cause additional fatigue damage.

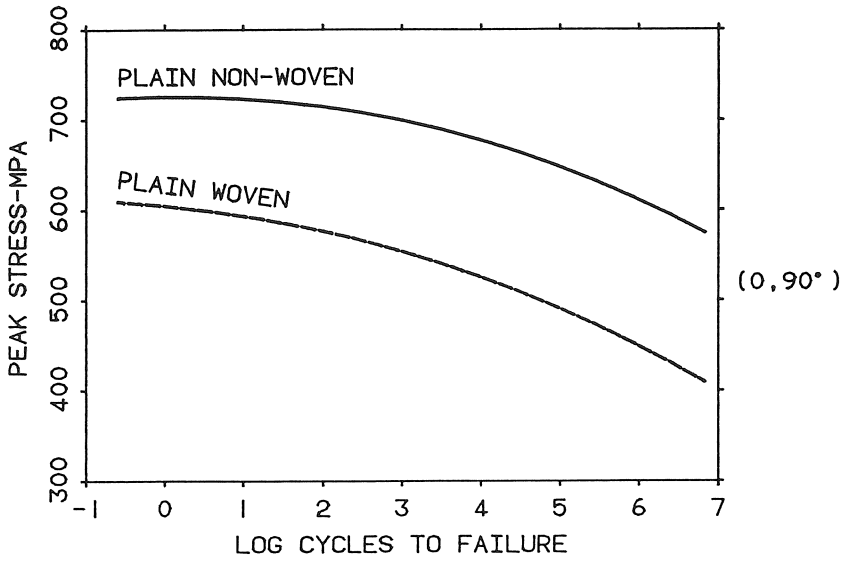

Figure 3.24: Life time plots for [0, 90] wovens and cross-plies, dynamically loaded along the 0° direction.

Optical microscopy and C-scanning show large transversal cracks through the 90° layers, together with delaminations which tend to grow with increasing number of cycles. In non-woven material, this effect uncouples the 90° layers from the 0° plies. However, in the woven

case, the 90° layers remain connected to the 0° plies and exert a stress concentrating influence on them. Consequently, the cross-over points will cause more damage, resulting in a steeper Wöhler curve in case of [0,90] woven fabrics.

[± 45] composites however perform better under fatigue conditions if the fibres are interwoven (Fig. 3.25). Woven [± 45] laminates can survive the non-wovens for a factor 10. The smaller damage extension in the woven case is probably due to the reduced tendency for the damage to grow, thanks to the presence of the holding cross-over points.

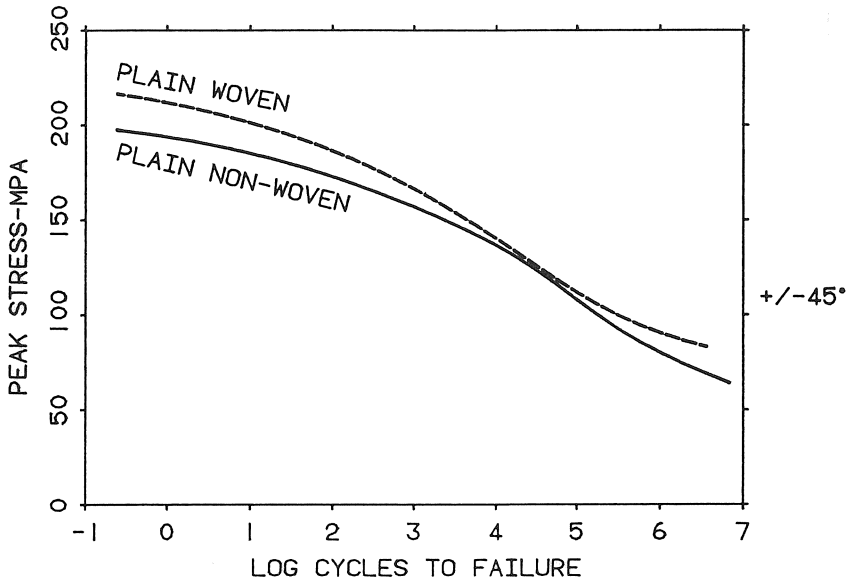

Figure 3.25: Life time plots for [±45] wovens and cross-plies, dynamically loaded along the 0° direction.

3.4.3.5 Literature survey conclusions

According to literature, woven fabrics, with fibres lying in the direction of the load (as in a [0,90] lay-up), show reduced stiffness, strength and fatigue life as compared to similar non-woven cross-plies. The stronger the interweaving is pronounced, the higher the reduction is.

In load directions in between the fibre orientations however, woven

fabrics, e.g. [±45] woven laminates, show better strength, stiffness and fatigue performance.

In impact situations, the area of impact damage produced is smaller for the woven laminates. This results in improved residual compressive strength as compared to non-woven materials. However, residual tensile strength of woven laminates can be significantly lower.

3.4.4 Definition of winding strategy

By winding strategy is understood the time sequence of the fibre laydown in a particular cross-section of the wound structure. Consider e.g. a circumference with 30 fibre strands in the $+\alpha$ direction and 30 in the $-\alpha$ direction (Fig. 3.26).

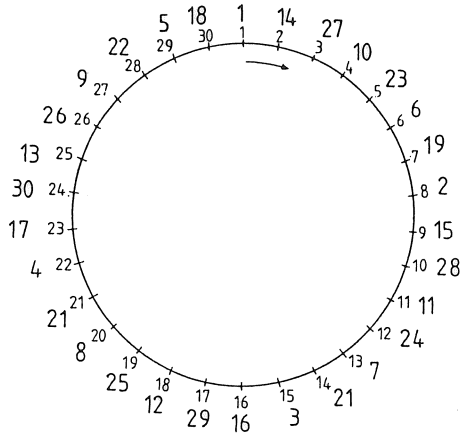

Figure 3.26: Numbering according to a winding strategy "7/30".

A strategy called "7/30" indicates that, at every new cycle, the mandrel has turned over a fraction 7/30 of the circumference. This strategy has following winding sequence : 1 8 15 22 29 6 ...This means that fibre number 8 is laid during the second cycle, fibre number 15 during the third one ...and that only during the last cycle, fibre number 24 is wound onto the mandrel.

The winding strategy strongly determines the interweaving of the fibres. A strategy "29/30" or "1/30", in which the next fibre is adjacent to the immediately previous one (to the left or to the right), corresponds to what is called in literature a "layered structure". In

this case there is almost no interweaving. On the contrary, "7/30" and "23/30" strategies, in which spaces between fibres can be filled up long time after these fibres have been laid, show many cross-overs, resulting in a highly interwoven structure. The strategies "7/30" or "23/30" and "29/30" or "1/30" are extreme situations. In between these cases there exist other feasible strategies with intermediate interweaving degrees.

To make a classification possible, a concrete definition of interweaving degree is needed. To introduce this definition, a graphical method will be used. Again 30 points along the circumference of the tube are considered. These points are numbered from 1 to 30 (Fig. 3.26). In Fig. 3.27 this circumference is developed and presented by the inclined line segment. It is assumed that the $+\alpha$ and $-\alpha$ fibres start at the same point, e.g. point 1. Then, from every point, the $+\alpha$ and $-\alpha$ fibres are drawn, starting with the last one in time, which of course lies at the upper surface. Therefore the winding strategy sequence is followed, starting at the last number. By successively considering all circumferential points, and reminding in every cross-over point which direction lies at the upper surface, one can obtain plots like Fig. 3.27.

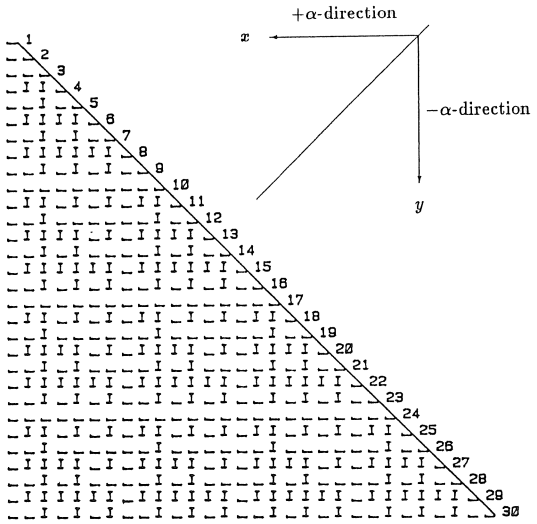

Figure 3.27: Graphical representation of the fibre interweaving.

The horizontal dashes show that in that particular cross-over point, the fibre along the x-axis ($+\alpha$ direction) lies at the upper surface, a

vertical dash indicates that the fibre along the y-axis ($-\alpha$ direction) lies on top. These plots provide a visual representation of the interweaving. The more frequent the changes | — | — are, the more intensive the fibres are interwoven.

To express the degree of interweaving by a numerical value, following steps have been attempted : for every horizontal line ($2 \rightarrow 30$) the dash-changes are counted and added. The same addition is performed for the vertical direction. The average is then divided by the maximum number of changes that can be achieved in an analogous plain-weave structure. This ratio finally defines the interweaving degree.

Based upon the just now defined interweaving degree, following classification (Table 3.5) can be made :

strategy	interweaving degree
23/30	0.497
7/30	0.483
19/30	0.476
11/30	0.448
17/30	0.379
13/30	0.324
29/30	0.097
1/30	0.000

Table 3.5: Interweaving degree for different winding strategies.

Only those strategies "$x/30$" in which x and 30 do not have a common divisor are valid. Other strategies, for example "5/30", with sequence : 1 6 11 16 21 26 1 6 11..., do not permit the fibres to reach every point of the circumference because, after 6 cycles, the first fibre position is overlaid again.

So, to resume this definition section, it can be stated that, depending on winding strategy, the winding process results in either a layered cross-ply, either a woven composite.

3.4.5 Influence of winding strategy

To prove that interweaving winding methods can provide interesting properties, as could be expected from woven fabric literature, the influence of the winding strategy, -determining the fibre interweaving-,

on the performance of filament wound tubes and vessels has been investigated.

3.4.5.1 Tubes

Glass fibre/epoxy tubes with a winding angle of $\pm 25°$ were wound according to the "7/30", "17/30" and "29/30" winding strategies. The tubes have a diameter of 70 mm and contain 30 fibre strands along their circumference in both directions, resulting in a 1.2 mm thickness. After winding, curing and mandrel removal, the tubes were sliced into rings of 12 mm width. These rings were then tested for stiffness and strength using a split-disk test procedure.

Mandrel

To start the investigation, a mandrel enabling different winding strategies to be achieved was needed. In case of a cylindrical mandrel, continuing pure geodesic winding and guaranteeing a stable way of returning the fibre requires the ends to have a smaller diameter, e.g. using conical or spherical end caps. If these are wound geodesically, different winding angles can be realized, but for one specific angle the strategy is fixed.

Therefore, it has been decided to use a cylindrical mandrel without end caps. However, to be able to return the fibre, now a certain overlength is needed on which the winding angle changes non-geodesically from its constant value $+\alpha°$ on the definite tube part to $0°$ and further back to $-\alpha°$. Thanks to friction, these slow deviations from the geodesic paths do not detract from the winding accuracy. With a pure cylindrical mandrel, totally different strategies can be realized by simply altering the length of the wound tube. Besides, it has the additional advantage that the mandrel can be removed by a simple pushing-through operation. In case of end caps, mandrel removal requires additional sawing or turning, which could possibly damage the mandrel.

The mandrels used for the tube winding were made of ertalon or polyethylene and turned cylindrical. Thanks to pre-heating and applying a suitable release agent, their removal caused no problems.

Manufacturing data

Material

- E-glass : 2400 Tex
- resin : Araldyte LY556
- hardener : HY917
- accelerator : DY070
- mandrel :
  - ertalon
  - polyethylene
  - diameter : 70 mm

Winding conditions

- winding angle : $\pm 25°$
- 30 fibres along the circumference in each direction, resulting in a 1.2 mm thickness
- mandrel pre-heating at 60° C
- impregnation bath temperature: 40° C
- winding environment temperature : 80° C, using an infra-red lamp
- fibre tension : low to ensure stable non- geodesic returning
- curing : 10 hours at 75° C, no pressure applied

After curing and mandrel removal, the tubes have been sliced into rings of 12 mm width. Although the test pieces were narrow, which could cause boundary effects to influence the measurements, broader rings could not be tested because of the limited maximum force of the hydraulic tensile test machine used (12 kN).

Tensile test

Test procedure

To examine the tensile stiffness and strength of the filament wound rings, *split-disk* tests have been performed, situated between the standardized *N.O.L. ring-split* tensile test and the *elongated ring* or *race-track* test.

The *N.O.L. test* (Fig. 3.28) allows for the specimen to be fabricated by filament winding and tested in a conventional, universal testing machine without special fixtures. However, it has the disadvantage that no flat section is available to attach strain gages.

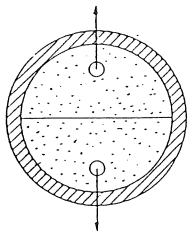

Figure 3.28: Schematic representation of the N.O.L. ring tensile test.

In order to provide a flat surface for bonded-on strain gages, a similar type of test can be performed, using an elongated specimen design. This *elongated ring* or *race-track* specimen is shown in Fig. 3.29.

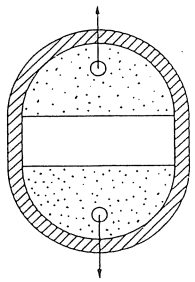

Figure 3.29: Schematic representation of the race-track tensile test.

In both specimen types, substantial bending moments occur near the corner of the disks.

Within this research, both tests have been combined by using circular test pieces with smaller disks. Finite element simulation of this test

procedure will also show significant bending in the free ring sections, with maximum bending stresses at the edges of the disks.

The applied disks are circular segments with an outer radius equal to the inner radius of the composite ring. Since each disk is smaller than one half circle, there will be a gap of 13 mm between both disks, when being put into the ring (Fig. 3.30). The upper disk is gripped by an hydraulic cylinder, the lower disk is fixed to a dynamometer. While the upper grip is pulled upwards with a speed of 6 mm/min, its displacement and the force acting on the lower grip are measured respectively by a LVDT (Linear Variable Differential Transformer) and a dynamometer. For each specimen, the maximum force before rupture and the slope of the tensile curve in its linear region are determined.

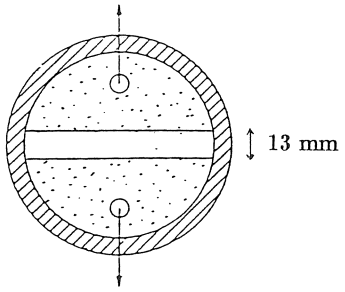

Figure 3.30: Schematic representation of the tensile test, performed at the K.U.Leuven.

Test results

The results of the tensile tests, together with their standard deviations, are presented in Table 3.6. Because of a scatter on the specimens' width, the measured maximum force is referred to a width of 10 mm instead of 12 mm. The equivalent stiffness is defined as the total force for 1 mm displacement in case of a test piece with a width of 10 mm. For each strategy type, 2 tubes have been wound. From each tube, 6 or 7 test pieces have been cut and tested.

These test results show that winding strategy and therefore interweaving has only little influence on structural stiffness. On the other hand, they reveal a 30 % higher strength for woven specimens "7/30" and "17/30", when compared to "29/30". This experience answers to the expectations based on literature data concerning woven fabrics, loaded in between their fibre orientations. In this study, $\pm 25^{\circ}$

strategy	equivalent stiffness [N/mm]	maximum force [N]	number of specimens
"7/30"	4846 ± (378)	7227 ± (1077)	12
"17/30"	4744 ± (452)	6907 ± (1025)	14
"29/30"	4506 ± (460)	5512 ± (723)	13

Table 3.6: Tensile test results.

laminates, charged along the 0° direction, have been compared. The "7/30", which shows the most interweaving, is also the strongest. The "29/30", which can be considered as cross-ply (no interweaving) has a 30 % lower strength.

The test simulation, discussed in the next paragraph, will predict failure to occur at the edges of the disks. In practice however, the position of failure showed a broad scatter around the mid-plane of the ring, reaching to the corners of the upper and lower disks.

Macroscopic inspection of the "29/30" test pieces showed that failure was caused by shear in the resin between the two layers. No fibres were broken and the surface was very regular. On the contrary, the fractured surface of the "7/30" type was much more irregular. There was no shear failure between two layers because of the cross-over points. The damage was dispersed over the whole cross-section. As well, a number of fibres were broken. In "17/30" strategies, a combination of both failure types could be seen.

Test simulation by means of finite elements

A major problem in structural analysis and strength prediction of filament wound components are the material data that must be introduced in the model. Determining properties of filament wound specimens is a rather difficult task, because most standardized test procedures to define material data for strength analysis use flat specimens. Therefore, unidirectional hoop windings consisting of glass fibres, impregnated with epoxy resin, have been wound on a flat square drum, permitting flat specimens to be cut out of it (Ref. [13] and [66]). Unfortunately, the quality of these specimens did not answer the needed requirements for obtaining significant strength properties, since the flat drum sides did not allow an appropriate compaction and uniform resin distribution of the resulting laminates .

However, the fibre volume fraction of most filament wound test specimens was measured to be situated between 40.5 % and 49.1 % with an average of 44.8 %. As this corresponds to the fibre content in commercially available and well-tested *Scotchply-1002* (45 %), which is a glass fibre/epoxy prepreg, it has been suggested to replace the unknown design variables by the well-known *Scotchply* data (Ref. [78]).

To justify this *Scotchply* data utilization, it can be mentioned that, unlike the strength measurements, the elastic properties of the flat filament wound specimens did quite well correspond to the *Scotchply* stiffness, as can be concluded from Table 3.7. The measured moduli are an average from tensile and compression test results.

	measured data	Scotchply-1002 data
E_l [MPa]	36031 $\pm$ 3499	38600
E_t [MPa]	9499 $\pm$ 1723	8270
ν	0.30	0.26

Table 3.7: Stiffness comparison between filament wound specimen measurements and *Scotchply* data.

Thanks to this comformity, it has been decided to simulate the tensile test by means of finite elements (Fig. 3.31), using *Scotchply* stiffness and strength properties.

The ring specimen, introduced in the finite element code, has following dimensions : a width of 12 mm, 35 mm radius and 1.2 mm thickness. The fibres are oriented at $\pm 25°$ with respect to the circumferential direction.

Difficulties arise in simulating the contact surface between the two disks and the composite ring. In reality, this contact is a free joint, meaning that the composite can slide over the segments, once friction has been overcome. As this is difficult to simulate, an approximation has been introduced by prohibiting the contact points of the finite element mesh to rotate in any direction.

The load is represented by an internal pressure acting onto the ring's contact surface. The pressure distribution is taken sinusoidal, resulting in a vertical force of 10000 N.

Fig. 3.32 shows the deformed specimen, albeit exaggerated to obtain a clear picture. The ring part in between the two disk segments clearly suffers from significant bending moments.

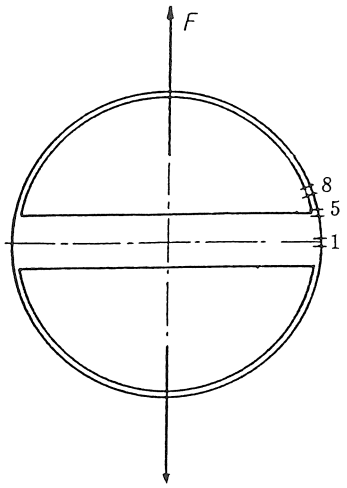

Figure 3.31: Schematic representation of the simulated tensile test.

The corresponding stresses have been incorporated into the *Tsai-Wu* failure criterion (Eq. 1.1), using *Scotchply-1002* strength properties (Table 3.8).

The resulting safety factors, referred to a tensile load of 10000 N, are gathered in Table 3.9. This table indicates a shift of the dangerous locations from the inside ($-25°$ layer) to the outside ($+25°$ layer), which is due to the sign change of the curvature. From the analysis results one can expect the rings to resist a maximum tensile load of $0.52 \cdot 10000$ N $= 5200$ N. Probably, rupture will occur in element 5, at the corner of the disk segment. This maximum force applies to a layered ring of 12 mm width. For comparison with the test results, which are referred to a width of 10 mm, a rupture load of $\frac{10}{12} \times 5200$, being 4333 N, will be considered. Test specimens with a "29/30" strategy could resist a maximum tensile load of 5512 N (Table 3.6) with a standard deviation of 723 N, exceeding the predicted value for at least 21 %.

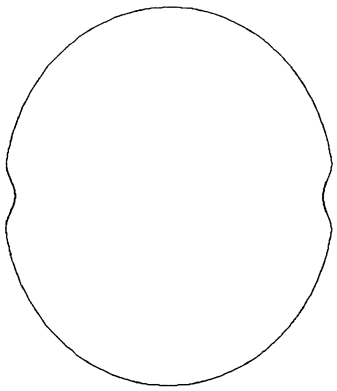

Figure 3.32: Deformed state of the ring specimen during the tensile test.

	Scotchply-1002 data
X_t [MPa]	1062
Y_t [MPa]	31
X_c [MPa]	610
Y_c [MPa]	118
S [MPa]	72

Table 3.8: *Scotchply* strength properties.

element	$+25°$	$-25°$
1	2.13	0.65
2	1.87	0.81
3	1.35	0.96
4	0.84	1.47
5	0.52	1.83
6	1.19	1.19
7	1.20	1.19
8	1.21	1.20

Table 3.9: Safety factors according to the ring test simulation by means of finite elements.

Following considerations however have to be made :

- Safety factors are calculated using the *Tsai-Wu* criterion, based on a first-ply failure.
- Assumptions have been made concerning the contact surface and load distribution.
- A very important factor is the composite's thickness. Small variations among thickness can have significant implications because the rings are subjected to bending. In case of a 1.3 mm thickness, the maximum computed load is 4 916 N, which is only 11 % below the measured force.
- In the filament wound rings, the fibre distribution is not uniform over the cross-section. The outside contains more resin than the inside.
- Finally, *Scotchply* data have been used instead of data measured on the filament wound specimens.

From these tensile test simulations, predictions of the maximum tensile load have been obtained, which, taking into account all assumptions, quite well correspond to the measured values. As employing *Scotchply* data leads to conservative strength predictions, they can be accepted for safe glass fibre/epoxy filament winding design.

Residual stresses

Curing at elevated temperatures gives rise to residual stresses when the composite is used at room temperature. Although these temperature caused stresses can not be avoided, their influence can be reduced in case the fibres are interwoven. To demonstrate this, again the "7/30" and "29/30" test pieces are once more compared.

When a "7/30" ring is given an axial cut, no deformation occurs. Residual stresses are compensating each other at every interweaving point.

On the contrary, the "29/30" test pieces can show large deformations when being given an axial cut. These deformations depend on the laminate lay-up. When a "29/30" tube is cut into slices, the first ring has e.g. a $+25°$ lay-up along the whole circumference. The next specimen then already shows a small area with a $\pm 25°$ lay-up which is extending in the next specimen ...and so on. The test piece with only one stable lay-up is a simple cross-ply laminate, which will deform

when cooled down, giving an helical shape to the cut ring, whose two ends have separated in the axial direction over a quite large distance (Y_{max}) (Fig. 3.33).

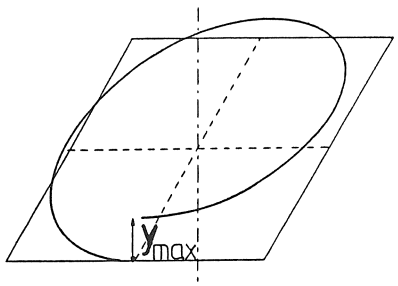

Figure 3.33: Deformation of a cut ring, due to residual stresses.

Test pieces with a $\pm 25°$ lay-up over one half of the circumference and $\mp 25°$ over the other half, have two parts which tend to deform in opposite directions. This gives rise to two compensating torsions, resulting in no axial displacement of the two ends, only an anglular distorsion. Laminate lay-ups in between show deformations between 0 and Y_{max}.

A quite good agreement has been ascertained between computed and measured values of axial displacement. Using the principle of virtual work, it can be stated that : (Fig. 3.34)

$$\frac{P \cdot Y}{2} = \int_0^L \frac{M_w^2 \cdot dx}{2 \cdot G \cdot I_p} \tag{3.17}$$

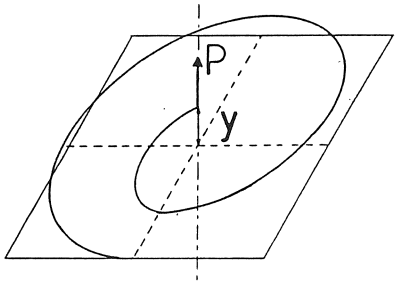

Figure 3.34: Deformation of a cut ring, due to a tensile load P.

With $M_w = P \cdot R$, R being the radius of the ring, and $L = 2\pi \cdot R$, the vertical displacement Y due to a force P equals :

$$Y = \frac{M_w \cdot 2\pi \cdot R^2}{G \cdot I_p} \tag{3.18}$$

For the considered rings, $M_w/G \cdot I_p$ corresponds to the torsional curvature caused by a temperature difference of 75° - 20° = 55° C. Using *Scotchply* data, Tsai's computer program *Genlam* (Ref. [78]) calculates this torsional curvature and returns : -1.5/m = -1.5/1000mm.
Consequently, Y_{max} becomes :

$$Y_{max} = (-1.5/1000)2\pi 35^2 = -11.5mm \tag{3.19}$$

This is the axial displacement for a pure cross-ply. If the laminate lay-up changes over one part of the circumference, twice this part must be subtracted from the total length of the circumference.

Three rings have been investigated :

		measured Y	calculated Y
		[mm]	[mm]
50 % +25°	50 % −25°	0	0
11 % +25°	89 % −25°	6	9
16 % +25°	84 % −25°	10	8

Table 3.10: Measured and computed deformations of the cut rings, due to residual stresses.

The measured deformations correspond quite well with the computed predictions. Both reveal substantial residual stresses in cross-plied tubes. Thanks to the alternating lay-up, these residual stresses are not built up in case of a woven lay-up.

Summary

The influence of the winding strategy of filament wound tubes has been investigated. Different winding strategies with varying interweaving degree have been tested for stiffness, strength and residual stresses and deformations. It has been found that interweaving of the fibres has positive influence on the strength and residual stresses and almost no influence on stiffness. *Scotchply* data have been shown to provide conservative strength predictions for glass/epoxy filament wound components.

3.4.5.2 Pressure vessels

The influence of winding strategy has also been investigated on pressure vessels (Ref. [63]). Both interwoven and cross-plied vessels consisted of a cylindrical part with a 125 mm radius, closed by two optimally shaped end caps (3.3.3.2). In both cases the fibre angles and layer thicknesses were the same; the cylinder shell contained a 0.93 mm layer of $\pm 9°12'$ windings, covered by a layer of hoop windings with a 1.78 mm thickness. The only difference was the length of the cylinder, which determined the sequence of the fibre lay-down. Two extreme strategies have been chosen; a shorter cylinder, with a length of 134 mm, giving a cross-plied lay-up and a longer cylinder (326 mm), resulting in an interwoven laminate. Both types of vessels were pressurized using water and checked for leaking. Before performing the static burst tests, the vessels were first fatigued between 0.025 and 0.6 MPa during 33000 cycles at 1 Hz frequency (Fig. 3.35).

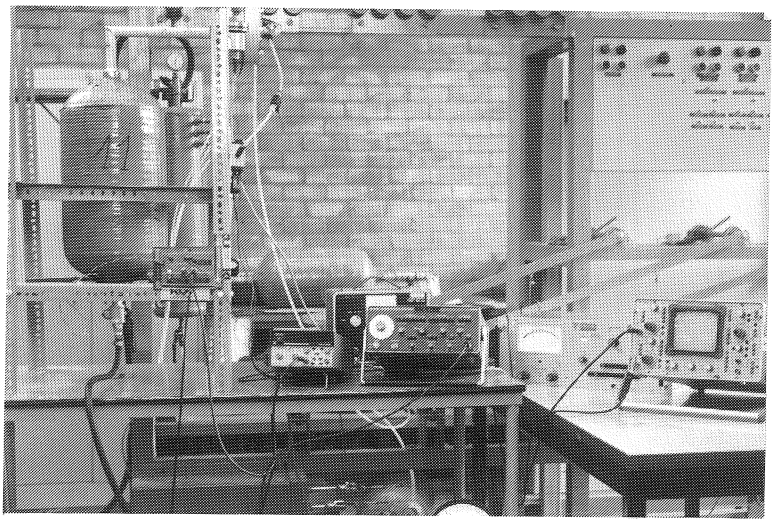

Figure 3.35: Filament wound pressure vessel during fatigue loading by means of an alternating water pressure.

On the end caps, the vessels with interweaving showed better performance as compared to the cross-plied vessels (1.8 MPa for the wovens against 1.4 MPa for the cross-plies). On the contrary, the cylin-

ders with a layered lay-up could stand higher pressures before leaking. The woven cylinders started leaking at 1.6 MPa while most layered cylinders could not be pressurized until leakage within the limited available pressurization. These results can be explained as follows : at the end caps it is obvious that the woven case is better because the random distribution of the fibres uniformly spreads out the discontinuities between the different height levels of the fibres. In the cross-plied case however, the laminate is built up like a fan, creating a large discontinuity where the last fibre meets again the first one. This discontinuity of course provides an ideal initiation for leaking.

On the cylinder the non-woven vessels faired slightly better. Here the penalty of the fibre crossings is probably more pronounced. The biaxial stress state in the pressurized vessel loads the almost longitudinal, helical windings and the circumferential hoop windings both along and perpendicular to their fibre directions. As literature only provides comparising data for uniaxial loading conditions, the biaxial results can not immediately be interpreted. Nevertheless the experiments revealed a better performence for the non-woven cylinders.

From these experiments it can be concluded that the ideal vessel would be one with an intermediate degree of interweaving, resulting in an initiation of leaks at the same pressure for the end caps as for the cylinder.

3.4.6 Conclusions

Although most filament winders prefer layered structures, interweaving winding processes can have several advantages. First, they practically do not require special geometrical demands. Second, they can affect the mechanical properties in a positive sense. To confirm this, the influence of winding strategy, including interweaving of the fibres, on the performance of filament wound tubes and pressure vessels has been investigated. Both tube and vessel results have shown that interweaving winding methods can have positive influences on the composite's performance. Consequently, they can be considered as appropriate manufacturing alternatives.

3.5 Detailed stress analysis comments

When performing detailed analysis, the question rises how to take the specific winding properties, characteristic for the interweaving of the fibres, into account in the design stage. Or, if the designer is limited to classic calculation techniques, which assume non-woven, layered plies, what safety factors should he apply?

Most composite calculations are based on the *classical laminate theory*, in which the laminate is considered to be built out of perfectly bonded laminae which are stacked on top of each other, with infinitesimal thin interfaces; displacements vary continuously over the thickness, laminae do not slip and plane sections remain plane and perpendicular to the mid-plane. It is also assumed that the stresses in the thickness direction are small and may be neglected.

At first sight, these assumptions do not answer to the specific properties, characteristic for filament wound components. However, in practice laminate theory offers quite good results for wound parts, in particular for their elastic behaviour. In filament winding literature typical winding-related failure criteria or strength predictions are not often treated, although a lot of filament wound applications require to be dimensioned based on strength instead of stiffness. Many researchers however (Ref. [79], Ref. [93] and [45]) have found out that quadratic failure criteria, as e.g. the *Tsai-Wu* criterion, give reasonable agreement between theoretical and experimental results on filament wound components.

Tsai (Ref. [78]) proposes to solve the problem of interweaving by giving laminate theory an empirical hand : *"predictions of elastic constants and strengths of fabrics, filament wound and braided structures can be made using classical micro- and macromechanics with appropriate correction factors"*.

Employing empirical aid is characteristic for all branches of composite calculations. According to Venkayya (Ref. [81]), for the analysis of bolted joints often a 2-D-anisotropic plate theory is used, in which appropriate correction factors are applied.

Laminate plate theory does not include the thickness direction. Excluding the third dimension is not only a weak point of simple laminate programs. Even sophisticated finite element programs often show the same shortcoming. This is also confirmed by researchers in aeronautic industries, who investigated the problems concerning bolted joints in

composites. Even single shear joints, where the third direction is very important because secondary bending creates additional stresses, are 2-D calculated, using empirical corrections.

Of course these days do offer a lot of finite element programs which indeed take into account the thickness direction. For filament wound structures there even exist computer codes which can model the winding pattern, the resulting layer boundaries, cross-over points, interweaving etc ... Such a detailed model has already been used to simulate the strength loss in spherical pressure vessels (Ref. [39]).

The question arises whether 3-D calculations can be financially justified. *"Computational procedures must not be so sophisticated and full of details that they become too time-consuming and expensive to use in daily analysis work"* (Ref. [20]). Moreover, the third direction is not the only obscure point; often external loads are not well known, there remain uncertainties about failure mechanisms and relevant input data are difficult to obtain.

In the Department of Mechanical Engineering, the finite element code *Systus* has been used, which only provides composite calculations based on *classical laminate theory.* However, this code has proved to be a relevant numerical computation tool for filament winding design purposes.

3.6 Conclusion

In this chapter, additional aspects the designer has to consider when designing a filament wound component have been discussed. A design methodology has been presented, taking into account these filament winding related design considerations. Two concrete examples, designed according to this method, have been described in detail.

Winding strategy, determining the interweaving of the fibres in a filament wound component, has proved to be an important design parameter. An investigation of the influence of winding strategy on the performance of tubes and vessels has shown that, beside flexibility, the little appreciated interweaving ways of winding can provide satisfying end product quality.

This chapter has been confined to axisymmetric composite components. However, the presented design methodology can be extended to non-axisymmetric structures, as will be discussed in chapter 4.

Chapter 4

Design of non-axisymmetric filament wound composites

4.1 Introduction

In filament winding design, restrictions imposed by the winding process very much complicate the design procedure. If moreover, non-axisymmetrical shapes are concerned, which have to be wound geodesically, the design's complexity will be even more pronounced. Further, also the control of the winding process will include more difficulties.

Hence, to guide the unexperienced designer, a design and control strategy will be discussed for non-axisymmetric filament wound composites. These strategies have been developed in collaboration with colleague J. Scholliers. From a series of feasible geodesic patterns, a proper selection must be made. Their coverage will correspond to a specific laminate lay-up, which must be checked by structural analysis and eventually, some additional patterns or layers must be provided. Once the resulting composite can answer to the strength and stiffness requirements, control commands can be set up to materialize the proposed winding patterns.

An important step in this strategy is the link between a given set of winding paths and the corresponding laminate lay-up. Therefore, the software that has been developed to automatically generate the lay-up data out of the winding pattern description will be discussed in

detail.

Finally, the proposed strategy is illustrated in the light of the design of a filament wound T-connection. After the geometry has been defined, a finite element analysis is performed on an isotropic T-part. It would be possible to translate the resulting isotropic stress state into ideal fibre orientations all over the structure. However, finding a set of geodesic paths which together completely cover the mandrel is already such a problem, that it is impossible to take into account the ideal fibre direction everywhere on the T-part. Therefore, the design is conceived as a problem of verification. From a proper selection of geodesic patterns the equivalent laminate lay-up is computed, which is then used as input to a finite element control analysis. Locally overloaded areas are then to be reinforced by supplying additional, well-oriented fibres. For, the final set of patterns to be wound must provide the composite T-part with the required load-bearing capacities.

4.2 Additional difficulties, due to non-axisymmetry

When the filament winding technique is applied for manufacturing non-axisymmetrical components, additional concerns are involved as well in the DESIGN stage as during the CONTROL stage.

4.2.1 Design problems

Covering mandrels of asymmetrical shape can pose a number of difficulties, which do not appear when the component has an axis of symmetry. For, in case of axisymmetry, one and the same geodesic line can be repeated along the circumference, thereby effecting total coverage in a controllable manner. On non-axisymmetrical parts however, two consecutive paths, which have only a small initial shift, very fast diverge as soon they encounter areas of the surface that are not identical. Consequently, filament winding of such shapes will require a large number of individual winding paths to be generated, which, when combined, completely cover the mandrel's surface. Since all of these are unique, a major design problem will be the selection of appropriate starting conditions and corresponding geodesic paths, which together result in a laminate lay-up that is able to answer to the desired

strength and stiffness specifications.

Further, the computations themselves of geodesic lines are more complicated, since the law of *Clairaut* (Eq. 3.1), relating the mandrel's radius with the winding angle, does not apply to arbitrary surfaces, only to surfaces of revolution. To yet compute geodesic lines, other methods as e.g. triangularisation (Ref. [33]), in which the mandrel surface is modelled by means of plane triangles, or numerically solving the differential equation, derived from the definition of a geodesic path (Ref. [42], Ref. [36] and [9]), can be appealed on.

4.2.2 Control problems

Beside a more complex design process, complications also appear in the field of control. The large amount of individual geodesic paths causes the number of data, required to control the winding unit, to become much higher than the rather limited control data in case of axisymmetry. For winding complex non-axisymmetrical shapes, usually also a winding machine with more degrees of freedom is needed, with in accordance more axes to be controlled.

Further, problems can arise when the geometry shows local *concavities*. For these can include danger for *collisions* between the feed-eye and the mandrel and cause *fibre bridging* in case the fibre makes simultaneous contact in two separate points of the mandrel surface.

Until now, filament winding of non-axisymmetrical shapes has been commonly performed using the *teach-in* method. With the *teach-in* method, control data are determined experimentally. The operator continuously leads the feed-eye throughout the winding process, *teaching* it how to lay down the fibre along the desired path, and records the positions of the different winding machine axes at regular time intervals. With this method, instantly a collision-free control program is generated and a direct visual control of the mandrel's covering is provided. However, the *teaching* operation is very time-consuming and occupies the machine for a long, unproductive time. Moreover, it is extremely difficult to accurately position and orient the fibre on the mandrel, as specified by the designer. Since *teaching* is done statically, on a point-to-point basis, the recorded position-versus-time relationship of the feed-eye can result into severe machine accelerations when the program is run dynamically.

Therefore, it is far more interesting to compute the control data

in advance and to use an *off-line* control program, since this frees the machine for production runs only. The accuracy of the fibre placement will increase and sudden accelerations can be smoothed out. Moreover, the control program can first be simulated to check whether there are any collisions.

Filament winding using small fibre strands results in long production times, which can be shortened by employing wider tapes. But, when winding wide tapes, these can tend to rotate along their own length axis, which is referred to as *fibre twisting.* Fibre twisting introduces wrinkles in the surface, causing voids and weak spots, and should therefore be avoided. This can be accomplished by using an appropriate strategy for the motion of the feed-eye and the mandrel. Furthermore, it is favourable to align the feed-eye with the fibre as much as possible, thereby avoiding unnecessary wrinkles.

4.3 Design and control methodology for winding non-axisymmetrical composites

The successive elements constituting the proposed strategy are schematically represented in Fig. 4.1. The aspects within this flow chart that are typical for non-axisymmetrical design will be discussed more in detail.

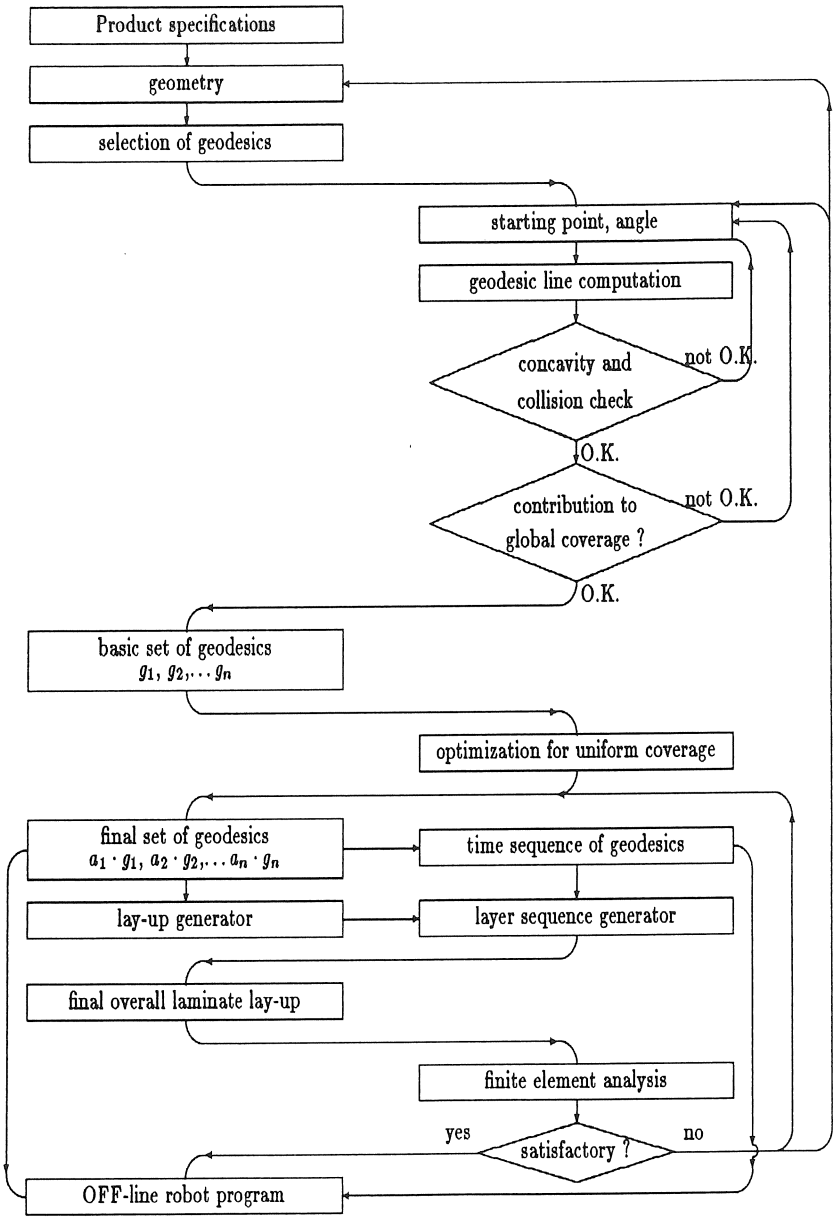

Figure 4.1: Design methodology for non-axisymmetric filament wound composites.

4.3.1 Shape definition and surface modelling

The shape may be completely determined by other design requirements, or it may have to be determined as a part of the filament winding design task. But even if the shape is given, its specification usually only concerns an inside mandrel surface, and the determination of the thickness and the outside shape will still form part of filament winding design.

Once the geometry has been defined, a mathematical representation of the component's surface must be drawn up. A three-dimensional CAD surface modeller can be used to make a drawing of the mandrel. Within the filament winding research team, the ANVIL-5000 CAD system has been used. The mandrel is divided into several blending surfaces. The corresponding geometrical data are made accessible for an external program by creating an IGES file, which is an international standardized format for interchanging data between CAD systems. The IGES format allows for the mathematical parameters describing the mandrel's geometry to be extracted and used in subsequent calculations.

4.3.2 Pattern development

Once the geometry of the surface has been defined, the computation of winding paths can start. The major condition in generating fibre trajectories is, however, that they should be non-slipping. This can be accomplished by either winding along geodesic lines or by slightly deviating from them, counting on friction effects. Similar to the axisymmetric components, the winding research emphasized in this chapter has been concentrating on geodesic winding only.

A computer code *CAWAR* (*Computer Aided filament Winding of Asymmetrical shapes using Robots*)(Ref. [68]) has been developed by colleague J. Scholliers for calculating geodesic paths on components which are composed of several individual surfaces of revolution. These computations require the differential equations describing the geodesic lines to be solved. The parameters representing the differential equations are determined by the geometry of the surface, stored in the IGES file.

A geodesic line on a surface is defined to be a curve for which the second order derivative is perpendicular to the surface. This can be

mathematically represented by means of a system of two differential equations of second order (Ref. [9]). For bodies with rotational symmetry, this system can be converted into a normal-system of four differential equations, which allows for simple numerical solving. A unique solution requires four initial conditions to be specified. These are imposed by choosing the starting point and orientation of the geodesic line.

Beside computing geodesic lines, *CAWAR* continuously checks their curvatures in order to assure that no local concavities do occur. For, in case the geodesic line is locally concave, the fibre will be released from the mandrel's surface and follow a shorter path through the air.

4.3.3 Pattern selection

When designing a composite part, an important issue is to align the fibres with the principal load directions. To have an idea about where and in what directions the highest stresses occur, the designer usually starts with performing some isotropic analysis. The isotropic results could then indicate the ideal fibre orientations all over the structure. However, searching for a set of geodesic lines which together completely cover the surface is already such a problem, that it is almost impossible to additionally take into account the ideal fibre directions everywhere on the component. Therefore the design should be considered as a problem of verification. For a chosen set of geodesic paths, the corresponding laminate must be checked for stiffness and strength. Problem areas must be locally reinforced by adding fibres along geodesic paths that answer to the specific needs at the undercovered places.

To allow for a proper selection, maps are made which symbolize the geodesic trajectories for varying starting points and starting angles. Based on these maps, a set of geodesic patterns is assembled which results in a global surface covering. To obtain an equally covered surface, geodesic curves are selected which are as parallel to each other as possible. For every individual geodesic fibre path, the equivalent contribution to the laminate thickness all over the component is computed. An optimization program then combines multiples of each geodesic line, until a minimum of the thickness variation over the entirely wound composite has been reached. From this new set of geodesic lines, also the time sequence is determined.

4.3.4 Structural analysis

To evaluate the selected set of winding patterns, a structural analysis must be performed. Therefore, a finite element model of the composite component is set up. From the proposed set of geodesic fibre patterns, an equivalent laminate lay-up all over the structure must be determined. A computer code *LUPGEN (Lay-Up GENerator)* (4.4.1) has been developed, which automatically translates the geodesic data into corresponding layers, fibre angles and thicknesses for every element of the finite element mesh of the composite structure. The computer code *LAYSEQ (LAYer SEQuence)* (4.4.2) then permutates the present layers for every element, taking into account the real time sequence of the considered geodesic trajectories during manufacture. Finally, *LAYSEQ* outputs the real laminate lay-up in every element according to the format, required as input to the finite element code. The stress state in the loaded composite and the corresponding safety factors will eventually reveal overloaded areas that will need additional covering. To locally reinforce these critical zones, additional geodesic lines will be applied, which answer as much as possible to the specific strength or stiffness needs in the considered undercovered elements.

4.3.5 Machine control commands

For winding non-axisymmetrical components, the winding robot presented in paragraph 2.5.2 has been used. In Fig. 4.2 this robot is schematized within its winding environment.

The robot is an articulated PUMA-762 with six degrees of freedom. The external axis, which carries the mandrel, is linked with the robot through a specially developed hardware board. The robot is off-line programmable in the VAL-II language of Unimation. A software routine takes care of the synchronization between the robot and the external axis.

For every member of the chosen set of geodesic lines, *CAWAR* computes the positions of the feed-eye, which is mounted at the end point of the robot, and the corresponding angular positions of the mandrel axis, which together will lead to the desired filament winding pattern. This requires the feed-eye to be on the tangent to the geodesic curve in the contact point on the mandrel. Once the distance between the feed-eye and the contact point has been chosen, the three coordinates of

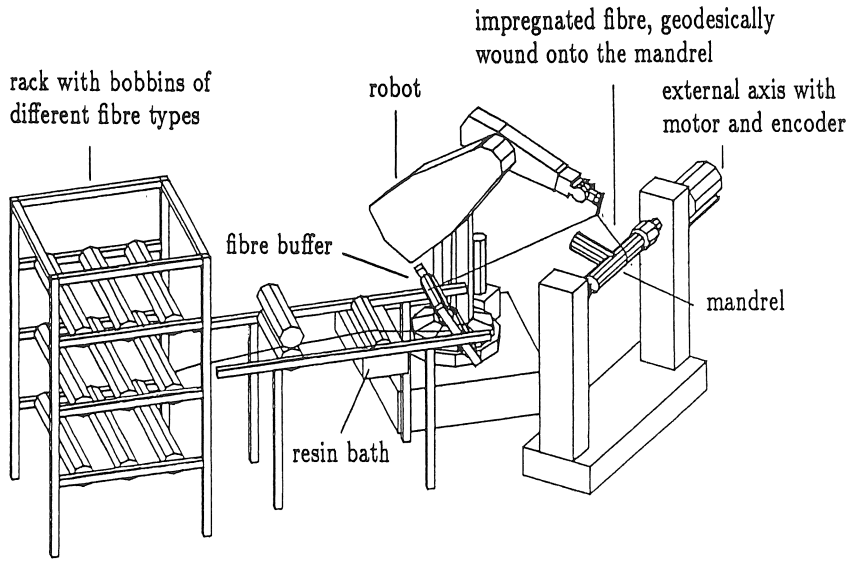

Figure 4.2: Filament winding robot with external axis.

the feed-eye position can be determined. To the feed-eye however, also an orientation can be given. In the ideal case, three conditions for this orientation can be formulated, by requiring that the orientation of the fibre in the contact point and in the feed-eye are equal. Consequently, for a given offset, six conditions can be stated. The filament winding equipment, robot plus external axis, has however seven degrees of freedom, thereby allowing to still vary the angular axis positions at which a particular point on the mandrel is wound. Consequently, an additional condition is needed to obtain a completely determined system. The best solution would be to define this condition as to minimize the accelerations. Since this would significantly complicate the computations, rotating the external axis as to make the tangent vector horizontal has been chosen as extra condition.

However, it must be taken care of that the calculated position of the feed-eye can be reached, without any collisions. Collisions between the feed-eye and the mandrel can easily occur in case the component has concave parts. Collision control is very difficult since a strategy has to be developed to prohibit collisions between two continuously moving objects, whose movements depend on each other.

To assure a continuous winding process, the successive fibre paths have to be linked together. Usually, in case of non-axisymmetrical

shapes, pins are provided along the circumference of the end sections of the mandrel, to allow for the fibre's returning. While determining the time sequence of the successive geodesic patterns, it has been taken care of that the end point of the previous path and the starting point of the next one coincide at the same pin circle and, moreover, that both pins involved are as close as possible to each other, thereby reducing superfluous material loss.

The successive robot paths are linked and a VAL-II program is set up. Within this program, developed by colleague J. Scholliers, the SYNCHRO routine realizes the synchronization of the motion of the external axis with the motion of the robot. The velocity of the axis is computed, based on a kinematic model of the motion of the robot between two points. The generated program is an off-line robot program, which can be downloaded to the robot controller.

As soon as all control data are available and the impregnated fibre is fixed onto the mandrel at the correct starting pin, the winding process can begin.

4.4 Automatic laminate lay-up generator

To allow for a structural finite element analysis of the designed filament wound component, the proposed global coverage patterns must be translated into an equivalent laminate lay-up. Therefore, a fortran link has been written between the geodesic data and the finite element program. This link contains two computer codes. The first one is called *LUPGEN*, which stands for *Lay-UP GENerator*, and which computes for every element what layers a specific set of geodesics corresponds to, their fibre angles and layer thicknesses. The second program, *LAYSEQ*, meaning *LAYer SEQuence*, transforms these data into the real laminate lay-up for every element, taking into account the time sequence of the individual, eventually repeatedly applied geodesics. The resulting equivalent laminate lay-up can be used as input to the finite element code. Both *LUPGEN* and *LAYSEQ* can be called from a command procedure, named *LUPRO*, allowing for the basic laminate lay-up to be created, additional lay-up to be generated and the real stacking sequence to be computed. A concise manual is given in appendix D.

4.4.1 LUPGEN

LUPGEN transforms geodesic data into layers with corresponding thicknesses and fibre angles in every element. An overview of the procedure thereby followed is presented in Fig. 4.3.

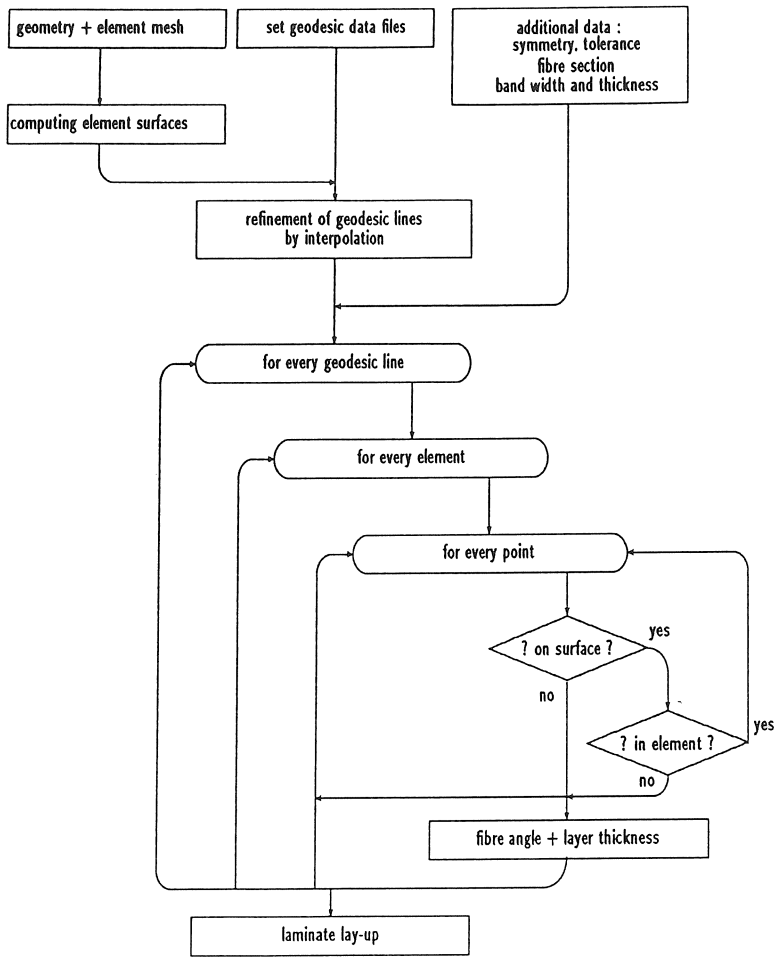

Figure 4.3: *LUPGEN* : *laminate Lay-UP GENerator.*

As is indicated in the scheme of Fig. 4.3, the input of *LUPGEN* consists of three types of data files. The first one contains information about the geometry and the element mesh. The second type of files are geodesic data files, each representing the coordinates of the points describing a particular geodesic line. In the third type, some additional data concerning eventual symmetry planes of the structure, tolerances, fibre section etc... are specified.

First the surface areas of all elements are computed. The dimensions of the smallest element serve as criterion to interpolate between the specified points of the geodesic lines. These are then refined until the point grid is finer than the element grid, in order to assure that, later on, no elements will be missed. Then, all geodesic lines are successively investigated. Each time it is checked which elements the geodesic path crosses, what the fibre angle then is and what thickness the covering corresponds to. Finally the laminate lay-up in every element can be determined.

To define this lay-up, following strategy is applied : all geodesic lines specified in the data set are investigated. For every geodesic line, all elements are verified and for every element, the program goes through all points describing the considered geodesic path. First it is checked whether the point is situated on the surface through the element. If yes, it is additionally examined whether the point also lies in between the element borders. Each time, it is stored how many successive points of a geodesic line do lie on the element. From this fibre segment (Fig. 4.4), an average fibre angle is computed and referred to the local axes of the element. Also the length of the fibre segment crossing the element is calculated. To this fibre segment, a volume is attached by multiplying the length by the cross-section of the fibre. This volume is then spread out over the surface of the element by dividing the volume by the element's area. This way, an equivalent layer thickness is obtained, corresponding to a fibre passing over the element with a well-defined orientation.

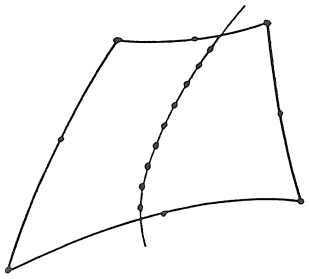

Figure 4.4: A geodesic line crossing the element.

This spreading-out simplification closely approximates reality in case that several parallel fibre strands cross the element (Fig. 4.5(a)). For, many very thin layers with the same fibre orientation will then together result into the real layer thickness. It is obvious that for geodesic lines from which there is only one specimen crossing the element in a particular direction, this way of modelling looses a little of its relevance (Fig. 4.5(b)).

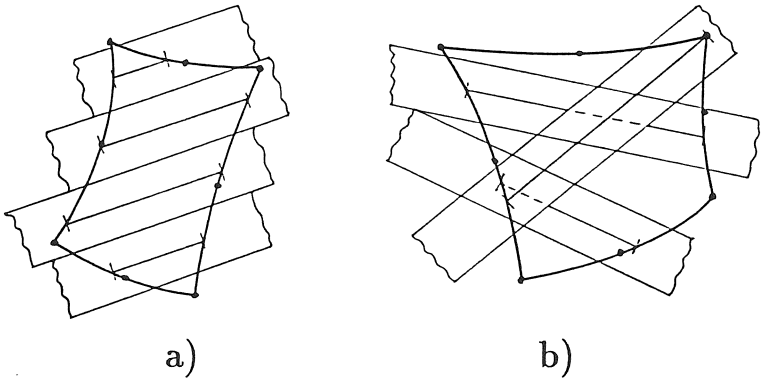

Figure 4.5: Graphical representation of the lay-up generation.

Furthermore, this strategy is only suited for an element mesh whose elements are large when compared to the mutual distance between adjacent geodesics. For, to very small elements, over which by coincidence several fibre bundels would pass, every time the entire fibre cross-section would be assigned, resulting in an exaggerated thickness. Therefore some other strategies to define the laminate lay-up have been tried out and compared. For example, a lay-up generator has been investigated, in which the fibres were considered as bands with a specific band width. A geodesic line was then assumed to cover right off a whole element area, in case the distance from the centre of the element to the geodesic line was less than half the band width. This lay-up generation specifically answers to the case where wide fibre bands with respect to the element size, corresponding to large distances between the individual geodesics, are concerned.

However, the first method has proved to be the most accurate one for the case of the T-connection, presented in 4.5, and will therefore be discussed more in detail.

Throughout *LUPGEN*, a parametric representation in the parameters η_1 and η_2 is used to describe the surface of each element (Ref. [5]). In this set of parameter equations, the coordinates of a point on the surface through the element are expressed as a combination of the coordinates of the element nodes, x_i, y_i and z_i, multiplied by weight functions ϕ_i in η_1 and η_2 : (Fig. 4.6)

$$\begin{aligned} x &= \sum_{i=1}^{8 or 6} \phi_i x_i \\ y &= \sum_{i=1}^{8 or 6} \phi_i y_i \\ z &= \sum_{i=1}^{8 or 6} \phi_i z_i \end{aligned} \tag{4.1}$$

with $\phi_i = f(\eta_1, \eta_2)$.

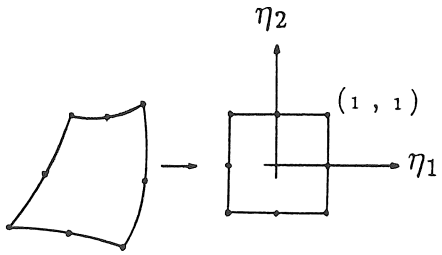

Figure 4.6: Parametric representation of the element surface.

Depending on its shape, the element is represented by 6 or 8 nodes. In order to check whether a particular point lies on an element, an approximating linearized equation of the surface in $\triangle\eta_1$ and $\triangle\eta_2$, going through the centre of the element is used :

$$\begin{aligned} x &= x_0 + \left.\frac{\partial x}{\partial \eta_1}\right|_{x=x_0} \Delta\eta_1 + \left.\frac{\partial x}{\partial \eta_2}\right|_{x=x_0} \Delta\eta_2 \\ y &= y_0 + \left.\frac{\partial y}{\partial \eta_1}\right|_{y=y_0} \Delta\eta_1 + \left.\frac{\partial y}{\partial \eta_2}\right|_{y=y_0} \Delta\eta_2 \\ z &= z_0 + \left.\frac{\partial z}{\partial \eta_1}\right|_{z=z_0} \Delta\eta_1 + \left.\frac{\partial z}{\partial \eta_2}\right|_{z=z_0} \Delta\eta_2 \end{aligned} \tag{4.2}$$

This system of three equations and only two unknowns must be solvable, which requires the determinant to be zero. Therefore, it is tested whether the determinant is smaller than a certain tolerance. If yes, it is additionally ascertained whether the point also lies in between the borders of the element. For this purpose, $\triangle\eta_1$ and $\triangle\eta_2$ have to be solved and checked whether they lie between certain limits. If yes, the considered point is accepted to be on the element.

In case the structure to be wound shows one or more planes of symmetry, this symmetry can be incorporated to simplify the modellization. For example, the T-connection that will be discussed later has two perpendicular planes of symmetry, therefore requiring only one quarter of the structure to be modelled and only one fourth of all geodesic lines to be investigated. However, it is possible that a geodesic line, starting in the quadrant of the model, proceeds in another quadrant. Yet, because of symmetry, one knows that for every geodesic pattern there are three equivalents, starting from each of the

other quadrants. To take this symmetry into account, it is determined for every geodesic point in what quadrant it is situated and then the proper mirroring is applied, required to bring the point into the modelled quadrant. For this mirrored point the same checks are performed and, depending on its origin quadrant, the sign of the fibre angle is reversed. But, by immediately taking into account the mirrored points, the real stacking sequence gets lost. This can however afterwards be reconstructed by means of the *LAYSEQ* routine. The output of *LUPGEN*, which directly serves as input to *LAYSEQ*, therefore contains for every element, beside the present layers, their fibre angles and thicknesses, also data concerning their origin, being the reference number of the corresponding geodesic, its quadrant of start and the quadrant of the corresponding geodesic points, giving rise to that particular layer.

4.4.2 LAYSEQ

Based on the output of *LUPGEN*, *LAYSEQ* will compute the real stacking sequence of the layers by permutating the present layers, having in mind the real time sequence of the fibre lay-down, starting in all four quadrants. This geodesic sequence information is stored in a separate file, which specifies for every present geodesic line the number of times it must be repeated, with for each time, the serial number of the four equivalent geodesic members, leaving off from the four quadrants.

Unfortunately, the resulting lay-up data will often constitute too much information to be handled in the finite element code. Therefore, an artificial data reducer has been built in, allowing for too thin layers to be dropped and successive layers of quite identical orientations to be combined to one single layer with average fibre angle. If more data reduction is required, the facility is provided to further compact the number of individual layers by combining alternating layers (1 with 3, 3 with 5... and 2 with 4, 4 with 6...).

The final laminate lay-up for every element is written in a special format, corresponding to the way the applied finite element code requires the material data to be specified.

4.4.3 Selection of basic geodesic patterns

Before running the automatic lay-up generator, an appropriate set of geodesic lines must be defined. This preliminary selection is principally

performed on a visual basis, using maps which represent the paths the geodesic lines describe on the structure for varying starting points and angles. A more detailed description of the selecting procedure is given further, for the case of a T-connection.

Once a first choice of geodesic patterns to be applied has been made, *LUPGEN* is run for each geodesic line individually, resulting in their individual contribution to the laminate thickness in every element. These thickness contributions are then used as input to an optimization routine with following strategy :
one starts with one copy of every member of the initial set of geodesics. Then, successively, that specific geodesic line is added which most strongly decreases the maximum-over-minimum thickness ratio among all elements. If no such geodesic exists, the geodesic line is repeated which will increase the minimum thickness at the most. Finally, this strategy will lead to a collection of geodesic lines, each of them repeated an appropriate number of times and together covering the structure as uniformly as possible.

4.4.4 Time sequence of the geodesic patterns

Not only for the actual winding process, but also for design purposes, it is necessary to know how the successive winding patterns will be linked to each other.

To allow for the fibres to start and finish at variable orientations, usually pin circles are attached at the end sections of the mandrel, with each pin representing a possible start or end point of a geodesic fibre path. In order to properly arrange the desired set of geodesic patterns, each time a successor is chosen, which starts at the same pin circle where the previous geodesic line was terminated and at a pin which is not too remote. The final time sequence of the individual geodesic lines must then be translated into the proper format, required by *LAYSEQ*, in order to generate the real stacking sequence of the laminate lay-up, corresponding to the proposed set of geodesic patterns.

4.5 Design of filament wound T-connections for pipelines

4.5.1 Introduction

As it is the case in many industrial areas, composite pipes and T-connections are trying to conquer their metal equivalents. Since a better corrosion resistance is one of their major benefits, they can offer interesting substitution facilities (Ref. [62]). In this section a design is proposed for a filament wound T-connection.

4.5.2 Geometry definition

Although functional substitution can be obtained, the original metal shape can not just be copied into a composite equivalent. For, the geometry of the T-part must be windable. But a classic T-connection consists of two intersecting cylinders with eventually an additional collar to locally reinforce the intersection (Ref. [2]). In case of filament winding, such a discontinuity must be avoided. To improve the windability and the quality of the laminate in the cross-area, a smoother shape is proposed (Ref. [25]), built out of 8 basic parts, 3 cylinders, 1 half cylinder, 2 torus segments and 2 plane segments to connect the torusses and the cylinders. Such a rounded-off geometry (Fig. 4.7) has the additional advantage of reducing the stress concentrations in the connection and the energy losses in the pipes.

However, the proposed geometry immediately includes an important penalty, connected with local concavity. For, the rounded elements are convex in the circumferential direction, but concave in the longitudinal direction. Consequently, a lot of geodesic lines will not be acceptable since they are locally concave and therefore cause the fibres to bridge.

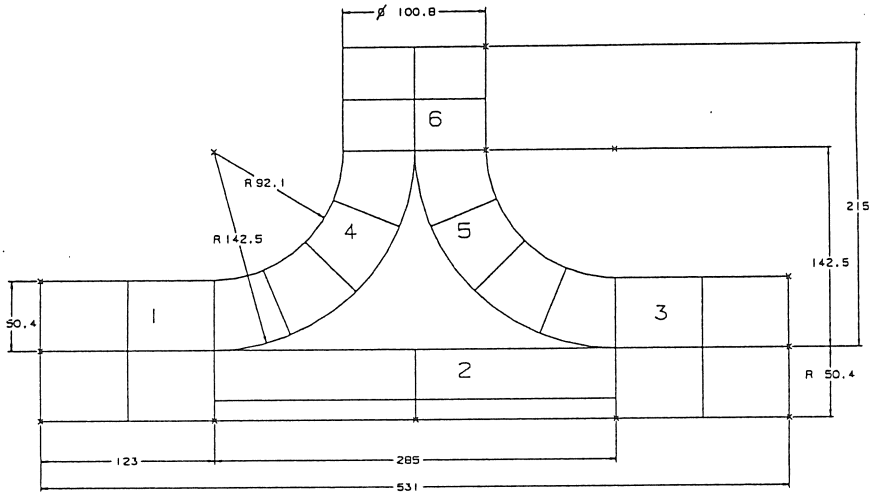

Figure 4.7: Proposed geometry of the T-connection to be filament wound.

4.5.3 Isotropic analysis

4.5.3.1 Purpose and benefit

When designing composites, the classical method is to start creating a model, to define relevant loading conditions and to perform a preliminary isotropic stress analysis. The resulting stress state can then be used as indicator for the ideal laminate lay-up in every area of the structure. In this optimal lay-up, the fibres are aligned with the directions of the highest stresses.

But, for a non-axisymmetric part, as e.g. a T-connection, the path of the geodesics varies very quickly with small changes in starting position and orientation. Hence, assembling a set of geodesic patterns which together completely cover the mandrel is already such a problem, that it is almost impossible to additionally take into account the ideal fiber direction in every element. Besides, the ideal fiber angle will change, depending on the loading conditions, which are, except for an internal pressure, not very well known.

Therefore it was decided to conceive the design problem as a problem of verification. For a set of geodesic lines, which completely and as uniformly as possible cover the mandrel, the equivalent laminate lay-up is defined and used as input to a finite element analysis. The resulting stress state is investigated and the safety factors all over the structure are checked. If necessary, some additional geodesics or layers are applied to locally reinforce the overloaded or undercovered problem areas. The final set of geodesics should then result in a composite structure, able to resist the imposed loads.

However, before performing complicated composite calculations, first a model was set up for an isotropic T-connection. These isotropic computations could then serve as check for the model's relevance. It is obvious that testing out a model is a complicated task, once simulating composite materials, since, with e.g. 20 layers and 3 stresses pro layer, interpreting the results becomes quite difficult. Beside the possibility to check the model, the isotropic results offer the opportunity to indicate some problem areas which will probably also occur in the composite case, and therefore deserve some special attention. These expected problem areas can then be accounted for from the initial selection of geodesic lines on.

4.5.3.2 Finite element model

For the strength computations, the finite element code *SYSTUS* has been used, allowing for isotropic as well as composite analysis. An initial steel model with a 3 mm thickness has been set up and various boundary and loading conditions have been investigated.

Fig. 4.8 shows the finite element mesh, albeit in deformed state, due to a 1 MPa internal pressure. For simplicity reasons, the end sections are assumed to be clamped so they do not deform. Thanks to symmetry, only one quarter of the structure has to be simulated. The torus and the cylindrical parts are modelled using quadrilateral elements. For the flat segment, trilateral elements are used. Because of numerical stability and accuracy, it has been decided to perform a quadratic analysis, meaning that in the middle of every element side an additional node is provided. A first sight on Fig. 4.8 reveals an unexpected deformation. If the T-part is assumed being a foot, the instep is compressed while the ankle-joint is expanding.

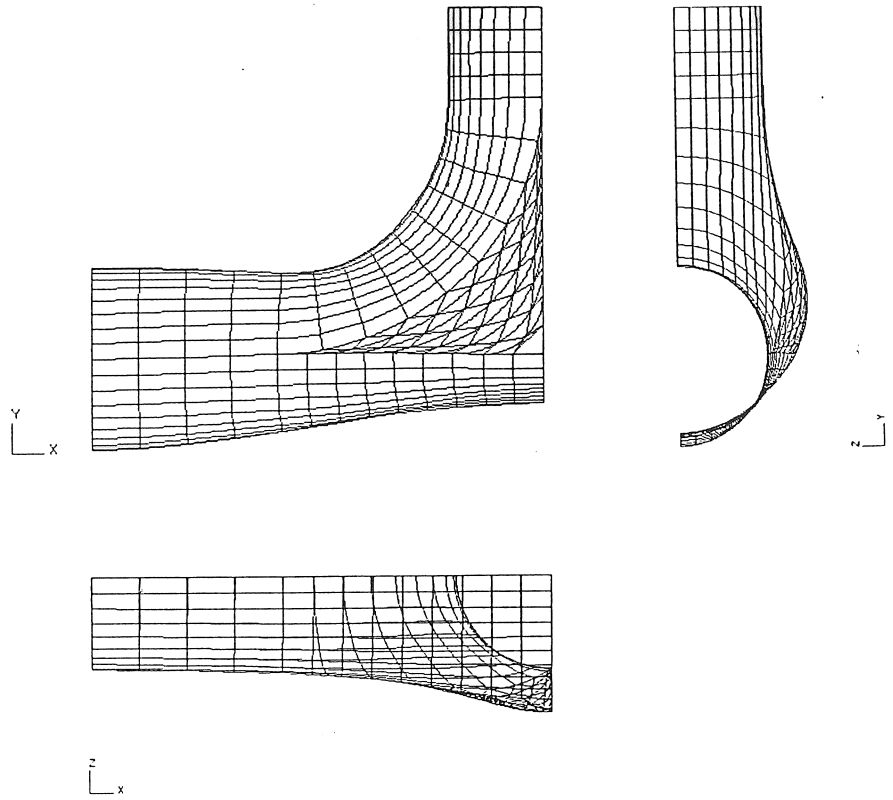

Figure 4.8: Deformed mesh of a clamped T-part, due to an internal pressure.

The corresponding stress state is visualized by means of the *Von Mises* stresses, at the inside (Fig. 4.9) and at the outside (Fig. 4.10) of the T-part. These plots show high bending stresses in the flat segment, close to the torus.

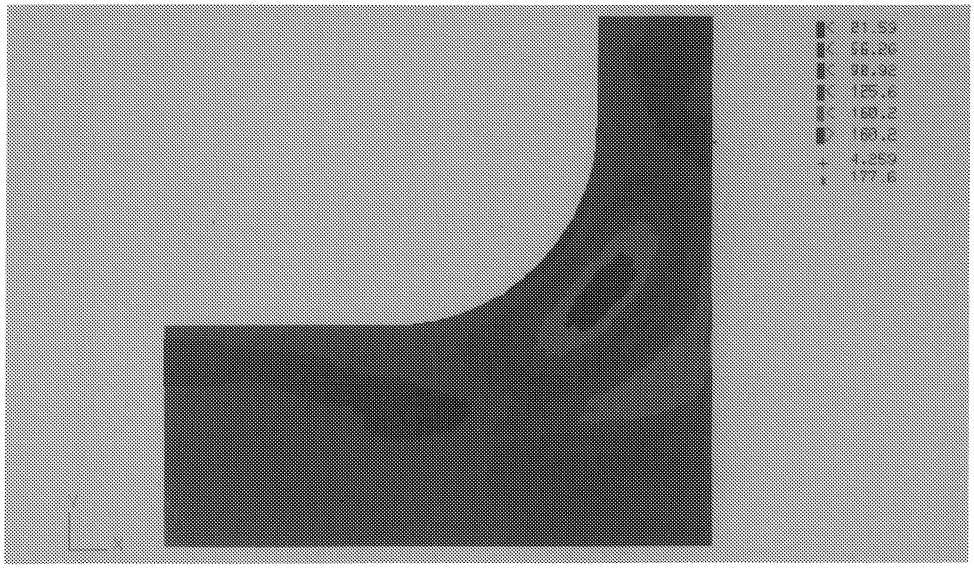

Figure 4.9: *Von Mises* stresses at the inside of the clamped T-part, due to an internal pressure.

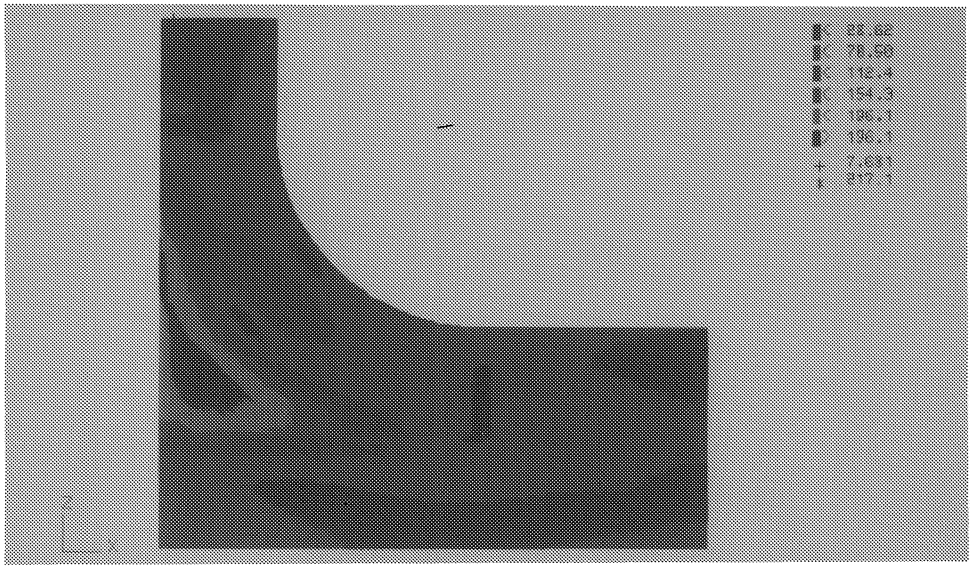

Figure 4.10: *Von Mises* stresses at the outside of the clamped T-part, due to an internal pressure.

Beside an internal pressure, other loading conditions have been investigated, such as a longitudinal shear force, which causes a deformation and a stress state shown in Fig. 4.11 and Fig. 4.13, a transverse shear load (Fig. 4.12 and Fig. 4.14) as well as longitudinal and transverse bending moments.

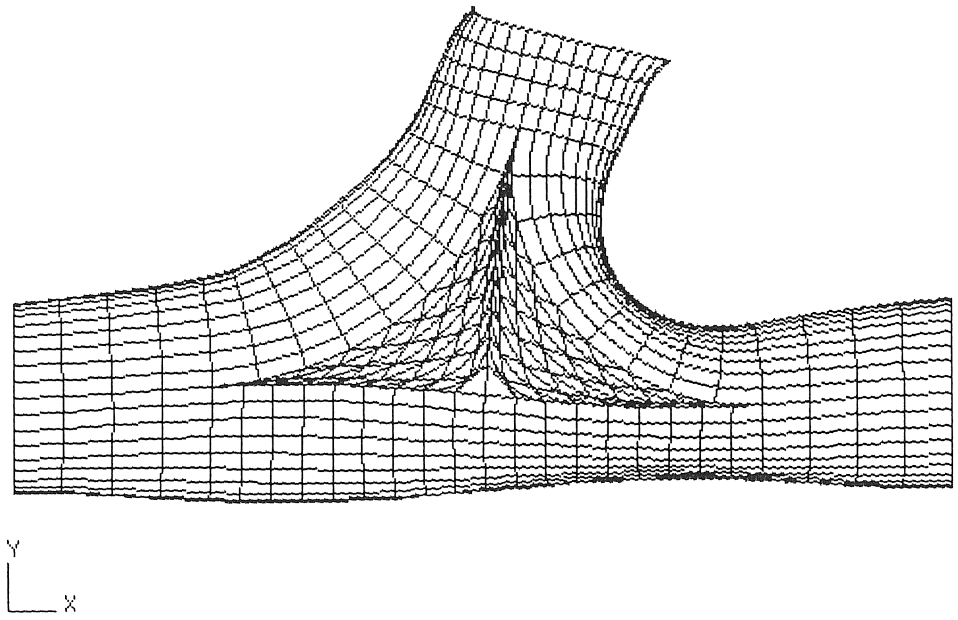

Figure 4.11: Deformed state of the T-part, due to a longitudinal shear force.

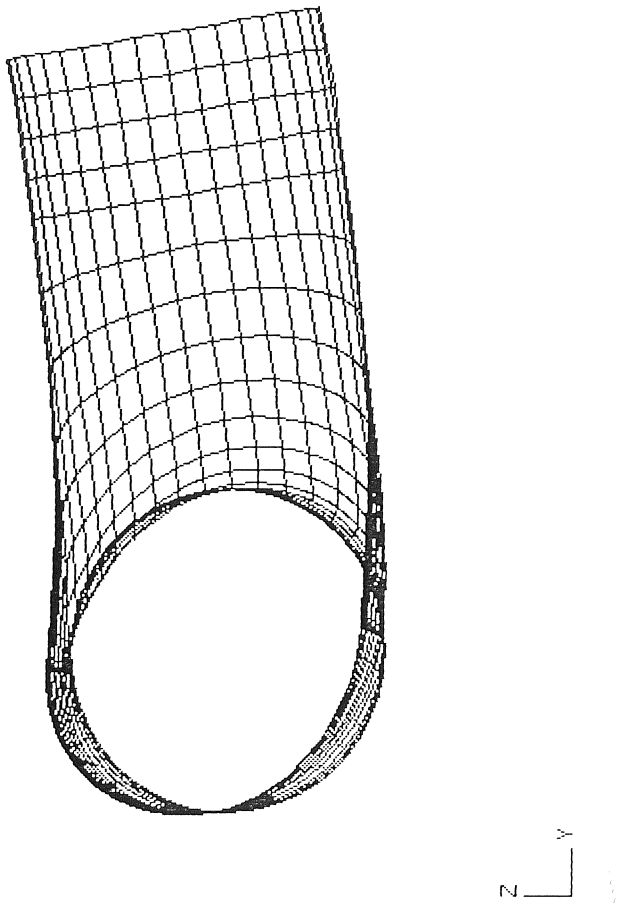

Figure 4.12: Deformed state of the T-part, due to a transverse shear force.

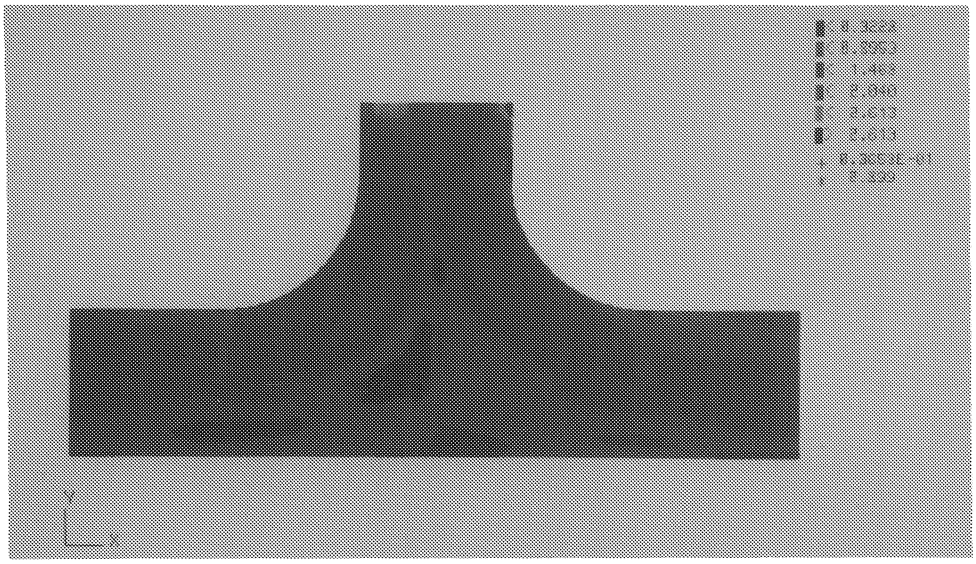

Figure 4.13: *Von Mises* stress distribution in the T-part, due to a longitudinal shear force, to the left at the inside, to the right at the outside.

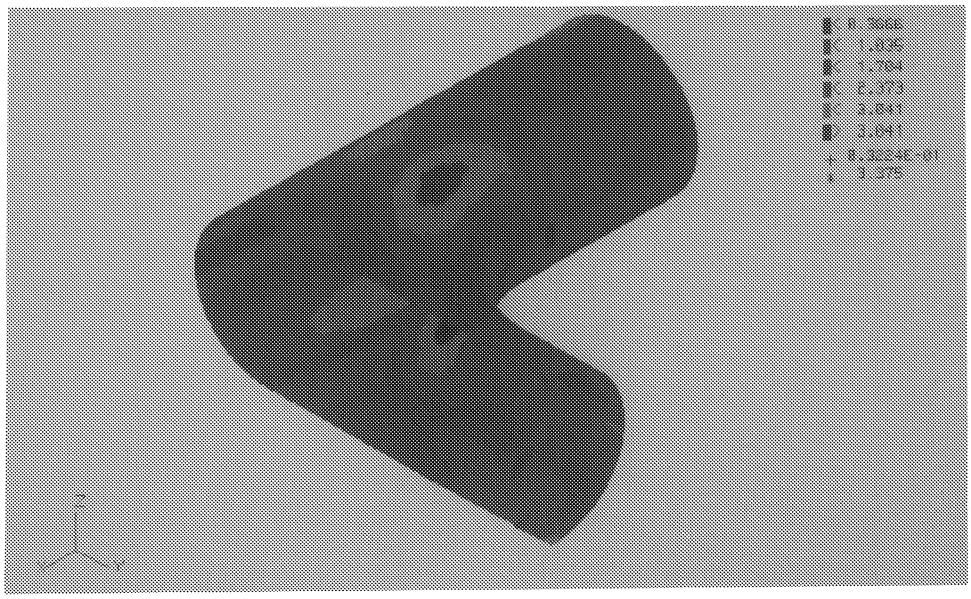

Figure 4.14: *Von Mises* stress distribution in the T-part, due to a transverse shear force, underneath at the inside, above at the outside.

Furthermore, the influence of the boundary conditions has been examined, going from free, non-loaded edges to the presence of infinitely stiff flanges with pressure acting on them.

The case of free edges is presented in Fig. 4.15. The deformed mesh shows that the end sections deform into ellipses. To check this unexpected behaviour, the cylinders have been extended to a high degree. The whole elongated T-part has been pressurized, hoping that the elliptical deformation would smooth out towards the ends and that the end sections would show uniform radial expansion. Computations indead showed that the initial floating elliptical deformation finally declined into a pure circular expansion.

From practical consideration, however, including a shortage of numerical data concerning the external loads and the unknown on-the-field boundary conditions, it has been decided to design the composite T-connection for the case that stiff flanges close the ends and an internal pressure is applied.

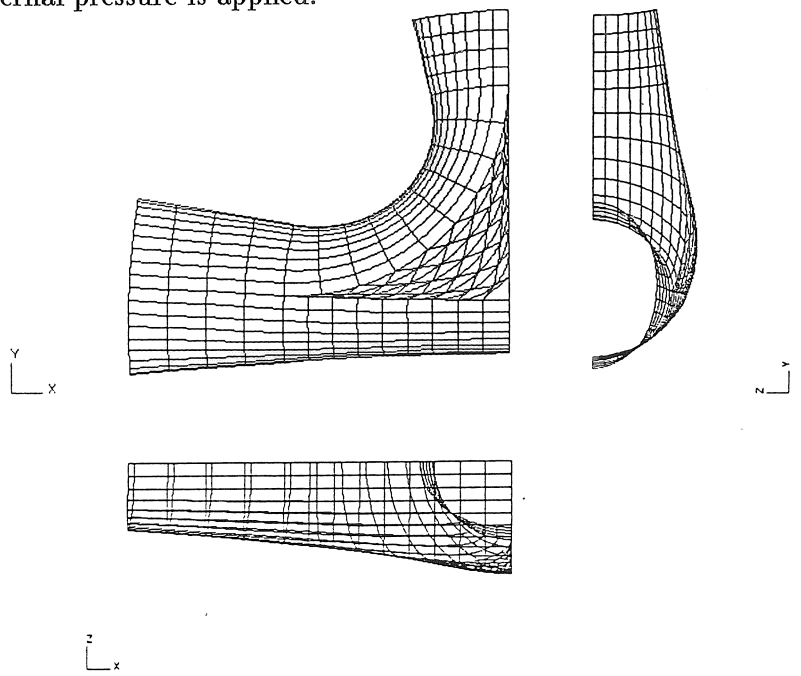

Figure 4.15: Deformed state of the T-part, with free edges and loaded by an internal pressure.

4.5.4 Basic pattern development and selection

To allow for the computation of geodesic trajectories, the T-part is modelled within the CAD system ANVIL-5000 and an IGES file is created.

Since the geodesic software only applies to surfaces of revolution, the structure must be divided into cylindrical segments, torusses and plane sections. So, the T-part is modelled by 8 different surfaces : 3 cylinders, 1 half cylinder, 2 torus segments, and 2 plane elements (Fig. 4.16).

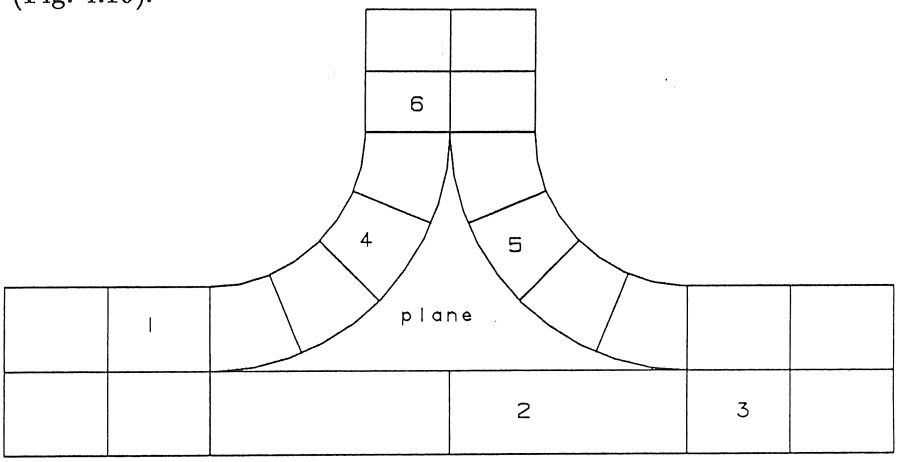

Figure 4.16: CAD drawing of the T-part, divided into individual surfaces of revolution.

There are three different physical locations for a geodesic line to start : at the upper edge of the vertical cylinder and at the left or right edge of the horizontal tube. At these end sections, pin circles are provided which allow for an almost complete freedom in the selection of geodesic lines.

For the computation of the geodesic lines, the *CAWAR* code is used (Ref. [68]). To get a better view on the trajectories the computed geodesic lines follow on the T-part's surface, colleague J. Scholliers has performed an investigation of the feasible combinations of starting position and starting orientation for several internal boundaries of computational start. The geodesic lines obtained are symbollically represented in maps, proper to a particular starting boundary. Fig. 4.17 (a) shows a map with the lower edge of the vertical cylin-

der taken as starting section. The starting positions are represented in abscis, the starting orientations in ordinate. The corresponding conventions are shown in Fig. 4.18.

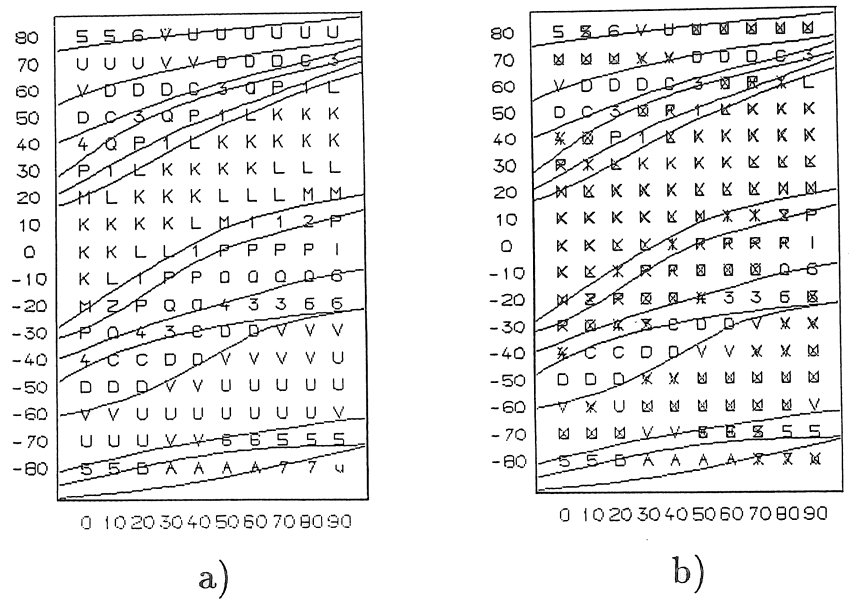

Figure 4.17: Geodesic trajectory map for geodesics starting at the lower edge of the vertical cylinder.

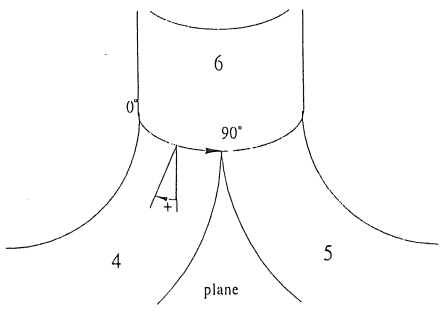

Figure 4.18: Map conventions.

Each symbol corresponds to a particular surface sequence, defined in Table 4.1. A character refers to a single sequence, a digit to a group of successive surfaces. The reference numbers of the individual surfaces are shown in Fig. 4.16.

code	surface sequence	code	surface sequence
A	6-4-*plane*-5-*plane*-2-1	K	6-4-1
B	6-4-*plane*-5-*plane*-2-*plane*-4-1	L	6-4-*plane*-2-1
C	6-4-*plane*-2-*plane*-5-3	M	6-4-*plane*-2-*plane*-4-1
D	6-4-*plane*-2-3		
P	6-4-*plane*-2-4-6	U	6-4-*plane*-5-3
Q	6-4-*plane*-2-*plane*-5-6	V	6-4-*plane*-5-*plane*-2-3
1	6-4-2-*plane*-4-*plane*-2-...	5	6-4-5-*plane*-2-*plane*-4-...
2	6-4-2-*plane*-4-*plane*-5-...	6	6-4-5-*plane*-2-*plane*-5-...
3	6-4-2-*plane*-5-*plane*-2-...	7	6-4-5-*plane*-4-*plane*-2-...
4	6-4-2-*plane*-5-*plane*-4-...	8	6-4-5-*plane*-4-*plane*-5-...

Table 4.1: Symbollic representation of surface sequences.

Fig. 4.19 shows a geodesic line of the "K"-family, with a surface sequence : 6 - 4 - 1.

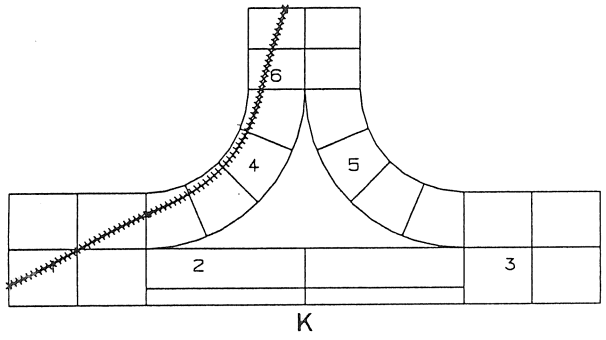

Figure 4.19: Geodesic line of the "K"-family.

In Fig. 4.20 a member of the "C"-surface sequence group is represented.

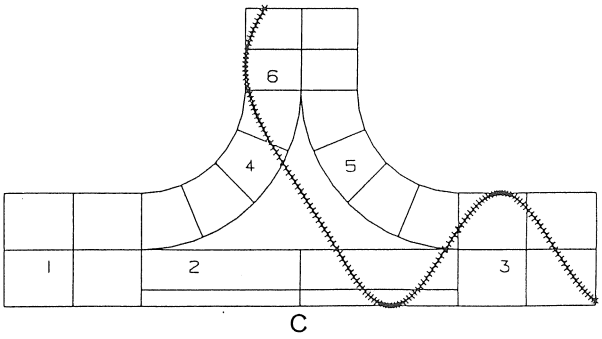

Figure 4.20: Geodesic line of the "C"-family.

On each of the geodesic lines, a concavity test is performed. The results of this concavity check are shown in Fig. 4.17 (b). A "X" refers to a locally concave geodesic line. For this particular map, only 36 % of all possible geodesic lines can be approved of. Only surface sequences A, B, C and D provide satisfying results. Consequently, these will have to contribute to the global covering of the T-part. From these surface sequences, a further investigation for proper geodesic patterns has to be carried out. Therefore a diagram is set up, representing the relation between starting point and end point for a particular surface sequence, with the starting points being situated at the lower rim of the vertical cylinder and the end points somewhere at the right edge of the left cylinder. From this diagram, those geodesic paths are selected for which the mutual distance at the start and at the end section are as equal as possible. This way, a large band of parallel geodesic curves is obtained, as shown in Fig. 4.21.

The same selection strategy is applied to other starting boundaries. Each time, maps are drawn and areas are looked for, in which the geodesic trajectories do not depend very much on the starting position. This means that a specific surface sequence is valid for a large series of start positions, with quite similar winding angles. Consequently, these most stable combinations should be used as basis to the final coverage.

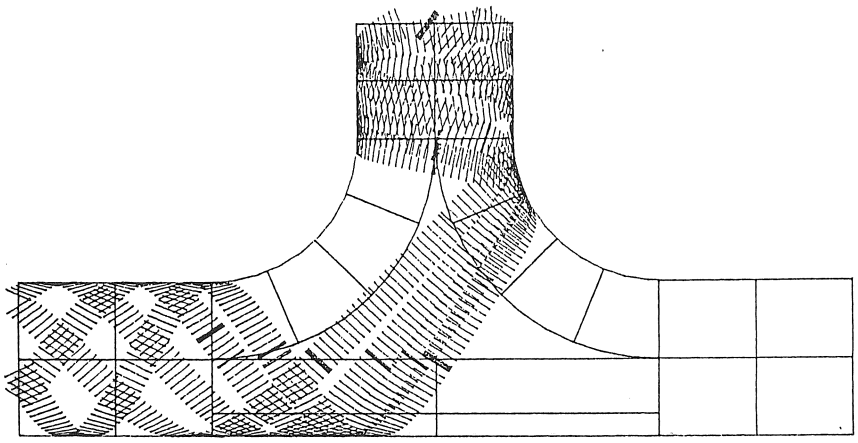

Figure 4.21: Partly covered T-connection, with "*parallel*" fibre bands.

4.5.5 Optimization for uniform coverage

The basic pattern selection has resulted in 59 individual geodesics, with a 5 mm band width and an internal point distance of 2 mm. One single fibre strand is assumed to have a 1.57 mm^2 cross-section. This corresponds to the dimensions of a 2400 tex glass fibre, impregnated with an epoxy resin to a 45 % fibre volume percentage.

For each individual geodesic line, *LUPGEN* computes the contribution to the laminate thickness in every element. With these thickness contributions, the optimization routine, described in (4.4.3), is run. Each of the geodesics is repeated an appropriate number of times, as to cover the structure as uniformly as possible. Finally the 59 different geodesic paths have been rearranged into 468 separate trajectories, including copies of the same paths or members of the same geodesic family, but starting from other quadrants. In spite of the optimization, the ratio between the maximum and minimum occurring thickness could not be reduced more than to a minimum of 4.3. The thickness variation over the composite T-part's surface is represented in Fig. 4.22 by means of coloured vectors.

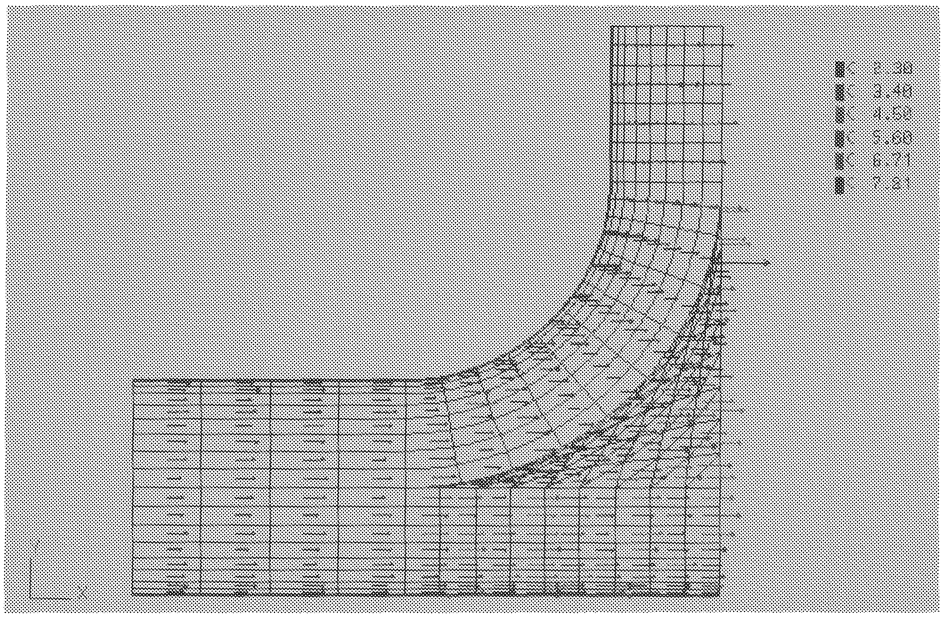

Figure 4.22: Thickness variation over the composite T-connection.

4.5.6 Time sequence of the geodesic patterns

Not only for the robot control during winding, but also for design purposes, it is necessary to know how the successive winding patterns will be linked to each other.

To allow for the fibres to start and finish at variable orientations, pin circles have been attached at the end sections of the mandrel (Fig. 4.23). Each pin represents a possible point for a geodesic fibre path to start or to end.

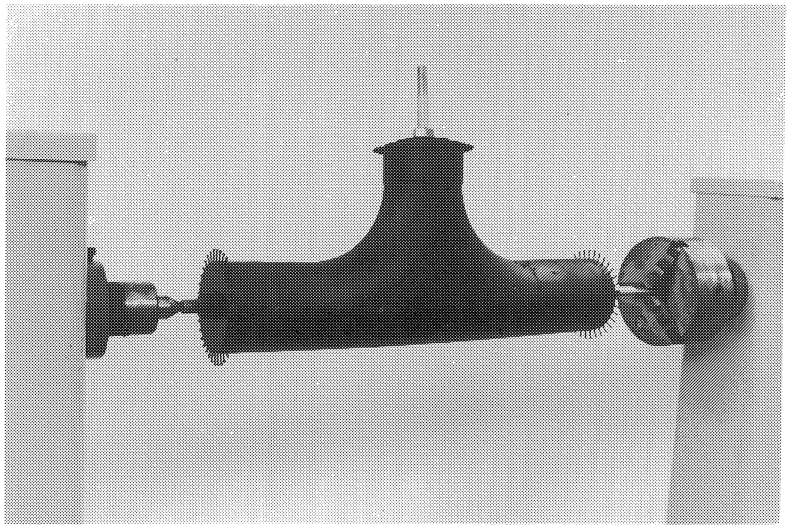

Figure 4.23: Pin circles at the end sections to allow for the fibre's returning.

To obtain an appropriate arrangement of the desired geodesic patterns, each time a successor is chosen, which starts at the same pin circle where the previous geodesic line was terminated, and at a pin which is as close as possible. The final time sequence of the individual geodesic lines must then be translated into the proper format, required by *LAYSEQ*, in order to compute the real stacking sequence of the laminate lay-up, corresponding to the proposed set of geodesic patterns.

4.5.7 Automatic lay-up generation

Based on the final group of geodesic paths, their frequency and time sequence, the previously computed layers are repeated and permutated until they correspond to the real laminate lay-up in every element of the finite element mesh. This mesh contains elements with a surface area varying between $270.5mm^2$ for the largest quadrilateral elements on the tube ends and $8.2mm^2$, which is the surface area of the smallest trilateral element on the flat segment. Since the geodesic lines were specified with an internal point distance equal to 2 mm, which is small when compared to the average element dimensions, no additional interpolation between these points has been performed within the lay-up generator. For practical reasons however, the data reducer within *LAYSEQ* had to be applied, allowing for layers thinner than 0.05 mm to be dropped and successive layers of less than 20° difference in fibre orientation to be combined and averaged. Furthermore, an alternating compaction has been carried out, resulting in a maximum number of layers equal to 27.

4.5.8 Finite element analysis

The same input file used for the isotropic computations can also be applied for the composite analysis, except for the material data, which have to be adapted. The output file, resulting from *LAYSEQ*, can directly be included in the isotropic data file (Fig. 4.24).

```
definition
 t-part, loaded by a 10 bar internal pressure
option shell
two-dimensional generate 1
NODES
 301 / 265.5 215 -50.4
 302 / 215.1 215 0
 303 / 215.1 142.5 0
 304 / 265.5 142.5 -50.4
 305 / 123 50.4 0
 306 / 0 50.4 0
 307 / 0  0 -50.4
 308 / 123 0 -50.4
 309 / 123  -50.4 0
 310/ 0 -50.4 0
 311/ 265.5 0 -50.4
 312/ 265.5 -50.4 0
ELEMENTS
 310 / 304 303 302 301
 320 / 304 308 305 303
 330 / 307 306 305 308
 340 / 310 307 308 309
 350 / 309 308 311 312
 360 / 308 304 311
EDGES
 3100 / 301 304 4
 3101 / 301 302 9 50.4 90
 3102 / 302 303 4
 3103 / 304 303 9 50.4 90
 3104 / 303 305 9 -92.1
 3105 / 308 305 9 50.4 90
 3106 / 305 306 4
 3107 / 307 306 9 50.4 90
 3108 / 308 307 4
 3109 / 309 308 9 50.4 90
 3110 / 310 307 9 50.4 90
 3111 / 309 310 4
 3112 / 311 308 9
 3113 / 312 309 9
 3114 / 311 312 9 50.4 90
 3115 / 304 308 9 -142.5
 3116 / 304 311 9
verify
MATERIAL PROPERTIES
 element inter   1 / composite zc= 0 psi=0
 layer  1/PCA 1 table 31 criter 2  h=  0.31985143 psi=  -0.002
 layer  2/PCA 1 table 31 criter 2  h=  0.27343372 psi=  20.252
 layer  3/PCA 1 table 31 criter 2  h=  0.07525004 psi= -24.266
 layer  4/PCA 1 table 31 criter 2  h=  0.09408101 psi= -20.822
 layer  5/PCA 1 table 31 criter 2  h=  0.45932910 psi=  74.191
 layer  6/PCA 1 table 31 criter 2  h=  0.16936174 psi=   0.001
 layer  7/PCA 1 table 31 criter 2  h=  0.08527137 psi=  17.959
 layer  8/PCA 1 table 31 criter 2  h=  0.33872348 psi=   0.001
 element inter   2 / composite zc= 0 psi=0
 layer  1/PCA 1 table 31 criter 2  h=  0.41393250 psi=  -2.228
 layer  2/PCA 1 table 31 criter 2  h=  0.18816090 psi=  19.391
 layer  3/PCA 1 table 31 criter 2  h=  0.44800356 psi= -26.496
 layer  4/PCA 1 table 31 criter 2  h=  0.35674110 psi=  74.111
 layer  5/PCA 1 table 31 criter 2  h=  0.37633139 psi= -34.489
 layer  6/PCA 1 table 31 criter 2  h=  0.16932492 psi=  -0.006
```

```
 element inter   3 / composite zc= 0 psi=0
.....
 element inter 351 / composite zc= 0 psi=0
 layer  1/PCA 1 table 31 criter 2  h=  0.82998699 psi= -82.059
 layer  2/PCA 1 table 31 criter 2  h=  0.22087100 psi= -21.080
 layer  3/PCA 1 table 31 criter 2  h=  0.30565211 psi=  66.344
 layer  4/PCA 1 table 31 criter 2  h=  0.28268209 psi= -89.010
 layer  5/PCA 1 table 31 criter 2  h=  0.24584711 psi=  89.508
 layer  6/PCA 1 table 31 criter 2  h=  0.30565211 psi=  66.344
 layer  7/PCA 1 table 31 criter 2  h=  0.22087100 psi= -21.080
 layer  8/PCA 1 table 31 criter 2  h=  0.24584711 psi=  89.508
 layer  9/PCA 1 table 31 criter 2  h=  0.55020821 psi= -84.926
 layer 10/PCA 1 table 31 criter 2  h=  0.30565211 psi=  66.344
 layer 11/PCA 1 table 31 criter 2  h=  0.24584711 psi=  89.508
 elem inter 28 to 36 118 to 126 154 to 162 / e=210000 nu=0.3 h=30
TABLES
 31 / el=38.6*3 et=8.27*3 nult=0.34 glt=4.14*3 nutt=0.34
 2 / 2 1062 31 72 72 610 118 -0.5
CONSTRAINTS
 nodes inter  13 to 19 4 235 to 251 11 201 to 217 / ux   rz   ry
 nodes inter 2 37 to 43 3 61 to 77 5 95 to 101 6 / ry  rx   uz
 nodes inter 184 to 200 9 160 to 166 10 / uz   rx  ry
 nodes inter 12 / ux uz rx ry rz
 nodes inter 1 / ux uy rz ry
LOADS
1 inter pressure
  / pz=1.0 local
  nodes inter 1 2 / fy=50.5
  nodes inter 20 to 36 / fy=110.
  nodes inter 6 10 / fx=-50.5
  nodes inter 102 to 118 143 to 159 7 / fx=-110.
return
save data 1008
return
solve double
return
save data resu 1008
return
stress layer extract
return
save data resu 1009
retu
end
```

Figure 4.24: Input file to the *SYSTUS* finite element code, corresponding to the composite T-part, loaded by an internal pressure of 1 MPa.

Furthermore, it is specified in this input file that the *TSAI-WU* failure criterion should be applied and that an output on layer-level is desired. (For the syntax of the corresponding commands, the reader is referred to appendix C). Some results of the finite element analysis, corresponding to an internal pressure of 1 MPa, are graphically represented. In Fig. 4.25, the most loaded layer in each element is selected and its boundary is painted in accordance with the value of the applied failure criterion.

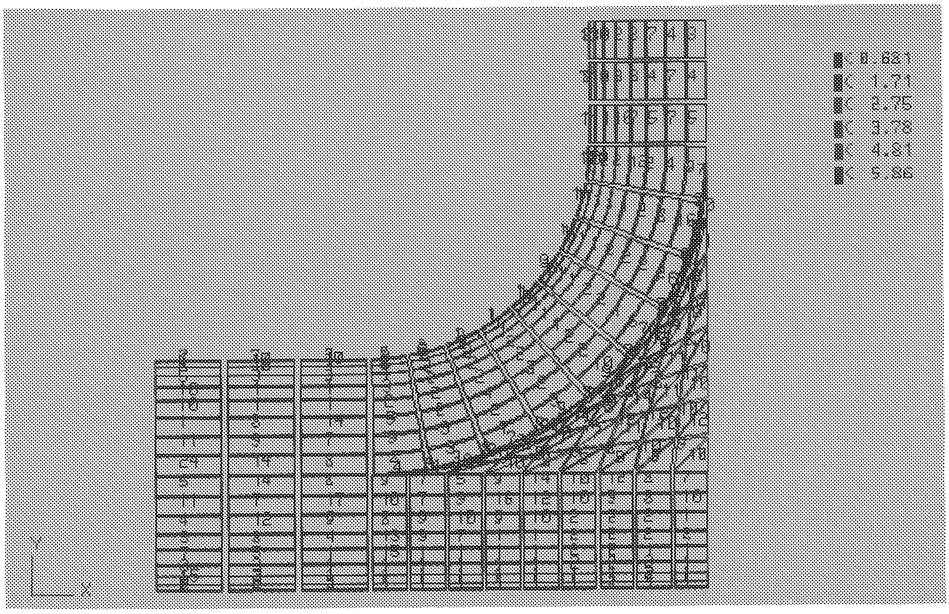

Figure 4.25: Failure criterion in the most loaded layer of each element, corresponding to an internal pressure of 1 MPa.

Values exceeding 1 indicate damaged layers (see 1.5.1.2). On the contrary, layers with a failure criterion result smaller than 1 can be considered to be safe. Beside the failure criterion, also the serial number of each most loaded layer is specified. From this plot, it can be concluded that, analogous to the isotropic T-part, the composite equivalent suffers from significant bending stresses in the flat segment. When

zooming in on this flat part, Fig. 4.26 is obtained.

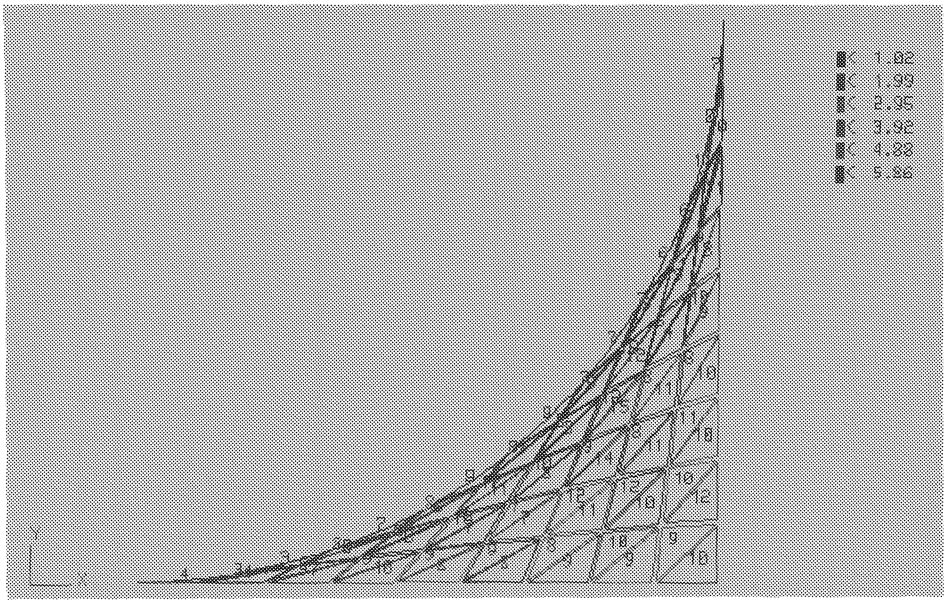

Figure 4.26: Failure criterion in the most loaded layers on the flat segment of the T-part, loaded by an internal pressure of 1 MPa.

Further selection reveals that internal element 314 is the most critical one. For this element, the numerical results from the *stress layer extract* command (C.4.1.1) are tabulated in Table 4.2, giving the two-dimensional stress state referred to both the element axes and the fibre related system of coordinates, followed by the failure criterion value and ratio.

Table 4.2 indicates, by means of an *asterix*, that layers 9, 11 and 12 are not able to sustain the 1 Mpa internal pressure, since their safety factor, referred to as *ratio*, is less than 1. The most loaded layer of element 314 and of all elements is layer 12. Due to high transverse stresses, perpendicular to the fibre direction, this layer would fail at a pressure which is only a fraction 0.285 of the applied 1 MPa load.

*****STRESS LAYER EXTRACT

STRESSES IN A LAYER

ELEMENT INT.NO.	LOAD	LAYER	STRESSES IN ELEMENT AXES SXX	SYY	SXY
314	1	1	-.138E+03	-.218E+03	0.143E+03
314	1	2	-.757E+02	-.358E+02	0.397E+01
314	1	3	-.948E+02	-.272E+02	0.194E+02
314	1	4	-.195E+02	-.595E+02	0.177E+02
314	1	5	0.108E+02	0.230E+02	-.187E+02
314	1	6	-.311E+01	0.131E+02	-.191E+02
314	1	7	0.175E+02	0.117E+03	-.231E+02
314	1	8	0.209E+02	0.131E+03	-.214E+02
314	1	9	0.945E+02	0.392E+02	-.336E+02
314	1	10	0.120E+03	0.217E+03	-.142E+03
314	1	11	0.473E+02	0.272E+03	-.504E+02
314	1	12	0.642E+02	0.776E+02	-.429E+02

ELEMENT INT.NO.	LOAD	LAYER	STRESSES IN FIBER AXES SLL	STT	SLT	CRITERION TYPE	VALUE	RATIO	
314	1	1	-.327E+03	-.299E+02	-.313E+01	TSAI	-.273E+00	0.361E+01	
314	1	2	-.706E+02	-.409E+02	0.139E+02	TSAI	-.481E+00	0.287E+01	
314	1	3	-.980E+02	-.240E+02	0.124E+02	TSAI	-.349E+00	0.466E+01	
314	1	4	-.657E+02	-.132E+02	-.494E+01	TSAI	-.227E+00	0.916E+01	
314	1	5	0.365E+02	-.269E+01	-.217E+01	TSAI	-.826E-01	0.200E+02	
314	1	6	-.157E+02	0.256E+02	-.249E+01	TSAI	0.810E+00	0.118E+01	
314	1	7	0.119E+03	0.159E+02	0.193E+02	TSAI	0.420E+00	0.188E+01	
314	1	8	0.130E+03	0.218E+02	0.236E+02	TSAI	0.634E+00	0.140E+01	
314	1	9	0.101E+03	0.331E+02	-.275E+02	TSAI	0.111E+01	0.925E+00	*
314	1	10	0.319E+03	0.182E+02	0.127E+01	TSAI	0.339E+00	0.209E+01	
314	1	11	0.276E+03	0.438E+02	0.418E+02	TSAI	0.158E+01	0.725E+00	*
314	1	12	0.326E+02	0.109E+03	-.204E+02	TSAI	0.585E+01	0.285E+00	*

Table 4.2: *stress layer extract* results in internal element 314.

4.5.9 Proposal for reinforcement

Since the finite element results only locally show significantly lower safety factors, the most plausible solution is to search for geodesic patterns which pass through the overloaded elements, if possible with a direction parallel to the principal stress direction, thereby increasing the overall safety factor.

4.5.10 Final remarks

For filament winding T-connections, an appropriate and windable geometry has been proposed. For this geometry, a whole set of geodesic patterns has been defined, which together completely cover the mandrel and provide the resulting composite T-part with sufficient laminate thickness to answer to the internal pressure load. The control data, corresponding to winding these geodesic trajectories, can now be computed and downloaded to the robot controller and the robot can start performing its winding task.

4.6 Conclusion

Filament winding has for a long time been limited to simple axisymmetric geometries. With the advent of more sophisticated winding machines however, having a number of independently controllable axes of motion, winding complex shapes has become reality. Consequently, it is self-evident to have dedicated one chapter of this filament winding thesis to the design of non-axisymmetric composites.

Based on the experience with axisymmetric design, a strategy has been developed for handling non-axisymmetric design problems.
Within this strategy, the design has been converted into a problem of verification. For an initial set of geodesic coverage patterns, the equivalent laminate lay-up is determined. The resulting composite structure is then analyzed and a final set of covering paths is assembled, providing the composite laminate with the required stiffness and strength.

The proposed strategy has been discussed in detail and, in illustration, been applied onto a T-connection. The design of a filament wound T-connection has shown to be very complex and remains susceptible of improvements.

Conclusion

Thanks to the anisotropic nature of their fibre reinforcement, composite materials provide the designer with a powerful tool for tailoring light-weight and corrosion resistant structural components, which can optimally answer to their performance requirements. To take maximum benefit of this design potential, composite designers and manufacturers are very much concerned with orienting the fibres in the principal load directions.

A widely used manufacturing technique, particularly suited to meet this fibre alignment in composite structures, is filament winding. For, filament winding allows a high-speed and accurate lay-down of continuous fibre reinforcement along predescribed patterns.

In former days, filament winding used to be quite restrictive; problems arised because of the required mandrel, which could be complex and expensive. Moreover, geometry had to be such that the mandrel could be removed. Winding was limited to geodesic patterns and reverse curvatures were impossible to wind. Furthermore, the cured structure had a poor external surface and usually showed a lot of voids.

However, new technologies and new materials have enabled filament winding to circumvent the earlier drawbacks.

Nowadays, a variety of mandrel material types has become available to meet specific requirements. Particularly the attendance of soluble and washable mandrel materials has solved many mandrel removal problems. New material forms, the use of prepregs and thermoplastic resins, have rendered the winding process more flexible by allowing deviations from geodesic paths. Thereby, the fibre directions and laminate lay-up can closer meet the loading conditions. Reverse curvatures must not be avoided anymore, also thanks to reshaping possibilities after winding.

New technologies and more advanced equipment, combined with computer control facilities, have, through a closer control of winding parameters, fibre tension, fibre placement, resin distribution, curing and compaction cycles, resulted in a higher end product quality. Integrated CAD/CAM has reduced design problems and cost and has led to the automation of filament winding design, development and manufacturing. Thanks to these evolutions, filament winding has conquered versatile application areas by delivering composite components

with high mechanical properties and excellent reproducibility.

Approaching any structural design problem implies three tasks : selecting the material, defining an appropriate configuration and finding a production technique for manufacturing. This approach essentially applies to all types of materials, conventionals as well as composites. However, unlike e.g. metals, which can be designed according to a linear process, composites need a more integrated design procedure as they require the material to be designed along with the structure.

Design and manufacturing obviously interact with each other. In the course of this thesis, only wet filament winding has been performed, in which the fibre is impregnated with resin just before being wound onto the mandrel. Since wet winding does not provide much friction, as compared to prepreg winding, the fibre paths were to be limited to geodesic patterns. Unfortunately, geodesic winding is quite restrictive in that the law of *Clairaut* must be regarded, which completely fixes the fibre trajectory once the starting conditions of fibre position and orientation have been determined. This limited freedom in feasible winding angles clairly complicates the design process, since the major benefit of composites, their potential to align the fibres with the directions of the mechanical loads, can not be fully utilized.

Furthermore, beside the applied winding technique, also the type of winding unit used, its size and degrees of freedom, together with its control capacities, restrict the attainable geometries and the windable dimensions. The numerically controlled two-axis winding machine developed for this research was confined to simple axisymmetric structures, such as the tubes, spinning pots and pressure vessels, discussed in chapter 3. The available robotic winding cell on the contrary, having seven degrees of freedom, was able to handle a more complex non-axisymmetric T-connection, as has treated chapter 4.

In order to make a maximum profit of the great potential offered by fibre reinforcement anyhow, in spite of the only limited fibre orientation freedom, a design methodology has been proposed for geodesically wound composites. The emphasis in this design strategy is laid on finding an optimal compromise between, on the one hand, the almost unlimited tailoring facilities of composites, and, on the other hand, the restrictions imposed by the winding process. Finally, the design procedure results in a semi-optimal geometry and winding pattern.

In illustration, the proposed design methodology has been dis-

cussed in detail, by referring to some practical axisymmetric examples. A first application regarded the already mentioned composite spinning pots, which "unfortunately" were just a substitution of their aluminum equivalents. The second example concerned pressure vessel design, allowing an optimal definition of the dome shape. For both designed components, the material choice has resulted in an epoxy matrix, reinforced by E-glass fibres.

But even when the geometry and the laminate lay-up of a filament wound component have been defined and more or less suboptimized, there remains a final degree of freedom, being the winding strategy. Winding strategy refers to the time sequence of the fibre lay-down and is related to the interweaving of the fibres. With filament winding, one can obtain layered structures as well as components with interwoven fibres. Although most filament winders prefer layered composites, interweaving winding processes have revealed interesting advantages; first, they practically do not require special geometrical demands. Second, they can affect the mechanical properties in a positive sense. To confirm this, the influence of winding strategy, including interweaving of the fibres, on the performance of filament wound tubes and pressure vessels has been investigated. Both tube and vessel results have shown that interweaving winding methods can have positive influences on the composite's performance. Consequently, they can be considered as appropriate manufacturing alternatives.

From chapter 3, one can conclude that in filament winding design, even in case of only axisymmetric components, the restrictions imposed by the winding process very much complicate the design procedure. If, moreover, non-axisymmetrical shapes are concerned, which have to be wound geodesically, the designer has to deal with an additional complexity. Furthermore, also the control of the winding process includes more difficulties. Therefore, the axisymmetric design methodology has been extended into design and control strategies for non-axisymmetric filament wound composites. From a series of feasible geodesic patterns, an appropriate set has to be selected. This set represents a specific surface coverage. The corresponding laminate lay-up must be checked by structural analysis. Depending on the resulting stress state, one has to provide additional patterns or layers to strengthen the overloaded or undercovered areas. Once the designed composite is able to meet the strength and stiffness requirements, control commands can be set up

for the winding robot, in order to filament wind the proposed winding patterns.

An important part in this strategy is the transition between a given set of winding paths and the corresponding laminate lay-up. To realize this link, a computer program has been developed which automatically generates the lay-up data out of the winding pattern information.

In illustration, the proposed design method has been applied to a filament wound T-connection. After defining an appropriate geometry, a finite element analysis was performed on an isotropic T-part. Theoretically, it would have been possible to translate the resulting isotropic stress state into ideal fibre orientations all over the structure. However, searching a set of geodesic patterns which together completely covered the mandrel was already such a problem, that, from a practical point of view, it was considered as impossible to additionally take into account the ideal fibre direction everywhere on the T-part. Consequently, the T-part design has been approached as a problem of verification. From an appropriate selection of geodesic patterns, the equivalent laminate lay-up has been computed. This lay-up was then introduced in a finite element control analysis. Locally overloaded areas were to be reinforced by supplying additional, well-oriented fibres. Finally, the selected series of fibre patterns should provide the composite T-part with the required performance characteristics.

Bibliography

[1] ASME, *Boiler and Pressure Vessel Code, Section 10, Fibreglass-reinforced plastic pressure vessels*, New York, 1986.

[2] ASME, *Boiler and Pressure Vessel Code, Section III, division 1, subsection NB-class 1 components NB3000-Design.*

[3] *Annual Book of ASTM Standards*, American Society for Testing and Materials.

[4] JOSEF BAER, MASCHINENFABRIK, *Servo-Fadenspannungsregler STC*, Weingarten, Germany.

[5] BREBBIA C.A., TELLES J.C.F., WROBEL L.C., *Boundary element techniques, theory and application in engineering*, Springer-Verlag, 1984.

[6] BROUTMAN L.J., SAHU S., *A new theory to predict cumulative fatigue damage in fiberglass reinforced plastics*, Proceedings of the 2nd Conference on Composite Materials -testing and design- , p.170-188, ASTM, U.S.A., 1972.

[7] BROWN R.T., *Computer programs for structural analysis*, Engineered Materials Handbook, Volume 1, Composites, ASTM International, 1987.

[8] BRUNSWICK CORPORATION, *Filament wound pressure vessels*, October 1985.

[9] BRYON S., VAN AELST O., *Robotsturing voor het wikkelen van composietstukken*, 87 EP 06, KUL, Louvain, May 1987.

[10] CALLIUS E.P., SPRINGER G.S., *Modelling the filament winding process*, Fifth International Conference on Composite Materials ICCM-V, San Diego, July 1985.

[11] CURTIS P. T., BISHOP S. M., *An assessment of the potential of woven carbon fiber reinforced plastics for high performance applications*, Composites, volume 15 no.4, 259-265, October 1984.

[12] CURTIS P.T., MOORE B.B., *A comparison of the fatigue life of woven and non-woven CFRP laminates*, Proceedings of the 5th International Conference on Composite Materials, p 293-313, San Diego, 1985.

[13] DE BUYSER L., DECKERS J., *Berekeningsmodellen voor gewikkelde komposietstrukturen*, 88 EP 03, KUL, Louvain, May 1988.

[14] DE JONG TH., *Stresses in pin-loaded anisotropic plates*, Proceedings of the AGARD conference, Madrid, Spain, May 1987.

[15] DE MEESTER P., WEVERS M., *Non-destructive testing of composites*, 3d International Composite Materials Workshop, KUL, Louvain, June 1988.

[16] DRITT ET AL., *United States Patent*, 4,005,233, January 1977.

[17] DROPEK R.K., *Numerical design and analysis of structures*, Engineered Materials Handbook, Volume 1, Composites, ASTM International, 1987.

[18] EGERTON M.W., GRUBER M.B., *Thermoplastic filament wound parts demonstrating properties in crush tube and torque tube applications*, 34th International SAMPE Symposium, May 1989.

[19] ELLIMAN D.G., SORENTI P., BROWN L., SHEARING M., MIDDLETON V., OWEN M.J., *A cell for the manufacture of composite components by filament winding*, Adv. Manuf. Eng., Vol. 1, October 1988.

[20] ERIKSON I., *An analysis method for bolted joints in primary composite aircraft structures*, Proceedings of the AGARD conference, Madrid, Spain, May 1987.

[21] EUI-JIN JUN, KWANG-JOON YOON, TSAE-WOOK KIM, *Development of filament wound S-2 glass/epoxy pressure vessels*, Proceedings of the International Symposium on Composite Materials and Structuring, p 261-266, Peking, 1986.

[22] EVANS D.O., VANIGLIA M.M., *Fibre placement process study*, 34th International SAMPE Symposium, May 1989.

[23] GOSNELL R.B., *Thermoplastic resins*, Engineered Materials Handbook, Volume 1, Composites, ASTM International, 1987.

[24] HANAQUD S., *Comparative evaluation of woven graphite/epoxy composites*, NASA 159001, July 1979.

[25] HILLE E.A., MENGES G., KÖNIG W., *Faserwickeltechnik - Methoden zur Herstellung geometrisch komplizierten Bauteile*, Doktorarbeit an der Abteilung Maschinenbau der "Technische Hochschule", Aachen, January 1981.

[26] HULL D., LEGG M.J., SPENCER B., *Failure of glass/polyester filament wound pipes*, Composites, January 1978.

[27] ISHIKAWA T., CHOU T.W., *Stiffness and strength behaviour of woven fabric composites*, Journal of materials science 17, 3211-3220, 1982.

[28] JANSSENS H., *Design of composite-metal joints with Ansys*, Proceedings of the Composite Materials Workshop : level 2, KUL, Louvain, June 1989.

[29] JAYASINGHE S., JOHNSON C., *An integrated approach to finite element analysis of advanced composite structures*, 33rd International SAMPE Symposium, March 1988.

[30] JONES R.M., Proceedings of the *In search of excellence* workshop on composite materials -design and analysis-, VUB, Brussels, Belgium, April 1987.

[31] KAPANIA R.K., *A review on the analysis of laminated shells*, Transactions of the ASME journal of pressure vessel technology, Vol. 111, p. 88-96, May 1989.

[32] KIM R.Y., *Fatigue strength*, Engineered Materials Handbook, Volume 1, Composites, ASTM International, 1987.

[33] KIRBERG K.W, MICHAELI W., MENGES G., SEIFERT A., *Process simulation in filament winding*, 2nd International Conference : Automated Composites 88, P.R.I., Noordwijkerhout, Netherlands, September 1988.

[34] KÖNIG W., GRASS P., *Bohr- und Fräswerkzeuge für faserverstärkte Kunststoffe*, VDI-Z Bd.128 NR. 3, February 1986.

[35] KÖNIG W., TRASSER F.-J., *Bearbeitung faserverstärkter Kunststoffe mit Wasser- und Laserstrahl*, VDI-Z Bd.129 NR. 11, November 1987.

[36] KORN G.A., KORN T.M., *Mathematical handbook for scientists and engineers*, Mc Graw-Hill, 1968.

[37] KROLEWSKI S., *Economic comparison of advanced composite fabrication technologies*, 34th International SAMPE Symposium, May 1989.

[38] LARK R.F., *Recent advances in lightweight, filament wound composite pressure vessel technology*, Proceedings of "The Energy Technology Conference on Composites in pressure vessels and piping (PVP-PB-02)", p. 17-49, Houston, Texas, September 1977.

[39] LEAVESLEY P. J., KNIGHT C. E., *An analytical model of strength loss in filament wound spherical vessels*, Transactions of the ASME, Vol. 109, p. 352-356, August 1987.

[40] LEE R.J., *The damage tolerance of high performance composites*, Composite Structures, p. 536-554, Applied Science Publishers, 1981.

[41] LEISSA A.W., *Instability considerations*, Engineered Materials Handbook, Volume 1, Composites, ASTM International, 1987.

[42] LLOYD-THOMAS D.G., ECKOLD G.C., WELLS G.M., *Asymmetric filament winding*, 2nd International Conference : Automated Composites 88, P.R.I., Noordwijkerhout, Netherlands, September 1988.

[43] LOCKETT F.J., *The provision of adequate material property data*, Sixth International Conference on Composite Materials ICCM-VI, London, 1987.

[44] LOSSIE M.L., *DECOMPS*, Internal manual to the DECOMPS computer code, KUL, Louvain, 1987.

[45] MARLOFF R.H., RAGHAVA R.S., *Failure analyses of filament wound graphite/epoxy cylinders under biaxial loading*, 30th National SAMPE Symposium, March 1985.

[46] MASSARD T.N., PATTERSON J.M., *Laminate ranking as a tool for laminate sizing*, Engineered Materials Handbook, Volume 1, Composites, ASTM International, 1987.

[47] MCCARVILL W.T., *Filament winding resins*, Engineered Materials Handbook, Volume 1, Composites, ASTM International, 1987.

[48] MEASURIA U., COGSWELL F.N., *Aromatic polymer composites : broadening the range*, Sampe journal, September/October 1985.

[49] MIDDLETON V., OWEN M.J., ELLIMAN D.G., SHEARING M., *Developments in non-axisymmetric filament winding*, Proceedings of the "First international conference on automated composites", University of Nottingham, United Kingdom, September 1986.

[50] MITINE B.S, STEPHANYTCHEV E.I., PICHUGIN V.S., *Fabrication of composite shells by wet-winding process using expanded mandrel*, 30th National SAMPE Symposium, March 1985.

[51] MORRIS E., *High-pressure, high-performance filament-wound carbon/epoxy pressurant tanks with seamless aluminum liners for expandable launch vehicles and spacecraft*, 34th International SAMPE Symposium, May 1989.

[52] MORRIS E.E., *Composite pressure vessels for aerospace and commercial applications*, Proceedings of "The Energy Technology Conference on Composites in pressure vessels and piping (PVP-PB-02)", p. 89-128, Houston, Texas, September 1977.

[53] NOTON B.R., *Cost drivers in design and manufacture of composite structures*, Engineered Materials Handbook, Volume 1, Composites, ASTM International, 1987.

[54] NUISMER R.J., TAN S.C., *Constitutive relations of a cracked composite lamina*, Journal of Composite Materials, 1987.

[55] OUELLETTE P., HOA S.V., *Buckling of filament wound reinforced plastic vessels under external pressure*, 41st Annual Conference, Reinforced Plastics / Composites Institute, The Society of the Plastics Industry, January, 1986.

[56] PETERS S.T., HUMPHREY W.D., *Filament winding*, Engineered Materials Handbook, Volume 1, Composites, ASTM International, 1987.

[57] PHILPOT R.J., BUCKMILLER D.K., COLEGROVE J.E., *Design and manufacturing of high performance recreational products via filament winding*, 34th International SAMPE Symposium, May 1989.

[58] PIESSENS R., *Differentiaalvergelijkingen - deel2*, course book p. 320, Faculty of Applied Sciences, KUL, Louvain, 1984.

[59] PIGGOT M.R., *Load bearing fibre composites*, Pergamon press, 1980.

[60] POON C., *Literature review on the design of mechanically fastened composite joints*, Proceedings of the AGARD conference, Madrid, Spain, May 1987.

[61] PRICE M.R., VANDIVER T., *Jannaf Interim mechanical test standards for filament wound composites*, 34th International SAMPE Symposium, May 1989.

[62] REVIE H.H., BANKS W.M., *Experimental stress analysis of glass reinforced plastic pipes with Tee pieces*, 44th Annual Conference, Composite Institute, The Society of the Plastics Industry, February 1989.

[63] ROBBERECHTS B., ROLLIER F., *Het wikkelen van axisymmetrische drukvaten in komposietmateriaal*, 89 EP 01, KUL, Louvain, May 1989.

[64] ROWAN J.H.C., *Advanced filament winding : evolution and revolution*, Composite materials, May 1988.

[65] RYBICKI E.F., SCHUESER D.W., FOX J., *An energy release rate approach for stable crack growth in the free-edge delamination problem*, Journal of Composite Materials, Vol. 11, 1977.

[66] SCHILDERMANS D., VAN GENECHTEN P., *Geodetisch wikkelen van rotatiesymmetrische komposietstrukturen*, 88 EP, KUL, Louvain, May 1988.

[67] SCHOLLIERS J., *Robotic filament winding of non-axisymmetrical parts*, Proceedings of the Composite Materials Workshop : level 2, KUL, Louvain, May 1989.

[68] SCHOLLIERS J., LOSSIE M., VAN BRUSSEL H., *Wikkelen van T-stukken*, Internal research report, KUL, Louvain, February 1989.

[69] SCHULTE K., *Damage development in composite materials under static loading*, 3d International Composite Materials Workshop, KUL, Louvain, June 1988.

[70] SCHULTE K., *Damage development under cyclic loading*, 3d International Composite Materials Workshop, KUL, Louvain, June 1988.

[71] SCHWARTZ M.M., *Composite Materials Handbook*, McGraw-Hill Book Company, 1984.

[72] SHAW-STEWART D., *Filament winding - Materials & Engineering*, Pultrex Limited, Clacton-on-Sea, U.K.

[73] SHEPPARD L.M., *The revolution of filament winding*, Advanced materials & processes inc. metal progress, 7, 1987.

[74] SPENCER B.E., *Advances in power transmission using filament wound composites*, 34th International SAMPE Symposium, May 1989.

[75] SPENCER B.E., *Modelling the filament winding process*, 34th International SAMPE Symposium, May 1989.

[76] SPRINGER G.S., *Resin flow during the cure of fibre reinforced composites*, Journal of Composite Materials, Vol. 16, no. 5, p. 400-410, September 1982.

[77] SPRINGER G.S., *Environmental Effects on Composite Materials*, Technomic Publishing Company, Lancaster, Pennsylvania, 1984.

[78] TSAI S. W., *Composite design*, Think Composites, 1988.

[79] UEMURA M., FUKUNAGA H., *Filament wound cylinders under internal pressure*, J. Composite Materials, Vol. 15, p. 462, September 1981.

[80] VAN GEMERT D., *Finite element analysis*, 3d International Composite Materials Workshop, KUL, Louvain, June 1988.

[81] VENKAYYA V. B., RAMKUMAR R. L., TISCHLER V. A., SNYDER B. D., BURNS J. G., *Recent studies on bolted joints in composite structures*, Proceedings of the AGARD conference, Madrid, Spain, May 1987.

[82] VERCHERY G., *The analysis of transverse stresses in laminated composite structures*, Proceedings of the DESIGN conference, VUB, Brussels, April 1989.

[83] VERPOEST I., *The influence of the fiber-matrix interface on the hygro-mechanical properties of aramid-epoxy composites*, Proceedings of the European Symposium on Damage Development and Failure processes in Composite Materials, Louvain, May 1987.

[84] WANG A.S.D., *Strength, failure, and fatigue analysis of laminates*, Engineered Materials Handbook, Volume 1, Composites, ASTM International, 1987.

[85] WECK M., ZENDER H., HERBERG F., *Automatisierte Fertigung von Faserverbundbauteilen im Wickelverfahren*, VDI-Z 131, Nr. 5, May 1989.

[86] WELLS G.M., *Computer aided filament winding using non-geodesic trajectories*, Sixth International Conference on Composite Materials ICCM-VI, London, 1987.

[87] WEVERS M., VERPOEST I., DE MEESTER P., *Identification of fatigue failure modes in carbon fibre reinforced composites with the energy discriminating acoustic emission method*, Proceedings of the Stanford-KUL Symposium, Louvain, March 1989.

[88] WILDER R.V., *Microprocessor technology spurs mass production for composites*, Modern Plastics International, April 1988.

[89] WILSON B.A., *Filament winding...past, present and future*, 34th International SAMPE Symposium, May 1989.

[90] WILSON B.A., *Design/tooling/manufacturing interfaces*, Engineered Materials Handbook, Volume 1, Composites, ASTM International, 1987.

[91] WINKEL J.D., ADAMS D.F., *Instrumental drop weight impact testing of cross-ply and fabric composites*, Composites, Vol. 16, no. 4, October 1985.

[92] WOOD A.S., *The filament wound car frame and other practical miracles*, Modern Plastics International, July 1984.

[93] WURZEL D.P., *Torsional impact of filament wound tubes*, 34th International SAMPE Symposium, May 1989.

[94] XIAN-LI LI, DAO-HAI LIN, *Non-geodesic winding equations on a general surface of revolution*, Sixth International Conference on Composite Materials ICCM-VI, London, 1987.

Appendix A

Classical laminate plate theory

A.1 Introduction

The heart of laminated structures' analysis is embodied in the *classical laminate plate theory.*

A laminate is built up of several unidirectional laminae, each with its own fibre orientation, which are properly stacked one on top of the other. According to *laminate plate theory*, the laminae are assumed to be perfectly bonded with infinitesimal thin interfaces. Displacements vary continuously over the thickness, laminae do not slip and plane sections remain plane and perpendicular to the laminate's mid-plane. Transverse shear and through the thickness stresses are neglected. Hence, the laminate is considered as to only experience in-plane stress components.

The purpose of laminate plate theory is twofold : to obtain overall laminate in-plane and bending stiffness properties from the individual ply properties, enabling to compute an overall response to external loading, and, inversely, to translate the laminate strains and curvatures into individual ply stresses and strains.

This appendix gives a brief overview of *classical laminate plate theory.* For more details the reader should consult Ref. [78].

A.2 Definitions

The in-plane stress state acting on a lamina can be expressed with respect to two coordinate systems, termed *off-axis* and *on-axis* (Fig. A.1).

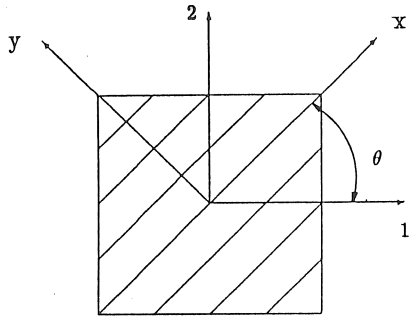

Figure A.1: *Off-axis (1,2)* and *on-axis (x,y)* coordinate systems.

A global *off-axis* system of coordinates $(1, 2)$ usually refers to the principal loading directions. This *off-axis* system is the same for every lamina. In each individual ply, a fibre-related *on-axis* system of coordinates (x, y) can be defined, with x parallel to the fibre direction and y oriented perpendicular to the fibres. The z-axis is directed perpendicular to the laminate and corresponds to the thickness direction. Following symbols will be used for the stresses and strains :

σ_x and ϵ_x : normal stress and strain in the fibre direction
σ_y and ϵ_y : normal stress and strain perpendicular to the fibre direction
σ_s and ϵ_s : shear stress and strain in the $x - y$ plane
σ_1 and ϵ_1 : normal stress and strain in the laminate's 1-direction
σ_2 and ϵ_2 : normal stress and strain in the laminate's 2-direction
σ_6 and ϵ_6 : shear stress and strain in the $1 - 2$ plane

A.3 Stress-strain relations on lamina level

A first set of equations relates the *on-axis* strains $(\epsilon_x, \epsilon_y, \epsilon_s)$ with the *on-axis* stresses $(\sigma_x, \sigma_y, \sigma_s)$ in a particular layer :

$$\begin{aligned} \epsilon_x &= \frac{\sigma_x}{E_x} - \frac{\nu_y}{E_y} \cdot \sigma_y \\ \epsilon_y &= -\frac{\nu_x}{E_x} \cdot \sigma_x + \frac{\sigma_y}{E_y} \\ \epsilon_s &= \frac{\sigma_s}{E_s} \end{aligned} \tag{A.1}$$

In these equations, E_x is the longitudinal Young modulus, E_y the transverse Young modulus, E_s the shear modulus, ν_x the longitudinal Poisson ratio and ν_y the transverse Poisson ratio.

Further in the text, following terminology will be used :

$$\begin{aligned} Q_{xx} &= \frac{E_x}{1 - \nu_x \cdot \nu_y} \\ Q_{yy} &= \frac{E_y}{1 - \nu_x \cdot \nu_y} \\ Q_{xy} = Q_{yx} &= \nu_x \cdot Q_{yy} = \nu_y \cdot Q_{xx} \\ Q_{ss} &= E_s \end{aligned} \tag{A.2}$$

Using (A.2), the inverse of (A.1) can be written in following matrix form :

$$\begin{bmatrix} \sigma_x \\ \sigma_y \\ \sigma_s \end{bmatrix} = \begin{bmatrix} Q_{xx} & Q_{xy} & \\ Q_{yx} & Q_{yy} & \\ & & Q_{ss} \end{bmatrix} \cdot \begin{bmatrix} \epsilon_x \\ \epsilon_y \\ \epsilon_s \end{bmatrix} \tag{A.3}$$

Secondly, the *on-axis* stresses can be expressed in terms of the *off-axis* stresses, according to :

$$\begin{bmatrix} \sigma_x \\ \sigma_y \\ \sigma_s \end{bmatrix} = \begin{bmatrix} m^2 & n^2 & 2 \cdot m \cdot n \\ n^2 & m^2 & -2 \cdot m \cdot n \\ -m \cdot n & m \cdot n & m^2 - n^2 \end{bmatrix} \cdot \begin{bmatrix} \sigma_1 \\ \sigma_2 \\ \sigma_6 \end{bmatrix} \tag{A.4}$$

where $m = \cos\theta, n = \sin\theta$, with θ being the angle between the (x, y) and the $(1, 2)$ coordinate system (Fig. A.1).

For the strains, analogous relations can be derived :

$$\begin{bmatrix} \epsilon_x \\ \epsilon_y \\ \epsilon_s \end{bmatrix} = \begin{bmatrix} m^2 & n^2 & m \cdot n \\ n^2 & m^2 & -m \cdot n \\ -2 \cdot m \cdot n & 2 \cdot m \cdot n & m^2 - n^2 \end{bmatrix} \cdot \begin{bmatrix} \epsilon_1 \\ \epsilon_2 \\ \epsilon_6 \end{bmatrix} \tag{A.5}$$

A last link to be specified concerns the relation between the *off-axis* stresses and strains :

$$\begin{bmatrix} \sigma_1 \\ \sigma_2 \\ \sigma_6 \end{bmatrix} = \begin{bmatrix} Q_{11} & Q_{12} & Q_{16} \\ Q_{21} & Q_{22} & Q_{26} \\ Q_{61} & Q_{62} & Q_{66} \end{bmatrix} \cdot \begin{bmatrix} \epsilon_1 \\ \epsilon_2 \\ \epsilon_6 \end{bmatrix} \tag{A.6}$$

The Q-terms in these equations can be computed from following formulae :

$$\begin{bmatrix} Q_{11} \\ Q_{22} \\ Q_{12} \\ Q_{66} \\ Q_{16} \\ Q_{26} \end{bmatrix} = \begin{bmatrix} m^4 & n^4 & 2 \cdot m^2 \cdot n^2 & 4 \cdot m^2 \cdot n^2 \\ n^4 & m^4 & 2 \cdot m^2 \cdot n^2 & 4 \cdot m^2 \cdot n^2 \\ m^2 \cdot n^2 & m^2 \cdot n^2 & m^4 + n^4 & -4 \cdot m^2 \cdot n^2 \\ m^2 \cdot n^2 & m^2 \cdot n^2 & -2 \cdot m^2 \cdot n^2 & (m^2 - n^2)^2 \\ m^3 \cdot n & -m \cdot n^3 & m \cdot n^3 - m^3 \cdot n & 2(m \cdot n^3 - m^3 \cdot n) \\ m \cdot n^3 & -m^3 \cdot n & m^3 \cdot n - m \cdot n^3 & 2(m^3 \cdot n - m \cdot n^3) \end{bmatrix} \cdot \begin{bmatrix} Q_{xx} \\ Q_{yy} \\ Q_{xy} \\ Q_{ss} \end{bmatrix} \tag{A.7}$$

A.4 Relation between laminate deformation and external loads

Until now, only links between stresses and strains in any particular layer have been expressed. In a second step, a relation will be formulated between, on the one hand, the external loads and, on the other hand, the global deformations of the loaded laminate, consisting of several individual layers.

First, a relation will be set up between the forces acting in the plane of the laminate and the corresponding global strains in this plane. The laminate is assumed to be symmetric and strains to remain constant over the thickness.

In an *off-axis* coordinate system (Fig. A.2), this relation becomes :

$$\begin{bmatrix} N_1 \\ N_2 \\ N_6 \end{bmatrix} = \begin{bmatrix} A_{11} & A_{12} & A_{16} \\ A_{21} & A_{22} & A_{26} \\ A_{61} & A_{62} & A_{66} \end{bmatrix} \cdot \begin{bmatrix} \epsilon_1 \\ \epsilon_2 \\ \epsilon_6 \end{bmatrix} \tag{A.8}$$

with $A_{ij} = A_{ji}$ and $A_{ij} = \int Q_{ij} \cdot dz$ (i=1,2,6) (j=1,2,6).

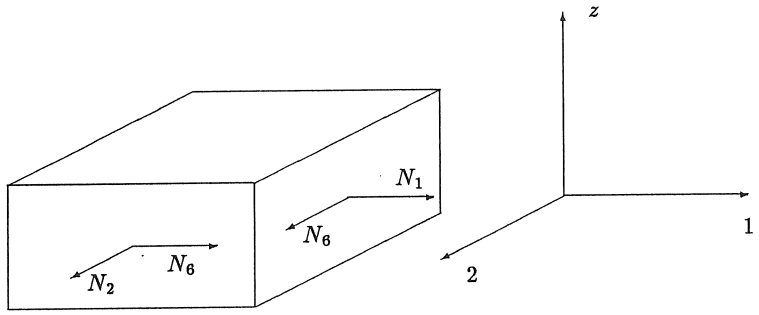

Figure A.2: In-plane forces acting on the laminate.

Second, a relation will be derived which connects moments (Fig. A.3) with curvatures, while still assuming a symmetric laminate. The strains at a particular z-coordinate can be expressed as :

$$\begin{aligned} \epsilon_1(z) &= z \cdot k_1 \\ \epsilon_2(z) &= z \cdot k_2 \\ \epsilon_6(z) &= z \cdot k_6 \end{aligned} \tag{A.9}$$

with k_1, k_2 and k_6 the curvatures, which are defined as :

$$\begin{aligned} k_1 &= -\frac{\delta^2 w}{\delta x_1^2} \\ k_2 &= -\frac{\delta^2 w}{\delta x_2^2} \\ k_6 &= -2 \cdot \frac{\delta^2 w}{\delta x_1 \cdot \delta x_2} \end{aligned} \tag{A.10}$$

In these equations, $w = f(x_1, x_2)$ represents the out-of-plane deformation of the laminate.

The relation between moments and curvatures can be written as :

$$\begin{bmatrix} M_1 \\ M_2 \\ M_6 \end{bmatrix} = \begin{bmatrix} D_{11} & D_{12} & D_{16} \\ D_{21} & D_{22} & D_{26} \\ D_{61} & D_{62} & D_{66} \end{bmatrix} \cdot \begin{bmatrix} k_1 \\ k_2 \\ k_6 \end{bmatrix} \tag{A.11}$$

with $D_{ij} = D_{ji}$ and $D_{ij} = \int Q_{ij} \cdot z^2 \cdot dz$, and ij referring to any combination of $(i = 1, 2, 6)$ and $(j = 1, 2, 6)$.

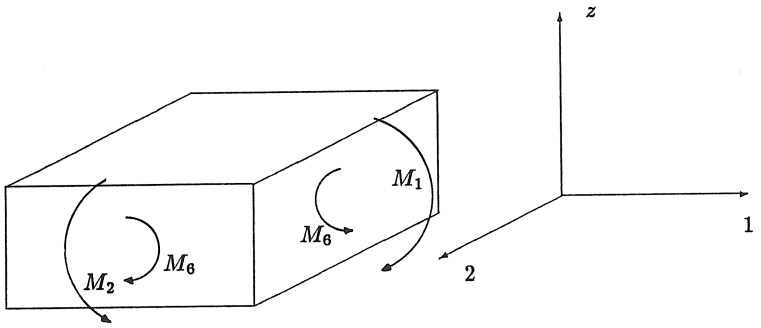

Figure A.3: Out-of-plane moments acting on the laminate.

Now, a combination of both loading types, in-plane forces and out-of-plane moments, has to be made. In such a combined loading condition, one assumes that the strain at a specific distance z above the neutral fibre can be written as :

$$\epsilon_i(z) = \epsilon_i^0 + z \cdot k_i \tag{A.12}$$

with $(i = 1, 2, 6)$ and ϵ_i^0 and k_i respectively the global laminate strain at the neutral fibre and the global laminate curvature. Based on this deformation field, one can relate the forces and moments with the strains and curvatures :

$$\begin{bmatrix} N_1 \\ N_2 \\ N_6 \\ M_1 \\ M_2 \\ M_6 \end{bmatrix} = \begin{bmatrix} \mathrm{A_{ij}} & \mathrm{B_{ij}} \\ \mathrm{B_{ij}} & \mathrm{D_{ij}} \end{bmatrix} \cdot \begin{bmatrix} \epsilon_1^0 \\ \epsilon_2^0 \\ \epsilon_6^0 \\ k_1 \\ k_2 \\ k_6 \end{bmatrix} \tag{A.13}$$

with $B_{ij} = B_{ji}$ and $B_{ij} = \int Q_{ij} \cdot z \cdot dz$, $(i = 1, 2, 6)$ and $(j = 1, 2, 6)$. The forces and moments are given pro unit width. In case of a symmetric laminate, the B_{ij}-matrix equals zero, meaning that there exists no coupling between forces and curvatures or moments and global laminate strains.

A.5 Computational sequence

To apply classical laminate plate theory onto a composite structure, following procedure must be followed :

For a given set of forces and moments pro unit width, the global laminate strains and curvatures in the $(1, 2)$ coordinate system can be computed (A.13). From these strains and curvatures, the *off-axis* strains $(\epsilon_1, \epsilon_2, \epsilon_6)$ at a specific z-value, corresponding to a particular layer, can be determined using (A.12). With (A.6), these *off-axis* strains can be translated into *off-axis* stresses $(\sigma_1, \sigma_2, \sigma_6)$. If one is interested in *on-axis* strains, (A.5) can be applied. And finally, through (A.3) also the *on-axis* fibre related stresses $(\sigma_x, \sigma_y, \sigma_s)$ can be determined, which can further be used as input to an appropriate failure criterion for strength prediction.

Appendix B

Netting theory based derivations for pressure vessel design

B.1 Derivation of the optimal end contour differential equation

B.1.1 Membrane theory

As the composite thickness of vessels for low pressure applications is usually small, it is allowed to model the structure as a membrane. Based on membrane theory, the axial and circumferential stresses, due to an internal pressure load, can be computed.

Consider the element $a\ b\ f\ e$, taken from the pressurized vessel shell (Fig. B.1). Due to symmetry, it is only subjected to normal stresses, being the meridional stress $\vec{\sigma_1}$ and the circumferential stress $\vec{\sigma_2}$.

Both stresses result in forces which have following components in the direction perpendicular to the mid-plane of the element :

$$2 \cdot \vec{F_1} = 2 \cdot \vec{\sigma_1} \cdot h \cdot ds_2 \cdot \sin \frac{d\theta_1}{2} \tag{B.1}$$

$$2 \cdot \vec{F_2} = 2 \cdot \vec{\sigma_2} \cdot h \cdot ds_1 \cdot \sin \frac{d\theta_2}{2} \tag{B.2}$$

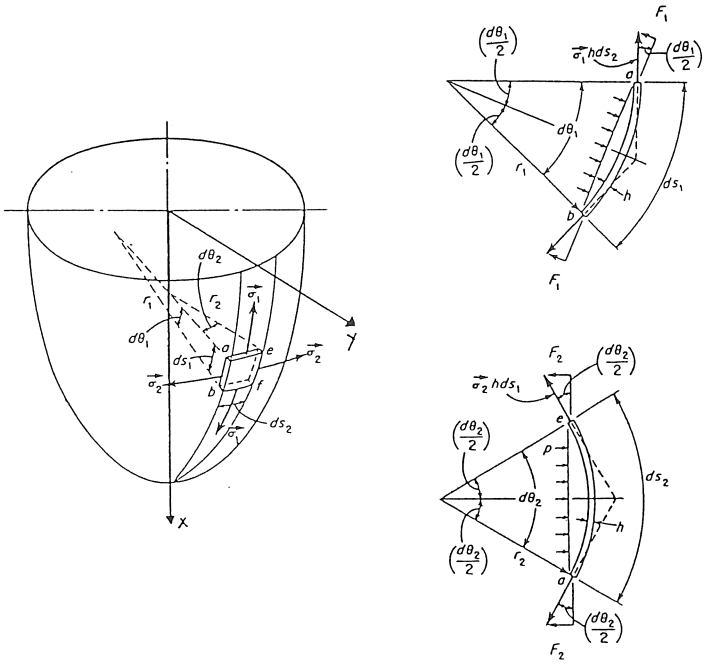

Figure B.1: Stress state in a pressurized membrane.

The total pressure force P acting on the element, due to a pressure p, is :

$$P = p \cdot (2 \cdot r_1 \cdot \sin \frac{d\theta_1}{2}) \cdot (2 \cdot r_2 \cdot \sin \frac{d\theta_2}{2})$$

with r_1 and r_2 being the principal radii of curvature of the shell surface :

r_1 : radius of curvature of meridian
r_2 : length of normal between point on shell and axis of rotation

Expressing that this pressure force must be in equilibrium with the sum of the forces given by (B.1) and (B.2) and taking into account that :

$$\sin \frac{d\theta_1}{2} = \frac{ds_1}{2 \cdot r_1}$$

and

$$\sin \frac{d\theta_2}{2} = \frac{ds_2}{2 \cdot r_2}$$

yields :

$$\frac{\sigma_1}{r_1} + \frac{\sigma_2}{r_2} = \frac{p}{h} \tag{B.3}$$

This equation assumes a constant pressure p and thickness h along the circumference.

The σ_1 stress can be found by expressing the equilibrium of a cut, perpendicular to the x-axis (Fig. B.2). Let y be the radius of this cut. Equilibrium then requires :

$$\pi \cdot y^2 \cdot p - 2 \cdot \pi \cdot y \cdot h \cdot \sigma_1 \cdot \sin\theta = 0$$

or

$$\sigma_1 = \frac{p \cdot y}{2 \cdot h \cdot \sin\theta} = \frac{p \cdot y}{2 \cdot h \cdot \frac{y}{r_2}} = \frac{p \cdot r_2}{2 \cdot h} \tag{B.4}$$

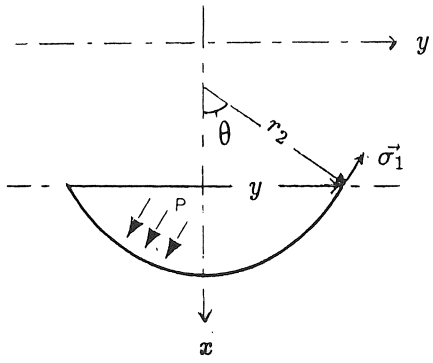

Figure B.2: Equilibrium of a cut, perpendicular to the x-axis.

The σ_2 stress is found by substituting (B.4) in (B.3) :

$$\sigma_2 = \frac{p \cdot r_2}{h} \cdot (1 - \frac{r_2}{2 \cdot r_1}) \tag{B.5}$$

Dividing (B.5) by (B.4) gives :

$$\frac{\sigma_2}{\sigma_1} = 2 - \frac{r_2}{r_1} \tag{B.6}$$

If one assumes the x-axis to coincide with the axis of rotation and the y-axis to be oriented in the radial direction, the principal radii of curvature of the element can be written as :

$$r_1 = -\frac{(1 + (\frac{dy}{dx})^2)^{\frac{3}{2}}}{\frac{d^2y}{dx^2}} \tag{B.7}$$

$$r_2 = y \cdot (1 + (\frac{dy}{dx})^2)^{\frac{1}{2}} \tag{B.8}$$

Dividing (B.8) by (B.7) gives :

$$\frac{r_2}{r_1} = \frac{-y \cdot y''}{1 + y'^2} \tag{B.9}$$

Substituting (B.9) in (B.6) finally results in :

$$\frac{\sigma_2}{\sigma_1} = 2 + \frac{y \cdot y''}{1 + y'^2} \tag{B.10}$$

B.1.2 Netting theory

According to netting theory, only the fibres take up the loads, without any contribution of the matrix. Hence, all fibres in all points are subjected to the same fibre stress σ_f. In filament winding, one layer of windings corresponds to an amount of fibres in the $+\alpha$ and an equal number of fibres in the $-\alpha$ direction with respect to the longitudinal *1-* axis (Fig. B.3). The *2-* axis is directed along the component's circumference.

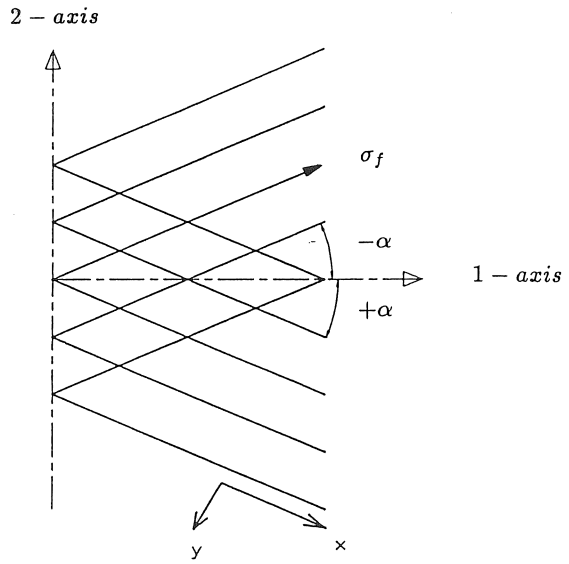

Figure B.3: Fibre orientations in one filament wound layer.

As all fibres are equally stressed, the mean stresses, referred to the *1-2* - axes, can be written as :

$$\sigma_1 = \sigma_f \cdot \cos^2 \alpha$$

$$\sigma_2 = \sigma_f \cdot \sin^2 \alpha$$

resulting in :

$$\frac{\sigma_2}{\sigma_1} = \tan^2 \alpha \tag{B.11}$$

Substituting (B.11) in (B.10) yields :

$$-\frac{y \cdot y''}{1 + y'^2} = 2 - \tan^2 \alpha \tag{B.12}$$

Additionally, it must be considered that the fibres lie along geodesic paths, which can be expressed by *Clairaut's* law :

$$y \cdot \sin \alpha = constant = Y_0$$

with Y_0 being the radius where the fibres are returned.
Hence,

$$\tan^2 \alpha = \frac{\sin^2 \alpha}{1 - \sin^2 \alpha} = \frac{Y_0^2}{y^2 - Y_0^2} \tag{B.13}$$

By incorporating (B.13) in (B.12), one obtains following equation :

$$-\frac{y \cdot y''}{1 + y'^2} = \frac{2y^2 - 3Y_0^2}{y^2 - Y_0^2} \tag{B.14}$$

This differential equation has to be numerically solved. The solution is a function $y(x)$, describing the netting profile end contour.

B.2 Derivation of the additionally required cylinder reinforcement

As equation (B.14) can not simultaneously be valid on a cylindrical surface and on the optimally shaped end contour which it is linked to, the cylinder requires additional reinforcement. Netting theory can be applied to compute the necessary hoop windings, by supposing the

longitudinal (t_{1-cyl}) and hoop windings (t_{2-cyl}) to be equally stressed. Following equilibrium equations can be written :

$$\sigma_1 \cdot (t_{1-cyl} + t_{2-cyl}) = \sigma_f \cdot t_{1-cyl} \cdot \cos^2 \alpha_{1-cyl} + \sigma_f \cdot t_{2-cyl} \cdot \cos^2 \alpha_{2-cyl} \tag{B.15}$$

$$\sigma_2 \cdot (t_{1-cyl} + t_{2-cyl}) = \sigma_f \cdot t_{1-cyl} \cdot \sin^2 \alpha_{1-cyl} + \sigma_f \cdot t_{2-cyl} \cdot \sin^2 \alpha_{2-cyl} \tag{B.16}$$

The circumferential windings can be considered having a fibre angle of 90°. Hence, using (B.6) with r_1 being ∞, (B.15) and (B.16) can be combined into the desired thickness relation :

$$\frac{t_{2-cyl}}{t_{1-cyl}} = 3 \cdot \cos^2 \alpha_{1-cyl} - 1 \tag{B.17}$$

Appendix C

SYSTUS manual for composites

C.1 Introduction

This appendix is meant to guide the *Systus* user who wants to analyze composite structures. *Systus* is a finite element code developed by FRAMATOME in France and runs on a VAX computer. The facilities within *Systus* that are specific for composites, together with the corresponding commands, will be briefly described.

In principle, the composite finite element analyses within *Systus* are very analogous to those for isotropic or general anisotropic materials. Only the input and output have been adapted to meet the composite nature. The laminate lay-up must be specified. From the global composite structure, the stiffness matrix is computed, which is handled in a classical way during the further calculation procedure. The global results can be withdrawn according to conventional methods. To obtain the output on layer-level, the user disposes of several numerical as well as graphical facilities.

C.2 Option *shell*

Before starting the analysis, a data file must be created describing the geometry, the material properties, the loading situation and the boundary conditions. In this file, also an option must be specified. The command *option* serves as to describe the type of the structure to

be analyzed and has two essential functions :

- indicating the number and type of the degrees of freedom for each node
- specifying the type of the analysis that must be carried out

Within the present-day *Systus* version at the Department of Mechanical Engineering's disposal, for composites only the option *shell* is operative. This applies to composite shells with arbitrary geometry, which are loaded statically, dynamically or thermically. Until now, in Mechanical Engineering no dynamic calculations have yet been performed for composites. Static loading conditions on the contrary have been frequently investigated and resulting stresses and deformations have proved to be quite acceptable. Thermal stresses however are still computed erroneously.

C.3 Composite shells

Shell structures are usually modelled by two-dimensional elements, the corresponding finite element analysis being associated with *plate theory*. *Plate theory* assumes the stresses and strains to vary lineary over the element's thickness. This assumption is quite realistic in case of thin plates or shells, subjected to small displacements (see chapter VIII.3.3 in manual).

C.3.1 Nodal degrees of freedom

- u_x : displacement in the X-direction
- u_y : displacement in the Y-direction
- u_z : displacement in the Z-direction
- r_x : rotation around the X-axis
- r_y : rotation around the Y-axis
- r_z : rotation around the Z-axis

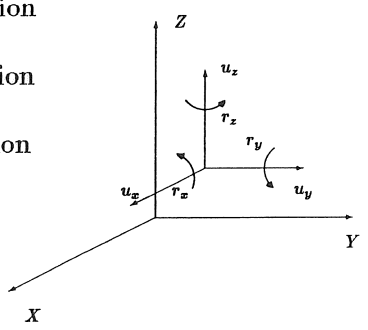

C.3.2 Loading components

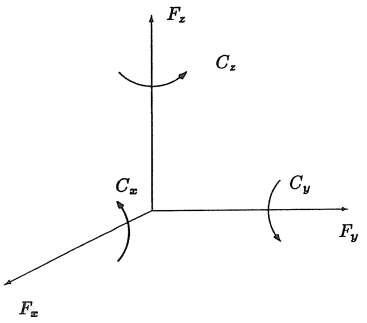

- F_x : force in the X-direction
- F_y : force in the Y-direction
- F_z : force in the Z-direction
- C_x : moment around the X-axis
- C_y : moment around the Y-axis
- C_z : moment around the Z-axis

C.3.3 Types of elements

For composites only elements of the type 2003-2004 (thin) or 2n06-2n08 (thick) can be used.

- 2003-2004 : simple elements, low computation cost but assessed to stiff for in-plane bending in case of a rough mesh
  - 2003 :
    * linear membrane displacements
    * cubic bending displacements
    * membrane-bending coupling provided
  - 2004 : computed by superposition of four 2003-shell elements
- 2n06-2n08 : these elements are to the mid-plane reduced versions of three-dimensional elements and are suited for thick shells (radius of curvature being smaller than ten times the thickness). Displacement functions are quadratic for bending and membrane effects. These elements guarantee high accuracy, yet require more computation time. 2n06-2n08 elements should be taken as flat as possible.

C.3.3.1 Note for thick shell elements

- The number of integration points is a function of n, as is shown in Table C.1 :

element type	n	default	1	2	3	4
trilateral	2n06	3	1	3	7	7
quadrilateral	2n08	4	1	4	9	16

Table C.1: Number of integration points for thick shells.

- The value $n = 2$ for a quadrilateral element corresponds to what is commonly referred to as *reduced integration.* Usually, reduced integration offers more accurate modelling of bending effects.

C.3.4 Laminate lay-up specification

Within the finite element model, a composite shell is built up by stacking successive plies, parallel to the shell's mid-plane through the nodes of the mesh. Each element has, within the global system of coordinates (X,Y,Z), an individual local system of axes, (x, y, z) (Fig. C.1). x and y are in-plane axes, determined by the definition sequence of the element nodes. The local z-axis is directed perpendicular to the element's mid-plane, according to the right-hand rule. The layers are stacked in the local z-direction of the element. To specify the laminate lay-up, sometimes a reference axis X_0 is invoked, making an angle ψ_0 with the local element axes. The fibre orientations of the various layers are then referred to this reference axis. Each layer is characterized by its thickness, its fibre orientation with respect to the reference axis, and by a reference to a table containing the corresponding material data. Further specifications can include the composite's density, temperature expansion coefficients both parallel and perpendicular to the fibres, and a reference to a table in which failure criterion data are specified.

syntax :

MATERIAL

element e_1 to e_2 / composite $ZC = zc$ $PSI = \psi_0$

layer l_1 to l_2 / table t_1 $H{=}h$ $RO{=}ro$ $PSI{=}\psi_i$ $LX{=}lx$ $LY{=}ly$ crit c_1

layer l_3 to l_4 / table t_2 $H{=}h$ $RO{=}ro$ $PSI{=}\psi_j$ $LX{=}lx$ $LY{=}ly$ crit c_2

...

element ...

...

TABLES

t_1 / El Et Nult Glt Nutt

t_2 / 21 coefficients

c_1 / 1, 4 coefficients; HILL

c_2 / 2, 7 coefficients; TSAI

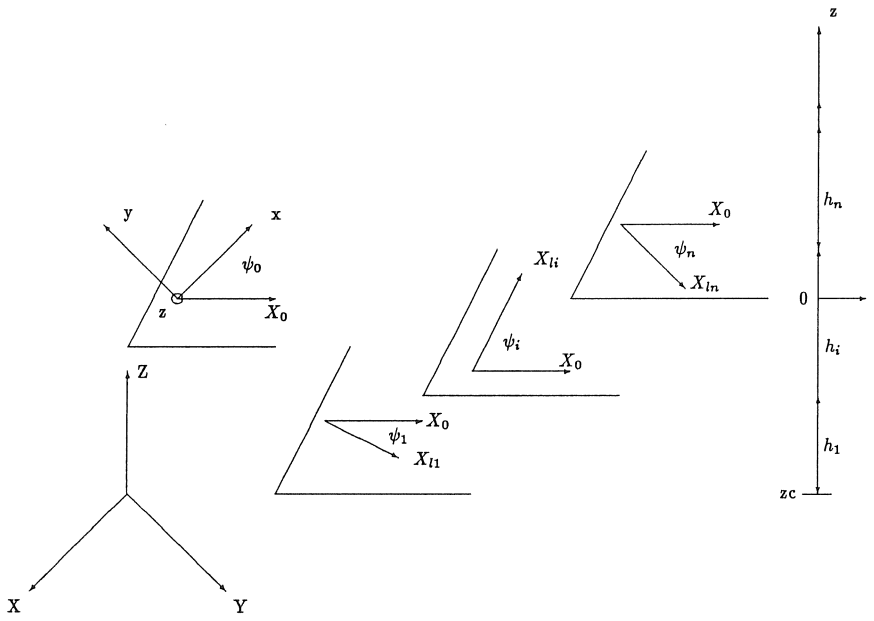

Figure C.1: Laminate related definitions.

C.3.4.1 Notice of parameters and labels

- ELEMENT SPECIFICATIONS
  - *composite*: indicates that a layered composite shell element is concerned
  - $ZC = zc$: 3-4 nodes : represents the distance between the describing main surface of the element through the nodes and the bottom surface of the composite shell. zc is always negative with default value 0. This distance is measured along the local z-axis. It should be noticed that it is the main plane in which forces act and nodal displacements are imposed. Therefore, it is recommended to define zc as to make the main plane and the mid-plane coincide, otherwise, additional bending moments are introduced. For elements with 6 or 8 nodes, zc has no meaning.
  - $PSI = \psi_0$: angle between the reference axis for the lay-up and the local system of axes of the shell element (positive from x to y).
- LAYER SPECIFICATIONS
  For every element, up to 60 layers can be considered.
  - *table* : number referring to a table with elastic constants
  - $H = h$: specifies the uniform element thickness. For elements with 6 or 8 nodes, it is possible to define a varying thickness. Then, in every node, the thickness must be specified, using a table. h is then taken negative and the absolute value of h indicates the number of the corresponding table.
  - $RO = ro$: density of the composite layer
  - $PSI = \psi_i$: fibre orientation of layer i, with respect to the reference axis X_0
  - $LX = lx$: thermal expansion coefficient in the fibre direction
  - $LY = ly$: transverse thermal expansion coefficient
  - *criterion* c_i : refers to a table with data concerning the failure criterion to be used. Two failure criteria are available : the Tsai-*HILL* and the *TSAI*-Wu criterion.

- TABELS CONTAINING MATERIAL PROPERTIES

  - *elastic constants*

    There are three possibilities :

    * In case of an isotropic layer, it is sufficient to specify the Young modulus E and the Poisson ratio ν.
    * Usually the composite consists of unidirectional layers with transverse isotropic properties. In this case, a table with 5 components is required :
      - E_l : longitudinal stiffness modulus
      - E_t : transverse stiffness modulus
      - nu_{lt} : in-plane Poisson ratio
      - G_{lt} : in-plane shear modulus
      - nu_{tt} : This transverse Poisson ratio is only significant for elements with 6 or 8 nodes.
    * In case of anisotropic layers, a relation between stresses and strains can be specified by means of 21 components of the stiffness matrix. This holds for a positive table number. In case of negative table numbers, the inverse matrix (flexibility matrix) is given.

      For $t > 0$:

$$\begin{bmatrix} \sigma_{ll} \\ \sigma_{tt} \\ \sigma_{zz} \\ \tau_{lt} \\ \tau_{lz} \\ \tau_{tz} \end{bmatrix} = \begin{bmatrix} (1) & (2) & (3) & (13) & (14) & (15) \\ & (4) & (5) & (16) & (17) & (18) \\ & & (6) & (19) & (20) & (21) \\ & & & (7) & (8) & (9) \\ & & & & (10) & (11) \\ & & & & & (12) \end{bmatrix} \begin{bmatrix} \epsilon_{ll} \\ \epsilon_{tt} \\ \epsilon_{zz} \\ \gamma_{lt} \\ \gamma_{lz} \\ \gamma_{tz} \end{bmatrix}$$

  - *failure criterion*

    * Tsai-*HILL*; this criterion is an extension of the *Von Mises* criterion for isotropic materials. It does not account for the difference in tension and compression strength.
    * *TSAI*-Wu; here the difference in tension and compression strength is incorporated in the failure criterion.

    Both criteria incorporate 5 stress components, σ_{ll}, σ_{tt}, τ_{lt}, τ_{lz} and τ_{tz}, all referred to a fibre-related coordinate system.

Following definitions are used :

* σ_{ll} : longitudinal normal stress (in fibre direction)
* σ_{tt} : transverse normal stress (perpendicular to the fibres)
* τ_{lt} : shear stress due to in-plane shear
* τ_{lz} : shear stress, due to shear in a plane perpendicular to the composite element, but parallel to the fibre direction
* τ_{tz} : shear stress, due to shear in a plane perpendicular to the composite element, and perpendicular to the direction of the fibres

For the strength properties, following symbols are used :

* X_t : longitudinal tensile strength (in fibre direction)
* X_c : longitudinal compression strength
* Y_t : transverse tensile strength (perpendicular to the fibres)
* Y_c : transverse compression strength
* R : shear resistance for shear in the lz- or lt-planes
* S : shear resistance for shear in the tz-plane

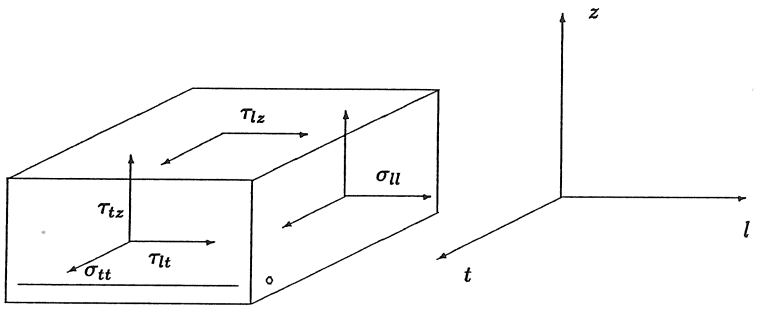

Figure C.2: Layer stresses.

* Tsai-*HILL*

$$HILL = (\frac{\sigma_{ll}}{X_t})^2 + (\frac{\sigma_{tt}}{Y_t})^2 - \frac{\sigma_{ll}\sigma_{tt}}{X_t^2} + \frac{(\tau_{lt}^2 + \tau_{lz}^2)}{R^2} + (\frac{\tau_{tz}}{S})^2 \qquad \text{(C.1)}$$

The *HILL* criterion only uses 4 strength components. Hence, only these four must be specified.
syntax :

TABLE
c_1 / 1 X_t Y_t R S

"1" refers to the criterion of *HILL*

* *TSAI*-Wu

$$TSAI = \frac{\sigma_{ll}^2}{X_t X_c} + \frac{\sigma_{tt}^2}{Y_t Y_c} + (\frac{1}{X_t} - \frac{1}{X_c})\sigma_{ll} + (\frac{1}{Y_t} - \frac{1}{Y_c})\sigma_{tt} + 2F_{lt}\sigma_{ll}\sigma_{tt} + \frac{(\tau_{lt}^2 + \tau_{lz}^2)}{R^2} + (\frac{\tau_{tz}}{S})^2 \qquad \text{(C.2)}$$

The value F_{lt} from the coupling term between longitudinal and transverse normal stresses is defined as follows :

$$F_{lt} = F_{lt}^* \sqrt{\frac{1}{X_t X_c Y_t Y_c}} \qquad \text{(C.3)}$$

with $-1 < F_{lt}^* < 1$

Usually F_{lt}^* is taken to be -0.5, which corresponds to the *Von Mises* criterion.
Since in the *TSAI*-criterion all 6 strength components are used, it is obvious that they must all be specified in the table, together with the value for F_{lt}^*.
syntax :

TABLE
c_2 / 2 X_t Y_t R S X_c Y_c F_{lt}^*

"2" refers to the *TSAI* criterion

(Here the manual is not always consistent; sometimes not F_{lt}^{*} but F_{lt} is said to be specified.)

C.3.4.2 Note concerning the lay-up definition

The local axes of 2003-2004 elements are defined differently from those of 2006-2008 elements. To obtain uniformity, it is possible to define the reference axis or the principal material direction according to a method which does not depend on the element type. The X_0 and X_i axes can be defined as the intersection of the plane through the shell element and a reference plane. This reference plane can be described as follows :

- either Ft=1 XX=xx YY=yy ZZ=zz KX=kx KY=ky KZ=kz

  In this case the reference plane is defined by three points : (xx,yy,zz), (kx,ky,kz) and the centre of the shell element.

- either $Ft = 2$ $XX = xx$ $YY = yy$ $ZZ = zz$

  The reference plane is now defined by its normal $N = (xx, yy, zz)$.

If PSI and Ft are both present, Ft has the upper hand over PSI.

C.3.4.3 General note to the input of data and commands

Data that belong together and should be on the same line, may continue on the following line if this line is preceded by an *asterix*.

C.3.5 Example

This example concerns a composite beam, clamped at one side and on the other side loaded by a shear force (Fig. C.3). The beam has a 2 m length, a 200 mm width and a 8 mm thickness. It consists of 8 glass fibre/epoxy layers, each of which is 1 mm thick and with an alternating fibre angle of 0° or 90°. The shear force is modelled by means of 5 shear forces in the 5 end point nodes of the quadratic element mesh, consisting of 2 rows of elements along the length axis. The elastic constants are shown in *table 31*. *Table 2* gives the strength properties according to the *TSAI*-criterion.

```
DEFINITION
checking SYSTUS for composites
OPTION SHELL
TWO-DIMENSIONAL GENERATE 1
NODES
    1 / −1000 −100 0
    2 / 1000 −100 0
    3 / 1000 100 0
    4 / −1000 100 0
ELEMENTS
    100 / 1 2 3 4
EDGES
    1000 / 1 2 10
    2000 / 2 3 2
VERIFY
MATERIAL PROPERTIES
    / composite zc = −8.0 psi = 0
    layer 1 3 5 7 / table 31 criterion 2 h = 1. psi = 90.
    layer 2 4 6 8 / table 31 criterion 2 h = 1. psi = 0.
TABLES
    31 / el=38.6 * 3 et=8.27 * 3 nult=0.34 glt=4.14 * 3 nutt=0.34
    2 / 2 1062 31 72 72 610 118 −0.5
CONSTRAINTS
    nodes inter 1 46 47 48 4 / ux uy uz rx ry rz
LOADS
1 clamped beam with point forces at the free end
    nodes inter 2 24 25 26 3 / fz = −1.
RETURN
SOLVE DOUBLE
RETURN
SAVE DATA RESU 10
```

The mesh and the internal numbering of the nodes and the elements are shown in Fig. C.4 and Fig. C.5. The deformed beam is presented in Fig. C.6.

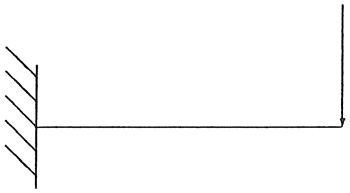

Figure C.3: Clamped beam.

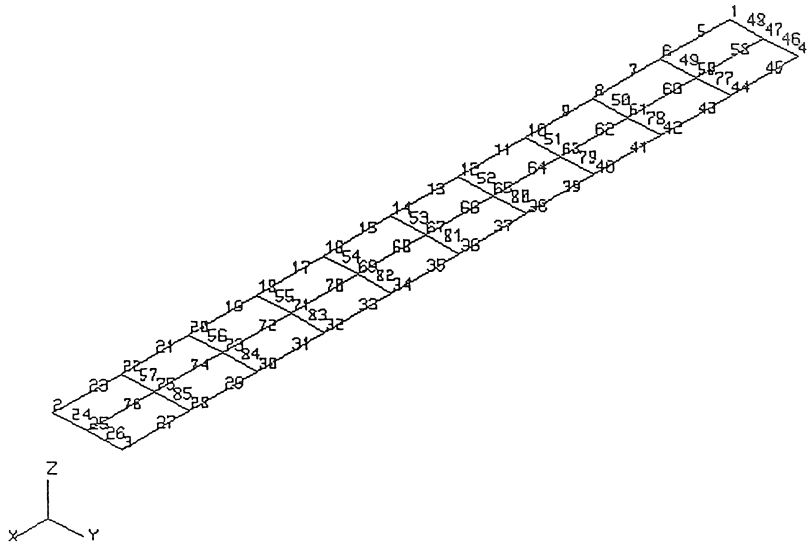

Figure C.4: Internal node numbering of the clamped beam.

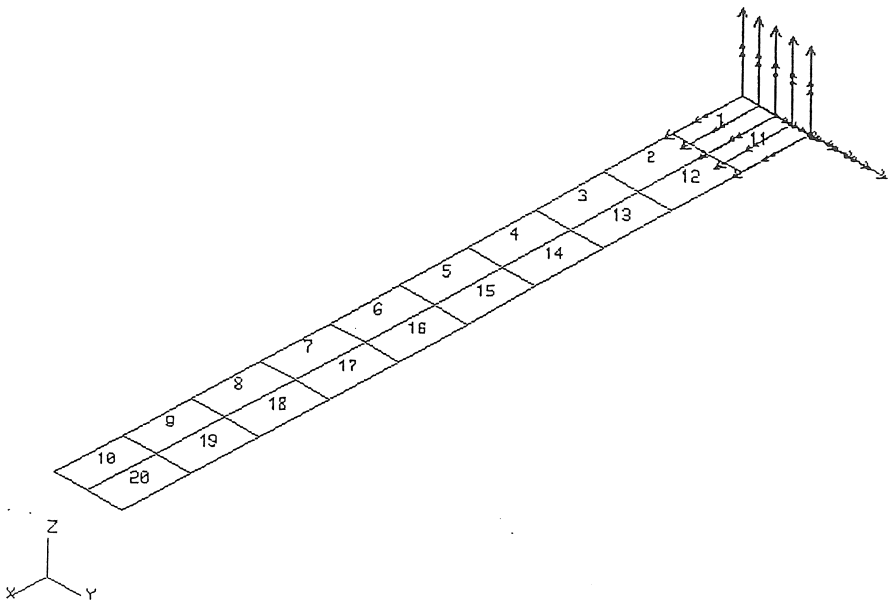

Figure C.5: Internal element numbering of the clamped beam.

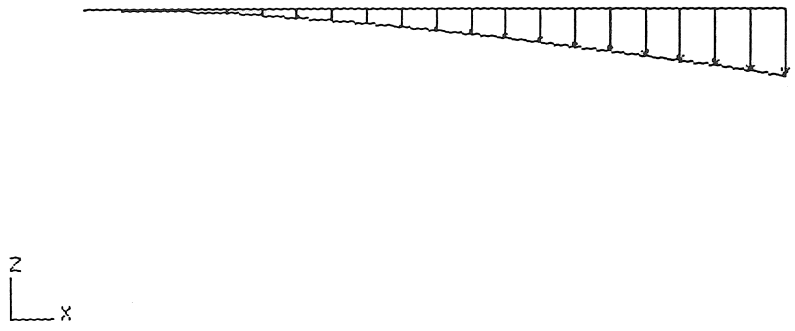

Figure C.6: Deformed state of the clamped beam, due to end point shear forces.

C.4 Postprocessing of the results

C.4.1 Numerically

With the command *SOLVE* the internal element forces are computed in the lower order *Gauss points* of the elements. These forces pro unit length are stored in the *stress*-file. To save this file, a *save data stress* must be executed. The internal element forces in the middle of the elements are stored in the *force*-file, which is automatically saved by a *save data results.*

For shells, the default numerical output after a *solve* command consists of 2 tables (Table. C.2). A first one contains the 6 displacement components (3 translations and 3 rotations) of all nodes present in the model. In the second table the internal element forces are given, including normal and shear forces and bending and torsional moments, expressed pro unit length.

LOAD CASE 1 : clamped beam with point shear forces at the free end

NODAL POINTS DISPLACEMENT

node no.		UX	UY	UZ
1	1	0.00E+00	0.00E+00	0.13E-28
2	2	-0.16E-01	-0.76E-05	-67.21
...	...	...	...	...

RX	RY	RZ
-0.69E-28	0.76E-27	0.00E+00
0.26E-04	0.50E-01	0.00E+00
...	...	...

ELEMENT INTERNAL FORCES

elem. no.		NX	NXY	NY
1	100	-0.36E-06	-0.76E-02	-0.31E-01
...	...	...	...	...
6	105	0.12E-06	-0.72E-05	-0.37E-04
...	...	...	...	...

MX	MXY	MY
-47.50	-0.52	-2.49
...	...	...
-22.50	0.53E-01	0.28E-03
...	...	...

Table C.2: Standard output resulting from a *solve* command.

When in addition the stresses in the individual layers are asked for, four alternatives can be chosen.

C.4.1.1 Stress layer extract

With this command, the stress components in the plane of the composite element are computed. To obtain this two-dimensional result, following syntax is used :

```
SEARCH DATA RESU 10
STRESS LAYER i EXTRACT
RETURN
```

- *layer i* : from layer i, the local axes referred stresses σ_{xx}, σ_{yy} and τ_{xy} in the middle of the element are computed in the upper, middle and lower fibre of this layer. These stresses are stored in the *force*-file. If no layer number is specified, the stresses in all layers are calculated.
- *extract*: indicates that a detailed output of the stress results will be given. It are only the stresses in the middle of the elements and of the layer thickness that are presented, as well in the local system of axis (σ_{xx}, σ_{yy} en τ_{xy}) as in the fibre related coordinate system (σ_{ll}, σ_{tt} en τ_{lt}). If in addition also a failure criterion was

specified (Tsai or Hill), the values from these criteria and the corresponding safety factors are also written to the output table. The label *extract* is necessary to obtain the output table.

- *stress layer strain* : this command generates a table, describing the strains and curvatures in the middle of each element.

Note :

- *extract* and *strain* can not be employed together
- Before asking for the results in a next layer, it is recommended to first execute a *return*, followed by again a *search data results.*

Example :

The results presented in Table C.3, concern element 6 in the middle of the beam.

layer	σ_{xx}	σ_{yy}	τ_{xy}	σ_{ll}	σ_{tt}	τ_{lt}
1	-.71E+00	.13E+00	.44E-02	.13E+00	-.71E+00	-.44E-02
2	-.25E+01	-.13E+00	.31E-02	-.25E+01	-.13E+00	.31E-02
...	...	...	...	...	...	...

	value	ratio
TSAI	-.17E-01	.17E+03
TSAI	-.13E-02	.46E+03
...	...	...

int.el.no.	LOAD	ϵ_{xx}	ϵ_{yy}	γ_{xy}
...	...	...	...	...
6	1	-.735E-05	-.293E-09	-.217E-09
...	...	...	...	...

c_{xx}	c_{yy}	c_{xy}
...	...	...
0.227E-04	-.273E-05	-.300-06
...	...	...

Table C.3: Output according to the *stress layer extract* command.

C.4.1.2 Postprocessing

The *postprocessing* module offers the possibility to compute stresses in the middle of each element, and for every layer in the upper, middle and lower fibre. Again the analysis is two-dimensional, thereby considering only the in-plane stress components. This module also allows for the *Tsai* or *Hill* safety factors to be determined. Following syntax is used :

POSTPROCESSING
SET (nr) (title)
FORCE COMPOSITE 1 2 3 4 5 6 / layer (nr) (Hill) X_t Y_t R S
ELEMENTS (nrs)
COMBINE
(title of the loading case)
RETURN
PRINT
SET (nr) COMBINE (nr) COMPONENT (nr)

Explanation to this syntax :

- *postprocessing* : refers to processing the results of the *solve*-computation.
- *set (nr) (title)* : the routine is provided with a number and title.
- The third line indicates that one wants to calculate the stresses in the upper, middle and lower fibre of layer i. If required, the stresses can be checked against a failure criterion, but then the corresponding parameters must be specified. (C.3.4.1)
- *element (nr)* : one can select particular elements.
- In the data file, several loading cases have been defined and to each of them a reference number has been given. If one wants to compute the stresses corresponding to load case i, following commands must be used :

COMBINE
LOAD i
RETURN

If one intends to combine several load cases, following syntax can be applied :

```
COMBINE
  (title) / 1 1 2 3
RETURN
```

By this, a new load case is created, being a combination of 1 times case 1 and 2 times case 3. To this new load case a new title can be given, which however must be preceded by a blanc.

- *print* : the command *print* is required to obtain an output of the results.
- The command *set (nr)* refers to the previously specified number.
- With *combine (nr)* only the results corresponding to the number *nr* under the *combine*-command of the routine are asked for.
- The results are presented in 10 columns. With the command *components nr*, the wished for column can be selected.

The 10 columns can be subdivided into 4 groups :

- group 1 :
  - 1-2-3 : σ_{ll}, τ_{lt} en σ_{tt}
- group 2 :
  - 4 : ψ, angle of the first principal stress
  - 5-6 : σ_1 and σ_2, principal stress components
- group 3 :
  - 7 : value of the *TSAI* or *HILL* criterion
- group 4 :
  - 8-9-10 : σ_{xx}, τ_{xy} en σ_{yy}

Example :

```
post
set 1 stresses
force composite 1 2 3 4 5 6 / layer 1 Tsai 1062 31 72 72 610 118 -0.5
elem inter 1 to 20
combine
load 1
return
print
```

el.no.	σ_{ll}	τ_{lt}	σ_{tt}	ψ	σ_1	σ_2
...	...	...	...	...	...	...
105	0.148	-.50E-02	-.802	-.300	0.148	-.802
	0.127	-.44E-02	-.709	-.298	0.127	-.709
	0.106	-.37E-02	-.617	-.296	0.106	-.617
...	...	...	...	...	...	...

TS/HI	σ_{xx}	τ_{xy}	σ_{yy}
...	...	...	...
-.19E-01	-.802	0.50E-02	0.148
-.17E-01	-.709	0.44E-02	0.127
-.15E-01			
...	...	...	...

Table C.4: Output according to the *postprocessing* module. (The element number 105 refers to the element with internal number 6.)

Components 1 to 10 refer to the lower fibre, 11 to 20 to the middle fibre and 21 to 27 to the upper one. For the upper surface of the layer, the stresses in the local system of coordinates are no longer given.

C.4.1.3 Average shell composite layer i extract

By the command *solve*, stresses in the *Gauss points* are computed. With *save data stress* these are stored in the *stre(nr).tit*-file. It has been found empirically that, for computing stresses, the most accurate results are obtained in the *Gauss points*. These stresses can afterwards be extrapolated to stresses in the nodal points. This extrapolation can

be performed, using the *average shell* command, which does only apply onto thick shells, modelled by means of quadratic elements (2n06-2n08). The syntax is as follows :

SEARCH DATA STRESS 10
AVERAGE SHELL COMPOSITE LAYER *i* EXTRACT
ELEMENTS ....
RETURN

For every node, values of σ_{xx}, σ_{yy}, σ_{zz}, τ_{xy}, τ_{xz} and τ_{yz} are given. These stresses are referred to the local axes of each element. *Average shell* thus considers a three-dimensional stress state. Beside the in-plane stress components, also the two transverse shear stresses are computed. σ_z is also provided but in principle should be zero.
Note : In case *average shell* is frequently used, it is recommended to perform a *search data stress* at every turn.

Example :

```
average shell composite layer 1 extract
elem inter 6
retu
```

node no.		σ_{xx}	σ_{yy}	σ_{zz}
14	1009	-0.7881	0.1418	0.6691E-20
15	1010	-0.7090	0.1275	0.8291E-21
...	...	...	...	...

τ_{xy}	τ_{xz}	τ_{yz}
0.2981E-02	-0.3127E-02	-0.1017E-02
0.4414E-02	-0.3030E-02	-0.5137E-04
...	...	...

Table C.5: Output according to the *average shell composite layer extract* command.

C.4.1.4 Shell

With the command *shell* (for thick shell elements 2n06-2n08), the stresses in the *Gauss points* are computed from the *stress*-file results. For each element and each layer, the coordinates (X,Y,Z) of the *Gauss points* in the middle of the layer are tabulated, followed by the corresponding three-dimensional stress components σ_{ll}, τ_{lt}, σ_{tt}, τ_{lz} and τ_{tz} with respect to the fibre related axes of that layer. (In the output's header however, the stresses in the local coordinate system are specified.) σ_z is not taken into account. Further, also the three principal stresses, σ_1, σ_2 and σ_3, and the eventual failure criterion value are returned. The syntax is the following :

SHELL
ELEMENTS....
COMPOSITE layer *m* to *l* criterion Hill..... Tsai.....
COMBINE
  title / (ci,ni)
....
COMPOSITE layer *n* ....
COMBINE
....
RETURN

Example :

```
shell
elem inter 6
composite layer 1 criterion Tsai 1062 31 72 72 610 118 -0.5
combine
  example / (1,1)
retu
```

ELEM.NO.		LAYER NO.		pts	X	Y	Z
6	105	1	58	1	42.3	-78.9	0.
				2	158.	-78.9	0.
				3	42.3	-21.1	0.
				4	158.	-21.1	0.

σ_{ll}	τ_{lt}	σ_{tt}	τ_{lz}	τ_{tz}
0.136	-0.373E-02	-0.755	0.811E-03	-0.438E-02
0.119	-0.505E-02	-0.663	-0.633E-03	-0.427E-02
0.135	-0.411E-02	-0.755	0.532E-03	-0.368E-02
0.119	-0.451E-02	-0.664	-0.286E-03	-0.374E-02

σ_1	σ_2	σ_3	HILL	TSAI
0.136	0.203E-04	-0.755		-0.179E-01
0.119	0.244E-04	-0.664		-0.157E-01
0.135	0.157E-04	-0.755		-0.179E-01
0.119	0.205E-04	-0.664		-0.157E-01

Table C.6: Output according to the *shell* module.

C.4.2 Graphically

C.4.2.1 Graphical data representation

Within the *plot* command, following representation facilities, specific for composites, are available :

- *vector element layer i* : the fibre orientation of layer i is shown by means of an arrow.
- *vector element material x,y or z* : the laminate thickness is presented by a coloured vector in the x, y or z-direction. (Notice that this command differs from the one in the manual.)

C.4.2.2 Graphical representation of the results

With the *paint* command, the stresses and safety factors in the different laminate layers can be graphically represented.

paint	laminated	criterion i ratio	surface layer j maxi mini	interval n choice n	load c	panel

Table C.7: Graphical output facilities.

- *laminated* : refers to results for composite materials from the *layer stress* procedure.
- i : number of the stress component :
  - 1 : σ_{ll}
  - 2 : σ_{lt}
  - 3 : σ_{tt}
- *criterion* : value of the failure criterion according to Tsai or Hill, as specified in the data file.
- *ratio* : (the manual says *margin*). Gives the safety factor according to the failure criterion used. This value represents the multiplicator by which the loads may be multiplied in order to reach a value 1 for the failure criterion.

- *layer j* : selects layer j of the laminate. Default, the values in the lower layer are given.
- *maxi* or *mini* : the most or least loaded layer is selected and its number appears on the mesh.
- *interval n* or *choice n* : refers to the division in colour intervals.

Default, the edges of the elements are painted in the colour, corresponding to the value that has to be drawn. With *panel* the elements are fully painted (in the manual *full* is mentioned). If one wants to show the results on the deformed mesh, *defo* must be added to the previously described command.

Appendix D

Manual to the laminate lay-up generating software for filament wound composites

This appendix is an addition to section 4.4.

D.1 LUPRO (Lay-Up command PROcedure)

LUPRO is a command procedure for generating the laminate lay-up for filament wound composites, corresponding to a well-defined set of geodesic winding patterns.

Within *LUPRO* following commands are available :

- BASLUP, to create the basic laminate lay-up
- ADDLUP, to create additional basic lay-up
- LUPSEQ, to compute the real lay-up sequence
- THEEND, to quit the lay-up generator

D.1.1 BASLUP

Within the BASLUP option, the computer code *LUPGEN* will be called to generate the basic lay-up data in each element of the finite element mesh of the filament wound component, which correspond to a specified set of winding patterns.

D.1.1.1 Input

- name of the SYSTUS-data file, containing data about the geometry and the finite element mesh. This file can be obtained from the *data* $****$*.tit* file, generated when running SYSTUS, by means of following procedure :

  search *data* $****$

  output data formatted extract

  file *mesh.* $****$

  return

- name of the file containing the total number of geodesic lines to take into account and the labels of the corresponding geodesic data files. These files are called *list01, list02, ... list55 ...*, their label being $1, 2 \ldots 55 \ldots$.
- name of the file to which the basic lay-up output must be written
- the file called *gegev.dat*, containing following information :

  1 : if $x - y$-plane is symmetry plane
  0.01 : proportional tolerance in view of the decision whether a point lies in or out of an element
  1.57 : wet fibre cross-section in mm^2
  5 : fibre band width in mm
  0.31 : fibre band thickness in mm
  20 : tolerance on angular difference for further compaction (°)
  0.05 : negligible layer thickness in mm

D.1.1.2 Output

- basic lay-up output file, containing for every element of the finite element mesh the number of layers covering that element. From

each layer, following data are specified :

- the label of the geodesic line of origin
- the quadrant where this line started
- the quadrant in which the points, corresponding to the geodesic segment crossing the element, were lying before eventual mirroring
- the fibre angle with respect to the local element axes
- the layer thickness

- a file containing the labels of eventual empty elements, which allows for a fast global coverage control

D.1.2 ADDLUP

ADDLUP requires as input the name of the original basic lay-up file, which is a result from previous computations. Starting from these data, ADDLUP continues with the BASLUP option for computing further lay-up data, corresponding to additional geodesic patterns.

D.1.3 LUPSEQ

The LUPSEQ option will transform the basic lay-up data into the real laminate lay-up, corresponding to the real time sequence of all winding patterns. For this purpose the *LAYSEQ* computer code is called for.

D.1.3.1 Input

- name of the basic lay-up file, which is computed from the BASLUP option
- name of the file containing the sequence data of the geodesic winding patterns. Such a sequence file can e.g. look as follows :

```
59
1        4
4        6        2        1
318      319      316      315
422      425      417      416
449      451      447      445
2        1
5        7        8        3
3   ...
...
```

This file includes following information :

- the number of basic geodesic patterns, considered when computing the basic lay-up (e.g. 59)
- for each considered geodesic line, it is indicated how frequent this line will be repeated within the global geodesic covering. In the example, the first geodesic trajectory is repeated four times. For symmetry reasons, one knows that from every geodesic line, three equivalent versions, starting in the three other quadrants, are also present. Consequently, the sequential number of all four versions of the same geodesic line must be specified within the sequence data file. In the given example file it is the version of the first specified geodesic line, starting in the fourth quadrant of the mandrel, which will be the first to be wound. Its mirrored copy, leaving from the third quadrant, will be the next one. The third winding is laid along a path corresponding to the second geodesic trajectory.

D.1.3.2 output

The output is a file containing the laminate lay-up in every element of the mesh, corresponding to the format required by the SYSTUS finite element code.